

RPGR 2018 GUILIN



OCTOBER 22-25, 2018 - CHINA

RECENT PROGRESS IN GRAPHENE & 2D MATERIALS RESEARCH

ABSTRACTS BOOK



 MAIN ORGANISERS

PHANTOMS
foundation



桂林市市徽

**GUANGXI INDUSTRY AND
INFORMATION COMMITTEE**

 **广西科学技术协会**
GUANGXI ASSOCIATION FOR SCIENCE AND TECHNOLOGY

WWW.RPGRCONF.COM/2018/

PLENARY CONTRIBUTIONS	<u>1</u>
KEYNOTE CONTRIBUTIONS	<u>3</u>
INVITED CONTRIBUTIONS	<u>17</u>
INVITED CONTRIBUTIONS (PARALLEL WORKSHOPS)	<u>32</u>
INVITED CONTRIBUTIONS (INDUSTRIAL FORUM)	<u>53</u>
ORAL CONTRIBUTIONS	<u>61</u>
POSTER CONTRIBUTIONS	<u>138</u>

Index alphabetical order

Plenary Speakers
Keynote Speakers
Invited Speakers
Oral
Poster

Speakers/Orals/Posters

	Page
Ahn, Jong-Guk (Chonnam National University, South Korea) <i>Surface Enhanced Raman Spectroscopy at Nanogap between Au Nanoparticles Separated by 2D hexagonal Boron Nitride</i>	Poster 139
Ai, Zizheng (State Key Lab of Crystal Materials, China) <i>BNNS@Ti3C2 Intercalation Electrocatalyst for Hydrogen Evolution Reaction</i>	Poster 141
Ando, Atsushi (National Institute of Advanced Industrial Science and Technology (AIST), Japan) <i>Morphology and electrical studies on NaCl-assisted CVD synthesis of WS2</i>	Poster 142
Bao, Qiaoliang (Monash University, Australia) <i>Photonic and Optoelectronic Device Applications Based on 2D Materials</i>	Invited (Plenary Session) 18
Bao, Lihong (Institute of Physics, Chinese Academy of Sciences, China) <i>Black Phosphorus and Its Analogue: Electrical Transport Properties and Devices</i>	Oral 64
Bao, Deliang (Institute of Physics, China) <i>Fabrication of Millimeter-Scale, Single-Crystal One-Third-Hydrogenated Graphene with Anisotropic Electronic Properties</i>	Oral 62
Belle, Branson (SINTEF, Norway) <i>Gamma ray radiation effects on hBN encapsulated Graphene Field Effect Transistors</i>	Poster 144
Bittencourt, Carla (University of Mons, Belgium) <i>Molybdenum Disulfide as Surface Enhanced Raman Scattering Substrates for Sensing Polycyclic Aromatic Hydrocarbons</i>	Oral 65
Blaskovic, Milan (National University of Singapore, Singapore) <i>Tunable interaction between graphene and a DNA molecule</i>	Poster 146
Bonaccorso, Francesco (IIT-Graphene Labs / BeDimensional, Italy) <i>Large scale production of 2D-materials for energy applications</i>	Invited (Plenary Session) 20
Cai, Yichao (Nankai University, China) <i>Graphene and Carbon Nanotube in Na-CO2 Battery</i>	Poster 148
Chang, Yung-Huang (National Yunlin University of Science and Technology, Taiwan, China) <i>Tunable Band Gap Energy from WSxSey Monolayer</i>	Poster 150
Chen, Jun (Nankai University, China) <i>Inorganic/organic and carbon composites for Li/Na Batteries</i>	Keynote 4
Chen, Hui (Institute of Physics, CAS, China) <i>Recovering edge states of graphene nanoislands on Ir(111) by silicon intercalations</i>	Oral 67

	Page
Chen, Zhaolong (Peking University, China) <i>High Brightness Blue/UV Light-Emitting Diodes Enabled by Directly Grown Graphene Buffer Layer</i>	Oral 68
Chen, Zongping (Zhejiang University, China) <i>Precision synthesis of structurally defined graphene nanoribbons by chemical vapor deposition</i>	Oral 69
Chen, Chang-Hsiao (Feng Chia University, Taiwan, China) <i>Chemical Vapor Deposition Synthesis of Large-Area Monolayer InSe</i>	Poster 151
Cheng, Hui-Ming (Chinese Academy of Sciences, China) <i>Fabrication of Graphene and Other 2D Materials by Exfoliation</i>	Keynote 5
Cho, Ah-Jin (Yonsei University, South Korea) <i>Evaluation of a WSe₂/MoS₂ Heterojunction in the Perspective of a Transparent Thin-film Solar Cell</i>	Poster 152
Chu, Hailiang (Guilin University of Electronic Technology, China) <i>Effect of Reduced Graphene Oxide on the Electrochemical Properties of Overlithiated Oxide Cathode Materials for Li-Ion Batteries</i>	Poster 154
Chua, Daniel (NUS, Singapore) <i>New varieties of Metal Sulphides / Phosphides for Electronics and Clean Energy applications</i>	Invited (Industrial Forum) 54
Ci, Haina (Peking University, China) <i>Vertically-oriented Graphene Growth at Low Temperature for Solarthermal Applications</i>	Poster 155
Cui, Xueping (Institute of Chemistry Chinese Academy of Sciences, China) <i>Fabrication of Transition Metal Dichalcogenides Nanoscrolls</i>	Poster 158
Cui, Ling zhi (Peking University, China) <i>Highly Conductive Nitrogen-doped Graphene Grown on Glass Towards Electrochromic Applications</i>	Poster 156
Dai, Xi (Nankai University, China) <i>Freestanding graphene/VO₂ composite films for highly stable aqueous Zn-ion batteries with superior rate performance</i>	Poster 159
Deng, Jianqiu (Guilin University of Electronic Technology, China) <i>High-performance V-based electrode materials for sodium-ion batteries</i>	Poster 161
Deng, Bing (Peking University, China) <i>Graphene as Electronic Materials: Controlled Growth of Single-Crystal Graphene Wafer</i>	Poster 160
Duan, Xiangfeng (University of California, USA) <i>Van der Waals Integration beyond 2D Materials</i>	Keynote 6
Eda, Goki (NUS, Singapore) <i>Photonics of 2D semiconductors</i>	Invited (Plenary Session) 21
Eginligil, Mustafa (Nanjing Tech University, China) <i>Circular Photogalvanic Photocurrents in 2D Materials</i>	Oral 70
Etemadi, Samaneh (Abalonyx AS, Norway) <i>Graphene Oxide acidity modifications</i>	Oral 71
Gao, Hongjun (Chinese Academy of Sciences, China) <i>Construction of Novel 2D Atomic/molecular Crystals and Its physical Property</i>	Keynote 7

	Page
Gao, Jie (Guilin University of Electronic Technology, China) <i>Enhanced Thermoelectric Performance in Graphene Quantum Dots/Te Nanowires composite film</i>	Poster 163
Garaj, Slaven (NUS, Singapore) <i>Nanofluidics with graphene and graphene-oxide membranes</i>	Invited (Parallel Workshop) 33
Geng, Fengxia (Soochow University, China) <i>Novel Inorganic Layered Materials: From Interlayer Chemistry, Delamination, toward Energy Storage Applications</i>	Oral 72
Ghimire, Mohan (Sungkyunkwan University, South Korea) <i>Graphene-CdSe quantum dot hybrid as a platform for the control of carrier temperature</i>	Oral 74
Guo, Wanlin (Nanjing University of Aeronautics & Astronautics, China) <i>Emerging Hydrovoltaic Technology</i>	Keynote 8
Hou, Yunpeng (Nankai University, China) <i>High-performance layered Ni-rich LiNi_{1-x-y}CoxAl_yO₂ cathode materials for lithium ion batteries</i>	Poster 164
Hsu, Hao-Lin (Green Energy Technology Research Center/Kun Shan University, Taiwan, China) <i>Application of Carbon Aerogel in the Adsorption of Polycyclic Aromatic Compounds from Diesel Exhaust</i>	Oral 75
Hu, Jinsong (Institute of Chemistry, Chinese Academy of Science, China) <i>2D Germanium Selenide for Photovoltaics and Optoelectronics</i>	Invited (Parallel Workshop) 35
Hu, Zhirun (University of Manchester, UK) <i>Printed Graphene For Chipless RFID Applications</i>	Oral 76
Huo, Shanshan (Graphene Enabled Systems Ltd, UK) <i>A New Model for Accelerating the Commercialisation of Graphene and other 2D Materials Research from Universities</i>	Oral 78
Ikeda, Keiichiro (Osaka Prefecture University, Japan) <i>Chemical Modification of Graphene Controlled by Substrate Surface Treatment with Self-Assembled Monolayers</i>	Poster 166
Iwasa, Yoshihiro (The University of Tokyo, Japan) <i>Symmetry Controlled Optical Properties in TMD Nanostructures</i>	Invited (Plenary Session) 22
Jang, Chan Wook (Kyung Hee University, South Korea) <i>Flexible perovskite resistive random access memories employing graphene transparent conductive electrodes</i>	Poster 168
Jia, Kaicheng (Peking University, China) <i>Copper Containing Carbon Feedstock for Growing High Quality Graphene</i>	Poster 169
Jiao, Chengli (Qingdao Institute of BioEnergy and Bioprocess Technology Chinese Academy of Sciences, China) <i>Induced Assembly of Two-Dimensional Metal–Organic Framework Nanosheets for Gas Separation</i>	Oral 80
Joe, Minwoong (SKKU, South Korea) <i>Dominant in-plane cleavage direction of CrPS₄ monolayer</i>	Poster 170

	Page
Kawanago, Takamasa (Tokyo Institute of Technology, Japan) <i>Two-Dimensional Inorganic/Organic Hetero Interface for Field-Effect Transistor Applications</i>	Invited (Parallel Workshop) 36
Kim, Keun Su (Yonsei University, South Korea) <i>Bandgap engineering of two-dimensional semiconductors</i>	Invited (Parallel Workshop) 38
Kim, Jong Min (Kyung Hee University, South Korea) <i>Use of Doped-Graphene Transparent Conductive Electrodes for High-Performance Si-Quantum-Dots-Based Solar Cells</i>	Oral 81
Kim, Gil-Ho (Sungkyunkwan University, South Korea) <i>Atomically Thin Tunneling Layer for Improved Contact Resistance and Dual Channel Transport in MoS₂/WSe₂ van der Waals Heterostructure</i>	Poster 171
Kim, Ju Hwan (Kyung Hee University, South Korea) <i>Multilayer graphene/conducting polymer/Si nanowires/Si/TiO_x hybrid solar cells</i>	Poster 173
Koshino, Mikito (Osaka University, Japan) <i>Effective theory for the flat band in the twisted bilayer graphene</i>	Invited (Plenary Session) 23
Kuester, Scheyla (École de technologie supérieure/NanoXplore Inc., Canada) <i>Electrical properties and electromagnetic shielding effectiveness of polycarbonate/acrylonitrile butadiene styrene/graphene nanoplatelets nanocomposites</i>	Oral 82
Lanza, Mario (Soochow University, China) <i>Building the hardware of future artificial intelligence systems: two-dimensional materials based electronic synapses</i>	Invited (Plenary Session) 24
Li, Lance (Taiwan Semiconductor Manufacturing Company, Taiwan) <i>Continue the transistor scaling with 2D materials: Challenges and Perspective</i>	Keynote 10
Li, Geng (Institute of Physics, CAS, China) <i>Construction of graphene/silicene heterostructure by Si intercalation</i>	Oral 84
Li, Jinshu (Sungkyunkwan University, South Korea) <i>Quasiparticle interference (QPI) in twisted bilayer graphene</i>	Oral 85
Li, Wenjiang (School of Materials Science and Engineering, China) <i>Nanoscale NEXAFS for Probing multi-layer graphene/copper nanowires composite</i>	Poster 174
Lin, Yen-Fu (National Chung Hsing University, Taiwan) <i>Performance potential and limit in van der Waals MoTe₂ Transistors</i>	Invited (Parallel Workshop) 39
Linchao, Zeng (Tsinghua-Berkeley Shenzhen Institute, China) <i>Integrated paper-based stretchable LIBs</i>	Poster 176
Liu, Hongyang (Institute of Metal Research, China) <i>Nano-Graphene Based Catalyst for Efficient Light Alkane Activation</i>	Invited (Parallel Workshop) 40
Liu, Chang-Hua (National Tsing Hua University, Taiwan) <i>Developing ultrathin light emitters and metalenses based on van der Waals materials</i>	Invited (Industrial Forum) 55

	Page
Liu, Zhongfan (Peking University, China) <i>CVD Graphene: Scalable Growth and Beyond</i>	Keynote 11
Liu, Zhibo (Institute of Metal Research, Chinese Academy of Sciences, China) <i>The boundaries of 2D Mo₂C superconducting crystals</i>	Oral 86
Liu, Yang (Guangxi University, China) <i>Asymmetric 3d Electronic Structure for Enhanced Oxygen Evolution Catalysis</i>	Poster 185
Liu, Fangming (Nankai University, China) <i>Anions inserted into graphite interlayers enhancing the electrodeposited metal hydroxides for oxygen evolution</i>	Poster 179
Liu, Jiaman (Tsinghua-Berkeley Shenzhen Institute, China) <i>Synthesis of wafer-scale single-layer h-BN and its use in proton transport membrane</i>	Poster 181
Liu, Mingqiang (Tsinghua-Berkeley Shenzhen Institute, China) <i>Controlled growth and doping of black phosphorus with tunable properties</i>	Poster 183
Liu, Bingzhi (Peking University, China) <i>Oxygen-assisted Growth of Highly Conductive Graphene with Controllable Domain Size on Glass</i>	Poster 178
Lu, Huibing (Guilin University of Technology, China) <i>Controllable synthesis of 2D Cr-doped MoO_{2.5}(OH)_{0.5} nanosheets and application in Lithium Ion Batteries</i>	Oral 87
Luo, Hao (Tsinghua University, China) <i>Probing and Modulating Interface Interactions in 2-Dimensional Materials and Their Heterostructures</i>	Oral 89
Ma, Ruisong (Institute of Physics Chinese Academy of Sciences, China) <i>Direct Four-Probe Measurement of Grain-Boundary Resistivity and Mobility in Millimeter-Sized Graphene</i>	Oral 90
Miao, Feng (Nanjing University, China) <i>Electronic Transport and Device Applications of 2D Materials</i>	Invited (Plenary Session) 26
Miao, Lei (Guilin University, China) <i>Enhanced Thermoelectric Performance in Graphene Quantum Dots/Te Nanowires Flexible Hybrid Film</i>	Invited (Parallel Workshop) 41
Moon, Pilkyung (NYU Shanghai, China) <i>Theory of Dirac Electrons in a Dodecagonal Graphene Quasicrystal</i>	Invited (Parallel Workshop) 42
Moon, Inyong (Sungkyunkwan University, South Korea) <i>Measurements of Fermi Level and Doping Concentration of 2D Transition Metal Dichalcogenide Using Kelvin Probe Force Microscopy</i>	Oral 91
Mugarza, Aitor (ICN2, Spain) <i>Engineering nanoporous graphene with atomic precision</i>	Invited (Parallel Workshop) 44
Munindra , (Delhi Technological University, India) <i>Quantum Capacitance Effect in Graphene-Metal-Oxide-Semiconductor Field Effect Transistor with Large Area Graphene Channel</i>	Oral 92

	Page
Novoselov, Kostya (University of Manchester, UK) <i>Materials in the Flatland</i>	Plenary 2
Oba, Tomoaki (Tokyo Institute of Technology, Japan) <i>Gated Four-Probe Method for Evaluation of Electrical Characteristics in MoS₂ Field-Effect Transistors</i>	Poster 187
Okamoto, Takuya (Tokyo Institute of Technology, Japan) <i>Three-Dimensional Spatial-Topology Effects, Magnetoresistance in Three-Dimensional Porous Graphene</i>	Poster 189
Park, Hamin (KAIST, South Korea) <i>Interlayer interaction in a van der Waals heterostructure of transition metal dichalcogenide and hexagonal boron nitride</i>	Oral 93
Park, YoungHee (Chonnam National University, South Korea) <i>Electrochemical Surface Modification of Two-Dimensional Hexagonal Boron Nitride for Generating Midgap Energy States</i>	Poster 191
Peng, Hailin (Peking University, China) <i>High-Mobility 2D Crystals: Controlled Synthesis and Functional Devices</i>	Keynote 12
Pu, Jiang (Nagoya University, Japan) <i>Room Temperature Valley Polarized Light-Emitting Diodes of Monolayer Transition Metal Dichalcogenides</i>	Oral 94
Qin, Jieqiong (Dalian Institute of Chemical Physics, Chinese Academy of Sciences, China) <i>Two-Dimensional Pseudocapacitive Nanosheets for All-Solid-State Micro-Supercapacitors</i>	Poster 193
Qiu, Jason Jieshan (Beijing University of Chemical Technology, China) <i>Synthesis and Applications of Carbon Dots</i>	Invited (Industrial Forum) 56
Reckmeier, Claas Julian (neaspec, Germany) <i>Cryogenic near-field imaging and spectroscopy at the 10-nanometer-scale</i>	Oral 96
Ren, Wencai (Chinese Academy of Sciences, China) <i>Graphene Oxide: Green Synthesis and Membrane Applications</i>	Keynote 13
Romano, Valentino (University of Messina, Italy) <i>An industrial scalable approach for graphene/carbon nanotubes hybrid flexible supercapacitors</i>	Oral 97
Sagar, Rizwan Ur Rehman (Tsinghua University, China) <i>Magneto-transport Properties of Graphene Foam</i>	Oral 99
Sasagawa, Akira (Tokyo Institute of Technology, Japan) <i>Direct observation of Plasmons in Graphene Quantum Dots with Scanning Near-Field Optical Microscopy</i>	Poster 195
Sato, Shintaro (Fujitsu Laboratories Ltd., Japan) <i>Application of Graphene and Graphene Nanoribbons to Electronic Devices Including Ultrasensitive Gas Sensors</i>	Invited (Industrial Forum) 57
Shamsul, Zakuan Azizi (NanoMalaysia Berhad, Malaysia) <i>Malaysia's Graphene Commercialization Progress - National Graphene Action Plan 2020</i>	Invited (Industrial Forum) 59
Shan, Suyan (Wenzhou Medical University, China) <i>The fibroblast growth factor modified nitrogen-containing graphene for regeneration of photo-damaged retinal pigment epithelial cells</i>	Oral 101

	Page
Shan, Jingyuan (Peking University, China) <i>Graphene-Armored Aluminum Foil as Current Collectors for High-voltage Lithium-Ion Battery with Enhanced performance</i>	Poster 197
Shi, Xiaoyu (Dalian Institute of Chemical Physics, Chinese Academy of Sciences, China) <i>Graphene based linear tandem micro-supercapacitors</i>	Poster 198
Shin, Gwang Hyuk (KAIST, South Korea) <i>Si-MoS₂ Vertical Heterostructure for High Responsivity Photodetector</i>	Oral 103
Shin, Seunghyun (Chonnam National University, South Korea) <i>Direct Covalent Functionalization of Single Layer 2H-MoS₂ Electrografting of Diazonium Salt: Influence of S vacancy and S-C bond on Photoluminescence of 2H-MoS₂</i>	Poster 199
Shin, Seung-Hyun (Kyung Hee University, South Korea) <i>MAPbI₃ Perovskite Solar Cells Employing Flexible n-Type Graphene Transparent Conducting Electrodes</i>	Poster 200
Shuan, Li (Peking University, China) <i>Annealing temperature effect on microstructure, optical and electrical properties of nanometer GdYOx high k films</i>	Poster 202
Son, Young-Woo (Korea Institute for Advanced Study, South Korea) <i>Effects of interlayer interactions on physics of layered crystals</i>	Invited (Plenary Session) 27
Su, Ching-Yuan (National Central University, Taiwan) <i>Rational Design of Nanostructured and Functionalized Graphene and Their Applications for Electronics and Energy Devices</i>	Invited (Parallel Workshop) 45
Su, Shubin (Shanghai Jiao Tong University, China) <i>Water-based Graphene Patterning under Ultraviolet Irradiation</i>	Poster 204
Sun, Li-Xian (Guilin Univ. of Electronic Technology, China) <i>Interfacing graphene with nanoparticles for energy and gas storage as well as sensors</i>	Invited (Plenary Session) 28
Sun, Jinhua (Chalmers University of Technology, Sweden) <i>Molecular pillar approach to construct functionalized graphene for energy storage</i>	Oral 104
Sun, Xiao (Peking University, China) <i>Rapid Growth of Large Single-Crystalline Graphene with Ethane</i>	Oral 106
Sun, Chia-Liang (Chang Gung University, Taiwan, China) <i>Photoassisted Electrochemical Biosensing Using Graphene Oxide Nanoribbons</i>	Poster 206
Sun, Yan (School of Materials Science and Engineering, China) <i>In-suit Assembled MoS₂/Reduced Graphene Oxide Aerogels as an Efficient Catalyst Application for HER Electrocatalysis</i>	Poster 208
Sun, Luzhao (Peking University, China) <i>Visualizing the Fast Growth of Large Single-Crystalline Graphene</i>	Poster 207
Takenobu, Taishi (Nagoya University, Japan) <i>Electrochemically Doped Light-Emitting Devices of Transition Metal Dichalcogenide Monolayers</i>	Invited (Parallel Workshop) 46
Tan, Zelin (National University of Defense Technology, China) <i>Photoluminescence properties of WS₂ under optical irradiation</i>	Poster 209

	Page
Tao, Li (Southeast University, China) <i>Emerging 2D Xenos for Innovative Nanoelectronics</i>	Invited (Parallel Workshop) 48
Tao, Haihua (Shanghai Jiao Tong University, China) <i>Patterning Graphene Film by Magnetic-assisted UV Photochemical Oxidation</i>	Oral 107
Tao, Lei (Institute of Physics, Chinese Academy of Sciences, China) <i>Band engineering of double-wall Mo-based hybrid nanotubes</i>	Oral 109
Terrones, Mauricio (The Pennsylvania State University, USA) <i>A review of Defects in 2D Metal Dichalcogenides: Doping, Alloys, Interfaces, Vacancies and Their Effects in Catalysis & Optical Emission</i>	Keynote 14
Tian, He (Tsinghua University, China) <i>Novel 2D devices based on graphene, BP and perovskite</i>	Oral 110
Wang, Hai (Guilin University of Technology, China) <i>Consideration on the structure of Mo-based anode materials for improving lithium storage performance</i>	Oral 113
Wang, Lin (Shanghai Institute of Technical Physics, China) <i>Toward Sensitive Terahertz Detection Based on Two-dimensional Materials</i>	Oral 115
Wang, Junying (Institute of Coal Chemistry, Chinese Academy of Sciences, China) <i>Co-synthesis of atomic Fe and few-layer graphene towards superior electrocatalysts of O₂ and CO₂</i>	Oral 114
Wang, Zhao (Guangxi University, China) <i>Low-temperature superlubricity of suspended graphene</i>	Oral 117
Wang, Hai (Max Planck Institute for Polymer Research, Germany) <i>Tailoring Graphene: from optical control of carrier density to bandgap engineering in graphene nanoribbons</i>	Oral 111
Wang, Chao (Dalian Institute of Chemical Physics, China) <i>In-situ investigations of the rechargeable aluminum ion battery by XPS, Raman and optical microscope</i>	Poster 210
Wang, Sen (Dalian Institute of Chemical Physics, Chinese Academy of Sciences, China) <i>Scalable Fabrication of Monolithic Micro-Supercapacitors with Tailored Geometries for On-Chip Energy Storage</i>	Poster 212
Wang, Yijing (Nankai University, China) <i>Rational design of 1D mesoporous MnO@C nanorods as anode material for improved Li-storage properties</i>	Poster 213
Wei, Qinwei (Institute of Metal Research, Chinese Academy of Sciences, China) <i>Green Controlled Synthesis of Graphene Oxide by Water Electrolytic Oxidation</i>	Oral 118
Wei, Jindi (Peking University, China) <i>Fabrication of a graphene edge based field emitter and its electron emission properties</i>	Poster 215
Wendelbo, Rune (Abalonyx, Norway) <i>Graphene Oxide Derivatives, Properties and Applications</i>	Invited (Industrial Forum) 60

	Page
Wu, ZhengMing (SwissLitho AG, Switzerland) <i>Fabrication of sub-20 nm Metal Electrodes on 2D Materials without a Charged Particle Beam</i>	Oral 120
Xia, Zhenyuan (Chalmers University of Technology, Sweden) <i>Three-Dimensional Multilayer Graphene-Fe₂O₃ Foam Composites and Their Application in Energy Storage</i>	Oral 122
Xia, Yongpeng (Guilin University of Electronic Technology, China) <i>Significant improved dehydrogenation of LiAlH₄ doped with two-dimensional Ti₃C₂</i>	Poster 216
Xin, Xing (Institute of Metal Research, Chinese Academy of Sciences, China) <i>Circular Graphene Platelets with Grain Size and Orientation Gradients Grown by Chemical Vapor Deposition</i>	Oral 124
Xu, Jian-Bin (The Chinese University of Hong Kong, China) <i>Optoelectronic Devices Based on Graphene-Like Materials and their Related Heterostructures</i>	Invited (Plenary Session) 30
Xu, Chuan (Institute of Metal Research, Chinese Academy of Sciences, China) <i>CVD-Grown High-Quality Ultrathin Mo₂C Crystals and Their Vertical Heterostructures with Graphene</i>	Oral 126
Xu, Chaochao (Guilin University of Electronic Technology, China) <i>Synthesis of bio-based porous carbon and its application in supercapacitors</i>	Poster 217
Yang, Aikai (Nankai University, China) <i>Organic Molecules Grafted onto Graphene Enable Superior Lithium-Ion Batteries</i>	Poster 218
Yang, Yusi (Peking University, China) <i>Weak Interlayer Interaction in Anisotropic GeSe₂</i>	Poster 219
Yao, Minjie (Nankai University, China) <i>Large-Area Reduced Graphene Oxide Composite Films for Flexible Asymmetric Sandwich and Microsized Supercapacitors</i>	Poster 220
Yin, Zhengxuan (Nankai University, China) <i>High Na/K-storage performance of bismuth enabled by ether-based electrolytes</i>	Poster 223
Yin, Shilu (Guilin University of Electronic Technology, China) <i>Synthesis and electrochemical properties of phosphorus doped GO/porous carbon</i>	Poster 221
Yu, Xuebin (Fudan University, China) <i>Graphene-Supported Complex Hydrides as Advanced Hydrogen Storage Materials</i>	Invited (Plenary Session) 31
Yue, Dewu (SKKU Advanced Institute of Nano Technology (SAINT), South Korea) <i>High Performance Two-dimensional Semiconductors established by using a Benzyl Viologen Interlayer</i>	Oral 127
Zahid, Muhammad (Istituto Italiano di Tecnologia, Italy) <i>Effect of 2D Nanomaterials on Gas Permeability and Mechanical Properties of Thermoplastic Polyurethane Nanocomposites</i>	Oral 128

	Page
Zhang, Yihe (China University of Geosciences, China) <i>Graphene Composites as Energy, Catalyst, Environmental and Biomedical Materials, and Full Utilization of Graphite-Mining</i>	Invited (Parallel Workshop) 49
Zhang, Hua (NTU, Singapore) <i>Synthesis and Applications of Novel Two-Dimensional Nanomaterials</i>	Keynote 16
Zhang, Zheng (University of Science and Technology Beijing, China) <i>Defects engineering for monolayer MoS₂ homojunction construction</i>	Oral 134
Zhang, Shaolin (Guangzhou University, China) <i>Preparation and mechanism of molybdenum diselenide nanosheets for ethanol detection</i>	Oral 132
Zhang, Jian (Guilin University of Electronic Technology, China) <i>Graphene quantum dots as interface materials for organic photovoltaic cells</i>	Oral 130
Zhang, Qiu (Nankai University, China) <i>Two-dimension Sulfide Anodes for Sodium-ion Batteries</i>	Poster 227
Zhang, Huanzhi (Guilin University of Electronic Technology, China) <i>Graphene-enhanced Composite Phase Change Materials for Thermal Energy Storage</i>	Poster 224
Zhang, Jincan (Peking University, China) <i>Super-clean graphene film: synthesis, transfer and applications</i>	Poster 226
Zhang, Shuqing (Tsinghua-Berkeley Shenzhen Institute, China) <i>High temperature half-metallicity in 2D CoGa₂X₄ (X=S, Se, Te)</i>	Poster 228
Zhao, Jijun (Dalian University of Technology, China) <i>Computational design of novel 2D electronic and magnetic materials</i>	Invited (Parallel Workshop) 50
Zheng, Jian (Institute of Chemistry Chinese Academy of Sciences, China) <i>Single Layer TMD Fabrication and Rolling up into Nanoscrolls</i>	Oral 135
Zhi, Wang (Institute of metal research, Chinese academy and sciences, China) <i>Electric-field control of magnetism in a few-layered van der Waals ferromagnetic semiconductor</i>	Oral 136
Zhou, Shuang (School of Materials Science and Engineering, China) <i>Reduced graphene oxide/carbon hybrid aerogels from cellulose and graphene oxide for oil/water separation</i>	Poster 229
Zhu, Min (South China University of Technology, China) <i>Highly reversible conversion reactions in lithiated SnO₂ based thin film anode materials</i>	Invited (Parallel Workshop) 51
Zou, Yongjin (Guilin University of Electronic Technology, China) <i>Functionalized porous carbon for high performance supercapacitors</i>	Poster 230



PLENARY CONTRIBUTIONS

K. S. Novoselov

School of Physics and Astronomy, University of Manchester, M13 9PL, UK

Materials in the Flatland

One of the most important “property” of graphene is that it has opened a floodgate of experiments on many other 2D atomic crystals: BN, NbSe₂, TaS₂, MoS₂, etc. The resulting pool of 2D crystals is huge, and they cover a massive range of properties: from the most insulating to the most conductive, from the strongest to the softest.

If 2D materials provide a large range of different properties, sandwich structures made up of 2, 3, 4 ... different layers of such materials can offer even greater scope. Since these 2D-based heterostructures can be tailored with atomic precision and individual layers of very different character can be combined together, - the properties of these structures can be tuned to study novel physical phenomena or to fit an enormous range of possible applications, with the functionality of heterostructure stacks is “embedded” in their design.

Already now such materials bring to life a number of exciting applications. In my lecture I will review some of them.



KEYNOTE CONTRIBUTIONS

Jun Chen

Key Laboratory of Advanced Energy Materials Chemistry (Ministry of Education),
College of Chemistry, Nankai University, Tianjin 300071, China

chenabc@nankai.edu.cn

Inorganic/organic and carbon composites for Li/Na Batteries

Electrode active materials have played a vital role in the working of rechargeable batteries because they are sources of electric energy with controlled electrode reactions. Either inorganic or organic electrode materials (particularly the positive electrode materials) show electrically insulating nature, which should be composited with carbon for enhancing the charge transport within the electroactive bulk. This report focuses on controlled synthesis of selected inorganic oxides and organic carbonyl salts with carbon composites via reduction-oxidation-transformation crystallization. Meanwhile, the as-synthesized inorganic/organic and carbon composites have demonstrated enhanced electrochemical performance in the application of rechargeable Li/Na (ion/metal) batteries (300~500 Wh/kg, safety and long cycling stability). It is demonstrated that electrode compositions of active inorganic/organic materials – conductive carbon (with various forms such as carbon black, carbon nanotubes and graphene) are necessary for the large-scale application of rechargeable batteries in the areas of electric vehicles and smart grids.

Keywords: Carbon composites, Inorganic oxides, Organic carbonyl salts, Rechargeable Li/Na batteries

Hui-Ming Cheng^{1,2}

¹ Tsinghua-Berkeley Shenzhen Institute, Tsinghua University, Shenzhen 518055, China

² Shenyang National Laboratory for Materials Science, Institute of Metal Research, Chinese Academy of Sciences, Shenyang 110016, China

hmcheng@sz.tsinghua.edu.cn; cheng@imr.ac.cn

Fabrication of Graphene and Other 2D Materials by Exfoliation

Graphene and other 2D materials have unique properties and is expected for various applications. Mass production of 2D materials is a prerequisite for their commercial use, but there are great challenges. Exfoliation of natural graphite and other layer materials are the most efficient method for fabricating 2D materials in powder or suspension form on large scale. However, currently, only graphene and graphene oxide can be produced on a ton scale, while it is difficult to mass produce other 2D materials.

We developed intercalation-expansion-liquid phase exfoliation and electrochemical exfoliation processes to produce graphene materials with high quality in large quantity from natural graphite, which may have wide applications in composites, energy storage, conductive inks, etc. Very recently, we have developed a grinding exfoliation technology that uses micro-particles as intermediaries to distribute an applied compressive force into a multitude of smaller shear friction forces that induce exfoliation of layered materials. This method can be used for mass production of many 2D materials, such as h-BN, black phosphorus, and MoS₂, with very high yield and high efficiency, indicating its universality in preparing 2D materials with a wide range of properties. These 2D materials can be used to fabricate polymer matrix composites and in many other applications.

Van der Waals Integration beyond 2D Materials

Semiconductor heterostructures are central for all modern electronic and optoelectronic devices. Traditional semiconductor heterostructures are typically created through a “chemical integration” approach with covalent bonds, and generally limited to the materials with highly similar lattice symmetry and lattice constants (and thus similar electronic structures) due to lattice/processing compatibility requirement. Materials with substantially different structure or lattice parameters can hardly be epitaxially grown together without generating too much defects that could seriously alter their electronic properties. In contrast, *van der Waals* integration, where pre-formed materials are “physically assembled” together through van der Waals interactions, offers an alternative “low-energy” material integration approach (vs. the more aggressive “chemical integration” strategy). The flexible “physical assembly” approach is not limited to materials that have similar lattice structures or require similar synthetic conditions. It can thus open up vast possibilities for damage-free integration of highly distinct materials beyond the traditional limits posed by lattice matching or process compatibility requirements, as exemplified by the recent blossom in *van der Waals* integration of a broad range of 2D heterostructures. Here I will discuss *van der Waals* integration as a general material integration approach beyond 2D materials for creating diverse heterostructures (e.g., semiconductor/semiconductor, dielectric/semiconductor and metal/semiconductor) with minimum integration-induced damage and interface states, enabling high-performing devices (including high speed transistors, diodes, flexible electronics) difficult to achieve with conventional “chemical integration” approach. A particular highlight is the creation of *van der Waals* metal/semiconductor contacts free of interfacial disorder and Fermi level pinning, thus for the first time enabling experimental validation of the Schottky-Mott rule first proposed in 1930s.

References

- [1] L. Liao, J. Bai, Y. Qu, Y. Lin, Y. Li, Y. Huang and X. Duan. *Proc. Natl. Acad. Sci.* **107**, 6711-6715 (2010) (DOI: 10.1073/pnas.0914117107).
- [2] L. Liao, Y. Lin, M. Bao, R. Cheng, J. Bai, Y. Liu, Y. Qu, K.L. Wang, Y. Huang and X. Duan. *Nature* **467**, 305-308 (2010) (DOI: 10.1038/nature09405).
- [3] R. Cheng, J. Bai, L. Liao, H. Zhou, Y. Chen, L. Liu, Y. Lin, S. Jiang, Y. Huang and X. Duan. *Proc. Natl. Acad. Sci.* **109**, 11588-11592 (2012) (DOI: 10.1073/pnas.1205696109).
- [4] W. J. Yu, Z. Li, H. Zhou, Y. Chen, Y. Wang, Y. Huang and X. Duan. *Nature Mater.* **12**, 246–252 (2013) (DOI: 10.1038/nmat3518).
- [5] R. Cheng, S. Jiang, Y. Chen, Y. Liu, N.O. Weiss, H.-H. Cheng, H. Wu, Y. Huang and X. Duan. *Nature Commun.* **5**, 5143 (2014) (DOI: 10.1038/ncomms6143).
- [6] Y. Liu, N. O. Weiss, X. Duan, H. C. Cheng, Y. Huang and X. Duan. *Nature Rev. Mater.* **1**, 16042 (2016) (DOI: 10.1038/natrevmats.2016.42).
- [7] Y. Liu, J. Guo, E. Zhu, L. Liao, S. Lee, M. Ding, I. Shakir, V. Gambin, Y. Huang and X. Duan. *Nature* **557**, 696-700 (2018) (DOI: 10.1038/s41586-018-0129-8).
- [8] C. Wang, Q. He, U. Halim, Y. Liu, E. Zhu, Z. Lin, H. Xiao, X.D. Duan, Z. Feng, R. Cheng, N. Weiss, G. Ye, Y.C. Huang, H. Wu, H.-C. Cheng, L. Liao, X. Chen, W.A. Goddard, Y. Huang and X. Duan. *Nature* **555**, 231-236 (2018) (DOI: 10.1038/nature25774).
- [9] B. Yao, S.-W. Huang, Y. Liu, A. K. Vinod, C. Choi, M. Hoff, Y. Li, M. Yu, Z. Feng, D.-L. Kwong, Y. Huang, Y. Rao, X. Duan and C. W. Wong. *Nature* **558**, 410-414 (2018) (DOI: 10.1038/s41586-018-0216-x).
- [10] Z. Lin, Y. Liu, U. Halim, M. Ding, Y. Liu, Y. Wang, C. Jia, P. Chen, X. Duan, C. Wang, F. Song, M. Li, C. Wan, Y. Huang and X. Duan. *Nature* (2018) (DOI: 10.1038/s41586-018-0574-4).

Hong-Jun Gao

Institute of Physics & University of Chinese Academy of Sciences, Chinese Academy of Sciences, Beijing
100190, P. R. China

hjgao@iphy.ac.cn

Construction of Novel 2D Atomic/molecular Crystals and Its physical Property

Control over charge and spin states at the single molecule level is crucial not only for a fundamental understanding of charge and spin interactions but also represents a prerequisite for development of molecular electronics and spintronics. While charge manipulation has been demonstrated by gas adsorption and atomic manipulation, the reversible control of a single spin of an atom or a molecule has been challenging. In this lecture, I will present a demonstration about a robust and reversible spin control of single magnetic metal-phthalocyanine molecule via attachment and detachment of a hydrogen atom, with manifestation of switching of Kondo resonance. Low-temperature atomically resolved scanning tunneling microscopy was employed. Using density functional theory calculations, the spin control mechanism was revealed, by which the reduction of spin density is driven by charge redistribution within magnetic 3d orbitals rather than a change of the total number of electrons. This process allows spin manipulation at the single molecule level, even within a close-packed molecular array, without concern of molecular spin exchange interaction. Moreover, I will talk about novel 2D atomic crystals, for example, the templates of PtSe₂ and CuSe recently developed for selective self-assembly of molecules, as well as for the functionalization of the same substrate with two different species. This work opens up a new opportunity for quantum information recording and storage at the ultimate molecular limit.

References

- [1] 1. L. Gao, S.X. Du, H.-J. Gao et al. Phys. Rev. Lett. 99, 106402 (2007).
- [2] 2. L.W. Liu, K. Yang, Y.H. Jiang, S.X. Du, and H.-J. Gao et al. Scientific Report 3, 1210 (2013).
- [3] 3. L.W. Liu, S.X. Du, and H.-J. Gao et al. Phys. Rev. Lett. 99, 106402 (2015).
- [4] 4. L.L. Jiang, H.-J. Gao, and F. Wang et al. Nature Materials 15, 840 (2016).
- [5] 5. X. Lin, and H.-J. Gao et al. Nature Materials 16, 717(2017).

Figures

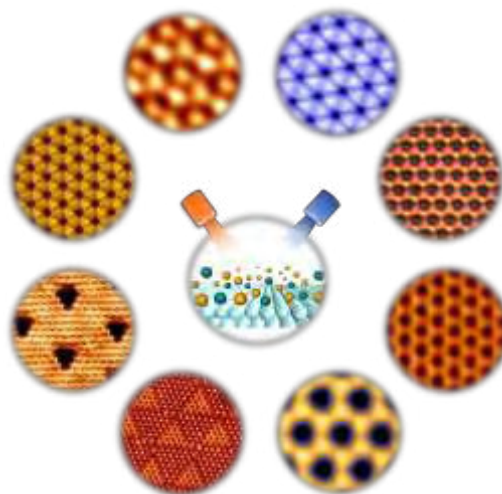


Figure 1: Different two-dimensional atomic crystals, silicene, germanene, PtSe₂, CuSe etc., constructed by molecular beam epitaxy.

Presenting Author: Wanlin Guo

Co-Authors: Zhuhua Zhang, Xuemei Li, Jun Yin

Institute of Nano Science, Nanjing University of Aeronautics and Astronautics.

Nanjing, 210016, China

wlguo@nuaa.edu.cn

Emerging Hydrovoltaic Technology

Water is not only the essence of life, but also the largest energy carrier on earth. Water covers about 70% of the earth's surface, absorbing 70% of the solar energy arriving the earth, and in the atmosphere it can exist in liquid, gaseous and solid states. In human history, through a variety of scientific principles, such as running water driven wheel, steam locomotives, water driven generator as well as the electrokinetic effects, the potential energy or kinetic energy of water can be converted into useful mechanical motion and electrical energy according to the principles of classical mechanics and electromagnetic dynamics. In recent years, we have theoretically and experimentally investigated the fluid-solid-electric coupling functionalization of graphene and other two-dimensional materials. It is found that carbon nanostructures can generate electricity from water energy by direct interaction with water, even by natural water evaporation from cheap carbon nanomaterials, a phenomenon that we termed as hydrovoltaic effect, which potentially extends the technical capability of water energy harvesting and enables creation of self-powered devices. Here, starting by presenting the water energy on the earth, fundamental properties of water and water-solid interfaces, we discussed basic mechanisms of harvesting water energy by carbon nanostructured materials and key aspects pertaining to water-carbon interaction. Experimental advances in generating electricity from water flows, waves, especially natural water-evaporation were then reviewed to show correlations in mechanisms and potential for integration, offering a prospect of harvesting energy from the nature cycle of water on the earth. Main challenges in promoting the energy conversion efficiency and scaling up the output power will be outlined, and finally discuss potential development and applications of the hydrovoltaic technology.

References

- [1] Penman, H. L. Natural Evaporation from Open Water, Bare Soil and Grass. *Proc. R. Soc. Lond. A* **193**, 120-145 (1948).
- [2] Yin, J., Zhang, Z., Li, X., Zhou, J. & Guo, W. Harvesting Energy from Water Flow over Graphene? *Nano Lett.* **12**, 1736-1741 (2012).
- [3] Yin, J., Zhang, Z., Li, X., Yu, J., Zhou, J., Chen, Y. & Guo, W. Waving potential in graphene. *Nat. Commun.* **5**, 3582 (2014).
- [4] Yin, J., Li, X., Yu, J., Zhang, Z., Zhou, J. & Guo, W. Generating electricity by moving a droplet of ionic liquid along graphene. *Nat. Nanotechnol.* **9**, 378 (2014).
- [5] Xue, G., Xu, Y., Ding, T., Li, J., ..., Zhou, J. & Guo, W. Water-evaporation-induced electricity with nanostructured carbon materials. *Nat. Nanotechnol.* **12**, 317 (2017).
- [6] Zhang, Z.H., ... Guo, W. Emerging hydrovoltaic technology, *Nat. Nanotechnol.* Accepted (2018).

Figures

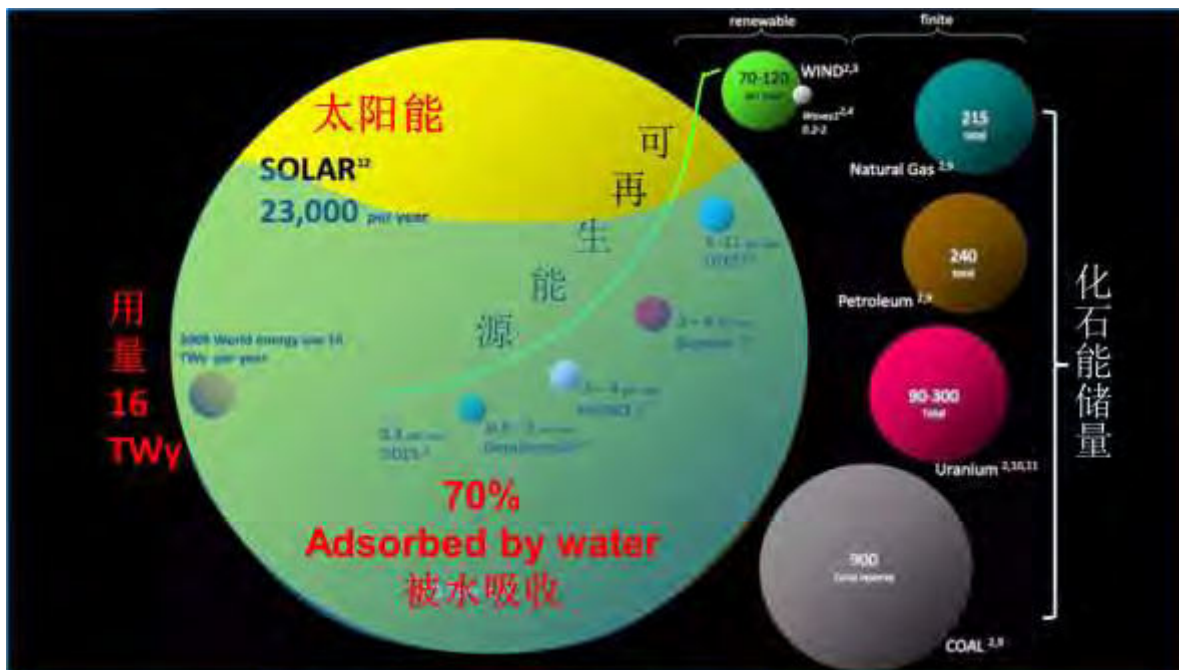


Figure 1: About 70% solar energy arrive the earth is adsorbed by water and half of adsorbed energy consumed by natural evaporation. The world energy consumption, reproducible energy, and the primary energy sources are illustrated in proportional to the solar energy.

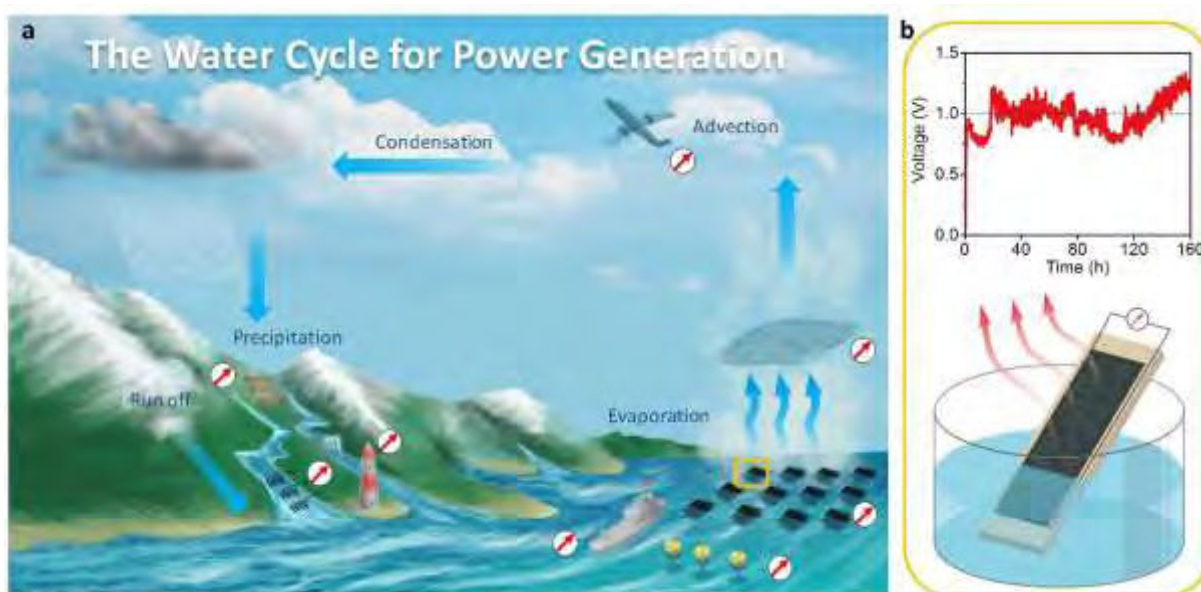


Figure 2: Harvesting the energy from the water cycle of the earth. (a) Devices for the energy harvesting(ref.6). (b) Electricity generation from natural water evaporation in ambient environment by carbon nanomaterials (ref.5).

Lance Li

Corporate Research, Taiwan Semiconductor Manufacturing Company (TSMC)
168 Park Ave 2, Hsinchu Science Park, Hsinchu 300

ljliv@tsmc.com.tw

Continue the transistor scaling with 2D materials: Challenges and Perspective

Internet of things and artificial intelligence demand further transistor performance improvements and device size scaling. In a conventional planar silicon field-effect transistor (FET), the gate controllability becomes weaker when its lateral dimension scales. Hence the transistor body thickness needs to be reduced to ensure efficient electrostatic control from the gate. When the silicon thickness reduces to a few nanometers, the fast mobility decay owing to the scatterings from imperfect silicon surfaces retards the further scaling. New materials with perfect surfaces are therefore needed and 2D semiconducting materials offer a chance to continue the scaling.

Silicon transistor evolution shall be discussed first. Many challenges are ahead for adopting 2D semiconductors as FET channel materials, including (1) selection of 2D materials, (2) reduction of contact resistance, (3) growth of wafer-scale and single-crystalline 2D materials, and (4) Integration of 2D materials to existing microelectronic fabrication processes. In this presentation, we will discuss on these challenges and possible approaches.

Zhongfan Liu

Beijing Graphene Institute (BGI)
Center for Nanochemistry (CNC), Peking University, Beijing 100871, China

zfliu@pku.edu.cn

CVD Graphene: Scalable Growth and Beyond

High quality graphene material itself is the footstone of future graphene industry. Hence scalable synthesis of graphene is extremely important, which will determine how far we can go with this wonderful two-dimensional (2-D) material. In fact, in spite of the great efforts on controlled synthesis since its first isolation in 2004, a huge gap still exists between the ideality and the reality. The ideal graphene material is composed of single crystalline hexagonal honeycomb lattice of sp^2 hybridized carbon atoms while the experimentally available graphene is a polycrystalline film with lots of structural defects and unexpected noncarbon impurities.

Over last ten years, we have made great efforts on the controlled CVD growth of graphene film from lab-scale fundamental studies to scalable instruments. The typical contributions include: roll to roll scalable growth technique and instrument, 4 inch single crystal graphene wafer and instrument, the fast growth technique, the doping growth with high carrier mobility, the CVD growth of superclean graphene, and etc. We have also succeeded in growing high quality graphene films on traditional glasses. The graphene endowed glass with extremely high thermal and electrical conductivities, leading to a new type of super graphene glasses. In a similar way, the graphene film has been deposited onto optical fibers under a high-temperature growth process, creating a graphene-decorated optical fiber. Various promising applications are demonstrated with these super graphene glass and graphene-covered optical fibers. The talk will give a brief overview of our last ten years studies on graphene synthesis and unique applications.

High-Mobility 2D Crystals: Controlled Synthesis and Functional Devices

The unique structure and properties of two-dimensional (2D) crystals have a large impact on fundamental research as well as applications in electronics, photonics, optoelectronics and energy sciences. Here our recent studies on the controlled synthesis of high-mobility 2D crystals such as graphene and layered bismuth oxychalcogenides (BOX, $\text{Bi}_2\text{O}_2\text{X}$: X = S, Se, Te), as well as their functional devices will be discussed. We achieved batch-fabrication of ultraclean graphene films and membranes towards their killer applications. In addition, novel air-stable ultrahigh-mobility semiconducting 2D BOX can be readily synthesized via chemical vapor deposition and fabricated into high-performance field-effect transistors and NIR photodetectors, in which pronounced quantum oscillations were also observed. Our studies suggest that high-quality 2D crystals hold great promise for future applications.

References

- [1] Wu, J.; Yuan, H.; Peng, H.; et al., *Nature Nanotech.* 2017, 12, 530.
- [2] Wu, J.; Tan C.; Peng, H.; et al., *Nano Lett.* 2017, 17, 3021.
- [3] Wu, J.; Liu, Y.; Tan, Z.; Peng, H.; et al., *Adv. Mater.* 2017, 29, 1704060.
- [4] Yin, J.; Hong, H.; Wu, J.; Tan, Z.; Liu, K.; Peng, H.; et al., *Nature Commun.* 2018, accepted.
- [5] Chen, C.; Wang, M.; Wu, J.; Peng, H.; Chen, Y., et al., *Science Adv.* 2018, accepted.
- [6] Zheng, W.; Peng, H.; et al., *Nature Commun.* 2015, 6, 6972.
- [7] Peng, H.; et al., *Nature Chem.* 2012, 4, 281.
- [8] Zhang, J.; Liu, Z.; Peng, H.; *Adv. Mater.*, 2017, 29, 1700639.
- [9] Xu, X.; Feng, D.; Peng, H.; Liu, K.; et al., *Nature Nanotech.* 2016, 11, 930.
- [10] Yin, J.; Wang, H.; Chen, Y.; Peng, H.; Liu, Z.; et al., *Nature Commun.* 2016, 7, 10699.

Wencai Ren

Shenyang National Laboratory for Materials Science, Institute of Metal Research, Chinese Academy of Sciences, Shenyang 11006, China

Contact@E-mail wcren@imr.ac.cn

Graphene Oxide: Green Synthesis and Membrane Applications

Graphene oxide (GO), an important derivative of graphene, has shown a great potential for many applications such as electronics, optoelectronic, energy storage, separation membranes, and composites. In this talk, I will first introduce a green water electrolytic oxidation method for scalable and highly efficient production of GO. Then, the influence of reduction degree on the performance of GO separation membranes will be discussed and a highly stable GO-based separation membrane with superior permeability will be demonstrated. Finally, I will introduce a scalable and efficient method to produce highly aligned and compact GO films. The synthesis of a variety of high-performance functional films by this method will also be demonstrated, including super-strong and highly conductive reduced GO films, reduced GO/single-walled carbon nanotubes hybrid films for flexible supercapacitors with record volumetric energy density, highly anisotropic graphene nanocomposites as well as various 2D nanosheet films and vertical heterostructures.

References

- [1] W.C. Ren, H. M. Cheng, *Nature Nanotechnology*, 9 (2014) 724.
- [2] S.F. Pei, Q.W. Wei, K. Huang, H.M. Cheng, W.C. Ren, *Nature Communications*, 9 (2018) 145.
- [3] Q. Zhang, X.T. Qian, K.H. Thebo, H.M. Cheng, W.C. Ren, *Science Bulletin*, 62 (2018) 788.
- [4] K.H. Thebo, X.T. Qian, Q. Zhang, L. Chen, H.M. Cheng, W.C. Ren, *Nature Communications*, 9 (2018)1486.
- [5] J. Zhong, W. Sun, Q.W. Wei, X.T. Qian, H.M. Cheng, W.C. Ren, *Nature Communications*, Accepted.

Mauricio Terrones

Department of Physics, Department of Chemistry, Department of Materials Science and Engineering and Center for 2-Dimensional & Layered Materials. The Pennsylvania State University, University Park, Pennsylvania 16802, USA & Institute of Carbon Science and Technology, Shinshu University, JAPAN

mut11t@psu.edu

A review of Defects in 2D Metal Dichalcogenides: Doping, Alloys, Interfaces, Vacancies and Their Effects in Catalysis & Optical Emission

In this presentation an overview of different defects in transition metal di-chalcogenides (TMDs) will be presented [1,2]. We will first focus on: 1) defining the dimensionalities and atomic structures of defects (Fig. 1); 2) pathways to generating structural defects during and after synthesis and, 3) the effects of having defects on the physico-chemical properties and applications. We will also emphasize doping and allowing monolayers of MoS₂ and WS₂, and their implications in electronic and thermal transport. We will also describe the catalytic effects of edges, vacancies and local strain observed in Mo_xW_(1-x)S₂ monolayers by correlating the hydrogen evolution reaction (HER) with aberration corrected scanning transmission electron microscopy (AC-HRSTEM) [3]. Our findings demonstrates that it is now possible to use chalcogenide layers for the fabrication of more effective catalytic substrates, however, defect control is required to tailor their performance. By studying photoluminescence spectra, atomic structure imaging, and band structure calculations, we also demonstrate that the most dominating synthetic defect—sulfur monovacancies in TMDs, is responsible for a new low temperature excitonic transition peak in photoluminescence 300 meV away from the neutral exciton emission [4]. We further show that these neutral excitons bind to sulfur mono-vacancies at low temperature, and the recombination of bound excitons provides a unique spectroscopic signature of sulfur mono-vacancies [4]. However, at room temperature, this unique spectroscopic signature completely disappears due to thermal dissociation of bound excitons [4]. Finally, hetero-interfaces in TMDs, will be studied and discussed by AC-HRSTEM and optical emission.

References

- [1] Z. Lin, M. Terrones, et al. "Defect engineering of two-dimensional transition metal dichalcogenides". 2D Materials 3 (2016) 022002.
- [2] R. Lv, M. Terrones, et al. "Two-dimensional transition metal dichalcogenides: Clusters, ribbons, sheets and more". Nano Today 10 (2015) 559-592.
- [3] Y. Lei, M. Terrones, et al. "Low temperature synthesis of heterostructures of transition metal dichalcogenide alloys (W_xMo_{1-x}S₂) and graphene with superior catalytic performance for hydrogen evolution". ACS Nano, 11 (2017), 5103-5112.
- [4] V. Carozo, M. Terrones, et al. "Optical identification of sulfur vacancies: Bound excitons at the edges of monolayer tungsten disulfide", Sci. Adv. 3 (2017), e1602813.

Figures

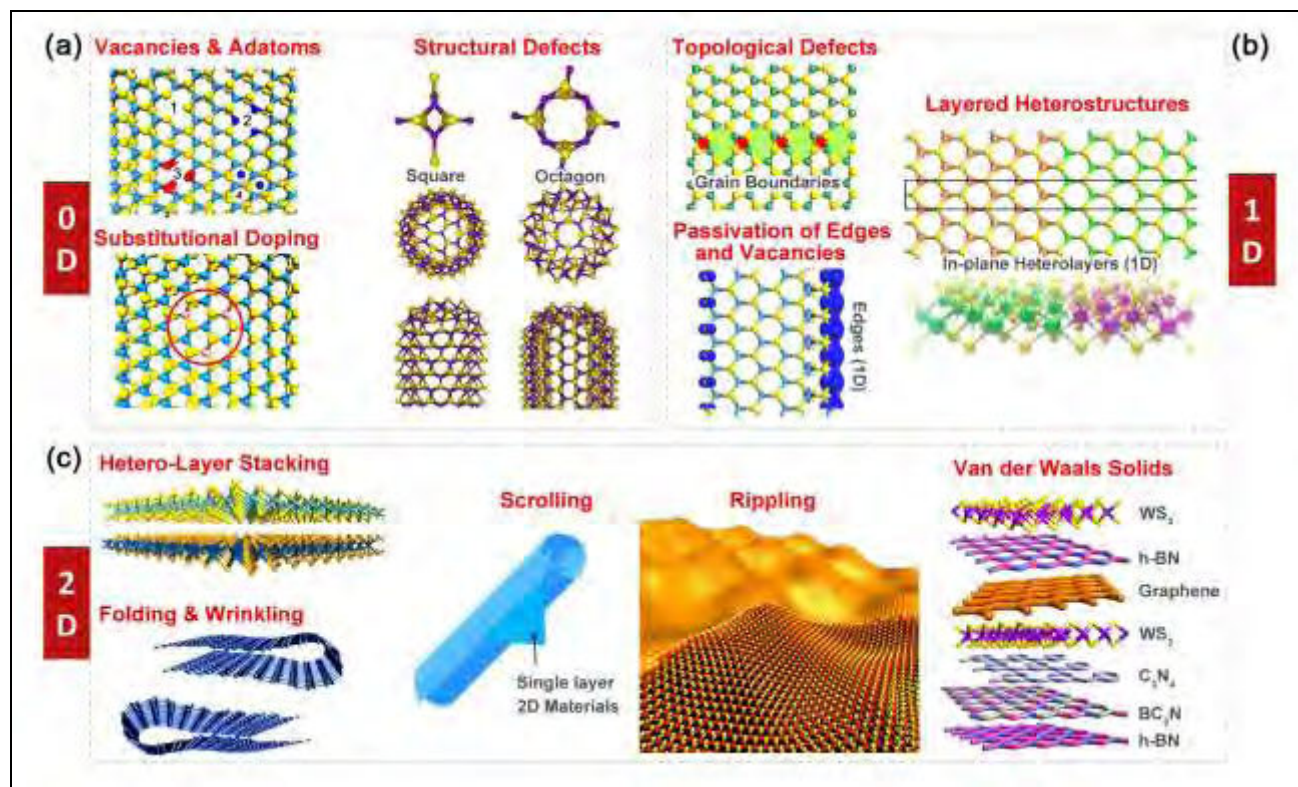


Figure 1: Different categories of defects in transition metal dichalcogenides according to their dimensionality.

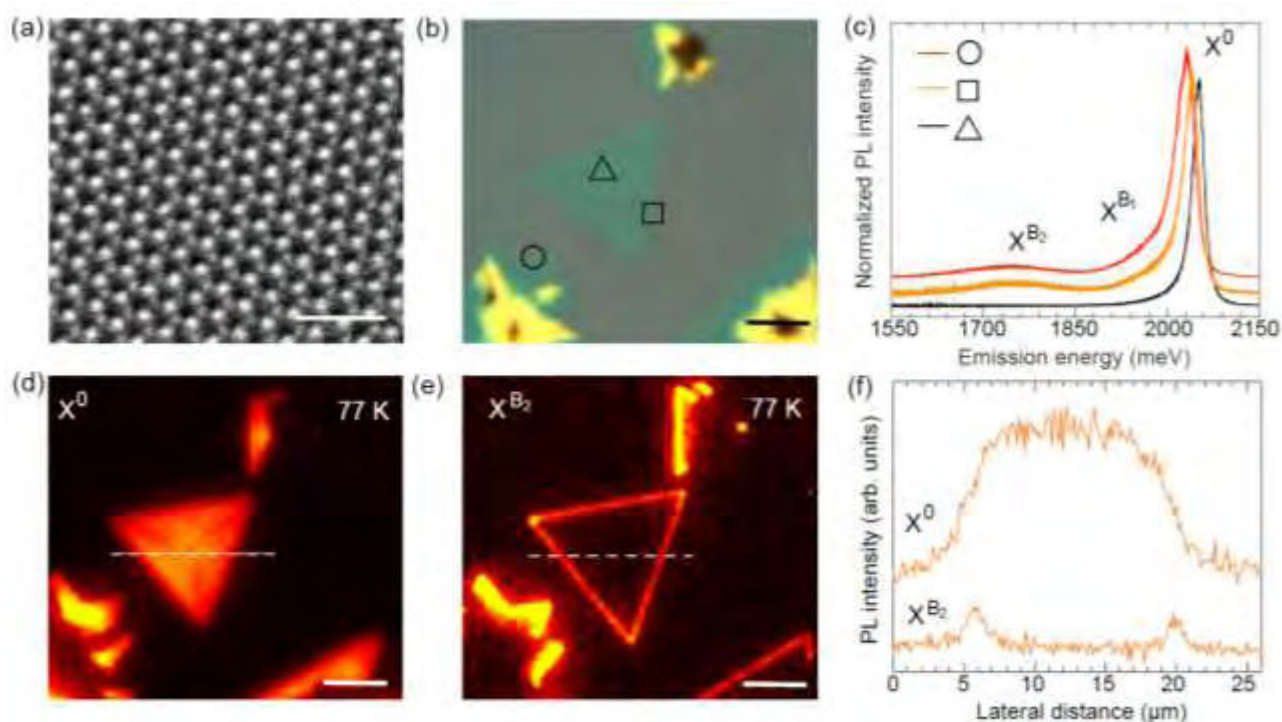


Figure 2: (a) Atomic structure of single layer 1H-WS₂. (b) Optical image of triangular WS₂. (c) PL spectra obtained from the marked regions in (b). Photoluminescence intensity image at 77 K of (d) X⁰ peak centered at 1970 meV and (e) X^B peak centered at 1690 meV. (f) X^B and X^B intensity profile acquired along the dashed line in (d) and (e).

Hua Zhang

Center for Programmable Materials, School of Materials Science and Engineering, Nanyang Technological University, 50 Nanyang Avenue, Singapore 639798, Singapore

HZhang@ntu.edu.sg

Synthesis and Applications of Novel Two-Dimensional Nanomaterials

In this talk, I will summarize the recent research on synthesis, characterization and applications of two-dimensional nanomaterials in my group. I will introduce the synthesis and characterization of novel low-dimensional nanomaterials, such as graphene-based composites including the first-time synthesized hexagonal-close packed (*hcp*) Au nanosheets (AuSSs) on graphene oxide, surface-induced phase transformation of AuSSs from *hcp* to face-centered cubic (*fcc*) structures, the synthesis of ultrathin *fcc* Au@Pt and Au@Pd rhombic nanoplates through the epitaxial growth of Pt and Pd on the *hcp* AuSSs, respectively, the first-time synthesis of 4H hexagonal phase Au nanoribbons (NRBs) and their phase transformation to *fcc* Au NRNs as well as the epitaxial growth of Ag, Pt and Pd on 4H Au NRNs to form the 4H/*fcc* Au@Ag, Au@Pt and Au@Pd core-shell NRNs, and the epitaxial growth of metal and semiconductor nanostructures on solution-processable transition metal dichalcogenide (TMD) nanosheets at ambient conditions, single- or few-layer metal dichalcogenide nanosheets and hybrid nanomaterials, the large-amount, uniform, ultrathin metal sulfide and selenide nanocrystals, other 2D nanomaterials, nanodots prepared from 2D nanomaterials, and self-assembled 2D nanosheets and chiral nanofibers from ultrathin low-dimensional nanomaterials. Then I will demonstrate the applications of these novel nanomaterials in chemical and bio-sensors, solar cells, water splitting, hydrogen evolution reaction, electric devices, memory devices, conductive electrodes, other clean energy, etc.



INVITED CONTRIBUTIONS

Qiaoliang Bao

Department of Materials Science and Engineering, and ARC Centre of Excellence in Future Low-Energy Electronics Technologies (FLEET), Monash University, Clayton, Victoria 3800, Australia

Tel: (+61) 3 9905 4927; E-mail: qiaoliang.bao@monash.edu

Photonic and Optoelectronic Device Applications Based on 2D Materials

Abstract

Our research interests are mainly focused on the light-matter interactions in 2D materials in terms of nonlinear light absorption, light modulation (amplitude, phase and polarisation), wave-guiding and photo-detection. This talk will give an overview of photonic and optoelectronic device applications based on these optical phenomena in 2D materials [1-5]. Firstly, to overcome the limit light absorption in graphene and obtain large nonlinear optical modulation depth, we developed a series of new saturable absorbers based on graphene heterostructures and other 2D materials, including graphene/Bi₂Te₃ [6-8], black phosphorus [9-11] and self-doped plasmonic 2D Cu_{3-x}P nanosheets [12] as well as 2D halide perovskite [13-14]. Depending on their nonlinear optical properties, either high energy Q-switched laser or ultrafast mode-locked pulse generation were demonstrated. Secondly, in order to fabricate improved graphene photodetectors working in different spectral ranges, we integrated graphene with other 2D materials with variant electronic structures, *for example*, graphene/perovskite for visible light detection [15-16], graphene/MoTe₂ and graphene/Cu_{3-x}P for near infrared light detection [17-18], and graphene-Bi₂Te₃ for broadband infrared light detection [19-20]. We show how photo-gating effect plays a significant role to amplify the photocurrent in the photodetectors as well solar cell device [21]. By fine tuning or aligning the electronic structure, we are able to engineer the depletion width in 2D material heterostructures, such as graphene/WS₂, MoS₂/WS₂ and WSe₂/WS₂ heterojunction [22-26], monolayer-bilayer WSe₂ heterojunction [27] and 2D perovskite *p-n* junction [28], so as to achieve higher photo-responsivity and large photo-active area. Lastly, the THz light modulation associated with plasmonic excitation in graphene/Bi₂Te₃, topological insulator Bi₂Te₃, graphene nanoribbon and 3D graphene was also investigated using either spectroscopic or real space imaging techniques [29-32]. We show how the plasmonic coupling happens in two Dirac materials, how high-order plasmonic modes are observed in 3D graphene structure, how multiple plasmonic modes at sub-wavelength are achieved in graphene nanoribbon and how edge chirality controls the plasmonic shift [29-32]. Furthermore, we update our recent progress on the synthesis of 2D non-layered perovskite nanosheets [13-14] and other form of low-dimensional perovskites [33-34] as well as their optoelectronic applications in waveguide [35-36], LED and solar cells [37-39]. In summary, the advances of 2D materials may pave the way for the next generation photonic and optoelectronic device applications.

Keywords: graphene; photonics; optoelectronics, 2D materials.

References

- [1] Bannur Nanjunda Shivananju *et al.*, *Advanced Functional Materials*, 27 (19) (2017)1603918.
- [2] Sathish Chander Dhanabalan *et al.*, *Nanoscale*, 8 (2016) 6410 – 6434.
- [3] Sathish Chander Dhanabalan *et al.*, *Advanced Science*, 4(6) (2017)1600305.
- [4] Joice Sophia Ponraj *et al.*, *Nanotechnology*, 27 (2016) 462001.
- [5] Sathish Chander Dhanabalan *et al.*, *Advanced Optical Materials*, 5(19) (2017)1700257.
- [6] Haoran Mu *et al.*, *ACS Photonics*, 2 (7) (2015) 832–841.
- [7] Fengnian Xia *et al.*, *Journal of Selected Topics in Quantum Electronics*, 23(1) (2016) 8800105.
- [8] Zhiteng Wang *et al.*, *Optical Engineering*, 55(8) (2016) 081314.

- [9] Haoran Mu *et al.*, *Advanced Optical Materials*, 3 (2015)1447-1453.
 [10] Yu Chen *et al.*, *Optics Express*, 23 (10) (2015)12823-12833.
 [11] Yingwei Wang *et al.*, *Applied Physics Letters*, 107 (2015) 091905.
 [12] Zeke Liu *et al.*, *Advanced Materials*, 28 (2016) 3535–3542.
 [13] Jingying Liu *et al.*, *ACS Nano*, 10 (3) (2016) 3536–3542.
 [14] Pengfei Li *et al.*, *ACS Applied Materials and Interfaces*, 9 (14) (2017)12759–12765.
 [15] Yusheng Wang *et al.*, *Advanced Optical Materials*, 3 (2015)1389.
 [16] Pengfei Li *et al.*, *Journal of Physics D: Applied Physics*, 50 (9) (2017) 094002.
 [17] Wenzhi Yu *et al.*, *Small*, 13 (24) (2017) 1700268.
 [18] Tian Sun *et al.*, *Small*, 13 (42) (2017)1701881.
 [19] Hong Qiao *et al.*, *ACS Nano*, 9 (2) (2015)1886–1894.
 [20] Jingchao Song *et al.*, *Advanced Electronic Materials*, 2(5) (2016)1600077.
 [21] Yusheng Wang *et al.*, *Advanced Materials*, 29(18) (2017)1606370.
 [22] Changxi Zheng *et al.*, *ACS Nano*, 11(3) (2017) 2785–2793.
 [23] Yunzhou Xue *et al.*, *ACS Nano*, 10 (2016) 573-580.
 [24] Zhipeng Li *et al.*, *ACS Applied Materials and Interfaces*, 9 (39) (2017) 34204-34212.
 [25] Zai-Quan Xu *et al.*, *ACS Nano*, 9 (6) (2015) 6178–6187.
 [26] Guoyang Cao *et al.*, *Nano Energy*, 30 (2016) 260-266.
 [27] Zai-Quan Xu *et al.*, *2D Materials*, 3 (4) (2016) 041001.
 [28] Qingdong Ou *et al.*, *Advanced Materials*, DOI: 10.1002/adma.201705792 (2018).
 [29] Qingyang Xu *et al.*, *Light: Science & Applications* 6 (2017) e16204.
 [30] Jian Yuan *et al.*, *ACS Photonics*, 4 (12) (2017) 3055–3062.
 [31] Yao Lu *et al.*, *JOSAB*, 33(9) (2016)1842-1846.
 [32] Jingchao Song *et al.*, *ACS Photonics*, 3 (10) (2016)1986–1992.
 [33] Jingying Liu *et al.*, *ACS Nano*, 10 (3) (2016) 3536–3542.
 [34] Yupeng Zhang *et al.*, *Chemical Communications*, 52 (2016)13637-13655.
 [35] Ziyu Wang *et al.*, *Nanoscale*, 8 (2015) 6258-6264.
 [36] Wenxin Mao *et al.*, *Angewandte Chemie*, 56(41) (2017)12486–12491.
 [37] Khan Qasim *et al.*, *Advanced Functional Materials*, 6 (2017)1606874.
 [38] Wei Li *et al.*, *Advanced Energy Materials*, 7 (20) (2017) 1700946.
 [39] Xiongfeng Lin *et al.*, *Nature Communications*, 8 (2017) 613.

Selective covers



Francesco Bonaccorso

Istituto Italiano di Tecnologia, Graphene Labs, Via Morego 30, Genova, Italy
BeDimensional Srl, Via Albisola 121, Genova, Italy

francesco.bonaccorso@iit.it

Large scale production of 2D-materials for energy applications

2D materials are emerging as promising materials¹⁻⁵ to improve the performance of existing devices or enable new ones.¹⁻⁵ A key requirement for the implementation of 2D materials in applications as flexible (opto)electronics and energy is the development of industrial-scale, reliable, inexpensive production processes,² while providing a balance between ease of fabrication and final product quality.

The production of 2D materials by solution processing^{2,6} represents a simple and cost-effective pathway towards the development of 2D materials-based (opto)electronic and energy devices, presenting huge integration flexibility compared to other production methods. Here, I will first present our strategy to produce 2D materials on large scale by wet-jet milling⁷ of their bulk counterpart and then an overview of their applications for flexible and printed (opto)electronic and energy devices.^{3,8,9,10,11,12,13,14}

References

- [1] A. C. Ferrari, F. Bonaccorso, et al., Scientific and technological roadmap for graphene, related two-dimensional crystals, and hybrid systems. *Nanoscale*, 7, 4598-4810 (2015).
- [2] F. Bonaccorso, et al., Production and processing of graphene and 2d crystals. *Materials Today*, 15, 564-589, (2012).
- [3] F. Bonaccorso, et. al., Graphene photonics and optoelectronics, *Nature Photonics* 4, 611-622, (2010).
- [4] F. Bonaccorso, Z. Sun, Solution processing of graphene, topological insulators and other 2d crystals for ultrafast photonics. *Opt. Mater. Express* 4, 63-78 (2014).
- [5] G. Iannaccone, et al., Quantum engineering of transistors based on 2D materials heterostructures. *Nature Nanotech* 13, , 183, (2018).
- [6] F. Bonaccorso, et. al., 2D-crystal-based functional inks. *Adv. Mater.* 28, 6136-6166 (2016).
- [7] A. E. Del Rio Castillo et. al., High-yield production of 2D crystals by wet-jet milling. *Mater. Horiz.* 5, 890 (2018).
- [8] F. Bonaccorso, et. al., Graphene, related two-dimensional crystals, and hybrid systems for energy conversion and storage. *Science*, 347, 1246501 (2015).
- [9] J. Hassoun, et al. An advanced lithium-ion battery based on a graphene anode and a lithium iron phosphate cathode *Nano Lett.* 14, 4901-4906 (2014).
- [10] F. Bonaccorso, et al. Functionalized Graphene as an Electron Cascade Acceptor for Air Processed Organic Ternary Solar Cells. *Adv. Funct. Mater.* 25, 3870-3880 (2015).
- [11] F. Biccari, et al. "Graphene-based electron transport layers in perovskite solar cells: a step-up for an efficient carrier collection" *Adv. Energy Mater.* 7, 1701349 (2017).
- [12] S. Casaluci, et al. Graphene-based large area dye-sensitized solar cell module. *Nanoscale* 8, 5368-5378 (2016).
- [13] A. Capasso, et al. Few-layer MoS₂ flakes as active buffer layer for stable perovskite solar cells. *Adv. Ener. Mater.* 6, 1600920, (2016).
- [14] L. Najafi, et al. MoS₂ Quantum Dot/Graphene Hybrids for Advanced Interface Engineering of CH₃NH₃PbI₃ Perovskite Solar Cell with Efficiency over 20 %. *ACS Nano* 2018 in press

We acknowledge financial support from the European Union's Horizon 2020 Graphene Flagship.

Symmetry Controlled Optical Properties in TMD Nanostructures

MoS₂ and related semiconducting transition metal dichalcogenide (TMD) family is regarded as a gapped graphene systems, the properties of which are controlled by the structural symmetry. The direct band gap at K and -K points that appears in monolayer MoS₂ is regarded as a mass gap opened by the in-plane broken inversion symmetry as compared with the Dirac cone in monolayer graphene. Effects of structural symmetry on TMDs can be investigated not only by thinning TMDs from bilayer to monolayer, but also by wrapping up the 2D sheets to tubular structures. In this presentation, we would like to report a couple of subjects related to the Berry curvature in 2D and 1D TMD nanostructures.

As a first topic, we report the exciton Hall effect [1]. Hall effect is a well known phenomena to determine the carrier density in semiconductors, in which carriers are subjected to the transverse motion due to the Lorentz force by the externally applied magnetic field. We found that exciton in monolayer MoS₂ shows a similar Hall effect without external magnetic fields. This transverse motion of excitons are driven by the Berry curvature of the K and K' bands, which works as an internal magnetic field in the momentum space. From the real space imaging of the exciton diffusion trajectories, we found that the valley diffusion length reached 2 μm at 50 K.

The second subject is related to TMD nanotubes. TMD nanotube was first synthesized a quarter century ago [2], however, the investigation of electronic properties have been started only several years ago [3]. Very recently, our group have discovered superconductivity in individual WS₂ multiwalled nanotubes through ionic gating [4], and photovoltaic properties of p-n junctions formed on the WS₂ nanotubes [5]. In particular we focus on the unique photovoltaic properties of WS₂ multiwalled nanotubes, which clearly reflects its structural symmetry.

References

- [1] M. Onga, Y. J. Zhang, T. Ideue, and Y. Iwasa, *Nat. Mater.* **16** (2017) 1193.
- [2] R. Tenne, L. Margulis, M. Genut, and G. Hodes, *Nature* **360** (1992) 444.
- [3] R. Levi, O. Bitton, G. Leitun, R. Tenne, and E. Joselevich, *Nano Lett.* **13** (2013) 3736.
- [4] F. Qin, W. Shi, T. Ideue, M. Yoshida, A. Zak, R. Tenne, T. Kikitsu, D. Inoue, D. Hashizume and Y. Iwasa, *Nat. Comm.* **8** (2017) 14465.
- [5] Y. J. Zhang, M. Onga, F. Qin, W. Shi, A. Zak, R. Tenne, J. Smet and Y. Iwasa, *2D Materials* **5** (2018) 035002.

Effective theory for the flat band in the twisted bilayer graphene

The recent discovery of the superconductivity and strongly correlated insulating state in the twisted bilayer graphene (TBG) attracts enormous attention [1,2]. TBG is a sandwich of two graphene layers stacked with a rotational orientation [Fig.1(a)]. There a slight rotation gives rise to a long-period moiré pattern, substantially modifying the electronic property. Due to the huge moire pattern, the unit cell of TBG includes more than 10,000 carbon atoms. It is a challenging problem to theoretically describe the many-body physics in such a complex system. Here we develop an effective theory to describe the many-body physics in TBG [3]. By using the realistic band model and with the aid of the maximally localized algorithm, we construct the Wannier orbital, which works as the effective composite “atom” on the moiré pattern. The effective atomic orbital has a characteristic three-peak structure [Fig.1(b)], and it leads to unexpected properties of many body states. For example, we find that an electronic excitation can be viewed as a pair creation of the fractional charges in units of $e/3$, which would possibly give rise to exotic physics. Our effective model dramatically reduces the fundamental complexity of the electronic system in TBG, and it would be greatly beneficial to future theoretical studies. It opens the way to explore the many-body physics in TBG.

References

- [1] Y. Cao, et al, Nature (556), 2018, 43.
- [2] Y. Cao, et al, Nature (556), 2018, 80.
- [3] M. Koshino, N. F. Q. Yuan, T. Koretsune, M. Ochi, K. Kuroki, and L. Fu, arXiv:1805.06819, to be published in Phys. Rev. X

Mario Lanza^{1*}

Yuanyuan Shi^{1,2}, Xianhu Liang¹, Bin Yuan¹, Victoria Chen², Haitong Li², Fei Hui¹,
Zhouchangwan Yu², Fang Yuan^{2,3}, Eric Pop², H.-S. Philip Wong²

¹ Institute of Functional Nano & Soft Materials, Collaborative Innovation Center of Suzhou Nanoscience and Technology, Soochow University, Suzhou, 215123, China

² Department of Electrical Engineering, Stanford University, Stanford, CA 94305, USA

³ Department of Applied Physics, The Hong Kong Polytechnic University, Hong Kong

MLanza@suda.edu.cn

Building the hardware of future artificial intelligence systems: two-dimensional materials based electronic synapses

Artificial intelligence (AI) systems are essential for modern societies because they can produce important progress in fields like economy (e.g. new jobs, powerful analysis tools), health (e.g. take care of elderly and children) and national security (e.g. autonomous machinery). Current AI systems rely on advanced computers to process a massive amount of data and carry out complex operations very fast (<1 ns/operation), and by using sophisticated algorithms they have been able to emulate some functionalities of animal brains (e.g. spiders, mice, cats). However, their computing capability and energy efficiency is still very far from that of human brains. The main reason is that traditional computers have a von Neuman structure, in which the data is computed in the central processing unit and stored in the memory unit. This produces a bottleneck that strongly limits the performance and enhances the power consumption of the entire system. On the contrary, the human brain uses an ultra-dense neural network to process and store the information in parallel. A human brain contains $\sim 10^{12}$ neurons, each of them electrically connected to other ~ 1000 neurons through synapses; therefore, the total number of synapses in a human brain is $\sim 10^{15}$. The synapses are biological membranes that can change their conductivity (when they receive an electrical impulse from a neuron) by segregating Ca^{2+} ions. The learning is achieved by: i) generating new synapses, and ii) modifying the conductivity of the synapses (a.k.a. synaptic weight). Depending on the learning process, the changes on the synaptic weight (produced by neuronal spikes) can last in a timescale from milliseconds to minutes (i.e. short term plasticity, STP) or for minutes or longer (i.e. long term plasticity, LTP).

In order to create more powerful and efficient AI systems, electronic engineers have started to consider the possibility of designing new electronic circuits that act as artificial neural networks. Several different electronic components, including three-terminal devices or field effect transistor based devices, ferroelectric switches and memory devices, have been suggested as the hardware implementation of electronic synapses for artificial neural networks. However, the designs have always resulted very complex and the performance too low (i.e. unable to emulate several simple learning rules that are readily carried out by biological synapses). Recently, two-terminal resistive switching (RS) devices based on a metal/insulator/metal (MIM) nanocells have been suggested as the ideal candidate device for the implementation of electronic synapses because their working principle resembles very well that of a biological synapse [1], i.e. changes in resistivity can be induced by applying electrical impulses to one of the electrodes, which produces the segregation of metallic and/or oxygen ions in the MIM cell. By using a wide range of metallic and insulating materials combinations, the emulation of LTP and its characteristic figures of merit has been readily achieved, including long term potentiation, long term depression, paired-pulse facilitation (PPF), paired-pulse depression (PPD), spike-timing dependent plasticity (STDP) and spike-rate dependent plasticity (SRDP) [2]. However, the traditional materials used in MIM-like electronic synapses have strong difficulties to generate progressive and linear resistivity changes, implement both STP and LTP in the same device, and generate stable and reproducible resistivity changes.

In our group we have solved some of these technological challenges by introducing two-dimensional (2D) materials in the structure of the RS devices. Some attempts of building electronic synapses using 2D materials have been reported [3], but those prototypes used planar configurations, which occupy much more space than vertical MIM cells, cannot be stacked three dimensionally and suffer from a higher device-to-device variability [4] (in fact, the RS industry only uses vertical configurations). Moreover, in most cases the 2D material was synthesized via mechanical exfoliation [5], which is not scalable and therefore unsuitable for building large-area synaptic networks. Here we report the first realization of vertical MIM-like electronic synapses using 2D materials produced by chemical vapor deposition (CVD), which is a scalable method [6]. By using multilayer hexagonal boron nitride (h-BN) sheets as RS medium, we have been able to implement both volatile and non-volatile RS simultaneously, which allows emulating several STP and LTP synaptic behaviors, including PPF, PPD, relaxation and STDP. The working regime can be selected by tuning the amplitude, duration and interval of the electrical stimuli. While until now all previous synaptic studies reported slow (0.1-100 s) erratic relaxation process during 0.1-100 s, here we show a fast ($\sim 200 \mu\text{s}$) and stable relaxation during more than 500 cycles, with a very low variability. The power consumption of the synapses in volatile regime is 0.1 fW in standby and 600 pW per transition, and we find that the pulse voltage plays a more important role in the potentiation of the synapses than the pulse time/interval. These performances are enabled by a novel switching mechanism that combines characteristics from CBRAM and ReRAM. The volatile and non-volatile nature of the RS has been confirmed at the nanoscale via CAFM, demonstrating excellent potential for scalability. This work represents an important advancement for the development of electronic synapses in terms of performance and, as only scalable processes have been used, these methods may be employed to build 2D materials synaptic networks.

References

- [1] P. A. Merolla, **Science** 345, 668-673 (2014).
- [2] M. A. Zidan et al. **Nat. Electron.** 1, 22-29 (2018).
- [3] H. Tian et al. **Nano Lett.** 15, 8013-8019 (2015).
- [4] F. Hui et al. **Adv. Electron. Mater.** 3, 1600195 (2017).
- [5] M. Wang et al. **Nat. Electron.** 1, 130-136 (2018).
- [6] Y. Shi et al. **Nat. Electron.** 1, 458-465 (2018)

Figures

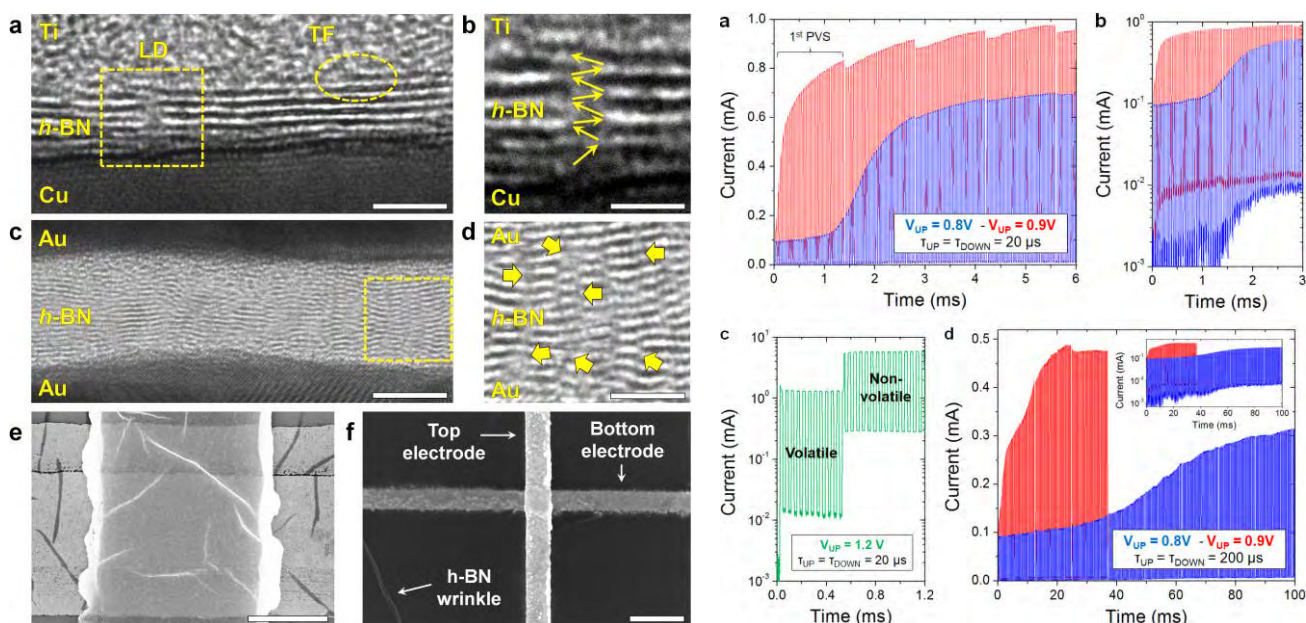


Figure 1: (Left) (a-d) Cross-sectional TEM images of the metal/h-BN/metal electronic synapses. (e-d) Top-view SEM images of the metal/h-BN/metal synapses with cross-point structure. (Right) (a-d) Potentiation of a h-BN based synapse by applying pulsed voltage stresses with different height, duration and interval. Reprinted with permission from Ref. [6]

Electronic Transport and Device Applications of 2D Materials

Two-dimensional (2D) materials have emerged as promising candidates for post-Moore electronics due to their unique electronic properties and atomically thin geometry. I will start with our studies on atomically thin semiconducting material rhenium disulfide (ReS_2) and type-II Weyl semimetal (WSM) tungsten ditelluride (WTe_2). We observed interesting in-plane anisotropic transport and mechanical properties of ReS_2 , together with its potential electronic and optoelectronic applications.[1] In thin tungsten ditelluride (WTe_2) flakes, we observed notable angle-sensitive negative longitudinal magnetoresistance (MR) and strong planar orientation dependence which reveal important transport signatures of chiral anomaly and type-II Weyl fermions. By applying a gate voltage, we further demonstrated that the Fermi energy can be tuned through the Weyl points via the electric field effect; this is the first report of controlling the unique transport properties *in situ* in a WSM system.[2]

By stacking layers of different 2D materials together, van der Waals (vdW) heterostructures offer unprecedented opportunities to create materials with atomic-level precision by design, and combine superior properties of each component. In the second part of my talk, I will show that robust memristors with good thermal stability, which is lacking in traditional memristors, can be created from a vdW heterostructure composed of graphene/ $\text{MoS}_{2-x}\text{O}_x$ /graphene.[3] Our latest results on high-performance mid-infrared photodetectors based on atomically thin vdW heterostructures made of black arsenic phosphorus and transition metal dichalcogenides will also be presented.[4]

References

- [1] Liu, et al., Nat. Comm. 6, 6991 (2015); Adv. Func. Mater. 26, 1938 (2016); Wang, et al., ACS Nano (2018).
- [2] Wang, et al., Nat. Comm. 7, 13142 (2016); Hao, et al., Adv. Func. Mater. (2018).
- [3] Wang, et al., Nat. Electronics 1, 130 (2018).
- [4] Long, et al., Science Adv. 3, e1700589 (2017); Nano Lett. 16, 2254 (2016).

Effects of interlayer interactions on physics of layered crystals

In this talk, I will review my recent studies on critical effects of interlayer interaction in determining electronic, structural and magnetic properties of layered two-dimensional crystals. It is shown that the structural stabilities, electronic energy bands as well as topological properties are critically dependent of nature of interlayer interactions between adjacent two-dimensional crystals. Examples includes twisted bilayer graphene, 1T'-type transition metal dichalcogenides and two-dimensional magnetic crystals.

Interfacing graphene with nanoparticles for energy and gas storage as well as sensors

Graphene, a very attractive two-dimensional carbon nanomaterial with superior electrical conductivity, excellent mechanical flexibility, and high thermal and chemical stability, has been widely used in many fields [1]. The extraordinary properties of graphene including high (ballistic) charge mobility and the potential for n- or p-doping can provide high conductivity materials depending on their structural quality. Multiple applications including as materials for gas and energy storage could be within reach if irreversible aggregation, or re-stacking, of graphene nanosheets could be inhibited. Furthermore, its chemical inertness makes it difficult to attach gas molecules on the surface of graphene directly and interfacing the graphene surface with other nanoparticles is a possible solution [2,3]. In our recent work, graphene oxide was enlisted as a substrate to induce nanosized MOFs. By growth nanosized Cu-BTC on the surface of graphene, the GO/Cu-BTC composite shows improved hydrogen storage and CO₂ capture performance. The composite material exhibited about a 30% increase in CO₂ and H₂ storage capacity (from 6.39 mmol g⁻¹ of Cu-BTC to 8.26 mmol g⁻¹ of CG-9 at 273 K and 1 atm for CO₂; from 2.81 wt% of Cu-BTC to 3.58 wt% of CG-9 at 77 K and 42 atm for H₂) [4]. By doping graphene with polyaniline and Pd nanoparticles, The resulting Pd-PANI-rGO nanocomposite was highly sensitive and selective to hydrogen gas, with fast response time in air at room temperature. The significantly enhanced sensitivity resulted from the faster spill-over effect, dissociation of hydrogen molecules on Pd, and the high surface area of the PANI-GO composite [5]. By doping graphene oxide with flower-like cobalt-nickel-tungsten-boron oxides, The Co-Ni-W-B-O/rGO composites resembled three-dimensional flowers with high surface area; they also exhibited superior electrochemical performance when compared to most previously reported electrodes based on nickel-cobalt oxides. Furthermore, the Co-Ni-W-B-O/rGO composite prepared in an ethanol solution showed much higher electrochemical performance than that the composite prepared in water. The Co-Ni-W-B-O/rGO electrode showed an ultrahigh specific capacitance of 1189.1 F g⁻¹ at 1 A g⁻¹ and exhibited an high energy density of 49.9 Wh kg⁻¹ along with remarkable cycle stability, which is promising for application in energy storage devices [6]. By spontaneous polymerization of pyrrole and formation of PB nanocubes on GO, The resultant supercapacitor based on PPy-PB-GO exhibits both double-layer and pseudocapacitance. The hybrid electrode showed a maximum specific capacitance of 525.4 F g⁻¹ at a current density of 5 A g⁻¹. It also exhibited excellent cyclic stability of 96% retention for up to 2000 cycles [7].

References

- [1] M.H. Yu, Y.C. Huang, C. Li, Y.X. Zeng, W. Wang, Y. Li, P.P. Fang, X.H. Lu, Y.X. Tong, *Adv. Funct. Mater.*, 25(2015)324–330.
- [2] S.H. Cho, J.S. Lee, J. Jun, S.G. Kim, J. Jang, *Nanoscale*, 6(2014)15181–15195.
- [3] H. Furukawa and O. M. Yaghi, *J. Am. Chem. Soc.*, 131(2009)8875–8883.
- [4] S. Liu, L. Sun, F. Xu, J. Zhang, C. Jiao, F. Li, Z. Li, S. Wang, Z. Wang, X. Jiang, H. Zhou, L. Yang, C. Schick, *Energy Environ. Sci.*, 6(2013)818–823.
- [5] Y. Zou, Q. Wang, C. Xiang, C. Tang, H. Chu, S. Qiu, E. Yan, F. Xu, L. Sun, *Int. J. Hydrogen Energy*, 41(2016)5396–5404.
- [6] C. Xiang, Q. Wang, Y. Zou, P. Huang, H. Chu, S. Qiu, F. Xu, L. Sun, *J. Mater. Chem. A*, 5(2017)9907–9916.
- [7] Y. Zou, Q. Wang, C. Xiang, Z. She, H. Chu, S. Qiu, F. Xu, S. Liu, C. Tang, L. Sun, *Electrochimica Acta* 188 (2016) 126–134.

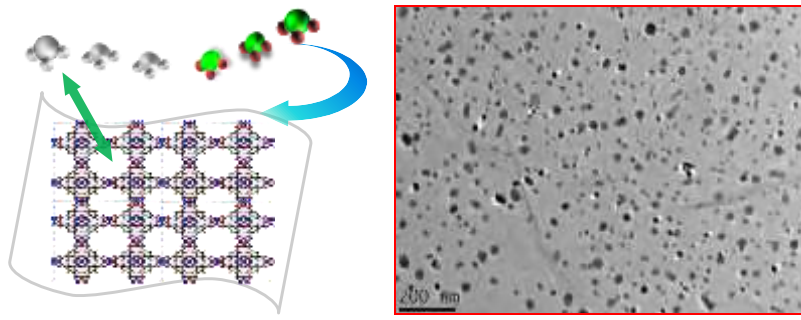


Figure 1: Graphene oxide induced nanosized Cu-BTC for gas adsorption.

Optoelectronic Devices Based on Graphene-Like Materials and their Related Heterostructures

Abstract

Graphene is a wonderful material thanks to its peculiar electronic, optical, thermal, and mechanical properties. In the past decade or so, advances in graphene-based devices have been evidently demonstrated, which shed light on the potential applications from visible to terahertz (THz) light waves. In order to enhance the performance of conventional graphene-based optoelectronic devices confined by the limited length of light-matter interaction on a nanometer scale, we develop the novel design and fabrication of high-performance graphene-based optoelectronic devices (particularly, photodetectors (from visible to the near-infrared regions) and THz modulators), by utilizing the extraordinary electronic and optical properties of graphene and its intrinsic transition characteristics. Similar strategies are applicable to other two-dimensional transition metal dichalcogenides (TMDs) and the related heterostructures.

References

- [1] Z. F. Chen, J. B. Xu, et al, accepted.
- [2] Z. F. Chen, X. M. Li, J. Q. Wang, L. Tao, M. Z. Long, S. J. Liang, L. K. Ang, C. Shu, H. K. Tsang, J. B. Xu, ACS Nano 11, 430-437 (2017)
- [3] L. Tao, Z. F. Chen, X. M. Li, K. Y. Yan, J. B. Xu, npj 2D Materials and Applications 1, 19 (2017)
- [4] L. Ye, P. Wang, et al., Nano Energy 37, 53 (2017)
- [5] X. D. Liu, Z. F. Chen, E. P. J. Parrott, B. S. Y. Ung, J. B. Xu, E. Pickwell-MacPherson, Advanced Optical Materials 5, UNSP 1600697 (2017)
- [6] Z. F. Chen, Z. Z. Cheng, J. Q. Wang, X. Wan, C. Shu, H. K. Tsang, H. P. Ho, J. B. Xu, Advanced Optical Materials 3, 1207-1214 (2015)

Figures

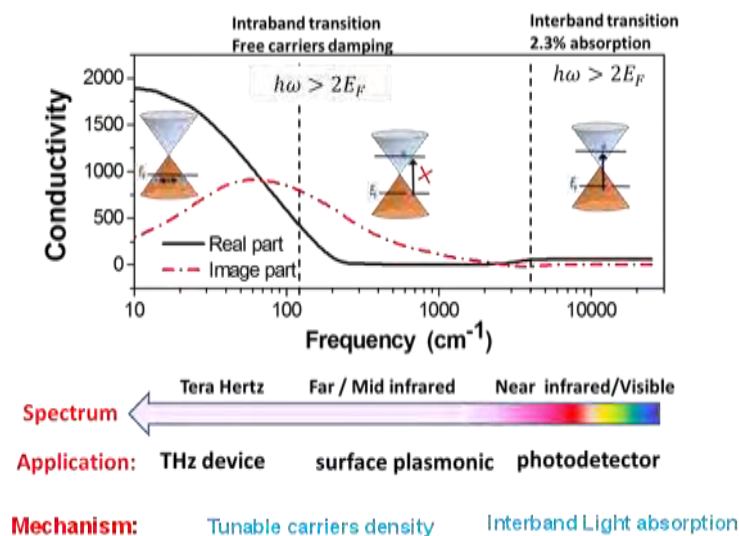


Figure 1: The conductivity of graphene in a broad spectral range.

Graphene-Supported Complex Hydrides as Advanced Hydrogen Storage Materials

Complex hydrides are a fascinating class of materials that can be used for several energy applications and devices, particularly as hydrogen storage materials owing to their high gravimetric and volumetric storage densities of hydrogen.^[1] Nevertheless, complex hydrides still suffer from sluggish kinetics and poor reversibility owing to the grain growth, phase separation, and particle agglomeration during hydrogen sorption cycles at elevated temperature.^[2] Downsizing materials to the nanometer scale is an effective way to relieve the inherent limitations to the diffusion of elements in the solid state and facilitate destabilization induced by excess surface energy.^[3] Graphene with ultrahigh surface area could serve as a structural support to promote the synthesis of the nanostructured materials, but also physically prevent agglomeration and phase segregation during the hydrogen absorption and desorption cycles.^[4,5] Therefore, space-confinement via graphene has been adopted as an effective tool to modify the hydrogen storage performance of complex hydrides. In this talk, I will first discuss the main ideas in this field, and then present some selected examples and our recent results of how the performance of complex hydrides can be improved through graphene.

References

- [1] Orimo S. I.; Nakamori Y.; Eliseo J. R.; Zuttel A.; Jensen C. M., *Chem. Rev.*, 2007, 107, 4111.
- [2] Niaz S.; Manzoor T.; Pandith A. H., *Renew. Sust. Energ. Rev.*, 2015, 50, 457.
- [3] Yu X. B.; Tang Z. W.; Sun D. L.; Ouyang L. Z.; Zhu M., *Prog. Mater. Sci.*, 2017, 8, 1.
- [4] Xia G. L.; Tan Y. B.; Chen X. W.; Sun D. L.; Guo Z. P.; Liu H. K.; Ouyang L. Z.; Zhu M.; Yu X. B., *Adv. Mater.*, 2015, 27, 5981.
- [5] Zhang H. Y.; Xia G. L.; Zhang J.; Sun D. L.; Guo Z. P.; Yu X. B., *Adv. Energy Mater.*, 2018, 8, 1702975.

Figures

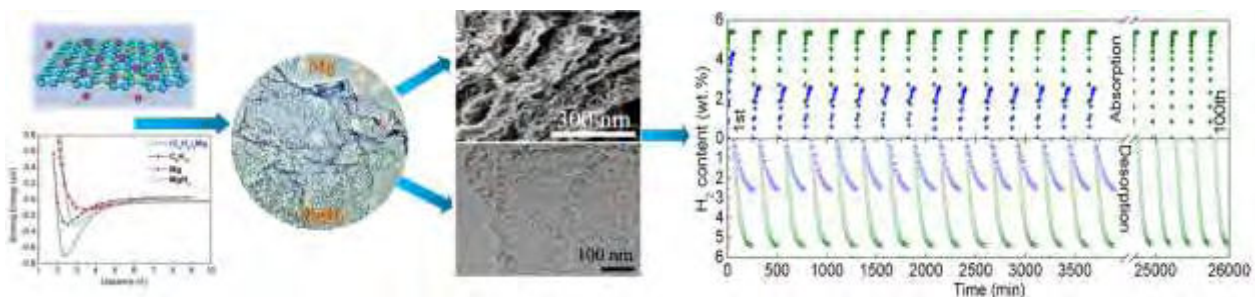


Figure 1: Self-assembly of metal hydrides nanoparticles on graphene and the induced excellent reversibility.



INVITED CONTRIBUTIONS

(PARALLEL WORKSHOPS)

Slaven Garaj

Department of Physics, Department of Biomedical Engineering and Centre for Advanced 2D Materials
National University of Singapore
Singapore

slaven@nus.edu.sg

Nanofluidics with graphene and graphene-oxide membranes

Water and ions show curious behavior when constricted by two-dimensional materials at the scales of few nanometers or less – the phenomena include the edge-enhanced ionic current in graphene nanopores [1,2], anomalous ionic flow in nanotubes, and frictionless water transport in graphene [3] and graphene-oxide (GO) nanochannels [4, 5]. Intimate understanding of such behavior would raise prospects in many applications, including filtration membranes, single-biomolecule analysis, supercapacitors, etc.

In this talk, I will present a systematic experimental investigation of the ionic flow in nanopores and nanochannels, as well as microscopic GO membranes. We investigated ionic flow in atomically-smooth graphene channels with height ranging from 0.7 – 3 nm and in chemically controllable GO channels. We identified several mechanisms that control ionic mobility in different systems: (a) mobility enhancement in smooth channels; (b) compression of the ionic hydration shell; (c) ionic electrostatic repulsion due to the membrane surface charge; and (d) chemically-specific interactions.

Armed with the insight into the physical mechanism governing the ionic flow, we are able to rationally engineer new membranes of desirable properties. With such tunability, we demonstrate a range of scaled-up membranes for desalination, electrodialysis and pervaporation, with properties matching or exceeding those of commercial membranes.

References

- [1] Garaj, S. *et al.* Graphene as a subnanometre trans-electrode membrane. *Nature* **467**, 190–193 (2010).
- [2] Garaj, S., Liu, S., Golovchenko, J. A. & Branton, D. Molecule-hugging graphene nanopores. *Proc Natl Acad Sci USA* **110**, 12192–12196 (2013).
- [3] Radha, B. *et al.* Molecular transport through capillaries made with atomic-scale precision. *Nature* **538**, 222–225 (2016).
- [4] Nair, R. R., Wu, H. A., Jayaram, P. N., Grigorieva, I. V. & Geim, A. K. Unimpeded Permeation of Water Through Helium-Leak-Tight Graphene-Based Membranes. *Science* **335**, 442–444 (2012).
- [5] Hong, S. *et al.* Scalable Graphene-Based Membranes for Ionic Sieving with Ultrahigh Charge Selectivity. *Nano Lett.* **17**, 728–732 (2017).

Figures

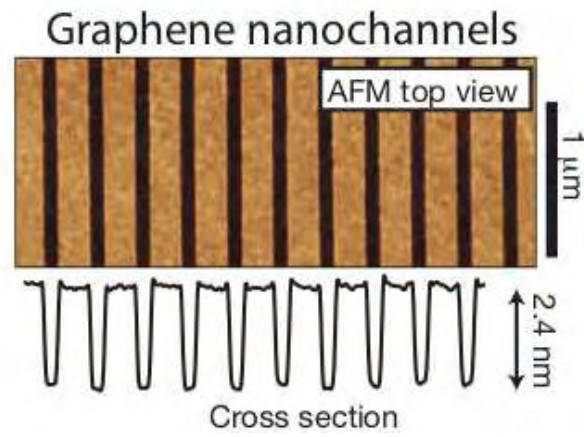


Figure 1: Atomic force microscopy of ultra-clean, atomically-smooth graphene nanochannels with height ranging from 0.7 – 3 nm, and micrometers long.

Jin-Song Hu

Ding-Jiang Xue, Shun-Chang Liu, Yu-Si Yang

Institute of Chemistry, Chinese Academy of Science, Beijing 100190, China

Contact: hujs@iccas.ac.cn

2D Germanium Selenide for Photovoltaics and Optoelectronics

Abstract: 2D germanium selenide including GeSe and GeSe₂ has attracted significant attention recently due to its intriguing in-plane anisotropic properties originated from the low-symmetry crystal structure, as well as earth-abundant and low-toxic constituents.^[1-3] As for GeSe, we reported the first GeSe thin-film solar cell with an efficiency of 1.48%,^[1] and systematically investigated the basic physical properties of GeSe films including refractive index, dielectric constant, carrier mobility, lifetime, and diffusion length,^[2] providing a solid foundation for the further development of GeSe solar cells. With regard to GeSe₂, we studied the in-plane anisotropic structural, vibrational, electrical, and optical properties from theory to experiment. Photodetectors based on GeSe₂ exhibit a highly polarization-sensitive photoresponse in short wave region due to the optical absorption anisotropy induced by in-plane anisotropy in crystal structure.^[3]

References

- [1] Xue, D.-J.; Liu, S.-C.; Dai, C.-M.; Chen, S.; He, C.; Zhao, L.; Hu, J.-S.; Wan, L.-J., *J. Am. Chem. Soc.* **2017**, *139* (2), 958-965.
- [2] Liu, S.-C.; Mi, Y.; Xue, D.-J.; Chen, Y.-X.; He, C.; Liu, X.; Hu, J.-S.; Wan, L.-J., *Adv. Electron. Mater.* **2017**, *3* (11), 1700141.
- [3] Yang, Y.; Liu, S.-C.; Yang, W.; Li, Z.; Wang, Y.; Wang, X.; Zhang, S.; Zhang, Y.; Long, M.; Zhang, G.; Xue, D.-J.; Hu, J.-S.; Wan, L.-J., *J. Am. Chem. Soc.* **2018**, *140* (11), 4150-4156.

Figures

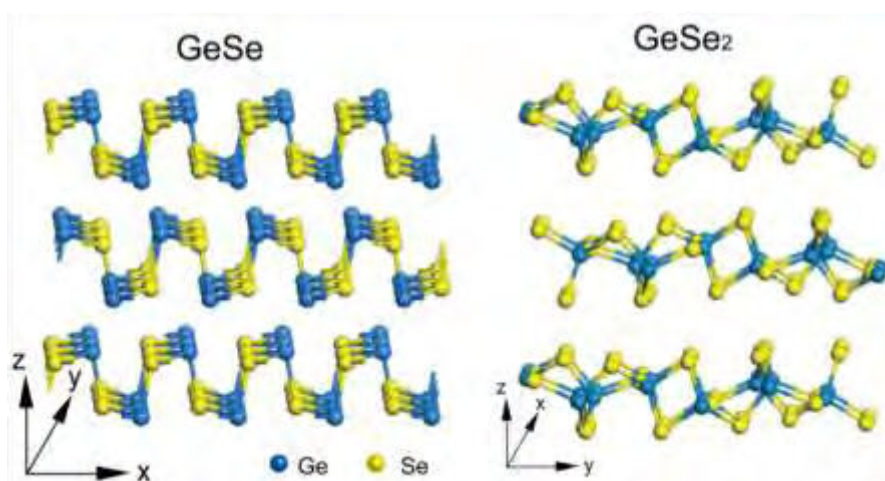


Figure 1: 2D crystallographic structure of GeSe and GeSe₂

Two-Dimensional Inorganic/Organic Hetero Interface for Field-Effect Transistor Applications

Two-dimensional (2D) materials, such as layered transition metal dichalcogenides (TMDC) semiconductors, are emerging research areas that involve multiple fields ranging from fundamental scientific interests to practical device applications [1]. Primary concerns of 2D materials to device applications is that conventional semiconductor process (e. g. high temperature anneal, ion implantation and thermal diffusion) is not applicable since these fabrication steps disrupt and spoil the 2D crystal structure, resulting in the degradation of characteristics or failure of devices [2]. In this context, molecular chemistry approaches to 2D TMDC have considerable attention because of their low temperature, low energy process [2]. In addition, amazingly rich chemistry and structure of organic molecules enables not only the tailoring of the properties of TMDC but also the fabricating of the functional devices [2].

This study describes our experimental results regarding the hybrid systems based on TMDC and organic self-assembled monolayer (SAM) for functional device applications [3]. The SAM is 2D organic molecular monolayer that spontaneously organizes at specific surface [4]. The SAM can tailor surface and interfacial properties including adhesive, hydrophilic, and hydrophobic properties [5]. A recent study has also demonstrated that a SAM can be utilized as ultrathin gate dielectric for field-effect transistors (FET) [6]. A phosphonic acid-based SAM can provide a low gate leakage current owing to its close-packed structure even when the physical thickness is 2.1 nm [6]. In this study, SAM-based gate dielectric with n-octadecylphosphonic acid (ODPA) is applied to the fabrication of molybdenum disulfide (MoS_2) FET [3]. Of particular interest in this study is how the MoS_2 /SAM structure affects the interfacial properties and electrical characteristics. The interfacial properties of semiconductor/dielectric structure fundamentally determines the device characteristics of FET. Since the terminal functional group of ODPA consists of a methyl group ($-\text{CH}_3$), an inert surface that has electrical and chemical stability is accomplished. Consequently, superior interfacial properties can be anticipated for the MoS_2 /SAM structure.

The fabrication process and device structure are summarized in Fig. 1. An Al gate electrode and Au source/drain contacts were prepared on a SiO_2/Si substrate by mask contact photolithography. The substrate was exposed to oxygen plasma to form AlO_x and a hydroxyl groups on the surface of Al. Then, the substrate was immersed in 2-propanol containing 5 mM ODPA for 1 h at room temperature. Mechanically exfoliated MoS_2 flakes were deterministically transferred to the substrate using a poly(dimethylsiloxane) (PDMS) elastomer and micromanipulator. Subthreshold slope (SS) of 69 mV/dec and no hysteresis were obtained from the I_d - V_g characteristics, indicating a low defect density at the MoS_2 /SAM interface (Fig. 2). TEM image highlights the flat and abrupt interface of the MoS_2 /SAM structure (Fig. 2). The fabricated FET device has a peak mobility of 13 cm^2/Vs from I_d - V_g and C-V characteristics (Fig. 3). This studies open up interesting directions for research on the functional devices based on 2D materials.

References

- [1] Q. H. Wang et al., *Nat. Nanotechnol.* 7, 699 (2012).
- [2] S. Bertolazzi et al., *Chem. Soc. Rev.* 47, 6845 (2018).
- [3] T. Kawanago et al., *Appl. Phys. Lett.* 108, 041605 (2016).
- [4] J. C. Love et al., *Chem. Rev.* 105, 1103 (2005).
- [5] J. E. Greene, *Appl. Phys. Rev.* 2, 011101 (2015).
- [6] H. Klauk et al., *Nature* 445, 745 (2007).

Figures

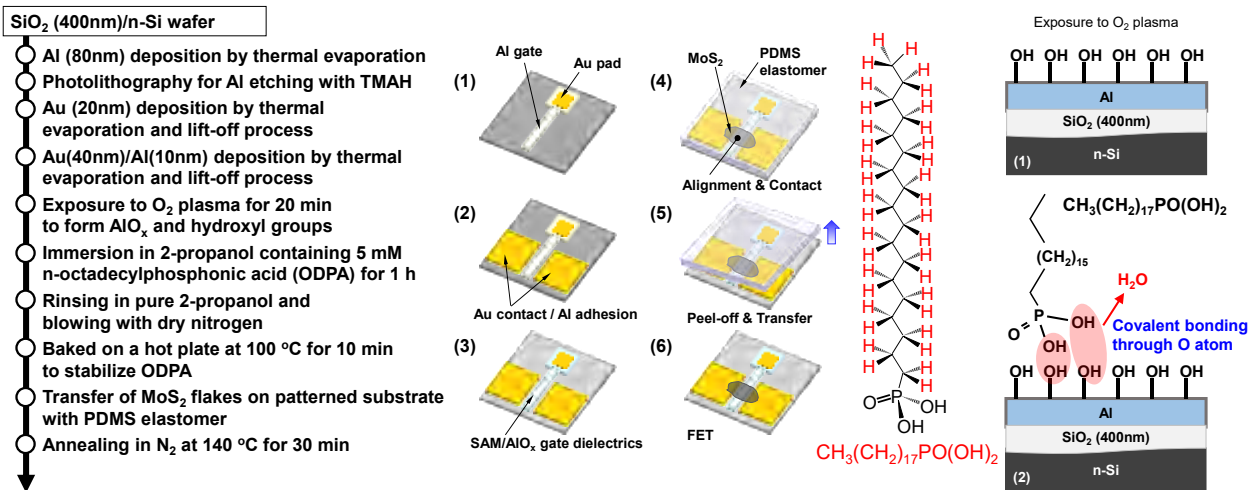


Figure 1: Fabrication process and device structure. Chemical structure of ODPA are also shown

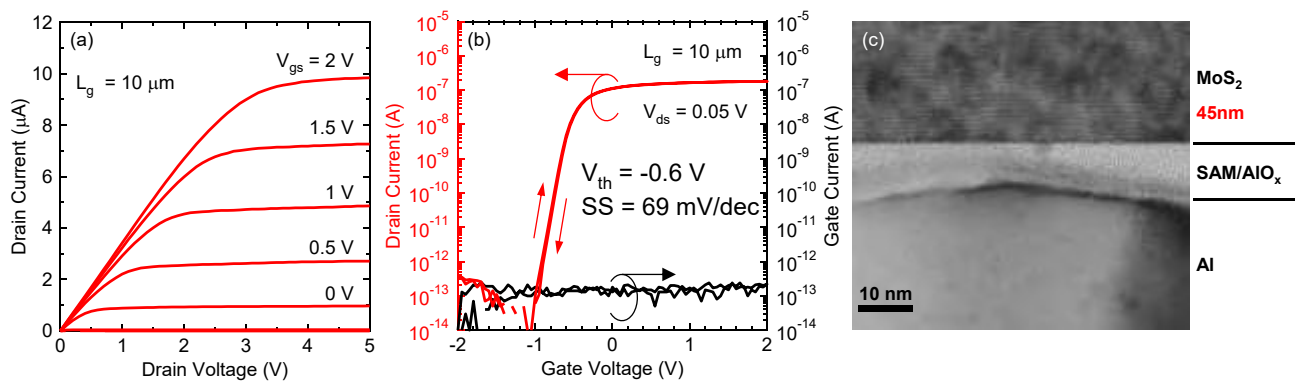


Figure 2: (a) I_d - V_d , (b) I_d - V_g characteristics and (c) TEM image of MoS₂ FET with SAM-based gate dielectric

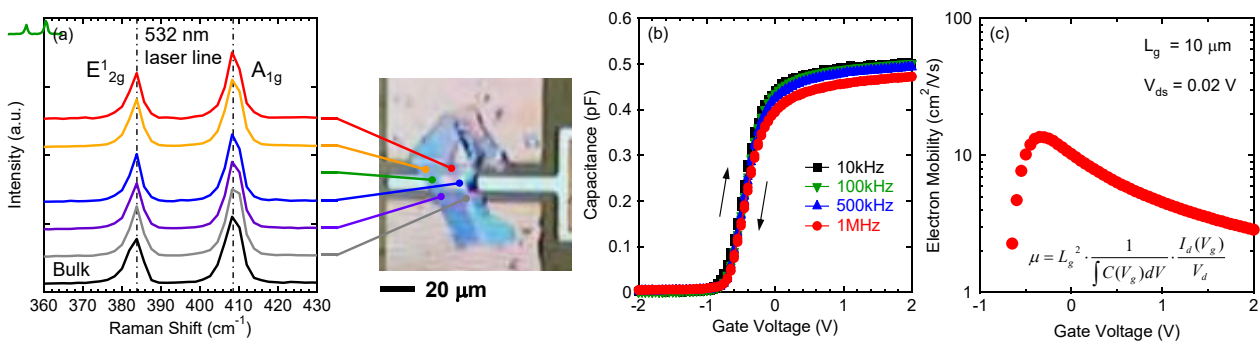


Figure 3: (a) Raman spectra, (b) C-V characteristics and (c) Mobility of MoS₂ FET with SAM-based gate dielectric

Keun Su Kim

Yonsei University, 50 Yonsei-ro, Seodaemun-gu, Seoul, Korea

keunsukim@yonsei.ac.kr

Bandgap engineering of two-dimensional semiconductors

Layered two-dimensional (2D) semiconductors, such as black phosphorus and transition-metal dichalcogenides, have emerged as a class of materials that may impact our future electronics technologies. Controlling their band structure widely with external parameters is important not only for application in various electronic and optical devices, but also to systematically study a novel quantum state of matter. In this talk, I will introduce our recent angle-resolved photoemission spectroscopy (ARPES) studies on a novel mechanism to modulate the band gap of black phosphorus [1] and $2H$ transition-metal dichalcogenides [2]. The widely tunable band gap of black phosphorus could be exploited to create a topologically nontrivial state with a pair of Dirac fermions protected by its unique crystalline symmetry [3]. Electron doping to the surface of transition-metal dichalcogenides can also be used to explore a novel composite particle arising from intervalley electron-phonon coupling [4].

References

- [1] J. Kim *et al.*, *Science*, 349 (2015) 723.
- [2] M. Kang *et al.*, *Nano Letters*, 17 (2017) 1610.
- [3] J. Kim *et al.*, *Physical Review Letters*, 119 (2017) 226801.
- [4] M. Kang *et al.*, *Nature Materials*, in press (2018).

Performance potential and limit in van der Waals MoTe₂ Transistors

Due to the versatile and tunable properties in nature, atomically thin transition-metal dichalcogenides (TMD) with the common formula MX₂, where M stands for a transition metal (Mo or W) and X is a chalcogen element (S, Se, Te), have garnered considerable attention for development of next-generation electronics from 2011. Among the TMD compounds, 2H-type molybdenum ditelluride (MoTe₂) has a smaller semiconducting gap in the range of 0.8 to 1.0 eV, which gives a high compatibility with modern Si thin-film processing. In this talk, I will present the synthesis, thickness identification of layered MoTe₂ materials as well as its electrical characterizations. In contrast to the unipolar features in widely studied MoS₂ transistors, van der Waals MoTe₂ transistors display the ambipolarity in charge transport, which is attributed to the existence of Schottky potential barriers between metals and conducting channel [1]. Through applying different controlled electric field, the modulation of such the potential barrier can be realized, allowing a low contact resistance for both n- and p-type channels, which will also be discussed. In addition, to deliberately explore the fluctuation mechanism of carrier trapping/de-trapping in such nanoscale electronics, I will demonstrate the origin of electric noise in van der Waals MoTe₂ transistors by means of the strategy of low-frequency noise measurements [2]. The experimental data clearly suggest that the dynamic processes at the channel surface such as gas absorptions/desorptions strongly affect its carrier transport. Eventually, using this feature of gas absorptions/desorptions, I will show a new doping concept, electrothermal doping [3]. The electrothermal doping adopted in obtaining p/n-type doping MoTe₂ transistors can provide an approach to create logic devices with desired performance.

References

- [1] Yen-Fu Lin, Yong Xu, Sheng-Tsung Wang, Song-Lin Li, Mahito Yamamoto, Alex Aparecido-Ferreira, Wenwu Li, Huabin Sun, Shu Nakaharai, Wen-Bin Jian, Keiji Ueno, and Kazuhito Tsukagoshi, *Adv. Mater.* 26, 3263 (2014).
- [2] Yen-Fu Lin, Yong Xu, Che-Yi Lin, Yuen-Wuu Suen, Mahito Yamamoto, Shu Nakaharai, Keiji Ueno, and Kazuhito Tsukagoshi, *Adv. Mater.* 27, 6612 (2015).
- [3] Yuan-Ming Chang, Shih-Hsien Yang, Che-Yi Lin, Chang-Hung Chen, Chen-Hsin Lien, Wen-Bin Jian, Keiji Ueno, Yuen-Wuu Suen, Kazuhito Tsukagoshi, and Yen-Fu Lin, *Adv. Mater.* 30, 1706995 (2018).

Figures

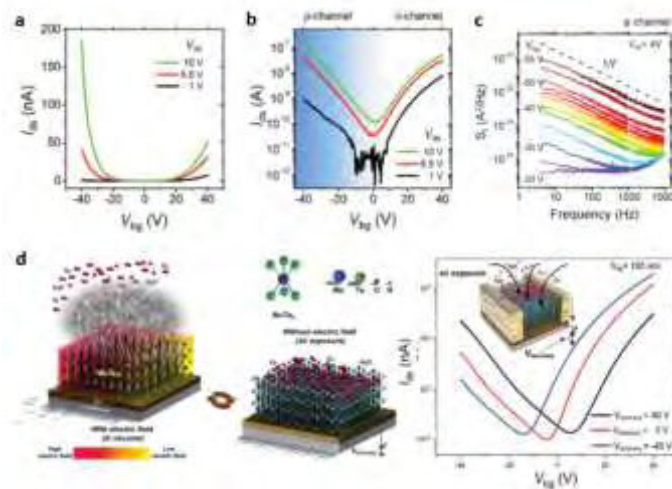


Figure 1: Room-temperature transfer characteristics of van der Waals MoTe₂ transistors under different V_{ds} values on a linear scale (a) and on a logarithmic scale (b). (c) Typical current fluctuations as a function of frequency under different V_{bg} values. (d) Schematic of a MoTe₂ channel processed by the electrothermal doping process and the corresponding transfer characteristics.

Nano-Graphene Based Catalyst for Efficient Light Alkane Activation

Nanocarbon is a term increasingly used to indicate the broad range of carbon materials having a tailored nanoscale dimension and functional properties that significantly depend on their nanoscale features. Recently, lots of studies have demonstrated that nanocarbons, such as carbon nanotube (CNT), porous graphene and nanodiamond (ND) can be used as metal free catalysts for the light alkane dehydrogenation reaction, showing their potential applications to replace the traditional metal oxide catalyst. In this report, we will not only present our recent studies about the exploration of nanocarbons (graphene and graphene@nanodiamond hybrid nanocarbons) as metal free catalysts for the industrial dehydrogenation reaction, but also we will introduce the fabrication of nanocarbon materials (hollow carbon sphere and hollow graphene nanoshell) embedded by Au and Pd nanoparticles used in catalytic oxidation and hydrogenation reaction, and the stabilization of Pd, Pt nanoparticles, especially the atomically dispersed metal species on the novel nanodiamond@graphene hybrid nanocarbons with core-shell structure for efficient light alkane dehydrogenation reaction. The detailed preparing process, characterization, catalytic performance and mechanism will be carefully discussed in the report [1-8].

References

- [1] H.Y. Liu, L.Y. Zhang, N. Wang, D. S. Su et al., *Angew. Chem. Int. Ed.*, 2014, 53, 1263;
- [2] L.Y. Zhang, H.Y. Liu, D.S. Su et al., *Angew. Chem. Int. Ed.*, 2015, 54, 15823;
- [3] X. R. Zhang, Z.S. Meng, H.Y. Liu and R.F. Lu et al., *Energy & Environmental Science*, 2016, 9, 841;
- [4] J Liu, H.Y. Liu and D.S. Su et al., *ACS Catalysis*, 2017, 7, 3349.
- [5] T. Hao, F. Huang, H.Y. Liu and J. Liu, et al. *Adv. Funct. Mater.*, 2018, 28, 1801737;
- [6] J. Diao and H.Y. Liu, et al. *ACS Catalysis*, 2018, 8, 10051;
- [7] F. Huang, H.Y. Liu and D. Ma, et al. *J. Am. Chem. Soc.* 2018, doi:10.1021/jacs.8b07476.

Figures

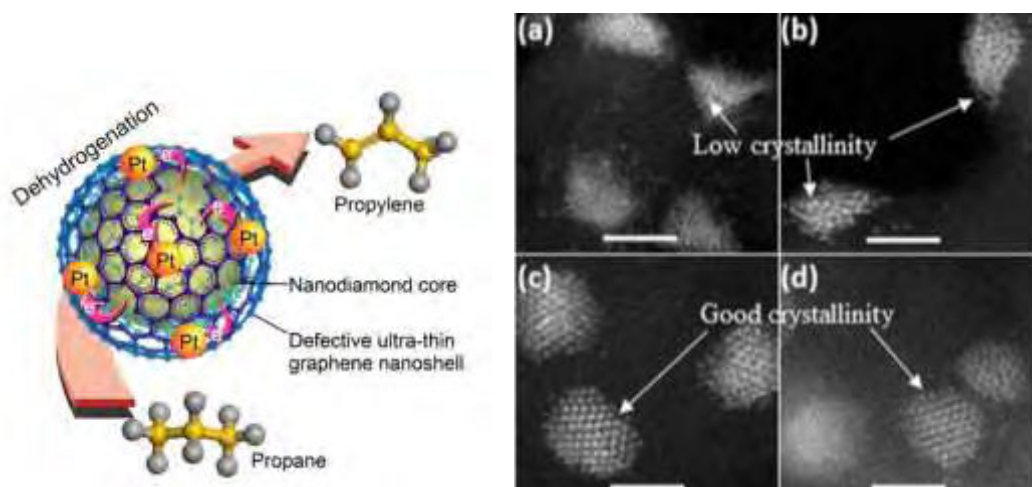


Figure 1: Scheme of Pt nanoparticles supported on the novel hybrid carbon support with a nanodiamond core and ultrathin graphene shell for the propane dehydrogenation reaction, HAADF-STEM images of the corresponding supported Pd nanoparticles: Pd/ND@G (a, b) and Pd/OLC (c,d).

Lei Miao

Jie Gao, Huajun Lai

Guilin University Of Electronic Technology, Guilin, China

nextyeargj@foxmail.com

Enhanced Thermoelectric Performance in Graphene Quantum Dots/Te Nanowires Flexible Hybrid Film

Graphene has been proved to be positive for reducing thermal conductivity in many thermoelectric nanocomposites. Here we prepared graphene quantum dots (GQDs) /Te nanowires flexible hybrid films on mica substrate through drop-cast method. After being annealed in H₂/Ar atmosphere, the hybrid films show enhanced thermoelectric performance due to the redox-reaction between GQDs and Te nanowires during annealing process. The thermoelectric performance of hybrid films can be further adjusted via changing size and percentage of GQDs in film. This work provides insights for the synthesis of graphene-based hybrid thermoelectric films.

Pilkyung Moon¹

Mikito Koshino², Young-Woo Son³

¹New York University Shanghai, Shanghai, China,

²Osaka University, Toyonaka, Japan, ³Korea Institute of Advanced Study, Seoul, Korea

pilkyung.moon@nyu.edu

Theory of Dirac Electrons in a Dodecagonal Graphene Quasicrystal

Quantum states of quasiparticles in solids are dictated by symmetry. Quasicrystals, which can have quasiperiodic orders (such as rotational symmetry) without spatial periodicity, have been used to study quantum states between the limits of periodic order and disorder. The study of the influence of quasiperiodic order has focused on extended wave functions of ordered states, pseudogaps, and fine structures of density of states. However, these studies have been limited to nonrelativistic fermions.

Recently, we reported that a relativistic Dirac fermion quasicrystal can be realized when the Dirac electrons in a single-layer graphene are incommensurately modulated by another single-layer graphene which is rotated by an exact 30° [1].

When two-dimensional atomic layers are stacked incommensurately, the interference between the two lattice arrangement leads to new order to the system. For example, the incommensurate stack of two graphene layers at a rotation angle other than 0 and 30° exhibits an extra periodicity in the form of moiré pattern (aka twisted bilayer graphene) [2]. The physical properties of twisted bilayer graphene are well described by the effective theory based on the moiré interference period [3-5]. However, such moiré periodicity disappears at a rotation angle of 30° , since the structure gains a 12-fold rotational symmetry which is not compatible with a translation. Mathematically, it is known that two honeycomb structures overlaid at 30° form a dodecagonal quasicrystal [6].

In this talk, I will discuss the theory of Dirac electrons in a dodecagonal graphene quasicrystal. I will first explain the emergence of the infinite number of Dirac cone replicas in ARPES in terms of the generalized Umklapp scattering. The contribution of multiple scattering to the unusually strong scattering signals associated with long wave vectors will be emphasized as well. In addition, I will show that the configuration of the Dirac cone replicas near the Γ point provides a solid evidence of the rotation angle at an exact 30° [1].

Moreover, I will report a rigorous effective model to describe the electronic structures of the graphene quasicrystal and show that very unique features, such as the neither localized nor extended states (aka critical states), arise in this system [7].

References

- [1] S. J. Ahn,* P. Moon,* T.-H. Kim,* H.-W. Kim, H.C. Shin, E. H. Kim, H. W. Cha, S.-J. Kahng, P. Kim, M. Koshino, Y.-W. Son,† C.-W. Yang,† and J. R. Ahn,† Science 361, 782 (2018) (*: co-first authors, †: co-corresponding authors).
- [2] C. Berger et al., Science 312, 1191 (2006).
- [3] J. M. B. Lopes dos Santos, N. M. R. Peres, and A. H. Castro Neto, Phys. Rev. Lett. 99, 256802 (2007).
- [4] P. Moon and M. Koshino, Phys. Rev. B 85, 195458 (2012).
- [5] P. Moon and M. Koshino, Phys. Rev. B 87, 205404 (2013).
- [6] P. Stampfli, Helv. Phys. Acta 59, 1260 (1986).
- [7] P. Moon, M. Koshino, and Y.-W. Son (in preparation).

Figures

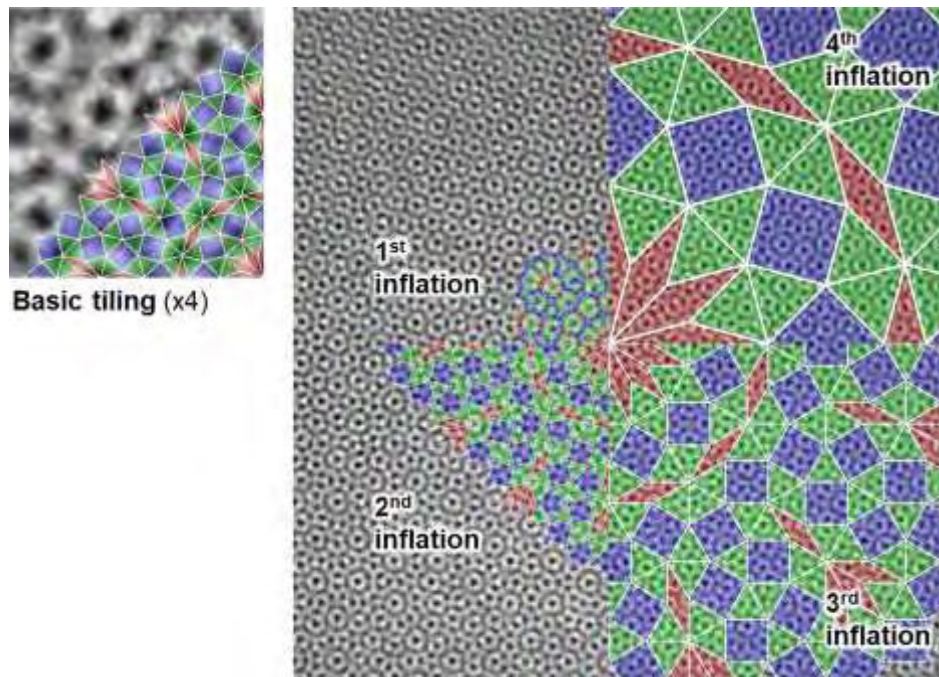


Figure 1: Color-coded dodecagonal tiling of the TEM image of a graphene quasicrystal [1].

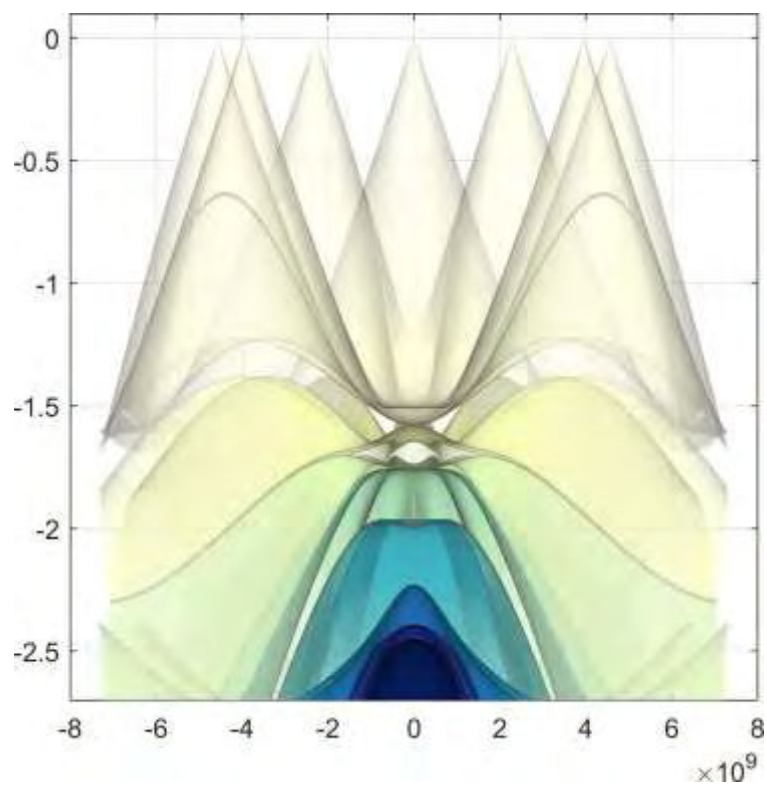


Figure 2: Electronic structures of a graphene quasicrystal calculated by the effective model [7].

Aitor Mugarza

Catalan Institute of Nanoscience and Nanotechnology (ICN2), CSIC and The Barcelona Institute of Science and Technology, Campus UAB, Bellaterra, 08193 Barcelona, Spain.

ICREA Institució Catalana de Recerca i Estudis Avançats, Lluís Companys 23, 08010 Barcelona, Spain

aitor.mugarza@icn2.cat

Engineering nanoporous graphene with atomic precision

Nanosize pores can turn semimetallic graphene into a semiconductor [1, 2] and from being impermeable into the most efficient molecular sieve membrane [3, 4]. However, scaling the pores down to the nanometer, while fulfilling the tight structural constraints imposed by applications, represents an enormous challenge for present top-down strategies.

Here we report a bottom-up method to synthesize nanoporous graphene comprising an ordered array of pores separated by ribbons, which can be tuned down to the one nanometer range [5]. The size, density, morphology and chemical composition of the pores are defined with atomic precision by the design of the molecular precursors. Our DFT-STs study reveal a highly anisotropic electronic structure, where orthogonal one-dimensional electronic bands with an energy gap of ~ 1 eV coexist with confined pore states that might sense passing ions and molecules. The semiconducting character of the nanomaterial has been further confirmed by fabricating field-effect transistors with state of art on/off ratios. The combined structural and electrical properties makes this nanoporous 2D material a highly versatile semiconductor for simultaneous sieving and electrical sensing of molecular species.

References

[1] J. Bai, X. Zhong, S. Jiang, Y. Huang, X. Duan, *Nat. Nanotechnol.* 5, 190–194 (2010).

[2] X. Liang et al., *Nano Lett.* 10, 2454–2460 (2010).

[3] S. Garaj et al., *Nature.* 467, 190–193 (2010).

[4] S. P. Koenig, L. Wang, J. Pellegrino, J. S. Bunch, *Nat. Nanotechnol.* 7, 728–732 (2012).

[5] C. Moreno et al., *Science* (80-.). 360, 199–203 (2018).

Figures

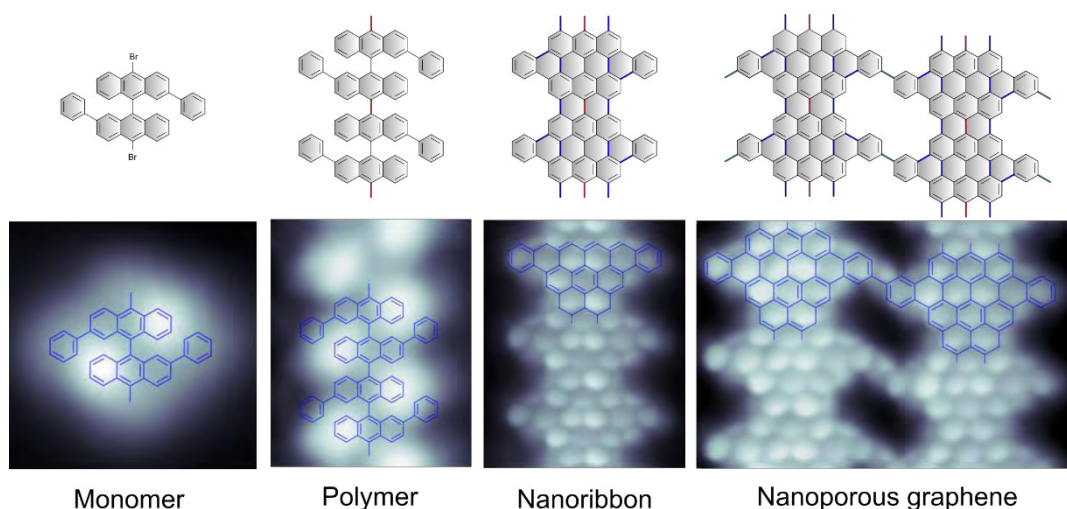


Figure 1: STM images (bottom) and schematic representation (top) of the precursor, intermediates and final product of the hierarchical synthesis of nanoporous graphene.

Rational Design of Nanostructured and Functionalized Graphene and Their Applications for Electronics and Energy Devices

2D materials, including graphene and MoS₂ and phosphorene, have attracted intensive interests due to their unique chemical and physical properties. These tremendous features make them as promising candidates for applications on nano-electronics, sensors, and energy storage. In this talk, three main related topics will be conducted: (1) The current developed approaches for the synthesis of 2D materials, such as Spiral-CVD graphene, printed MoS₂-nano-ribbon, and phosphorene. [1-7] In particular, the proof-of-concept on phosphorene-based RRAM device was demonstrated with reliable and superior performance, such as high on/off current ratio of $\sim 10^5$ and stable retention $> 10^4$ s. [8] (2) We demonstrate an all screen-printable solid-state micro-supercapacitor(MSCs), which was integrated with graphene/CNTs as hierarchical electrodes. It exhibits a high cycling stability after 1000 cycles and excellent mechanical flexibility. The extracted energy and power density of 16.4 mWh/cm³ and 294.8 W/cm³, which was, to our best knowledge, the highest performance for ultra-thin(< 5 μ m) MSCs. This work provides a scalable and cost-effective method to produce solid-state MSCs with high energy density. (3) Fluorinated graphene has been synthesized by various approaches; however, most of the processes using toxic chemicals with complex steps, which hinder the practical applications. Here, we report a novel hydrothermal method for fabricating FG through frequently used Nafion as reagents. The FG coated substrate shows high hydrophobic property, where the contact angle (water) of above 120° was achieved. Finally, the composite film with FG(0.75 wt%) as an additive in epoxy shows excellent anticorrosion ability with corrosion rate at 2.9×10^{-5} mm/year, which was $\sim 200\%$ enhanced if compare it with pristine epoxy. This work proposed a one-pot and green process for preparing FG in a scalable way, which is potential for applications in the sustainable environment in the future.

References

- [1] Y. M. Chen et al., *Nanoscale*, 8, 3555 (2016)
- [2] J. Y. Syu, et al., *RSC Advances*, 6, 8384 (2016)
- [3] C. H. Chen, et al., *Nanoscale*, 7, 15362 - 15373 (2015)
- [4] D. Dutta et al., *Nanoscale*, 10, 12612 (2018)
- [5] K. I. Ho, et al., *Advanced Materials*, 27, 6519 (2015)
- [6] K. I. Ho, et al., *Scientific Reports*, 4, 5893 (2014)
- [7] K. I. Ho, et al., *Small*, 989–997 (2014)

Electrochemically Doped Light-Emitting Devices of Transition Metal Dichalcogenide Monolayers

Recently, 2D layered materials have attracted much attention for exploring new electronic, optoelectronic, and photonic applications. Particularly, direct bandgap and unique electronic structure in monolayer transition metal dichalcogenides (TMDCs) provides a platform for exploring novel optoelectronic functionalities and devices [1,2]. One of the most interesting properties of TMDCs is topological features, such as a non-centrosymmetric two-dimensional crystal, strong spin-orbit interaction, non-zero Berry curvature and resulting spin-valley coupling [3]. Actually, circularly polarized light emission has been demonstrated [4,5].

Although the optical properties of TMDCs are very promising, light-emitting devices require intentional doping techniques to form p-n junction. However, reliable doping methods for TMDCs have not yet been fully established. Therefore, the fabrication of TMDC light-emitting devices are still limited, and this fundamental barrier has made investigating electroluminescence (EL) properties of TMDCs inevitably difficult [2]. To overcome this issue, we recently developed the electrochemical method to dope both holes and electrons [6-10], and proposed a simple approach to form p-n junction universally in TMDCs [11-13].

Firstly, as shown in Fig. 1, we fabricated ion-gel (a mixture of ionic liquid and triblock co-polymer) gated EDLTs (Electric Double Layer Transistors) using large-area TMDC monolayers, such as MoS₂ and WSe₂, grown by chemical vapor deposition [6-10]. The Fermi level of TMDCs can be continuously shifted by applying gate voltage, and we can induce both hole and electron transport in these devices. The hole mobility of WSe₂ can be enhanced up to 90 cm²/Vs at high carrier density of 10¹⁴ cm⁻², whereas the MoS₂ showed electron mobility of 60 cm²/Vs. By the combination of p-type WSe₂ and n-type MoS₂, we fabricated CMOS inverters [10].

Here, we use this technique to form p-n junction (Fig. 2) and apply this method into various forms of TMDCs, such as monolayer polycrystalline films (Fig. 3(a)), single crystalline flakes (Fig. 3(b)), and lateral heterojunctions (Fig. 3(c)), to achieve photo-detection [11] and EL emission [12,13]. Particularly, using single crystal samples, we have performed temperature and position dependent measurements of EL and investigated their optical properties. Very interestingly, we observed robust circularly polarized EL emission, arising from spin-valley coupling in TMDCs. Our approach paves a versatile way for using TMDCs in discovering new functional optoelectronic devices.

References

- [1] X. Xu, et al. Nat. Phys. 10, 343 (2014).
- [2] J. Pu and T. Takenobu, Adv. Mater. 30, 1707627 (2018).
- [3] D. Xiao, et al., Phys. Rev. Lett. 108, 196802 (2012).
- [4] K. F. Mak et al., Nat. Nanotechnol. 7, 494 (2012).
- [5] Y. J. Zhang, et al. Science 344, 725 (2014).
- [6] J. Pu, T. Takenobu, et al., Nano Lett. 12, 4013 (2012).
- [7] J. Pu, T. Takenobu, et al., Appl. Phys. Lett. 103, 23505 (2013).
- [8] J.-K. Huang, T. Takenobu, et al., ACS Nano. 8, 923 (2014).
- [9] Y.-H. Chang, T. Takenobu, et al., ACS Nano. 8, 8582 (2014).
- [10] J. Pu, T. Takenobu, et al., Adv. Mater. 28, 4111 (2016).
- [11] D. Kozawa, T. Takenobu, et al., Appl. Phys. Lett. 109, 201107 (2016).
- [12] J. Pu, T. Takenobu, et al. Adv. Mater. 29, 1606918 (2017).
- [13] M.-Y. Li, J. Pu, T. Takenobu, Adv. Funct. Mater. 28, 1706860 (2018).

Figures

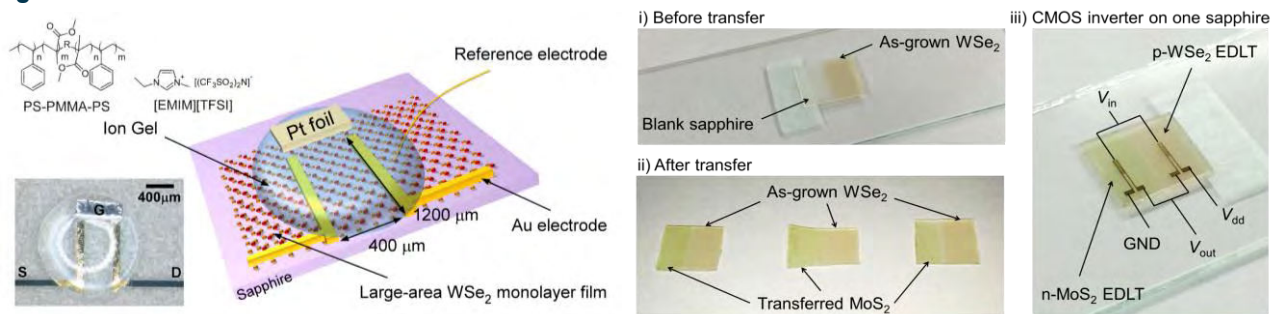


Figure 1: Schematic illustrations of ion-gel gated EDLT (left) and p-type WSe₂/n-type MoS₂ CMOS inverters (right).

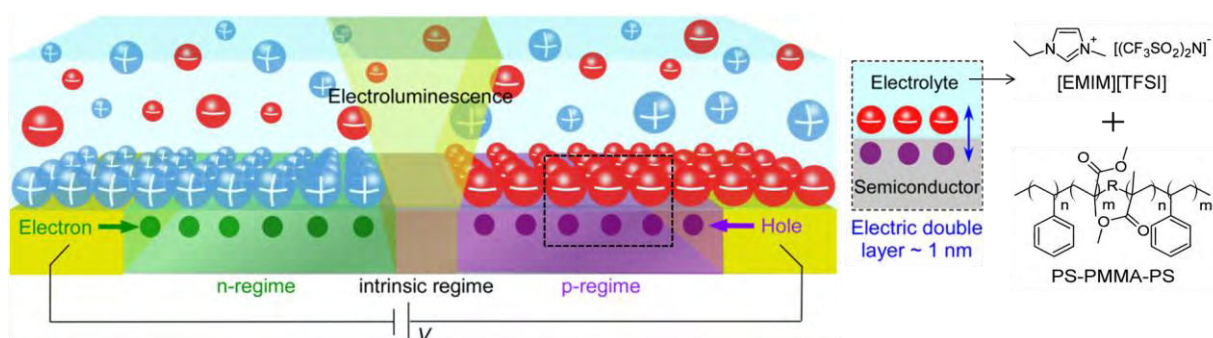


Figure 2: Schematic illustrations of a proposed light-emitting device.

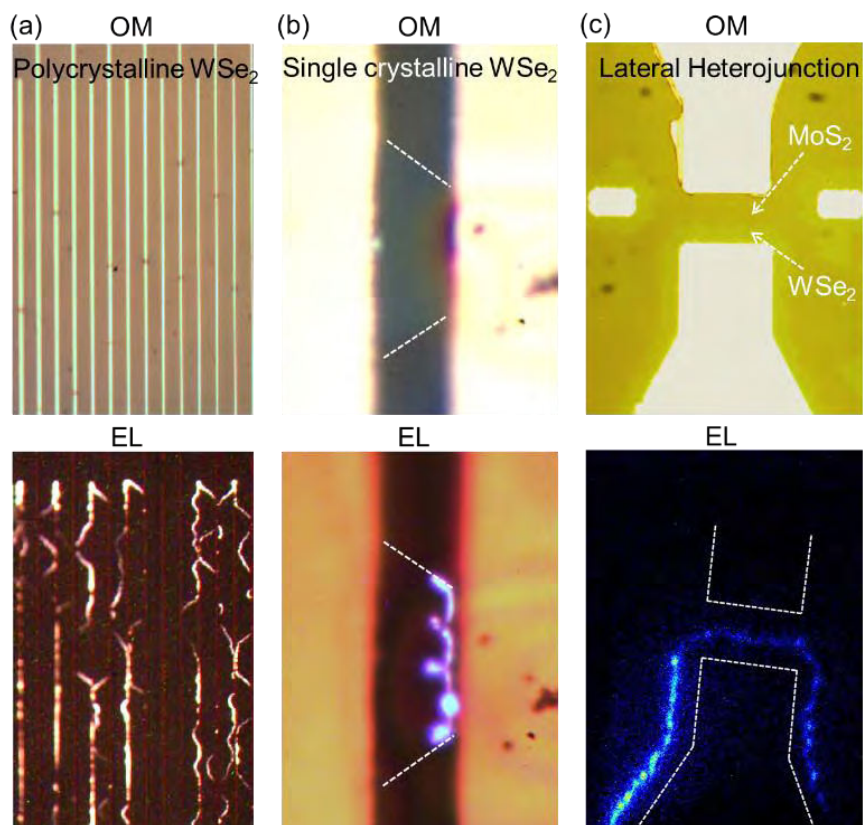
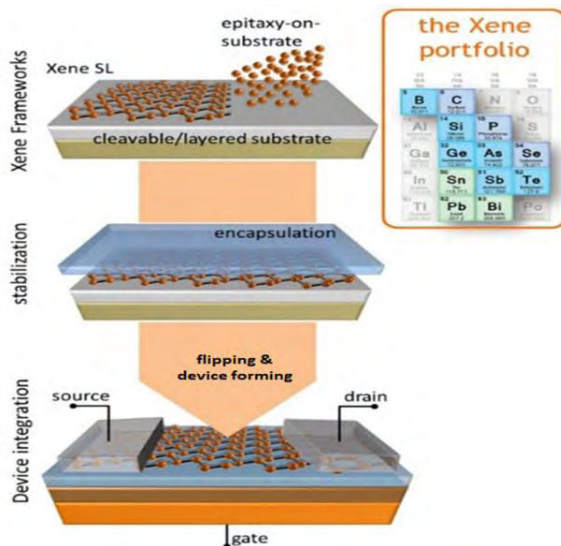


Figure 3: Optical microscope (OM) and electroluminescence (EL) images of various form TMDCs.

Emerging 2D Xenos for Innovative Nanoelectronics

Two-dimensional (2D) Xenos (monoatomic sheets, e.g. silicene and phosphorene) have collective properties of mechanical flexibility and tunable bandgap holding great promise for novel nanoelectronics beyond graphene. Nonetheless, there is a challenge in experimental device studies largely due to air-stability related material and process issues. This talk highlights state-of-the-art experimental progress in synthesis, stabilization and device integration of monolayer silicene and thicker derivatives. With a unique sandwich encapsulation process, we enabled silicene transistor debut^[1]. By tuning integration process and number of layers^[2], we further improved portability and reliability. Electrostatic characteristics of silicene field-effect transistor exhibits ambipolar charge transport with extracted mobility 100-200 cm²/V-s at residual carrier density $\sim 8 \times 10^9$ cm⁻², corroborating with theoretical predictions on Dirac cone in band structure. The electronic structure of silicene is expected to be sensitive to substrate interaction, surface chemistry, and spin-orbit coupling, holding great promise for a variety of novel applications, such as topological bits, quantum sensing and energy devices^[3]. We applied above strategy to phosphorene, few-layer black phosphorus, and demonstrated mobility 310-1500 cm²/Vs, gate modulation 10^{3-5} and intrinsic $f_T=20$ GHz on flexible polyimide substrates^[4,5]. Recent progress on silicene and phosphorene (transferable to other Xenos like stanine and germanene) represent a renewed opportunity for future nanoelectronics complementary to what is available in graphene^[6].



References

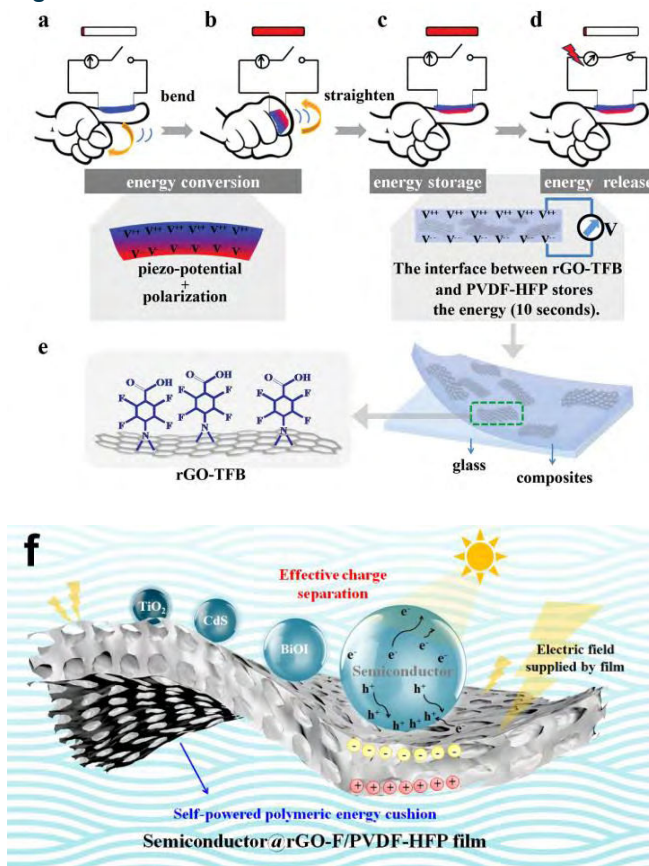
- [1] L. Tao, E. Cinquanta, D. Chiappe, et al., *Nature Nanotech.* 10 10 (2015).
- [2] C. Grazianetti, E. Cinquanta, L. Tao, et al., *ACS Nano* 11 3 (2017).
- [3] A. Molle, C. Grazianetti, L. Tao, et al., *Chem. Soc. Rev.* 47 16 (2018).
- [4] W. N. Zhu, M. N. Yogeesh, S. X. Yang, et al., *Nano Lett.* 15 3 (2015).
- [5] W. Zhu, S. Park, M. N. Yogeesh, et al., *Nano Lett.* 16 4 (2016).
- [6] S. Kabiri Ameri, R. Ho, H. Jang, et al., *ACS Nano* 11 8 (2017).

Figure: Xene device integration.

Graphene Composites as Energy, Catalyst, Environmental and Biomedical Materials, and Full Utilization of Graphite-Mining

Graphene is considered as one potential revolutionary material, due to its collective properties of mechanical strength and flexibility, tunable electronic behavior, optical transparency, etc. Most graphene-related applications are based on graphene composites, as a result of a trade off between performance and cost. In the past decade, our group has demonstrated a series of graphene composites aiming at energy storage and transformation^[1-5], photocatalysis^[6-9], biomedical devices^[10-13], etc. This presentation illustrates some typical works, such as a generator and in situ storage unit based on reduced graphene oxide (rGO)-PVDF-HFP film, and several novel graphene based-electrodes in lithium-ion batteries and super-capacitors. Meanwhile, the explosive development in graphene also stimulates exploitation of graphite. Consequently, a discussion about utilizing all the component during graphite-mining is also carried out, including the flake graphite, low grade graphite, tailings, and so on.

Figures



References

- [1] W. S. Tong, Y. H. Zhang et al, *Advanced Functional Materials*, 25 (2015) 7029-7037
- [2] H. T. Li, H. Dai, Y. H. Zhang et al, *Angew. Chem. Int. Ed.*, 56 (2017) 1-7
- [3] L. Q. Bai, Y. H. Zhang et al, *Nano Energy*, Accepted
- [4] L. Sun et al, *Chem. Commun.* 54 (2018) 10172–10175
- [5] L. Sun, Y. Zhang et al, *Nanoscale*, 9 (2017) 18552-18560
- [6] W. S. Tong, Y. H. Zhang et al, *Nano Energy*, 53(2018) 513–523
- [7] Q. Zhang, Q. An et al, *Nanoscale*, 7 (2015) 14002-14009
- [8] Q. Zhang, Y. H. Zhang et al, *Scientific Reports* 7 (2017) 12296
- [9] X. L. Yu, Y. H. Zhang et al, *Appl. Catal. B-Environ.* 182 (2016) 504-512
- [10] K. Nie, Q. An et al, *RSC Advances*, 5 (2015) 57389–57394
- [11] Y. Zhang, Q. An et al, *Small* 14(2018) 1802136
- [12] L. Liu, X. L. Yu et al, *New J. Chem.*, 41(17) (2017) 9008-9013
- [13] L. Liu, Y. H. Zhang et al, *Analyst*, 142(5) (2017) 780-786

Figure: (a-f) Schematic illustrations of rGO-PVDF-HFP film as both energy generator and in situ Storage Unit; (f) rGO-PVDF-HFP film as substrate for photocatalysis.

Computational design of novel 2D electronic and magnetic materials

Abstract

Theoretical design based on first-principles computations play an important role in the research and innovation of 2D materials. In the past few years, our group has designed a series of novel 2D electronic, magnetic and optoelectronic materials: (1) 2D semiconductor with high carrier mobility including monolayer δ -Cu₂S [1], GeAsSe, and SnSbTe [2]; (2) Janus group-III chalcogenide monolayers with enhanced piezoelectricity [3]; (3) monolayer group-III monochalcogenides by oxygen functionalization as 2D topological insulators [4]; (2) Y₂N monolayer as high-speed Dirac half-metal [5]; (5) monolayer MnB as 2D ferromagnet with high Curie temperature [6] (see Figure 1).

References

- [1] Y. Guo, et al., *Nanoscale Horizons* (2018)
- [2] Y. Guo, et al., *Frontier of Physics* 13 (2018) 138117
- [3] Y. Guo, et al., *Appl. Phys. Lett.* 110 (2017) 163102.
- [4] S. Zhou, et al., *npj Quantum Materials* 2018, 3, 16
- [5] Z. F. Liu, et al., *Nano Res.* 10 (2017) 1972.
- [6] Z. Jiang, et al., *Nanoscale Horizons* 3 (2018) 335.

Figures

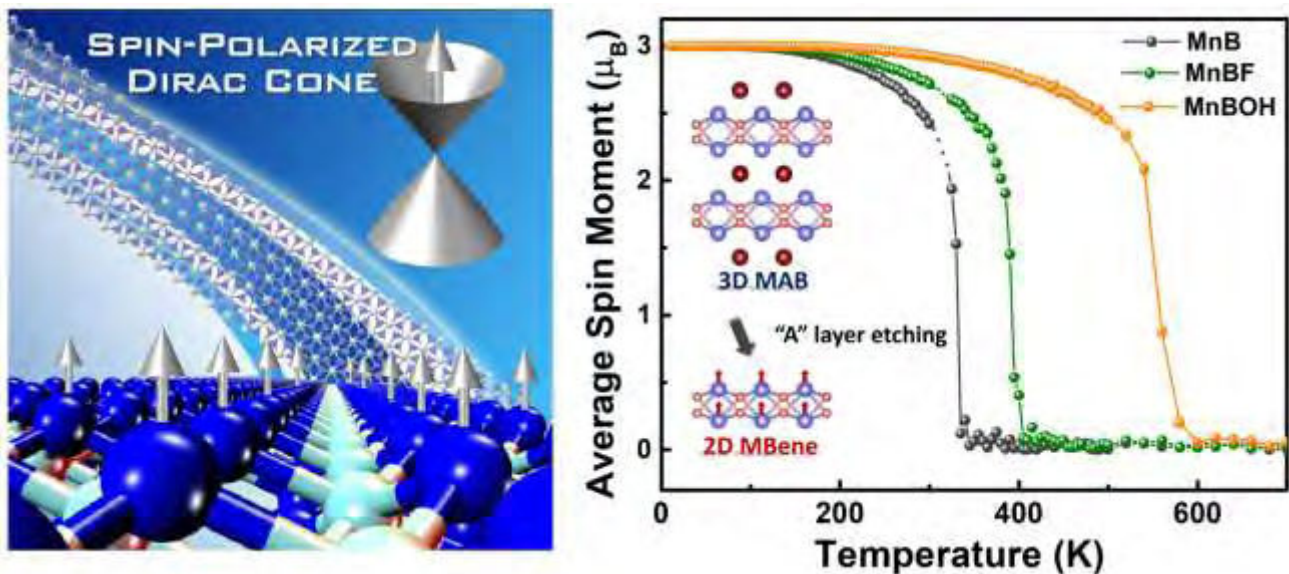


Figure 1: (left) Y₂N monolayer as a Dirac half-metal, (right) monolayer MnB as 2D ferromagnet with high Curie temperature.

Renzong Hu

Min Zhu

Guangdong Provincial Key Laboratory of Advanced Energy Storage Materials, School of Materials Science and Engineering, South China University of Technology, Guangzhou, China

msrenzonghu@scut.edu.cn

Highly reversible conversion reactions in lithiated SnO₂ based thin film anode materials

Tin dioxide (SnO₂) has been considered one of the most promising alternative anode materials for lithium batteries. In the past two decades, extensive studies have been directed to gaining a fundamental understanding of the lithiation/delithiation reactions to improve the performance of SnO₂-based electrodes. However, the conversion reaction in lithiated SnO₂ that produces Li₂O has long been believed irreversible and considered the main cause of large capacity loss and low initial Coulombic efficiency of SnO₂ and other oxide electrodes. Accordingly, a key question highlighted in Chiang's Perspectives (Building a better Battery, Science, 2010, 330, 1485) is how to overcome the irreversibility of Li₂O in SnO₂ anode to fully exploiting the limit of the capacity of the electrode materials.

Here we demonstrated that Li₂O can indeed be highly reversible in a SnO₂ thin film electrode with controlled nanostructure and achieved an initial Coulombic efficiency of ~95.5%, much higher than that previously believed possible (52.4%). In situ spectroscopic and diffraction analyses corroborate the highly reversible electrochemical cycling, suggesting that the interfaces and grain boundaries of nano-sized SnO₂ may suppress the coarsening of Sn and enable the conversion between Li₂O and Sn to amorphous SnO₂ when de-lithiated. Furthermore, we have found that the application of super-elastic films of NiTi alloy could accommodate the internal stress and volume change of lithiated nano-SnO₂ layer and thus effectively suppress Sn coarsening, to retain the high reversibility of the SnO₂ layer with reversible capacity more than 800mAh/g (based on SnO₂) for over 300 cycles, demonstrating stable charge capacities of ~400mAh/g in the potential ranges of 0.01-1.0V and 1.0-2.0V (vs. Li/Li⁺), respectively.

Furthermore, we designed a double-layer electrode of a SnO₂ film coated with an ALD Al₂O₃ Layer. The Al₂O₃ coating (~2 nm in thick) on the surface helps to maintain the structural stability of SnO₂ layer (~20 nm), while the inside filling Al₂O₃ increases the boundary integrity of SnO₂ nanocrystals, and acts as barriers to prevent the lithiation induced Sn coarsening during cycling. In particular, the Al₂O₃ layer stabilizing the solid electrolyte interphase formed on the surface of electrode, enabling enhanced roundtrip efficiency. Thus this SnO₂/Al₂O₃ electrode contributes superior electrochemical performance with a high ICE (88.1%), better reversible capacity retention (88.9% after 200 cycles) than that of the pure SnO₂ anode (30.6%), demonstrating that surface modification on nanograins of conversion type anode materials could be helpful for enhancing the reversibility and cyclability of the electrode, enabling high stable reversible capacity.

References

- [1] R.Z Hu, M. Zhu*, H. Wang, et al., *Acta Materialia*, 2012, 60:4695-4730.
- [2] H.P. Zhang, Z. W. Chen, R.Z. Hu*, et al., *Journal of Materials Chemistry A*, 2018, 6: 4374-4385.
- [3] R.Z. Hu, D.C. Chen, G. Waller, et al., *Energy & Environmental Science*, 2016, 9:595-603
- [4] R.Z. Hu, Y.P. Ouyang, D.C. Chen, et al., *Acta Materialia*, 2016, 109: 248-258.
- [5] R.Z. Hu, Y.P. Ouyang, T. Liang, et al., *Energy & Environmental Science*, 2017, 10:2017-2029.
- [6] R.Z. Hu, Y.P. Ouyang, T. Liang, et al., *Advanced Materials*, 2017, 29: 1605006.
- [7] H.Y. Zhang, R.Z. Hu*, Y.X. Liu, et al., *Energy Storage Materials*, 2018, 13:257-266

Figures

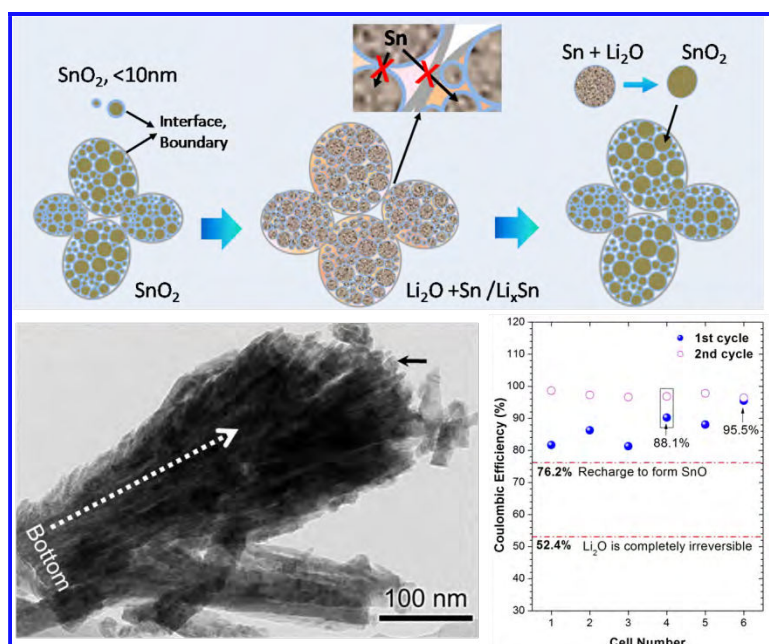


Figure 1: The high density interfaces and grain boundaries of nano-sized SnO₂ suppress the coarsening of Sn and enable the conversion between Li₂O and Sn to amorphous SnO₂ when de-lithiated, resulting in a high initial Coulombic efficiency of ~95.5% in pure SnO₂ film anodes.

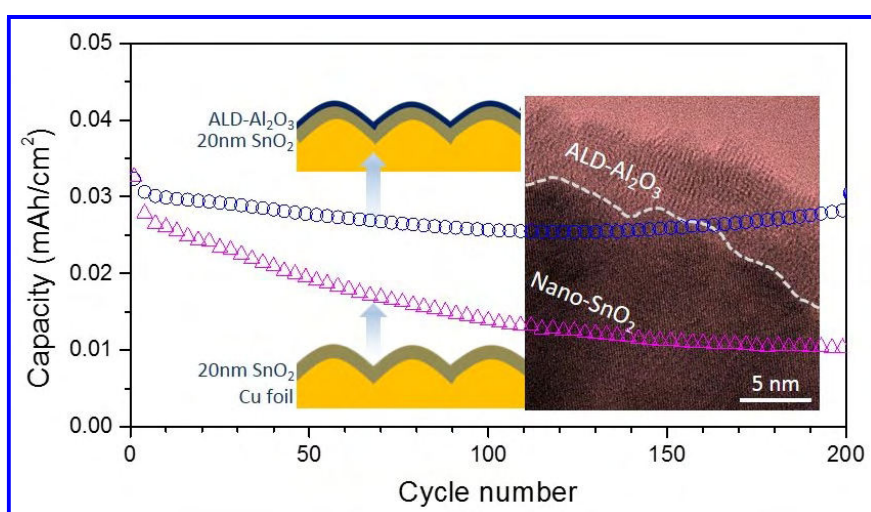


Figure 2: SnO₂/Al₂O₃ film electrode contributes superior electrochemical performance with a high ICE (88.1%), better reversible capacity retention (88.9% after 200 cycles) than that of the pure SnO₂ film anode (30.6%).



INVITED CONTRIBUTIONS

(INDUSTRIAL FORUM)

New varieties of Metal Sulphides / Phosphides for Electronics and Clean Energy applications

Abstract

Transition metal dichalcogenides (TMD) materials have attracted much attention due to their unique properties, ranging from low dimensional effects, good structural integrity, high electrical and thermal conductivity, and chemical stability. Increasingly, much of the applications have gradually progressed into different specific areas ranging from electronics to conductive coatings to biomedical technology.

In this talk, I will focus on new varieties of transition metal sulphides and phosphides, which are specifically designed and engineered. Two examples will be shown, the first is CuS, which is well known as a photosensitive material which possesses catalytical behavior. We will show there exist unique non-volatile memory behavior not previously known with low voltage switching of -3V and a switching speed of <20ms. Likewise, we will also show other forms of CoS where it has good water splitting capability. Likewise, we will demonstrate the more stable forms of metal phosphides, such as CoP and NiP where it has superior properties as compared to the more well studied sulphides in water splitting. We will also show some results where hybrid metal sulphides and phosphides can enhance catalytical reactions.

References

- [1] Yu S.H. and D.H.C Chua, ACS Applied Materials & Interface, DOI: 10.1021/acsami.8b02755
- [2] Ng Z.Q.C, R.K.K.Tan, A.Rath, A.T.S. Wee and D.H.C. Chua, Applied Physics Letters, doi: 10.1063/1.5027129

Figures

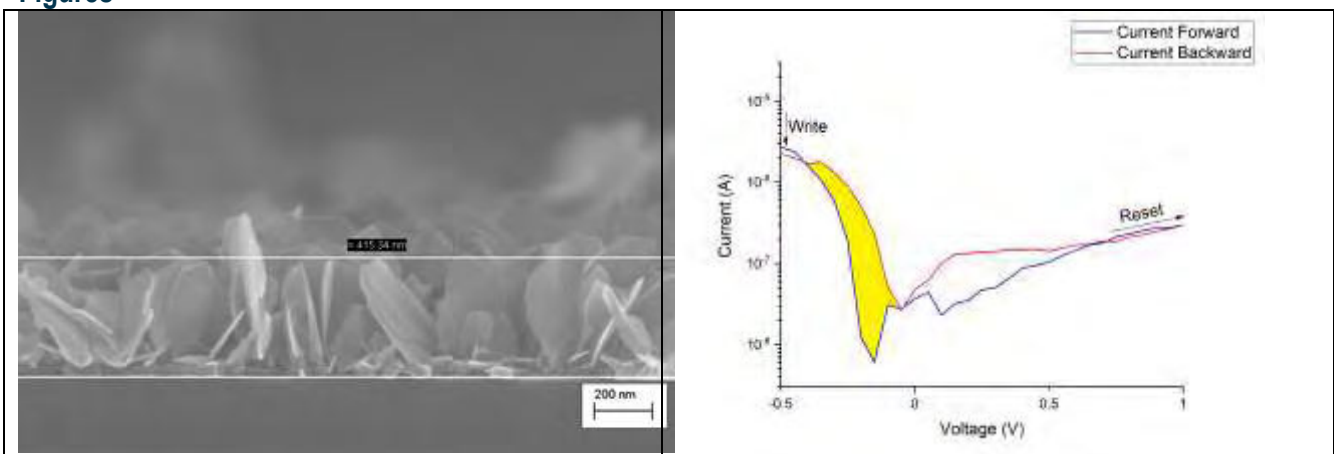


Figure 1: 2 dimensional flat plates of CuS with resistive random access memory behavior.

Chang-Hua Liu

Jiajiu Zheng, Shane Colburn, Taylor K. Fryett, Yueyang Chen, Xiaodong Xu, Arka Majumdar

Institute of Photonics Technologies, National Tsing Hua University

chliu@ee.nthu.edu.tw

Developing ultrathin light emitters and metalenses based on van der Waals materials

Van der Waals (vdW) materials have generated strong interest in recent years due to their unusual and superior optoelectronic properties. These materials can be integrated on any substrate without needing explicit lattice matching. This presents new opportunities for creating hybrid nano-structures which can take advantage of industrial semiconductor manufacturing technologies, while benefiting from the unique properties of vdW materials. Here, we will outline an architecture of ultrathin light emitter, composed of 2D heterostructures light emitting diode stacked with a photonic crystal cavity. The light emission near the cavity area is highly linear polarized with the degree of polarization $\sim 84\%$. More importantly, its emission intensity is enhanced by more than 4 times. As applying voltage pulses, we show the emitter can be modulated at 1 MHz speed at room temperature, faster than most of optoelectronics based on transition metal chalcogenides.

In addition to light emitters, we will demonstrate dielectric metalenses with their thickness approaching $\sim 0.14 \lambda$. Such features are realized by exploiting two-dimensional (2D) materials as dielectrics while leveraging incomplete phase design. Based on these design schemes, the developed ultrathin devices not only can be applied at 1310, 650 and 450 nm wavelength regimes, showing near diffraction-limited focusing, but also exhibit their capabilities for imaging applications. Due to the van der Waals (vdWs) nature of 2Ds, the fabricated dielectric metalenses can be transferred onto different substrates, including flexible substrates, for stretching and tunable focusing applications. Our work enables further downscaling of optical elements and opens the door for future imaging, spectroscopy, and energy harvesting applications.

References

- [1] C. H. Liu et al., Nano Lett. 17 (2017) 200-205.
- [2] C. H. Liu et al., arXiv:1807.03458.

Synthesis and Applications of Carbon Dots

Carbon atoms can bond together in different molecular configurations leading to different carbon allotropes including diamond, fullerene, carbon nanotubes, graphene, and graphdiyne. Carbon dots (CDs), which are generally surface-passivated carbon nanoparticles less than 10 nm in size, are other new members of carbon allotropes. CDs were serendipitously discovered in 2004 during the electrophoresis purification of single-walled carbon nanotubes. Similar to their popular older cousins, fullerenes, carbon nanotubes, and graphene, CDs have drawn much attention in the past decade and have gradually become a rising star because of the advantages of chemical inertness, high abundance, good biocompatibility, and low toxicity. Interestingly, CDs typically display excitation-energy- and size-dependent fluorescent behavior. Depending on their structures, the fluorescence from CDs is either attributed to the quantum-confinement effect and conjugated π -domains of the carbogenic core (intrinsic states), or determined by the hybridization of the carbon skeleton and the connected chemical groups (surface states). Compared with the traditional semiconductors, quantum dots, and their organic dye counterparts, fluorescent CDs possess not only excellent optical properties and small-size effect, but also the advantages of low-cost synthesis, good photo-bleaching resistance, tunable band gaps, and surface functionalities. For these reasons, CDs holds promise as emergent nanolights for bio-imaging, sensing, and optoelectronic devices. Additionally, CDs feature abundant structural defects at their surface and edges, excellent light-harvesting capability, and photo-induced electron-transfer ability, thus facilitating their applications in photocatalysis and energy storage and conversions. To date, remarkable progress has been achieved in terms of synthetic approaches, properties, and applications of CDs. This review aims to classify the different types of CDs, based on the structures of their carbogenic cores, and to describe their structural characteristics in terms of synthesis approaches. Two well-established strategies for synthesizing CDs, the top-down and bottom-up routes, will be highlighted. The diverse potential applications, in the bio-imaging and diagnosis, sensing, catalysis, optoelectronics, and energy-storage fields, of CDs with different structures and physicochemical properties, are summarized, covering the issues of surface modification, heteroatom doping, and hybrids made by combining CDs with other species such as metals, metal oxides, and biological molecules. The challenges and opportunities for the future development of CDs are also briefly outlined.

Application of Graphene and Graphene Nanoribbons to Electronic Devices Including Ultrasensitive Gas Sensors

Graphene, two-dimensional honeycomb carbon lattice, has excellent electrical properties, and is therefore a promising material for future electronic devices. We have been working on growth of nanocarbon materials, including graphene and carbon nanotubes, and their application to electronic devices, such as transistors, interconnects, and sensors. Furthermore, we recently work on bottom-up synthesis and application of graphene nanoribbons (GNRs). We here describe our recent progress.

We recently developed a gas sensor based on a graphene-gate transistor, where the gate of a Si transistor is replaced with monolayer graphene (Fig.1) [1]. If gas molecules adsorb on the graphene-gate surface, the Fermi level or work function of graphene can change, thus shifting the threshold of the transistor. This causes changes in the drain current if the gate voltage is kept constant. This graphene-gate sensor was found to be very sensitive to NO₂ and NH₃. As can be seen in the Fig. 2, the sensor can detect NO₂ with concentrations less than 1 ppb.

Graphene can also be utilized for high-frequency wave detection [2, 3]. We actually proposed a diode consisting of a GNR heterojunction (Fig. 3) for such a purpose [4]. The heterojunction consists of a hydrogen-terminated armchair-edge GNR (H-AGNR) and fluorine-terminated armchair-edge GNR (F-AGNR). Since there is a difference in electron affinity between them, we can construct a staggered-type lateral-heterojunction p-n diode. First principles simulations show that, due to band-to-band tunneling, the diode has a nonlinear reverse current of the order of kA/m. The junction capacitance is extremely small due to the small junction area. The voltage sensitivities of the GNR-based backward diode as a function of frequency are shown in Fig. 4. The diode can have a much better sensitivity for terahertz wave than a GaAsSb/InAlAs/InGaAs heterojunction diode [5].

We try to form GNRs having various widths and edge-terminations using a bottom-up approach [6]. In fact, we used a precursor shown in Fig. 5 (HFH-DBTA), aiming at synthesizing partially F-terminated AGNRs. The F atoms at the edges, however, were detached during the cyclodehydrogenation of partially-edge-fluorinated polyanthrylenes to form GNRs. We have found, by first principles calculations, that a critical intermediate structure, obtained as a result of H atom migration to the terminal carbon of a fluorinated anthracene unit in polyanthrylene, plays a crucial role in significantly lowering the activation energy of carbon-fluorine bond dissociation.

Incidentally, we have found that locally aligned GNRs are obtained when we use these precursors, as shown in Fig.6. Simulations show that this alignment is related to the relative strengths of precursor-precursor and precursor-substrate interactions. We have also fabricated a transistor using aligned GNRs as a channel. Transfer characteristics of the transistor are also described in the presentation.

This research was partly supported by JST CREST Grant Number JPMJCR15F1, Japan..

References

- [1] N. Harada, et al., IEDM 2016 (2016) p.476..
- [2] X. Cai, et al., Nat. Nanotech., 9, (2014) 814.
- [3] L. Vicarelli et al., Nat. Mater., 11, (2012) 865.
- [4] Harada, et al., Appl. Phys. Express, 10, 074001 (2017)
- [5] M. Patrashin, et al., IEEE Trans. Electron Devices, 62 (2015) 1068.
- [6] H. Hayashi, et al., ACS Nano, 11, 6204 (2017).

Figures

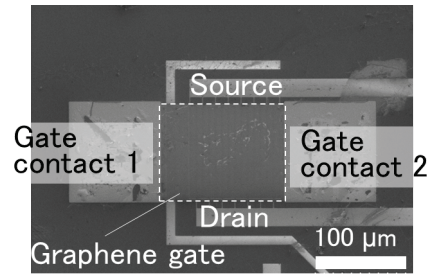
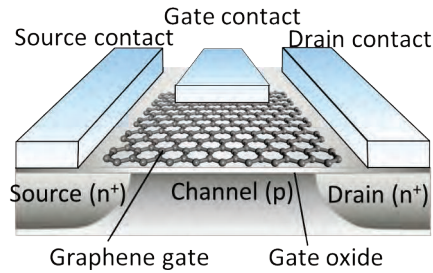


Figure 1: Schematic illustration (left) and scanning electron microscope image (right) of a gas sensor based on a graphene-gate transistor

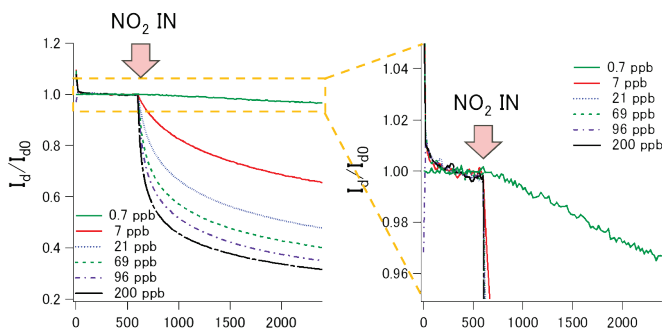


Figure 2: Dependence of the response (normalized drain current, I_d/I_{d0}) of a graphene-gate sensor on NO_2 concentrations.

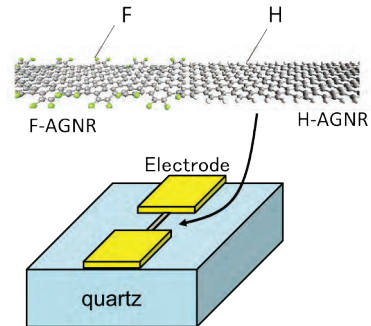


Figure 3: Schematic Illustration of a diode using a heterojunction of F-AGNR and H-AGNR concentrations.

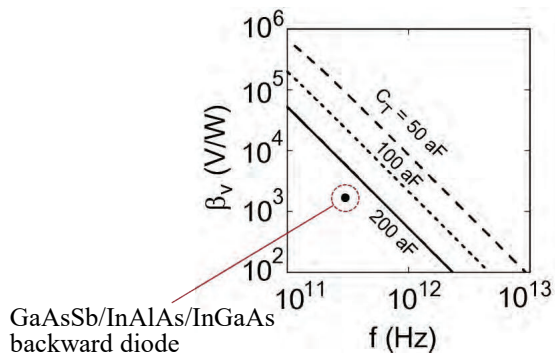


Figure 4: Calculated voltage sensitivity of a GNR backward diode, β_v , as a function of frequency with the total capacitance, C_T , as a parameter. The closed circle indicates β_v of a GaAsSb/InAlAs/InGaAs diode in Ref. 5.

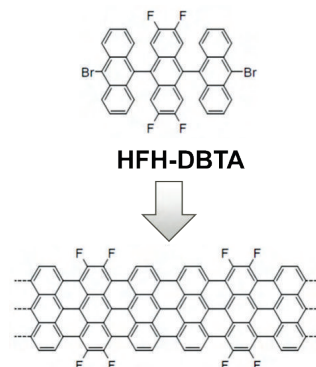


Figure 5: New precursor (above; HFH-DBTA) for synthesizing a partially F-terminated AGNR (below)

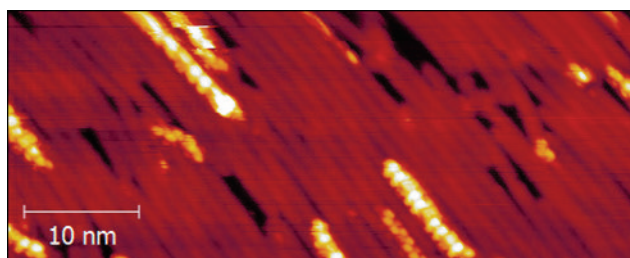


Figure 6: Locally-aligned AGNRs obtained from HFH-DBTA precursors.

Malaysia's Graphene Commercialization Progress National Graphene Action Plan 2020

NanoMalaysia's National Graphene Action Plan 2020 is supported by the country's 11th Malaysia Plan (2016-2020) as a catalytic support to expedite industrial adoption of graphene applications. Realizing the economic significance in the global market, more than 30 product development and pilot production projects have been initiated in the form of – government-industry-academia partnerships. These graphene based products are at the cusp of entering mainstream local and global markets.

References

Figures

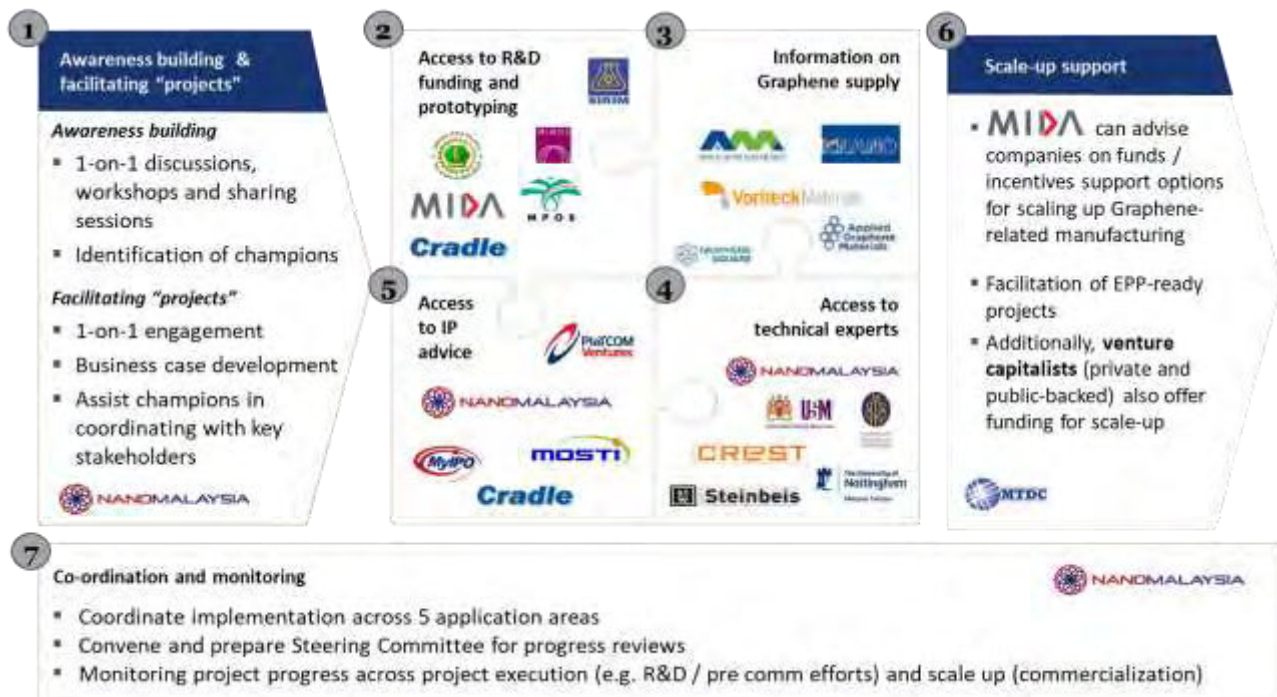


Figure 1: Framework of the National Graphene Action Plan (NGAP)

Rune Wendelbo

Samaneh Etemadi, Siamak Eqtesadi, Blerina Gjoka, Azadeh Motealleh and
Stephanie H. Santos

Abalonyx AS, Forskningsveien 1, 0373 Oslo, Norway

rw@abalonyx.no

Graphene Oxide Derivatives, Properties and Applications

Abstract

Graphene oxide, as prepared by the so called Hummers method¹ is a solid acidic compound that can be modified in a number of ways. It can be reduced, thermally, chemically or by light to become graphene-like rGO, partly reduced or fully reduced, it can be functionalized to become for example organophilic and it can be doped with N and B. The sheets can be small or large, all these variations giving rise to a family of related compounds with different properties, suitable for different application. Our company aims at offering all these varieties of GO to end-users, in Kg-quantities. In this process, it is essential to understand the stability or shelf-life of all these different forms, as well as the most suitable storage conditions. In Figure 1 and 2 below we compare dispersibility, color and X-ray diffractograms of standard graphene oxide stored for 3 months, 3 years and 6 years respectively, showing that standard GO is fairly stable for years. Now, we have undertaken a much wider study where we store a range of derivatives under different conditions (frozen, cool and ambient). These samples will be analysed regularly over the coming years in order to exactly define the changes that occur and how fast.

Potential applications of graphene oxide and graphene oxide derivatives include such diverse technologies as Load-speaker membranes, water treatment, polymer composites, protective coatings and medical. We see several applications now being piloted around the globe.

References

- [1] Hummers, William S.; Offeman, Richard E. (March 20, 1958). "Preparation of Graphitic Oxide". *Journal of the American Chemical Society*. **80** (6): 1339. Authors, Journal, Issue (Year) page (Arial Narrow 11)

Figures

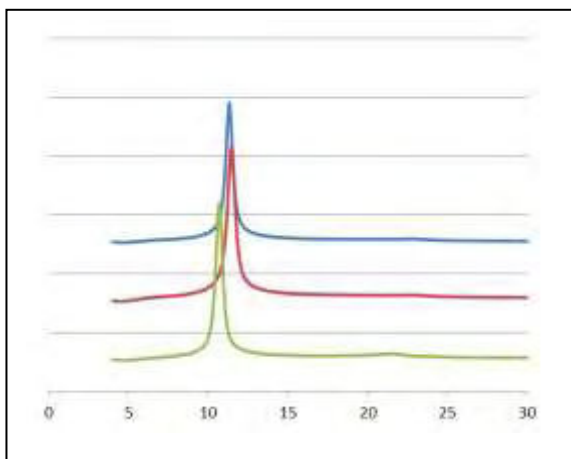


Figure 1: XRD patterns of GO aged 6, 3 and 0.3 years

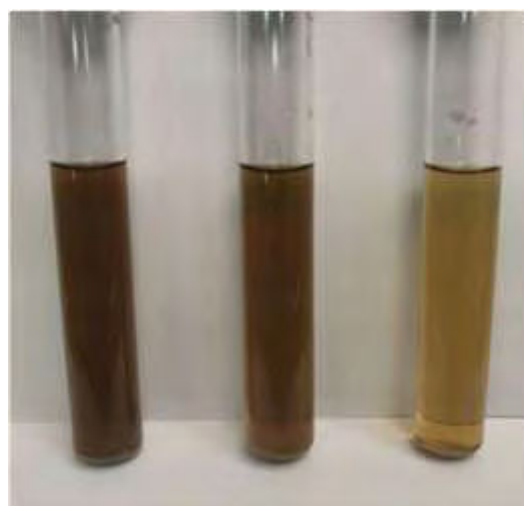


Figure 2: Suspensions of GO aged 6, 3 and 0.3 years



ORAL CONTRIBUTIONS

De-Liang Bao

Hui Chen, Dongfei Wang, Yande Que, Wende Xiao, Guojian Qian, Hui Guo, Jiatao Sun, Yu-Yang Zhang, Shixuan Du, Sokrates T. Pantelides, and Hong-Jun Gao

Institute of Physics, Chinese Academy of Sciences, 8th Nansan St. Beijing China.

dlbao@iphy.ac.cn

Fabrication of Millimeter-Scale, Single-Crystal One-Third-Hydrogenated Graphene with Anisotropic Electronic Properties

Periodically hydrogenated graphene is predicted to form new kinds of crystalline 2D materials such as graphane, graphone, and 2D C_xH_y , which exhibit unique electronic properties. Controlled synthesis of periodically hydrogenated graphene is needed for fundamental research and possible electronic applications. Only small patches of such materials have been grown so far, while the experimental fabrication of large-scale, periodically hydrogenated graphene has remained challenging. In the present work, large-scale, periodically hydrogenated graphene is fabricated on Ru(0001). The as-fabricated hydrogenated graphene is highly ordered, with a $\sqrt{3} \times \sqrt{3}/R30^\circ$ period relative to the pristine graphene. As the ratio of hydrogen and carbon is 1:3, the periodically hydrogenated graphene is named “one-third-hydrogenated graphene” (OTHG). The area of OTHG is up to 16 mm². Density functional theory calculations demonstrate that the OTHG has two deformed Dirac cones along one high-symmetry direction and a finite energy gap along the other directions at the Fermi energy, indicating strong anisotropic electrical properties. An efficient method is thus provided to produce large-scale crystalline functionalized graphene with specially desired properties.

References

- [1] Hui Chen, De-Liang Bao, Dongfei Wang, Yande Que, Wende Xiao, Guojian Qian, Hui Guo, Jiatao Sun, Yu-Yang Zhang, Shixuan Du, Sokrates T. Pantelides, and Hong-Jun Gao, *Adv. Mater.*, 30 (2018) 1801838.

Figures

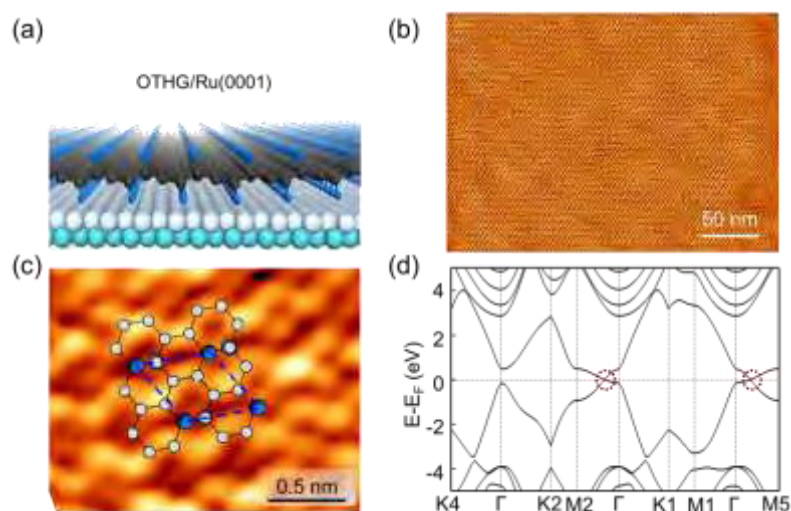


Figure 1: (a) Schematic showing the fabrication of periodically hydrogenated graphene on Ru(0001) through atomic hydrogen chemisorption. (b) A large-scale STM image of OTHG on Ru(0001), showing the formation of hexagonal patterns (Sample bias: $U = -20$ mV, Tunneling current: $I = 0.2$ nA). (c) Zoom-in STM image of the OTHG ($U = -2.0$ mV; $I = 1.0$ nA). The atomic model is superimposed on the STM image. (d) Calculated band structure of the OTHG, using the HSE06 hybrid functional method, showing anisotropic electronic properties. The two Dirac cones at E_F along two high-symmetry paths are indicated with red dashed rings.

Lihong Bao

Guocai Wang, Tengfei Pei, Ruisong Ma, Shixuan Du, Hong-Jun Gao

Institute of Physics, Chinese Academy of Sciences, Beijing, 100190, P. R. China

lhbao@iphy.ac.cn, hjgao@iphy.ac.cn

Black Phosphorus and Its Analogue: Electrical Transport Properties and Devices

Black phosphorus (BP) has attracted great attention due to its high hole mobility, and a sizable and tunable bandgap, meeting the basic requirements for logic circuits application. To realize a complementary logic operation, it needs to control the conduction type in BP FETs, *i.e.*, the dominant carrier types, holes (P-type) or electrons (N-type). Absence of reliable substitutional doping techniques makes this task a great challenge, however. In this talk, I will demonstrate that capping the thin BP film with a cross-linked poly-methyl-methacrylate (PMMA) layer can modify the conductivity type of BP by a surface charge transfer process, converting the BP layer from p-type to n-type. Combining BP films capped by cross-linked PMMA to a standard BP, a family of planar devices can be created, including BP gated diodes (rectification ratio $>10^2$), BP barristors (on/off ratio $>10^5$), and BP logic inverter (gain ~ 0.75), which are capable of performing current rectification, switching, and signal inversion operations. Furthermore, the conversion of a bidirectional rectifier to a polarity-controllable transistor in black phosphorus (BP) by dual gate modulation can be realized. Employing cross-linked PMMA as a top gate and combining it together with the global back gate of the SiO₂ substrate, well-defined unipolar transport (n- or p-type) in BP could get accessed.

References:

1. L. H. Bao, H. -J. Gao et al. Nano Letter 16, 6870 (2016).
2. L. H. Bao, H. -J. Gao et al. Adv. Electron Mater. 2, 1600292 (2016).
3. L. H. Bao, H. -J. Gao et al. 2D Mater. 4, 025056 (2017).

Carla Bittencourt¹

Malamatenia A. Koklioti², Xavier Noirfalise³, Izcoatl Saucedo⁴, Mildred Quintana⁴
and Nikos Tagmatarchis²

¹ University of Mons, Mons, Belgium

² Theoretical and Physical Chemistry Institute, National Hellenic Research Foundation, Athens, Greece

³ Materia Nova Research Center, Mons, Belgium

⁴ Universidad Autónoma de San Luis Potosí, San Luis Potosí, Mexico

carla.bittencourt@umons.ac.be

Molybdenum Disulfide as Surface Enhanced Raman Scattering Substrates for Sensing Polycyclic Aromatic Hydrocarbons

Transition metal dichalcogenides (TMDs) are at the forefront of the current research investigations of 2D layered materials beyond graphene [1]. Various methodologies for exfoliating TMDs have already been developed, mainly based on wet chemistry approaches allowing mass production of material suitable for basic research and proof-of-concept studies. Recently, the potential use of TMDs as SERS platforms promoting stable physicochemical tethering of aromatic molecules onto their surface have been announced, however, the Raman enhancement for organic species still modest [2]. In order to improve the SERS effect, TMDs need to be functionalized, for example by decoration with metal nanoparticles [3]. Different synthetic strategies have been employed for the fabrication of TMD-based SERS substrates ranging from simple wet chemistry procedures to sophisticated ones, involving micropatterning. Alternatively, oxygen and argon plasma treated MoS₂ sheets have been also examined, in which the creation of local dipoles resulted in enhanced SERS phenomena on MoS₂ surface [4]. Based on the aforementioned points, the preparation of robust sensing platforms using TMDs still remains a daunting challenge.

Herein, we report a simple one-pot functionalization of few-layered MoS₂ sheets, using nitrogen plasma treatment and simultaneous decoration with silver nanoparticles (Ag_{NPs}). The successful surface modification was evaluated through Raman and X-ray photoelectron spectroscopy (XPS), while transmission electron microscopy (TEM) imaging verified the decoration with Ag_{NPs}. N-MoS₂/Ag_{NPs} nano hybrids were employed as SERS substrates to detect Rhodamine B (RhB) at very low-concentration. Charge-transfer phenomena between RhB and N-MoS₂/Ag_{NPs}, along with the polarized character of the hybrid system, causing dipole-dipole coupling interactions, were associated to the Raman signal enhancement. Finally, considering the coordination of aromatic moieties via π -S interactions with TMDs, we used N-MoS₂/Ag_{NPs} hybrids, prepared with different functionalization parameters, as substrate for the sensitive recognition at low levels of polycyclic aromatic hydrocarbons. These widespread organic pollutants in the atmosphere are known to be highly carcinogen and mutagen species [5], therefore the engineering of highly-sensitive sensors capable of in-situ detection is a key technology for helping innovative environmental security policies. To this end we have investigated the performance of the N-MoS₂/Ag_{NPs} nano hybrids towards the detection of three hazardous aromatic hydrocarbons: pyrene, anthracene and 2,3-dihydroxy naphthalene were investigated, observing a sensitive detection at very low levels.

Rhodamine B (RhB), a Raman probe molecule, was selected as model analyte. For comparison, RhB was drop-casted onto bare Si as well as onto exfoliated MoS₂ (i.e. non-modified) and N-MoS₂/Ag_{NPs} for Raman signal detection. The Raman spectrum of the dye adsorbed on the Si substrate showed only a strong fluorescent background, while the Raman spectrum of RhB deposited onto as-exfoliated MoS₂ showed low intensity bands.

In sharp contrast, when SERS measurements were performed on N-MoS₂/Ag_{NPs} high intensity bands were observed (Fig. 1). The recorded Raman spectrum of RhB, shows distinct modes at 625 cm⁻¹ (C–C–C ring in plane bending), 760 cm⁻¹ (C–H out of plane bending), 943 cm⁻¹ (C–H stretching), 1195 cm⁻¹ (C–H in plane bending), 1278 cm⁻¹ (C–O–C stretching), 1360 cm⁻¹, 1505 cm⁻¹, 1563 cm⁻¹, 1648 cm⁻¹ (aromatic C–C stretching) and 1594 cm⁻¹ (C=C stretching), in full agreement with previous reports [6]. Focusing on the 1648 cm⁻¹ band, the SERS signal was enhanced by 8 times for the 10 s nitrogen plasma silver decorated substrates compared to the substrates functionalized only 5 s. This result emphasizes the influence of the amount of nitrogen-grafting and silver-nanoparticles size on MoS₂ in the Raman enhancement for detecting RhB. We choose the substrate with higher enhancement factor for SERS sensing of small quantities of pyrene, anthracene and 2,3-dihydroxy naphthalene.

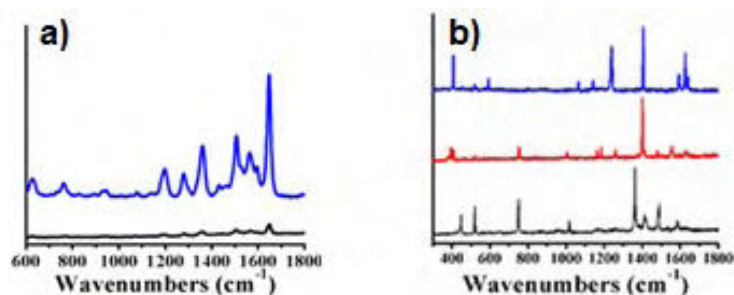


Figure 1: SERS spectra (514 nm) of (a) aqueous RhB (10⁻⁵ M) on exfoliated MoS₂ (black), and N-MoS₂/Ag_{NPs} (blue) substrates. b) pyrene (blue), anthracene (red) and 2,3-dihydroxy naphthalene (black) at 10⁻⁵ M deposited onto N10-MoS₂/Ag_{NPs} substrate.

The Raman spectra of the studied polyaromatics are governed by strong fluorescence background, making impossible the detection of characteristic Raman signals. However, in the recorded SERS spectrum of pyrene using N-MoS₂/Ag_{NPs} as substrate, seven distinctive modes at 407, 592, 1241, 1406, 1592, 1627, and 1643 cm⁻¹ can be identified, while for anthracene and 2,3-dihydroxy naphthalene bands at 752, 1006, 1183, 1402 and 1557 cm⁻¹ and at 448, 750, 1363, 1412, 1488 and 1585 cm⁻¹, were respectively observed. These bands can be divided into three main regions: (a) bands below 550 cm⁻¹, which are attributed to C–C out-of-plane bending vibrations, (b) bands at 600–1000 cm⁻¹ which are associated with C–H out-of-plane bending and at 1000–1300 cm⁻¹, which are related to C–H in-plane bending and rocking, and (c) bands at 1300–1650 cm⁻¹, which are due to aromatic C–C stretching [7]. These results testify the use of MoS₂ functionalized with nitrogen and silver particles as an effective SERS platform for the sensitive detection of polycyclic aromatic hydrocarbons. It is important to mention that the SERS detection of polycyclic aromatic hydrocarbons by other substrates requires special modification methodologies of metal nanoparticles to ensure effective interaction between the substrate and the analyte, as the aromatic rings exhibit low affinity for metals [8,9]. However herein, π -S interactions with MoS₂ were exploited, therefore the SERS application of functionalized TMDs as analytical, environmental and biomedical sensors can be envisioned.

References

- [1] Huang, X.; Zeng, Z.; Zhang, H., *Chem. Soc. Rev.*, 42 (2013) 1934
- [2] Ling, X.; Fang, W.; Lee, Y.-H.; Araujo, P. T.; Zhang, X.; Rodriguez-Nieva, J. F.; Lin, Y.; Zhang, J.; Kong, J.; Dresselhaus, M. S., *Nano Lett.*, 14 (2014) 3033
- [3] Jain, P. K.; Huang, X.; El-Sayed, I. H.; El-Sayed, M. A., *Plasmonics*, 2 (2007) 107
- [4] Sun, L.; Hu, H.; Zhan, D.; Yan, J.; Liu, L.; Teguh Jefri, S.; Yeow Edwin, K. L.; Lee Pooi, S.; Shen, Z., *Small*, 10 (2014) 1090
- [5] Conney, A. H. *Cancer Res.*, 42 (1982) 4875
- [6] Michaels, A. M.; Nirmal, M.; Brus, L. E., *J. Am. Chem. Soc.* 121 (1999) 9932
- [7] Long, D. A. *J. Raman Spectrosc.*, 35 (2004) 905
- [8] Guerrini, L.; Garcia-Ramos, J. V.; Domingo, C.; Sanchez-Cortes, S., *Anal. Chem.* 81 (2009) 953
- [9] Xie, Y.; Wang, X.; Han, X.; Song, W.; Ruan, W.; Liu, J.; Zhao, B.; Ozaki, Y., *J. Raman Spectrosc.*, 42 (2010) 945

Hui Chen

Yande Que, Lei Tao, Dongfei Wang, Wende Xiao, Yu-Yang Zhang, Shixuan Du*,
Socrates T. Pantelides, Hong-Jun Gao*

Institute of Physics & University of Chinese Academy of Sciences, Chinese Academy of Sciences, Beijing
100190, China

Department of Physics and Astronomy, Vanderbilt University, Nashville, Tennessee 37235, USA

sxdu@iphy.ac.cn; hjgao@iphy.ac.cn

Recovering edge states of graphene nanoislands on Ir(111) by silicon intercalations

It has been predicted by theory that free-standing graphene nanoribbons with zigzag edges have spin-polarized edge states with a promise for applications [1]. However, it has been widely reported that graphene nanoislands (GNIs) on metal substrates have no states that are localized at zigzag edges because of interaction with substrate electrons. Here, we demonstrate that edge states of GNIs with zigzag edges on Ir(111) can be recovered by intercalating a layer of Si atoms between GNIs and the Ir substrate. Using scanning tunneling microscopy and spectroscopy, in combination with density functional theory calculations, we show that GNIs are effectively decoupled from the Ir substrate by the intercalated Si layer, leading to the recovery of edge states that were originally suppressed by graphene-substrate interaction. We also find that edge states gradually shift to the Fermi level with increasing lateral sizes of the GNIs. In addition, theoretical calculations show that edge states of some irregular GNIs are spin-polarized, which suggests an avenue for construction of graphene-based spintronic devices.

References

- [1] P. Ruffieux *et al.* Nature 531 (2016), 489–492
- [2] Y. Li. *et al.* Adv. Mater. 25 (2013), 1967–1972
- [3] H. Chen *et al.* Nano Research 11 (2018), 3722

Figures

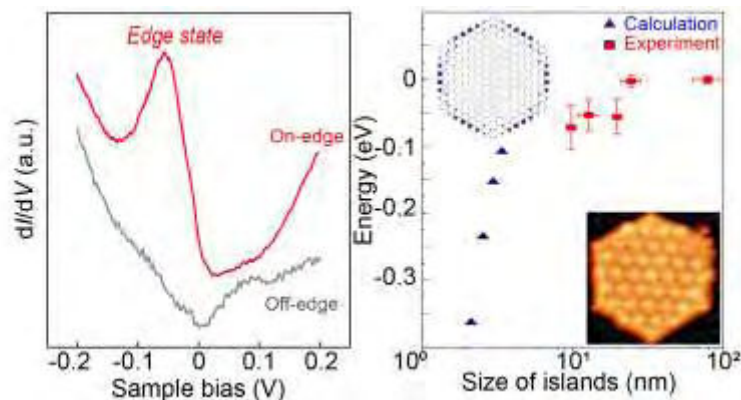


Figure 1: Appearance of edge states on the zigzag edge of GNI after Si intercalation. Right panel: The energy of the edge states versus lateral size of GNIs for both theoretical and experimental results

High Brightness Blue/UV Light-Emitting Diodes Enabled by Directly Grown Graphene Buffer Layer

Single-crystalline group-III nitrides (III-Ns, i.e. GaN, AlN) based light-emitting diodes (LEDs) with high-efficiency and long lifetime are the most promising solid-state lighting source compared with conventional incandescent and fluorescent lamps.^[1] However, the lattice and thermal mismatch between III-Ns and sapphire substrate always induce high stress and high density of dislocations and thus degrade the performance of LEDs.^[2] Here, we report the growth of high-quality III-Ns films with low-stress and low density of dislocations on graphene (Gr) buffered sapphire substrate for high-performance LEDs. Gr films are directly grown on sapphire substrate to avoid the tedious transfer process and III-Ns is grown by metal-organic chemical vapor deposition (MOCVD). The introduced Gr buffer layer greatly releases biaxial stress and reduces the density of dislocations in III-Ns film and multiple quantum well structures. The as-fabricated LED devices therefore deliver much higher light output power compared to that on bare sapphire substrate, which even outperforms the mature process derived counterpart. The III-Ns growth on Gr buffered sapphire only requires one-step growth, which largely shortens the MOCVD growth time. This facile strategy may pave a new way for applications of Gr films and bring several disruptive technologies for epitaxial growth of GaN film and its applications in high-brightness LEDs.

References

- [1] Kim, Y. et al. Nature 544 (2017), 340–343.
- [2] Chen, Z. L. & Liu, Z. F. et al. Adv. Mater., 30 (2018), 1801608.

Figures

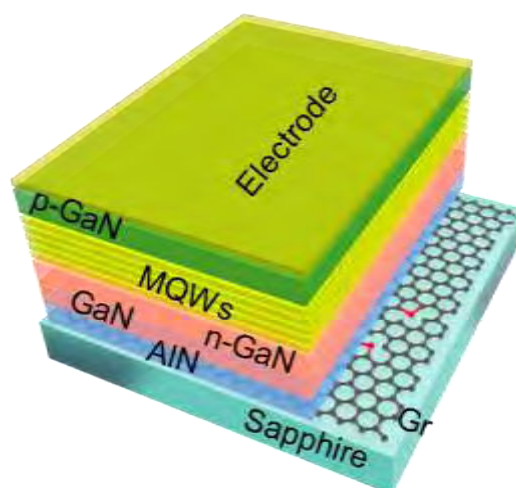


Figure 1: The structure of LEDs grown on Gr/sapphire substrates.

Zongping Chen

School of Materials Science and Engineering, Zhejiang University
38 Zheda Road, Hangzhou 310027, China

chenzp@zju.edu.cn

Precision synthesis of structurally defined graphene nanoribbons by chemical vapor deposition

Graphene nanoribbons (GNRs), quasi-one-dimensional narrow strips of graphene, have shown great promise for use as advanced semiconductors in electronics. Compared with the lack of structural control in GNRs fabricated by “top-down” approaches, atomically precise GNRs can be “bottom-up” synthesized by surface-assisted assembly of molecular building blocks¹. Such “bottom-up” synthesized ultranarrow (~1-2 nm) GNRs have demonstrated a wide range of bandgaps with visible to near-infrared absorption, rendering them highly interesting for a broad range of applications in next-generation transistors, as well as optoelectronic and photonic devices.

To establish facile and scalable on-surface synthesis of GNRs for real device applications, we demonstrate here an efficient chemical vapor deposition (CVD) process for inexpensive and high-throughput growth of structurally defined GNRs over large areas even under ambient-pressure conditions. This “bottom-up” CVD method allows the growth of chevron-type GNRs², armchair GNRs with various width³, N-doped GNRs as well as their heterojunctions, demonstrating the versatility and scalability of this process, which provides access to a broad class of GNRs with engineered structures and properties based on molecular-scale design. Moreover, with the CVD method, we have also recently demonstrated the highly efficient lateral fusion of armchair GNRs into wider GNRs, under the CVD growth at higher temperature⁴. The large-area availability of the CVD-synthesized GNR films enabled also the device integration and studies¹. The FET devices built on the transferred GNRs exhibited a high current on/off ratio of >6000, and a high photoresponsivity of ~105 A/W for small incident power in the visible-UV range, which is 8 orders of magnitude higher than the devices based on graphene. These results pave the way toward the scalable and controllable growth of GNRs, and provide practical solutions to the current challenges in graphene-based nanoelectronic, optoelectronic and photonic devices.

References

- [1] Talirz, L., Ruffieux, P. & Fasel, R. On-surface synthesis of atomically precise graphene nanoribbons. *Adv. Mater.* 28, 6222-6231 (2016).
- [2] Chen, Z. et al. Synthesis of graphene nanoribbons by ambient-pressure chemical vapor deposition and device integration. *J. Am. Chem. Soc.* 138, 15488-15496 (2016).
- [3] Chen, Z. et al. Chemical vapor deposition synthesis and terahertz photoconductivity of low-bandgap $n = 9$ armchair graphene nanoribbons. *J. Am. Chem. Soc.* 139, 3635-3638 (2017).
- [4] Chen, Z. et al. Lateral fusion of chemical vapor deposited $n = 5$ armchair graphene nanoribbons. *J. Am. Chem. Soc.* 139, 9483-9486 (2017).

Circular Photogalvanic Photocurrents in 2D Materials

Helicity dependent photocurrent (PC) is the electric current generated by elliptically polarized light incident on to sample plane. For the circular polarized light absorption, based on particular directions of optical field and the point group symmetries of the material, this PC can be mainly due to the circular photogalvanic effect (CPGE). The PC due to the CPGE has been studied in detail for III-V and II-VI semiconductor quantum wells as one kind of spin PCs in those materials. Recently, the CPGE current in 2D materials has attracted attention and been observed for oblique incidence and excitation perpendicular to the direction of current. Here first we provide a review about the CPGE current in 2D materials, starting with observation in graphene which has weak spin orbit coupling. The microscopic origin of the CPGE current in graphene is due to the quantum interference between Drude transitions and indirect intraband transition with intermediate states [1]. Then we demonstrate that in single layer graphene (1LG), bilayer graphene (2LG) [2], the carrier density dependence of the CPGE current follows the Fermi-Dirac distribution, as expected. Unlike 1LG, 2LG, and ABA stacked 3LG cases, the large enhancement of the CPGE current in ABC stacked 3LG is attributed to the coexistence of band gap opening and restored inversion symmetry [3]. On the other hand, monolayer transition metal dichalcogenide semiconductors, such as MoS₂, have a large direct band gap in their K valley, broken inversion symmetry and strong spin orbit coupling. They also exhibit CPGE current as a result of giant spin-valley coupling which can be controlled by circularly polarized light and global back-gating. A large CPGE current polarization was observed for excitation on π -resonance with exciton, which is negligible for off-resonance excitation [4]. Also a large on-off ratio of CPGE current as a function of carrier density was reported [5]. We also discuss the modulation of the CPGE current in monolayer MoS₂ upon doping with magnetic elements.

References

- [1] Jiang C. et al. *Physical Review B*, 84 (2011) 125429.
- [2] Qian X. et al. *Semiconductor Science and Technology*, (2018) just accepted.
- [3] Cao B. Et al. *European Graphene Forum proceedings*, (2017).
- [4] Eginligil et al. *Nature Communications*, 6 (2015) 7636.
- [5] Liu L. et al. *Bulletin of American Physical Society*, (2017) BAPS.2017.MAR.B33.4

Graphene Oxide acidity modifications

Graphene oxide (GO) as prepared by the “Hummers method”¹ is a solid acid with up to 2 mmol acid sites per gram. The acid sites are of various nature, but mostly carboxylic and hydroxylic groups (Fig.1). GO and GO-derivatives have been reported to have potential for a range of applications, such as corrosion protection, water treatment, composites, lubricants, energy storage, photo-catalysts, sensors, sports equipment, elastomers and load speaker membranes. For some of these applications, pH adjustment can be needed. In this study, we review how acidity can be adjusted by washing and by neutralization with bases, and how this affects fundamentally important properties such as dispersibility. Titration curves for “standard” GO and “water washed” GO are shown in Fig. 2, the standard GO having about 1.4 mmol acid sites per gram and the water washed GO having about 0.4 mmol acid sites per gram. From an industrial perspective, concerns, apart from relevant chemistry are costs, availability and hazards. Costs will inevitably come down with increased production volumes, to as little as 2 - 3 % of today’s price, according to our estimates. The keys to cost reduction are economy of scale and automation.

References

1. Hummers, William S.; Offeman, Richard E. (March 20, 1958). "Preparation of Graphitic Oxide". *Journal of the American Chemical Society*. **80** (6): 1339.

Figures

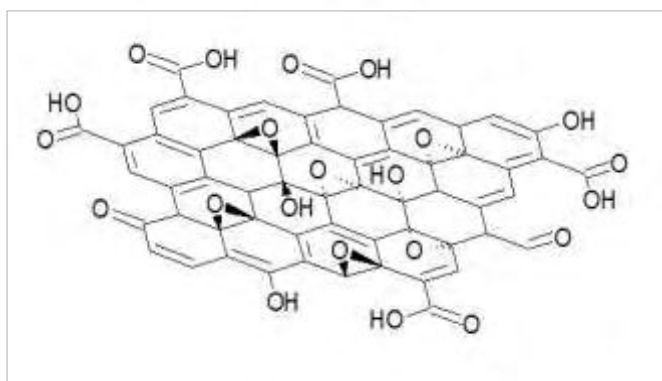


Figure 1: Schematic illustration of functional groups on GO.

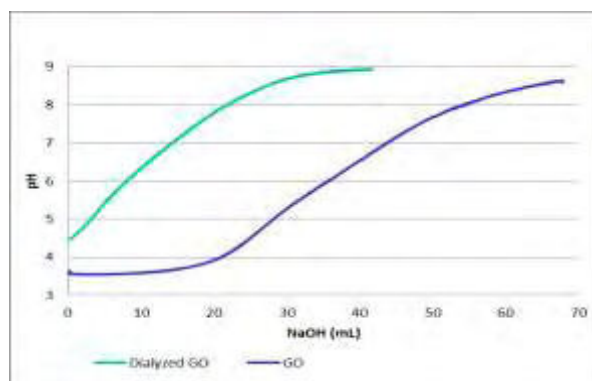


Figure 2: Titration curves for as produced GO compared to water-washed GO, 0.025 % dispersions titrated with NaOH.

Fengxia Geng

Tatsumasa Hoshide, Zhiqiang Wang, Weihong Liu, Takayoshi Sasaki
Soochow University, 199 Renai Road, Suzhou, China.

Contact: gengfx@suda.edu.cn

Novel Inorganic Layered Materials: From Interlayer Chemistry, Delamination, toward Energy Storage Applications

Molecularly thin two-dimensional (2D) nanomaterials, such as graphene and other inorganic analogues, delaminated from the corresponding three-dimensional counterparts with lamellar structures, are emerging as one of the most prevalent materials for their superior properties in diverse applications. The delamination arises from the unique structural characteristics of the layered parent precursor, that is, strong covalent bonding in the layers while weak van der Waals or electrostatic attractions between layers, resulting in easy interlayer expansions and even delaminations. In this talk, I will start by our study on how layered materials swell and what controls the reactions, which is critical to producing high-quality sheet materials.[1-2] It was found that the swelling behavior was regulated by the acid-base reaction and the osmotic pressure equilibrium, which are both substantially unselective and only molarity dependent. However, the nature of the intercalated ion was critical to the stability of the resulting swollen structure; that is, ions of higher polarity and smaller size help stabilize the highly expanded structure, while ions of low polarity and larger size readily lead to exfoliation. With the swelling and delamination rules, I will then move onto producing new 2D sheets, for example, titanium carbides covered with Al oxoanions showing strong optical absorption, particularly at near-infrared region.[3-5] Traditional methods in fabricating 2D MXene materials inevitably use highly noxious and strongly corrosive acid. Utilizing the amphoteric nature of interlayer Al and taking an organic base as the etchant, simultaneous surface functionalization by the hydrolyzed $\text{Al}(\text{OH})_4^-$ and intercalation of bulky ion into the gallery space was achieved, readily producing monolayer Ti_3C_2 sheets. Finally, the nanosheets were assembled into macroscopic structure directed to energy storage applications.[6-8] Employing the two-dimensional sheet form of titanium oxide, for the first time macroscopic fiber of titanium oxides was developed through a scalable wet-spinning process. Despite of the intrinsically weak Ti-O bond in molecular titania sheets, the optimal fiber manifested mechanical performance comparable to that documented for pristine fiber of graphene or carbon nanotubes, which should be credited to the highly-aligned stacking manner and enhanced sheet-to-sheet binding interactions. By a further in situ conformal hybridization with reduced graphene oxide, serving as efficient current collectors, a novel fiber electrode was obtained displaying excellent mechanical properties combined with favorable electrochemical performance in lithium-ion battery. Importantly, the storing capacities per unit length were especially competitive, considering the high linear densities of active materials as well as their close contact with current collectors, for which the powering period of an LED light could be extended from several seconds only up to >5 h.

References

- [1] F. X. Geng, R. Z. Ma, A. Nakamura, K. Akatsuka, Y. Ebina, Y. Yamauchi, N. Miyamoto, Y. Tateyama, T. Sasaki, *Nat. Commun.*, 4 (2013) 1632.
- [2] F. X. Geng, R. Z. Ma, Y. Ebina, Y. Yamauchi, N. Miyamoto, T. Sasaki, *J. Am. Chem. Soc.*, 14 (2014), 5491.
- [3] J. N. Xuan, Z. Q. Wang, Y. Y. Chen, D. J. Liang, L. Cheng, X. J. Yang, Z. Liu, R. Z. Ma, T. Sasaki, F. X. Geng, *Angew. Chem. Int. Ed.*, 47 (2016) 14569.
- [4] W. H. Liu, Z. Q. Wang, Y. L. Su, Q. W. Li, Z. G. Zhao, F. X. Geng, *Adv. Energy Mater.* 22 (2017) 1602834.
- [5] Z. Q. Wang, J. N. Xuan, Z. G. Zhao, Q. W. Li, F. X. Geng, *ACS Nano* 11 (2017) 11559.
- [6] T. Hoshide, Y. C. Zheng, J. Y. Hou, Z. Q. Wang, Q. W. Li, Z. G. Zhao, R. Z. Ma, T. Sasaki, F. X. Geng, *Nano Lett.*, 6 (2017) 3543.

- [7] J. Y. Hou, Y. C. Zheng, Y. L. Su, W. K. Zhang, T. Hoshida, F. F. Xia, J. S. Jie, Q. W. Li, Z. G. Zhao, R. Z. Ma, T. Sasaki, F. X. Geng, *J. Am. Chem. Soc.*, 40 (2015) 13200.
- [8] N. Liu, Z. Q. Wang, Z. Wang, J. S. Xia, Y. Chen, Z. G. Zhao, Q. W. Li, F. X. Geng, *ACS Nano* 8 (2017) 7879.

Figures

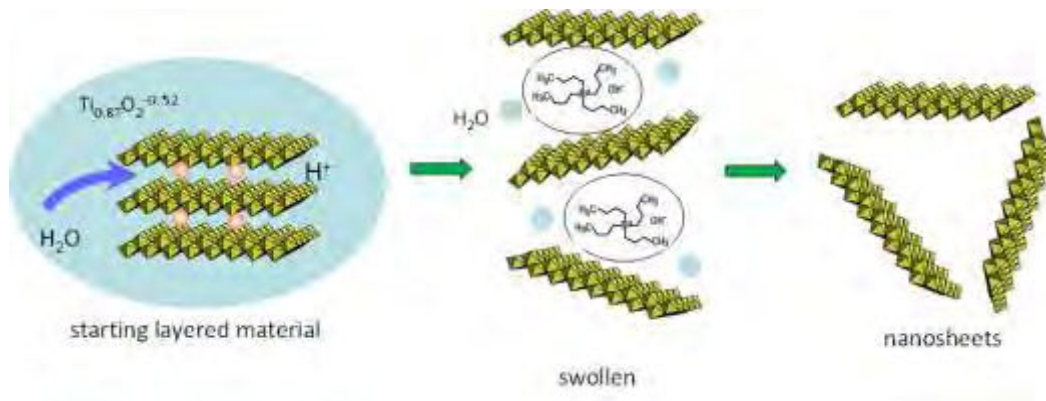


Figure 1: Delamination process of a layered structure.

Mohan Kumar Ghimire

Hamza Zad Gul, Hojoon Yi, Dang Xuan Dang, Wonkil Sakong, Nguyen Van Luan,
Hyun Jin Ji

Sungkyunkwan University, Gyeonggi do, Suwon, South korea

ghimiremohankumar@gmail.com

Graphene-CdSe quantum dot hybrid as a platform for the control of carrier temperature

In a graphene and quantum dots (QDs) hybrid structure, the graphene is known to play the role of an electrode that conducts the photoexcited carriers from the QDs to the electrodes. Thus, the yield of photocurrent of the QD ensemble is greatly enhanced [1]. However, in our study, the graphene provides a platform to control the energy relaxation of optically excited carriers from QDs. Thus, the temperature of photocarriers of QDs is controllable. Due to the moderate carrier temperature, the observed photocurrent from the hybrid structure reveals a photothermoelectric effect, which becomes even stronger when the Fermi energy, E_F , is located near the charge neutrality point (CNP) of the graphene. However, the photothermoelectric behavior weakens with increased E_F . Such a behavior originates from the varying electron-phonon coupling strength that is dependent upon E_F of the graphene [2].

References

- [1] S.H. Cheng, T.M. Weng, M.L. Lu, W.C. Tan, J.Y. Chen, Y.F. Chen, Nat. Sci. Rep.3 (2013) 2694.
- [2] M.K. Ghimire, H.Z. Gul, H. Yi, D.X. Dang, W. Sakong, N.V. Luan, H.J. Ji, S. C. Lim, FlatChem 6 (2017) 77-82.

Figures

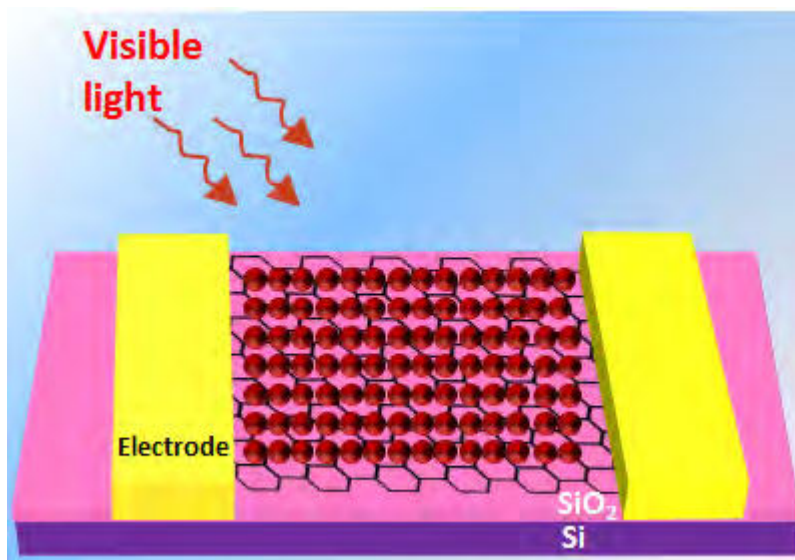


Figure 1: Schematic diagram showing light shining on graphene-CdSe QD hybrid FET

Hao-Lin Hsu¹

Chung-Yih Kuo², Jean-Hong Chen^{1, 4*}, Jih-Mirn Jehng³, Kai-Ying Liang⁴,
Ren-Long Zhang⁴ and Tian-Yi Zhou⁴

¹ Green Energy Technology Research Center, Kun Shan University, Tainan, Taiwan, R.O.C.

² Health Technology Center, Chung Shan Medical University, Taichung, Taiwan, R.O.C.

³ Department of Chemical Engineering, National Chung Hsing University, Taichung, Taiwan, R. O. C.

⁴ Department of Material Engineering, Kun Shan University, Tainan, Taiwan, R.O.C.

diago661228@gmail.com or kelvench@mail.ksu.edu.tw

Application of Carbon Aerogel in the Adsorption of Polycyclic Aromatic Compounds from Diesel Exhaust

Graphene-based materials, such as graphene oxide (GO) [1], reduced graphene oxide [2] and carbon aerogel (CA) [3], have attracted worldwide attention in recent years because of their outstanding properties. Graphene exhibits excellent physical and chemical properties and can be easily modified [4]. Graphene and graphite oxide materials exhibit excellent performance in adsorption with polycyclic aromatic hydrocarbons (PAHs) and their derivatives [5, 6]. In Taiwan, the number of car and motor vehicles has been progressively increasing. Moreover, the exhaust gases emitted by vehicles often contains many pollutants, including metal elements, suspended particular matter, volatile organic pollutants and PAHs etc [7]. Vehicular emissions of particulate and gas-phase PAHs are of particular interest because of their potentially toxic and probable human carcinogenic compounds [8]. Furthermore, rapid vehicular growth rate has increased vehicular emissions, which have become one of the principle anthropogenic sources of PAHs. Polyurethane foam (PUF) and commercial XAD polymer resin are the adsorbents announced by the EPA. In this study, we present reusable and efficient carbon aerogel (CA) adsorbent for particulate and gas-phase PAHs emitted from diesel vehicles. We demonstrate that CA material is highly adsorption efficiency for human carcinogenic compounds. Because of superior adsorption capacity of PAHs, CA is possible to be the excellent environmental and air pollution adsorbent material in the future.

References

- [1] D. C. Marcano et. al, ACS Nano 4, (2010) 4806.
- [2] H. He et. al, Chem. Mater. 22, (2010) 5054.
- [3] W. Wan et. al, Environ. Sci.: Nano 3, (2016) 107.
- [4] A. K. Geim, Science 324, (2009) 1530.
- [5] L. Li et. al, J. Environ. Qual. 42, (2013) 191.
- [6] J. Wang et. al, Environ. Sci. Technol. 48, (2014) 4817.
- [7] S. Chang et. al, J. Environ. Sci. Health C 27, (2009) 141.
- [8] C. Kuo et. al, Environ. Geochem Health 34, (2012) 77.

Printed Graphene For Chipless RFID Applications

Abstract

This paper presents screen printed graphene for chipless RFID applications. The highly conductive ink consists of multi-layer graphene nanoflakes and has been formulated specially for screen printing printed electronics. The frequency selective surfaces (FSS) periodic arrays are screen-printed on normal paper and attached onto FR4 for measurement. The measurement results show that the simple structure can encode 2 bits, indicating that screen printed graphene can be a viable solution to low-cost chipless RFID applications. In recent years, researchers have been trying to develop chipless RFID tags, often involving not printable patterns and complex decoding mechanisms [1]. The costs of the tags are mainly dependent on the cost of the IC chips as the mass production of transponder antennas is relatively cheaper. Additionally, the assembling implementation processes of the chips onto the tag antennas and the additional transportation add more cost down the production line. Hence, efforts have been put in developing chipless RFID tags without ICs, which means that the main cost of the tag can be removed.

The tagging of extremely low cost paper/plastic based items demands a fully passive and printable chipless tag as a low-cost, robust solution for simple applications. The primary potential benefit of the chipless tags is their capability to be directly printed on inventory items for a lower cost, providing a good alternative for traditional RFID tags with IC chips. For many applications, such as small business company applications and identifying classes of objects, a large ID string is not necessary.

The screen printed graphene technique has been reported in [2-4]. Different to antennas, printed graphene FSS arrays for chipless RFID applications are presented in this work. Frequency selective surfaces (FSS) are periodic structures that function as filters for microwave frequency waves. The resonating nature of these periodic structures at specific frequencies has been used as frequency selective filters and electromagnetic interference (EMI) shielding applications. Each data bit can be associated with the presence or absence of a resonant peak at a predetermined frequency in the spectrum by adding or reducing the resonating structures [5]. These tags have the advantage of extremely low fabrication costs benefiting from printed graphene technology and the chipless structure. The periodic FSS structure consists of concentric rings of different radius as multiple resonances are created. The ring structure has the advantage of its small length in terms of wavelength [6]. For the circular element, its length should be a multiple of half wavelength for resonance [7]. The resonance frequency is a function of the equivalent inductance L_{eq} and equivalent capacitance C_{eq} of the concentric rings. It should be noted that L_{eq} and C_{eq} are related to the radii and width of the rings, and the distance between the rings [8]. The structure of the samples prepared are shown in Fig.1(a). The sizes of the concentric rings are chosen to respond to the measurement range 2.6 to 3.95 GHz. Fig. 2(b) shows the Scanning Electron Microscope(SEM) image of the highly conductive printed graphene sample, showing the compact structure after compression.

A pair of identical standard gain horn antennas (2.95 – 3.95 GHz) are connected to measure the transmission(%) from antenna 1 to antenna 2 using a vector network analyzer (VNA), (FieldFox N9918A). A TRL (Thru-Reflect-Line) calibration was made for the cables to ensure the accuracy of the measurement. The measurement was first made without the printed graphene sample (DUT, device under test), then the DUT was pasted onto FR4 board (thickness:1.6 mm) to measure the transmission coefficients. When DUTs is absent, the

transmission is firstly measured from 2 to 5 GHz. This data is saved as reference. The measured transmission from antenna 1 to antenna 2 for different configurations then are normalized using the reference data to extract the response when the DUT is present. Fig. 1(c) shows the calculated transmission for different configurations. It can be seen that when the ring responsible for bit 1 is present, a resonance peak appears, same as the bit 2 ring, revealing the data bits can be encoded by adding or reducing the resonating structures. A 70% transmission can serve as a guidance line to observe the resonance as shown in Fig.1(c).

However, the resonant peak for bit 2 is relatively low due to the thin printed ring. The prepared sample's sheet resistance is measured to be 3 Ohms/sq. The small ring's resistivity is too high to resonate hence the lower resonant peak. This should be further addressed in future designs.

These results have proven that the screen printed graphene can provide bit encoding by its printed periodic structures. This is useful for chipless RFID applications in small business.

References

- [1] K. Finkenzeller and D. Müller, RFID handbook. Chichester: Wiley, 2012.
- [2] X. Huang, T. Leng, X. Zhang, J. Chen, K. Chang, A. Geim, K. Novoselov and Z. Hu, 'Binder-free highly conductive graphene laminate for low cost printed radio frequency applications', Appl. Phys. Lett., vol. 106, no. 20, p. 203105, 2015.
- [3] T. Leng, X. Huang, K. Chang, J. Chen, M. Abdalla and Z. Hu, "Graphene Nanoflakes Printed Flexible Meandered-Line Dipole Antenna on Paper Substrate for Low-Cost RFID and Sensing Applications", IEEE Antennas and Wireless Propagation Letters, vol. 15, pp. 1565-1568, 2016.
- [4] X. Huang, T. Leng, K. Chang, J. Chen, K. Novoselov and Z. Hu, "Graphene radio frequency and microwave passive components for low cost wearable electronics", 2D Materials, vol. 3, no. 2, p. 025021, 2016.
- [5] F. Costa, S. Genovesi and A. Monorchio, "A Chipless RFID Based on Multiresonant High-Impedance Surfaces", IEEE Transactions on Microwave Theory and Techniques, vol. 61, no. 1, pp. 146-153, 2013.
- [6] B. Munk, Frequency Selective Surfaces. Hoboken: John Wiley & Sons, 2005.
- [7] J. Huang, Te-Kao Wu and Shung-Wu Lee, "Tri-band frequency selective surface with circular ring elements", IEEE Transactions on Antennas and Propagation, vol. 42, no. 2, pp. 166-175, 1994.
- [8] S. Can, E. Karakaya, F. Bagcı, A. Yilmaz and B. Akaoglu, "Dual-Band Double-Cylindrical-Ring 3D Frequency Selective Surface", ETRI Journal, vol. 39, no. 1, pp. 69-75, 2017.

Figures

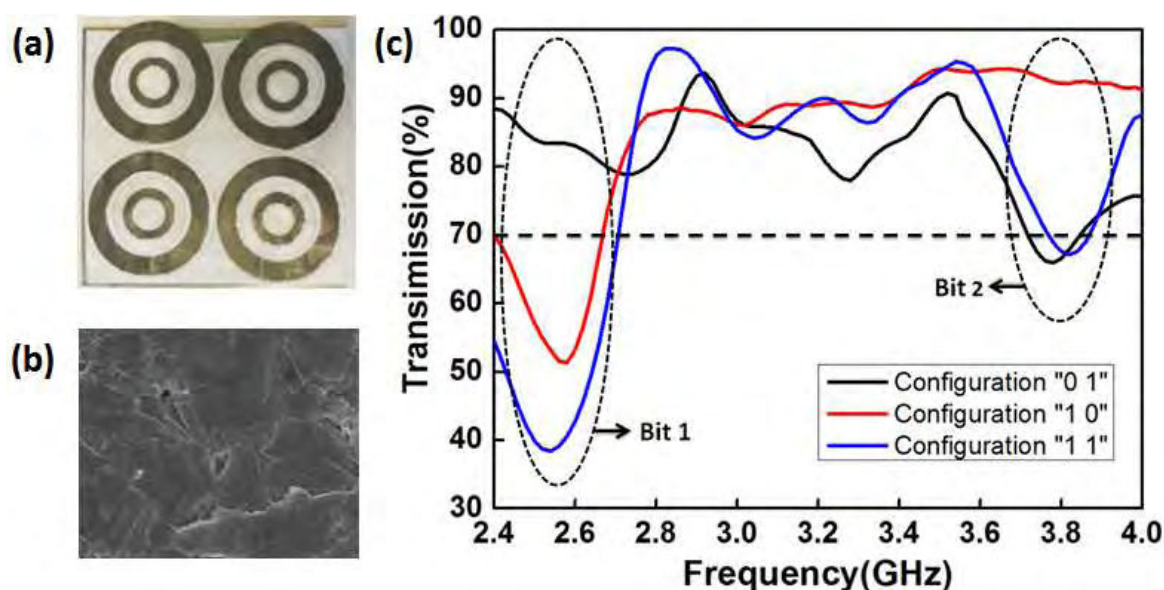


Figure 1: Printed Graphene For Chipless RFID Applications (a) Prepared screen printed graphene chipless RFID prototype tag (b) SEM image of the compact surface of highly conductive printed graphene sample (c) Measured transmission (%) from antenna 1 to antenna 2 for different configurations.

Dr Shanshan Huo – Senior Project Engineer

Andrew Wilkinson - CEO

Graphene Enabled Systems, Core Technology Facility, 46 Grafton Street, Manchester, M13 9NT, UK

shanshan.huo@graphene-enabled.com

A New Model for Accelerating the Commercialisation of Graphene and other 2D Materials Research from Universities

A vital stage in the adoption of a new material or technology is the creation of small entrepreneurial start-up businesses which are able to translate academic research into commercial products. To facilitate and drive the creation of these spin-out businesses and joint venture partnerships, The University of Manchester in the UK has set up a wholly owned subsidiary, Graphene Enabled Systems Ltd (GES). This organisation acts a facilitator - identifying and pre-qualifying deal opportunities, manufacturing high quality product demonstrators and putting together business plans for the potential spin-outs or joint-ventures.

Identifying and Evaluating Opportunities

GES has a process for identifying and evaluating new project ideas.

In the first part of the process new opportunities enter the 'funnel' from a variety of internal and external sources.

These ideas are then evaluated and empirically scored based on their commercial viability, competitive advantages, technical/operational feasibility and the strength of the University's IPs.

If an opportunity is considered suitable for a short to medium commercial exploitation and is potentially attractive to investors they enter a highly structured new product development(NPD) process.

As with any NPD process, when a project arrives at a specific 'mile-stone' or a gate it is formally reviewed and will not receive additional resource unless it has met the minimum criteria to move to the next stage of the development process.

This formal evaluation and gating process limits risks and increases the chance of a spin-out or joint venture being commercially and financially successful. GES regularly reviews the status of each project, highlighting any areas of concern that may result in a project being i) abandoned ii) recycled iii) delayed.

Outputs to Create Economic Impact

Projects that have been successfully passed through the GES evaluation and NPD process will have the following outputs:

- Comprehensive Business Plan – This will be structured in such a way to ensure the opportunity has undergone a process of due diligence.
- High-Quality Product Demonstrators – These will be designed and built to show the commercial viability of the technology and how it can be industrialised. These demonstrators (not prototypes) are invaluable tools for attracting commercial interest.
- Short Investment Prospectus – Key synthetic elements from the business plan and a description of the investment opportunity.

Graphene Enabled Systems is now successfully applying this model in the UK and is exploring how to collaborate with other Universities and industrial partners to proliferate this simple but effective model.

Spin-outs

Atomic Mechanics Ltd – Design, develop, manufacture and sale of a range of proprietary pressure sensors and human machine touch interfaces based on graphene-polymer membranes.

Grafine Ltd – Provide scientific and technical consultancy services to the multi-billion pound global elastomer industry.

Graphene Water Technologies Ltd – Develop a range of new, graphene enhanced membranes to clean polluted water and brines.

Laser Graphene Ltd – Manufacture equipment that will enable the ‘Laser Direct Writing’ of conductive tracks on low temperature substrates.

Riptron Ltd – Develop graphene based sensors to measure low concentrations of VOCs.

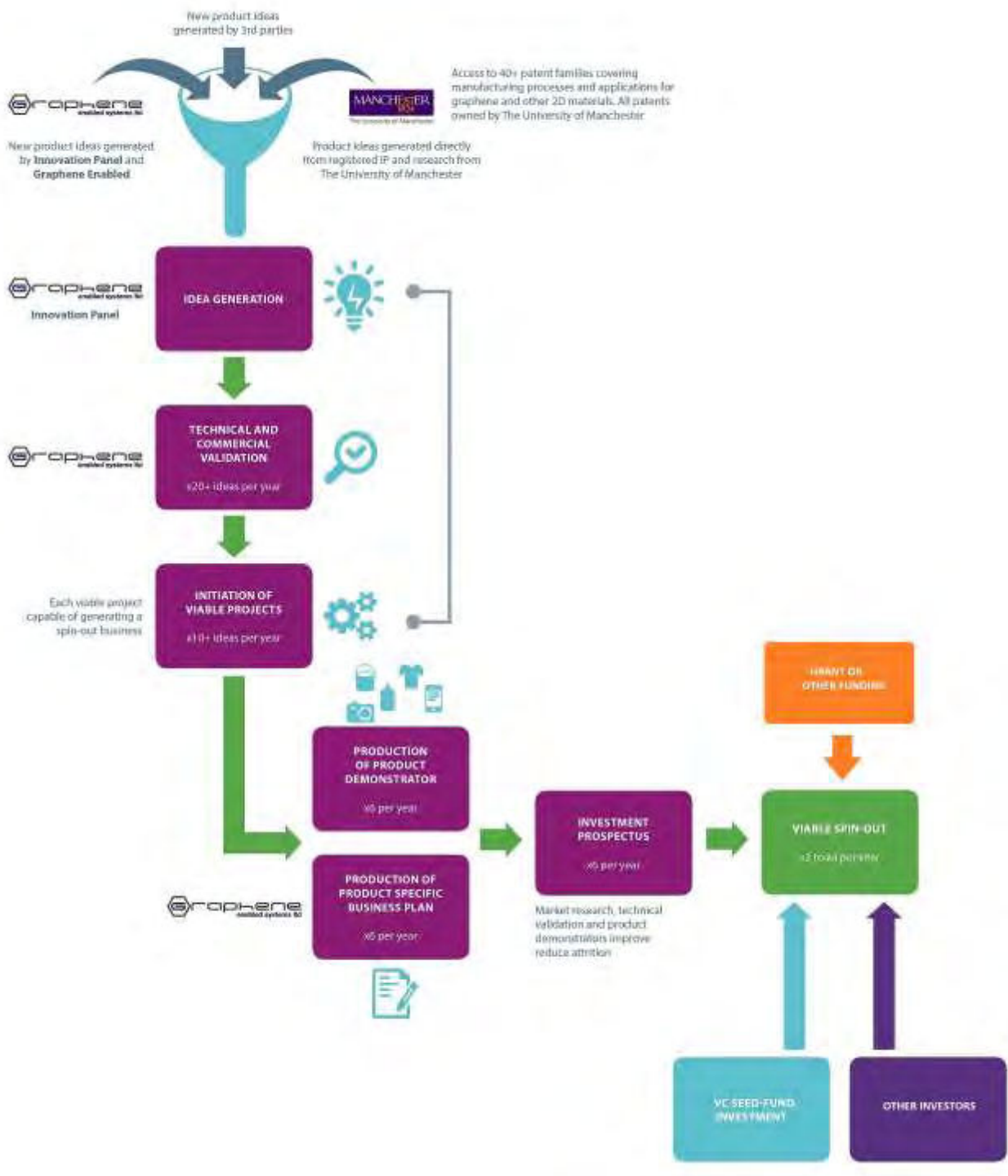


Figure 1: Flow Chart of Technology Commercialization Process

Induced Assembly of Two-Dimensional Metal–Organic Framework Nanosheets for Gas Separation

Metal–organic framework nanosheets (MONs), a new category of two-dimensional material composed of organic ligands and metal ions or clusters,^[1] have been considered as promising adsorbents and membranes for gas separation because of their structural diversity, extremely low mass-transfer barrier and precise molecule-size recognition.^[2] However, the mechanical strength and stability hinder the development of MONs-based adsorbents and membranes.^[3] Recently, we developed induced assembly strategy to fabricate MONs based composite adsorbents and composite membranes.^[4] Supports or fillers with functional groups (-OH, -COOH) are adopted, these functional groups act as nucleation or anchor sites for the growth or assembly of MONs. Taking advantage of the intimate interaction between MONs and the support or filler, metal organic framework (MOF) nanosheets confined in supports and continuous two-dimensional MOF composite membranes with enhanced performance and mechanical strength can be obtained. MOF nanosheet within the support exhibits an enhanced CO₂ adsorption capacity, which is 4 times higher than that of bulk MOF at 150 mbar and 273 K. Compare to parent unselective MONs membrane, GO/MONs membrane displays a remarkable H₂/CO₂ separation performance, with a superior H₂ permeance of 1.1×10⁻⁶ mol m⁻² s⁻¹ Pa⁻¹ and an ideal separation selectivity of 96.5.

References

- [1] M. Zhao; Y. Huang; Y. Peng; Z. Huang; Q. Ma; H. Zhang, *Chem. Soc. Rev.*, 47 (2018), 6267-6295.
- [2] Y. Peng; Y. Li; Y. Ban; H. Jin; W. Jiao; X. Liu; W. Yang, *Science*, 346 (2014), 1356-1359.
- [3] L. Prozorovska; P. R. Kidambi, *Adv. Mater. (Deerfield Beach, Fla.)* 2018, e1801179-e1801179.
- [4] C. L. Jiao; Z. Majeed; G.-H. Wang; H. Q. Jiang, *J Mater. Chem. A* 2018, 6, 17220-17226.

Figures

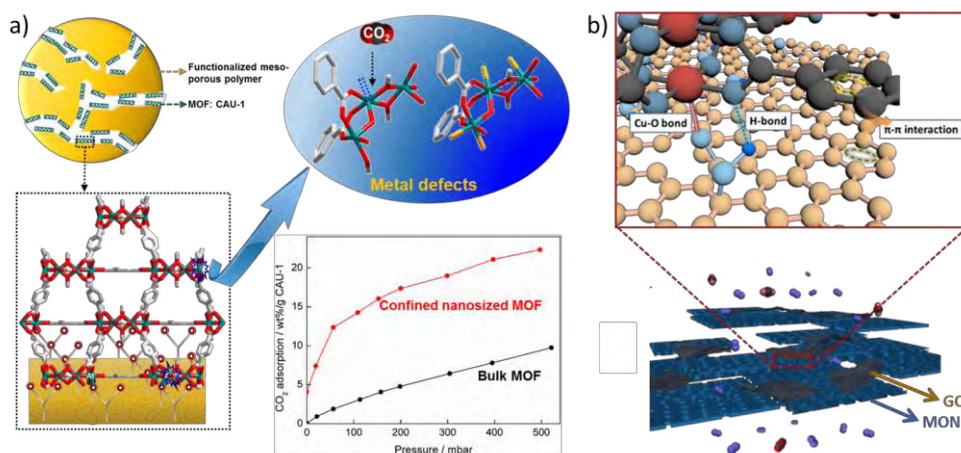


Figure 1: Scheme for the fabrication of: a) MOF nanosheets confined in porous support; b) MON (CuBDC)-GO composite membranes.

Use of Doped-Graphene Transparent Conductive Electrodes for High-Performance Si-Quantum-Dots-Based Solar Cells

Recently, various kinds of graphene/semiconductor heterojunction devices have been intensively studied due to the outstanding properties of graphene such as perfect transparency, high carrier mobility, and easy adjustment of the Fermi level by doping [1]. Even though Si is a principal material in semiconductor industries, it is of limited use in optoelectronic device applications because of the small- and indirect-bandgap nature [2]. To overcome this problem, Si quantum dots (SQDs) have been employed in optoelectronic devices based on quantum confinement effect [3]. Here, we employ doped-graphene transparent conductive electrodes (TCEs) for SQDs-based solar cells. Three kinds of dopants such as gold (III) chloride (AuCl_3), silver nanowires (Ag NWs), and bis(trifluoromethane sulfonyl)-amide (TFSA) are employed for efficient collection of the carriers photo-induced in SQDs. The TFSA-doped graphene TCE/SQDs solar cells show maximum power conversion efficiency (PCE) of 16.61%, much larger than ever achieved in their counterparts with metal TCEs. In particular, the long-term stabilities of the solar cells are remarkably improved by using TFSA for the graphene TCEs. After 700 h, the solar cells show 3.05/18.57/10.84% degradation from their initial PCEs for the TFSA/Ag NWs/ AuCl_3 -doped graphene TCEs, respectively. These results are very promising for the applications of the doped graphene TCE/SQDs heterojunctions in optoelectronic devices.

References

- [1] X. An, F. Liu, Y. J. Jung, and S. Kar, *Nano Lett.*, 3 (2013) 909-916
- [2] L. Pavesi, L. D. Negro, C. Mazzoleni, G. Franzò, and F. Priolo, *Nature*, 6811 (2000) 440-444
- [3] E.-C. Cho, S. Park, X. Hao, D. Song, G. Conibeer, S.-C. Park, and M. A Green, *Nanotechnology*, 24 (2008) 245201

Figures

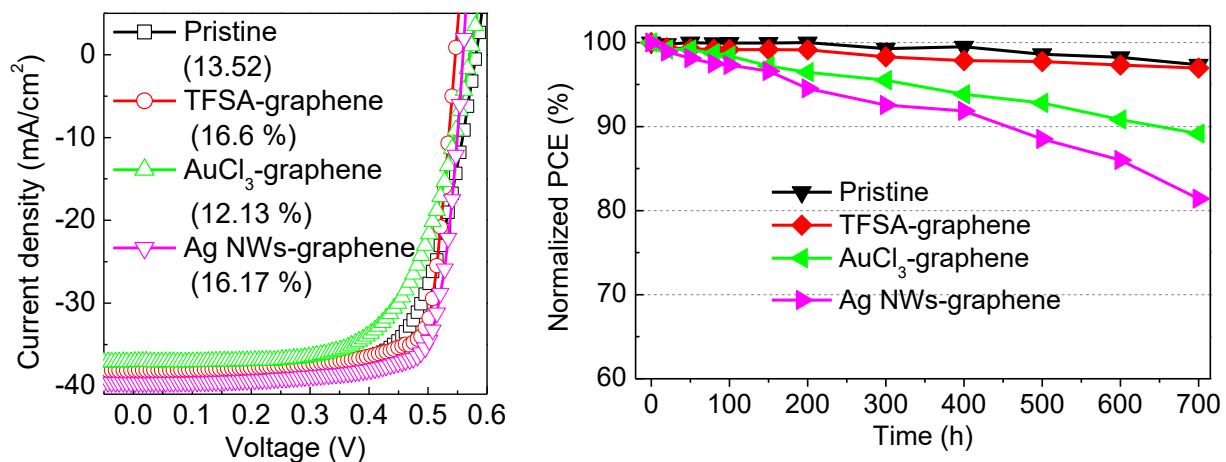


Figure 1: Photo J-V curves and long-term stabilities of the solar cells with TFSA/Ag NWs/ AuCl_3 -doped-graphene TCEs. Here, PCEs are indicated.

Scheyla Kuester^{1,2}

Rafael S. Kurusu^{1,2}, Emna Helal^{1,2}, Giovanna Gutierrez², Nima Moghimian², Éric David¹, Nicole R. Demarquette¹

¹École de technologie supérieure, 1100 Notre-Dame St W, QC H3C 1K3, Montreal, Canada

²NanoXplore Inc., 25 Montpellier Blvd, QC H4N 2G3, Montreal, Canada

scheylakuester@gmail.com

Electrical properties and electromagnetic shielding effectiveness of polycarbonate/acrylonitrile butadiene styrene/graphene nanoplatelets nanocomposites

In the current information age, the miniaturization of electronic systems and all the technical requirements for high technological applications are amplifying the complexity of developing electromagnetic interference (EMI) shielding materials for fully complying with electromagnetic compatibility (EMC) regulations [1, 2]. From an industrial perspective, the main challenge concerns the development of light cost-effective materials while combining other critical parameters such as easy processing, mechanical requirements, and esthetic factors. Electrically conductive polymer composites based on insulating polymer matrices and carbon particles have been shown to be the most promising materials for EMI shielding applications. Further, graphene-enhanced thermoplastics are showing to be more effective than the traditional carbon particles, such as carbon black and graphite [3].

In the present work, nanocomposites based on polycarbonate (PC), acrylonitrile butadiene styrene, and PC/ABS with different weight loadings of graphene nanoplatelets (GnP) were prepared in a twin screw extruder followed by compression molding for EMI shielding applications at NanoXplore Inc. As an attempt to improve the EMI shielding effectiveness (EMI-SE) with lower amounts of GnP, PC/ABS/GnP blends of 5 different morphologies with GnP content $\approx 15\text{wt}\%$ were designed. The effect of the blend's morphology and, consequently, the distribution of GnP networks of different configurations on the electrical and EMI shielding properties were evaluated. Figure 1 shows a schematic representation of the 5 different blends.

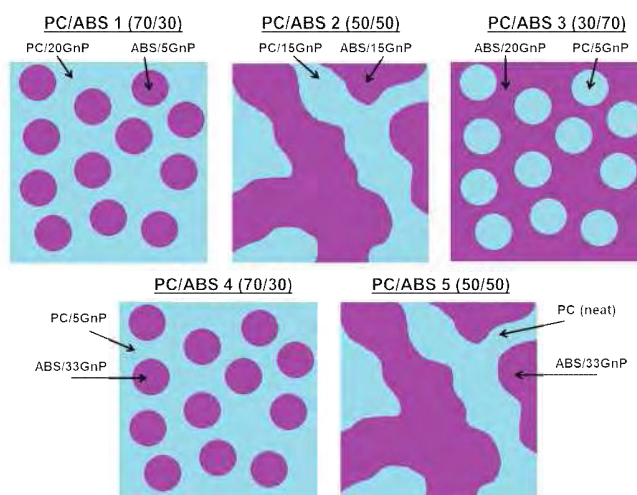


Figure 1: PC/ABS/GnP blends of different morphologies with $\approx 15\text{wt}\%$ GnP loading. Blend 1: PC/ABS blend (70 wt%/30 wt%) prepared from PC/20 wt% GnP and ABS/5 wt% GnP, Blend 2: PC/ABS blend (50wt%/50 wt%) prepared from PC/15 wt% GnP and ABS/15 wt% GnP, Blend 3: PC/ABS blend (30wt%/70 wt%) prepared from PC/5 wt% GnP and ABS/20 wt% GnP, Blend 4: PC/ABS blend (70 wt% wt%/30 wt%) prepared from PC/5 wt% GnP and ABS/33 wt% GnP, Blend 5: PC/ABS blend (50wt%/50 wt%) prepared from PC/0 wt% GnP and ABS/33 wt% GnP.

All 5 PC/ABS/GnP blends presented similar values of electrical conductivity which was very close to the one of ABS/GnP and PC/GnP nanocomposites with similar GnP concentration ($\approx 5E-2$ and $2E-1$ S.m⁻¹ for the compositions with 15 and 20wt% GnP loading, respectively). This behavior can be explained considering that at this concentration of GnP, the conductivity values are already in the plateau of conductivity after the electrical percolation threshold, and therefore the measurement is insensitive to changes regarding the morphology of the blends [3].

The EMI shielding properties were calculated from experimental data using suitable equations that can be found elsewhere [1, 4]. Figure 2 presents the EMI-SE of the different nanocomposites as a function of frequency.

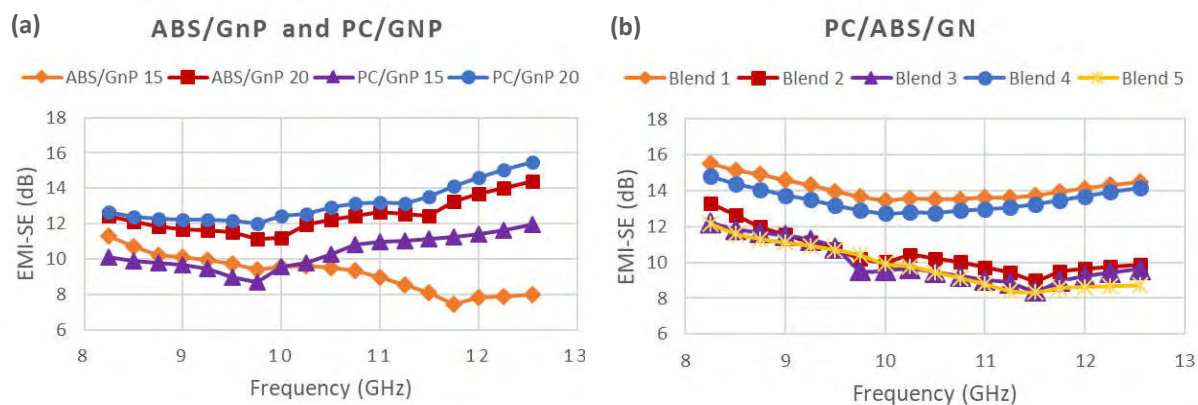


Figure 2: EMI-SE as a function of frequency of the a) PC/GnP and ABS/GnP nanocomposites and b) PC/ABS/GnP blends (≈ 2.5 mm thick)

As shown in the figure, PC/GnP presented higher EMI-SE than ABS/GnP. This result was already expected considering that PC has higher affinity with GnP than ABS according to thermodynamic predictions [5]. Further, differently than the results of electrical conductivity, the PC/ABS/GnP blends presented higher values of EMI-SE compared to the PC/GnP and ABS/GnP nanocomposites. For the PC/ABS (70 wt%/30 wt%) blends 1 and 4, where PC phase is continuous and the ABS phase is in form of droplets (with ≈ 15 wt% GnP loading), the EMI-SE of the blends were higher than the EMI-SE of PC/GnP and ABS/GnP nanocomposites with 20 wt% of GnP loading. These results can be explained considering the geometrical arrangement of the blends evaluated by rheological characterization (data not shown), where the domains of PC formed a close-packed conductive network (blend 1) and favored the formation of a highly GnP loading droplets network (blend 4) to interact with the electromagnetic radiation. Additionally, preliminary mechanical characterization (ongoing) showed a considerable increase of the mechanical properties of the PC/ABS/GnP blends compared to the PC/GnP nanocomposites.

As conclusion, it was possible to enhance the EMI-SE of the final material by controlling the morphology of the blends. PC/ABS/GnP blends of continuous PC phase showed to be potential candidates as EMI shielding materials for commercial applications.

References

- [1] Paul, C. R. (2006). Introduction to Electromagnetic Compatibility (EMC). In Introduction to Electromagnetic Compatibility (eds K. Chang and C. R. Paul). doi:10.1002/0471758159.ch1
- [2] Paul, C. R. (2006). EMC Requirements for Electronic Systems. In Introduction to Electromagnetic Compatibility (eds K. Chang and C. R. Paul). doi:10.1002/0471758159.ch2
- [3] Thomassin, J.-M., et al., *Polymer/carbon based composites as electromagnetic interference (EMI) shielding materials*. Materials Science and Engineering: R: Reports, 2013. **74**(7): p. 211-232.
- [4] Paul, C. R. (2006). Shielding. In Introduction to Electromagnetic Compatibility (eds K. Chang and C. R. Paul). doi:10.1002/0471758159.ch10
- [5] Sun, Y., Z.-X. Guo, and J. Yu, *Effect of ABS Rubber Content on the Localization of MWCNTs in PC/ABS Blends and Electrical Resistivity of the Composites*. Macromolecular Materials and Engineering, 2010. **295**(3): p. 263-268.

Geng Li

Lizhi Zhang, Lihong Bao, Yu-Yang Zhang, Shi-Xuan Du, Hong-Jun Gao
Institute of Physics & University of Chinese Academy of Sciences, Chinese Academy of Sciences, Beijing
100190, China

Contact@E-mail (gengli.iop@iphy.ac.cn)

Construction of graphene/silicene heterostructure by Si intercalation

Silicene-based van der Waals heterostructures have been theoretically predicted to have interesting physical properties, but their experimental fabrication has remained a challenge because of the easy oxidation of silicene in air. Here we report the fabrication of graphene/silicene van der Waals heterostructures by silicon intercalation. Density-functional-theory calculations show weak interactions between graphene and silicene layers, confirming the formation of van der Waals heterostructures. The heterostructures show no observable damage after air exposure for extended periods, indicating good air stability. The I-V characteristics of the vertical graphene/silicene/Ru heterostructures show rectification behavior.

References

- [1] J. H. Mao, L. Huang, Y. Pan, M. Gao, J. F. He, H. T. Zhou, H. M. Guo, Y. Tian, Q. Zou, L. Z. Zhang, H. G. Zhang, Y. L. Wang, S. X. Du, X. J. Zhou, A. H. Castro Neto, H. J. Gao, *Appl. Phys. Lett.* 2012, 100, 093101.
- [2] Y. Pan, H. G. Zhang, D. X. Shi, J. T. Sun, S. X. Du, F. Liu, H. J. Gao, *Adv. Mater.* 2009, 21, 2777.
- [3] G. Li, H. T. Zhou, L. D. Pan, Y. Zhang, L. Huang, W. Y. Xu, S. X. Du, M. Ouyang, A. C. Ferrari, H. J. Gao, *J. Am. Chem. Soc.* 2015, 137, 7099.
- [4] G. Li, L. Z. Zhang, W. Y. Xu, J. B. Pan, S. R. Song, Y. Zhang, H. T. Zhou, Y. L. Wang, L. H. Bao, Y. -Y. Zhang, S. X. Du, M. Ouyang, S. T. Pantelides, H. -J. Gao, *Adv. Mater.*, in press

Figures

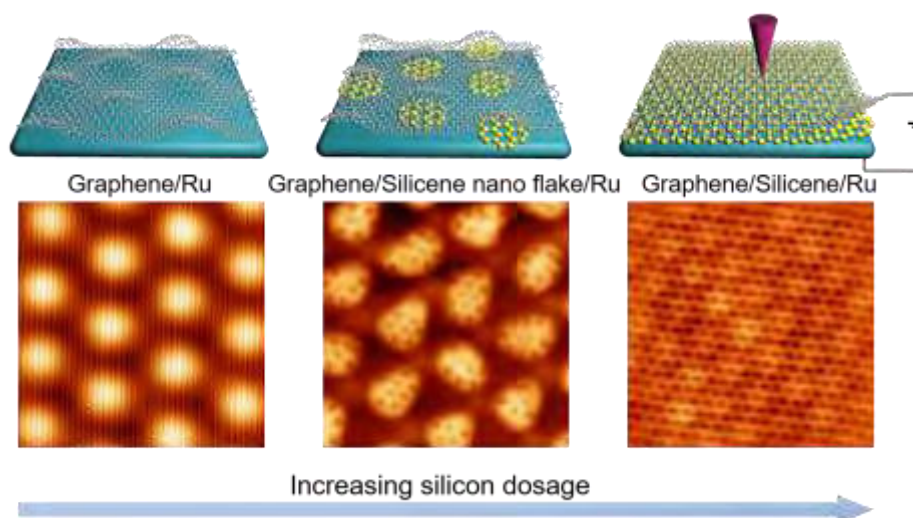


Figure 1: Formation of graphene/silicene heterostructure.

JinShu LI¹

Euyheon Hwang¹

¹Department of Nano Science and Technology, SKKU Advanced Institute of Nano-Technology (SAINT),
Sungkyunkwan University, Suwon, Korea

lijinshu@skku.edu

Quasiparticle interference (QPI) in twisted bilayer graphene

Twisted bilayer graphene, in which the lattice mismatch between neighboring layers gives rise to an additional potential modulation, creates novel electronic features distinct from graphene. Its most fascinating aspect is the Fermi velocity decreases with decreasing the twist angle between the two layers [1]. We calculate the effect of quasiparticle interference (QPI) on the spatial variations of the local density of states in twisted graphene in the neighborhood of an isolated impurity. A number of characteristic behaviors of interference are identified in the Fourier transformed spectrum of scanning tunneling microscope (STM), which can map the energy dependent local density of states by measuring the position dependence of the current /voltage characteristics [2]. Combining the powerful technique, STM, the QPI features may be analyzed to reveal information about the momentum space structure of the electronic states in twisted bilayer graphene [3]. We investigate quasiparticle interference in twisted bilayer graphene in two frameworks: the tight-binding model and the effective continuum model based on the Dirac equation. By using the T-matrix approximation to analyze the effect of a localized impurity on the local density of states in twisted bilayer graphene, we calculate the rotation angle dependence of QPI patterns, which are huge different from those of monolayer and bilayer graphene. Combing the experimental data from STM measurements for various energies and twisted angles, our calculated QPI results provide the scattering information of twisted bilayer graphene.

References

- [1] P. Moon, M. Koshino, Phys. Rev. B, 87, 205404, (2013).
- [2] S. A. Kivelson, I. P. Bindloss, E. Fradkin, V. Oganesyan, J. M. Tranquada, A. Kapitulnik, and C. Howald, Rev. Mod. Phys. 75, 1201 (2003).
- [3] K. McElroy, R. W. Simmonds, J. E. Hoffman, D. Lee, J. Orenstein, H. Eisaki, S. Uchida, and J. C. Davis, Nature (London) 422, 592 (2003).

Zhibo Liu¹

Chuan Xu¹, Ning Kang², Xiuliang Ma¹, Hui-Ming Cheng¹, Wencai Ren¹

¹Shenyang National Laboratory for Materials Science, Institute of Metal Research, Chinese Academy of Sciences, 72 Wenhua Road, Shenyang, China.

²Key Laboratory for the Physics and Chemistry of Nanodevices and Department of Electronics, Peking University, 5 Yiheyuan Road, Beijing, China.

zbliu10s@imr.ac.cn

The boundaries of 2D Mo₂C superconducting crystals

Domain (grain) boundaries have significant influence on the electrical, thermal, optical, mechanical properties of 2D materials. Ultrathin transition metal carbides (TMCs), known as MXenes, have attracted increasing attentions due to their promising applications in energy storage, electromagnetic interference shielding, water purification, sensors, and catalysis [1-4]. In this talk, we used aberration-corrected scanning transmission electron microscopy (STEM) to study the domain (grain) boundary structure of chemical vapor deposited high-quality 2D Mo₂C superconducting crystals [5,6]. For different regular shapes including triangles, rectangles, hexagons, octagons, nonagons, and dodecagons, the Mo atom sub-lattice in all these crystals has a uniform hexagonal closely-packed arrangement without any boundaries. However, except for rectangular and octagonal crystals, the C atom sub-lattices are composed of three or six domains with rotational-symmetry and well-defined line-shaped domain boundaries. We found that there is very small lattice shear strain perpendicular to a domain boundary. In contrast to the single sharp transition observed in single-domain crystals, transport studies across domain boundaries show a broad resistive superconducting transition with two distinct transition processes due to the formation of localized phase slip events within the boundaries, indicating a significant influence of the boundary on 2D superconductivity. We also studied the grain boundaries (GBs) of 2D Mo₂C crystals, which show dislocation structure or unique sawtooth pattern depending on the tilt angle. Moreover, we found two new $\Sigma 7$ GBs with different periodic structure and crystallographic orientation at tilt angle of $\sim 22^\circ$. These findings provide new understandings on not only the defect structure of 2D TMCs but also the influence of boundaries on 2D superconductivity, which would be helpful for tailoring the properties of TMCs through boundary engineering.

References

- [1] Ghidui, M., Lukatskaya, M. R., Zhao, M. Q., Gogotsi, Y. & Barsoum, M. W., *Nature*, 7529 (2014) 78-81.
- [2] Lukatskaya, M. R. et al., *Science*, 6153 (2013) 1502-1505.
- [3] Shahzad, F. et al., *Science*, 6304 (2016) 1137-1140.
- [4] Anasori, B., Lukatskaya, M. R. & Gogotsi, Y., *Nat. Rev. Mater.*, 2 (2017) 16098.
- [5] Xu, C. et al., *Nat. Mater.*, 11 (2015) 1135-1141.
- [6] Liu, Z. et al., *Nano Lett.*, 7 (2016) 4243-4250.

Huiping Lu

Hai Wang

Ministry-Province Jointly-Constructed Cultivation Base for State Key Laboratory of Processing for Non-ferrous Metal and Featured Materials, Guangxi Zhuang Autonomous Region, Guilin, China.

hbwanghai@gmail.com

Controllable synthesis of 2D Cr-doped $\text{MoO}_{2.5}(\text{OH})_{0.5}$ nanosheets and application in Lithium Ion Batteries

Abstract: α - MoO_3 has gained growing attention as anode materials for lithium-ion batteries (LIBs) due to its high theoretical capacity (1111 mAh g^{-1}). However, their key limitations are its low electronic conductivity and limited structural stability during charge-discharge process. Herein, we report a new 2D layered Cr-doped $\text{MoO}_{2.5}(\text{OH})_{0.5}$ (doped $\text{MoO}_{2.5}(\text{OH})_{0.5}$), existing good electrical conductivity and fast Li^+ diffusion pathways for high-performance LIBs by a unique “doping-adsorption” strategy. Compared with doped MoO_3 , doped $\text{MoO}_{2.5}(\text{OH})_{0.5}$ has larger expanded spacing of the (0/0) crystal plane for ultrafast Li^+ storage. Their lithiation-delithiation processes were studied by *ex situ* TEM combined with XPS analysis to reveal the mechanism of the reversible conversion reaction. Interestingly, for doped $\text{MoO}_{2.5}(\text{OH})_{0.5}$, it was found through the as-formed Li_xMoO_3 had an expanded (040) crystal plane with well-dispersed nano-dots after 10 cycles. Moreover, the pulverized electrode has a distinct open pore structure. This unique structural characterization would increase the effective surface of intermediate products Li_xMoO_3 to react with Li^+ and shorten the diffusion path to prompt electrochemical reaction. Additionally, the presence of Cr also played an important role in the reversible decomposition of Li_2O and enhanced specific capacity. When employed as an anode in LIBs, doped $\text{MoO}_{2.5}(\text{OH})_{0.5}$ delivers a capacity of 294 mAh g^{-1} at 10 A g^{-1} after 2000 cycles. Moreover, the reversible capacity after electrochemical activation, is quite stable throughout the cycling, thereby presenting a promising new anode materials for Li^+ storage.

References

- [1] C. Wang, L. Wu, H. Wang, W. Zuo, Y. Li, J. Liu, *Adv. Funct. Mater.*, 25 (2015) 3524-3533.
- [2] L. Cao, J. He, J. Li, J. Yan, J. Huang, Y. Qi, L. Feng, *J. Power Sources*, 392 (2017) 87-93.

Figures

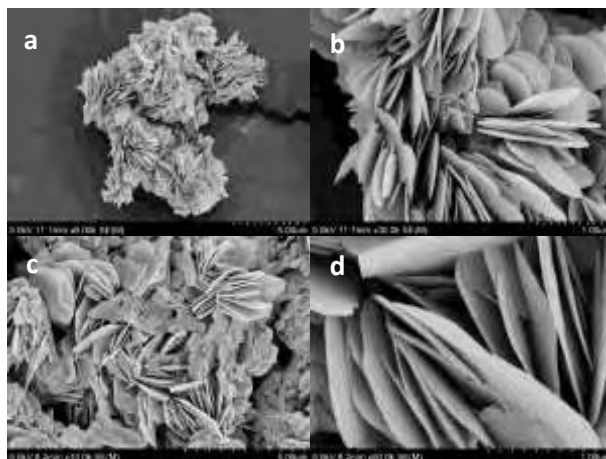


Figure 1: (a)-(b) FESEM images of 2D Cr-doped $\text{MoO}_{2.5}(\text{OH})_{0.5}$ and (c)-(d) 2D Cr-doped MoO_3 .

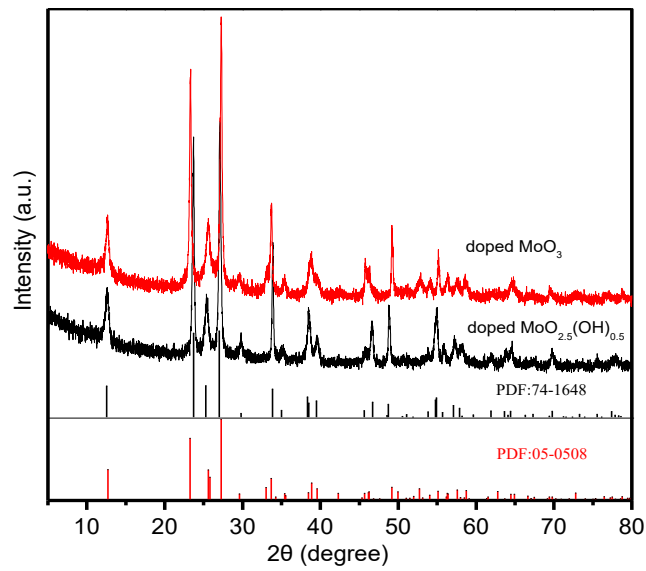


Figure 2: XRD patterns of doped MoO_3 and doped $\text{MoO}_{2.5}(\text{OH})_{0.5}$.

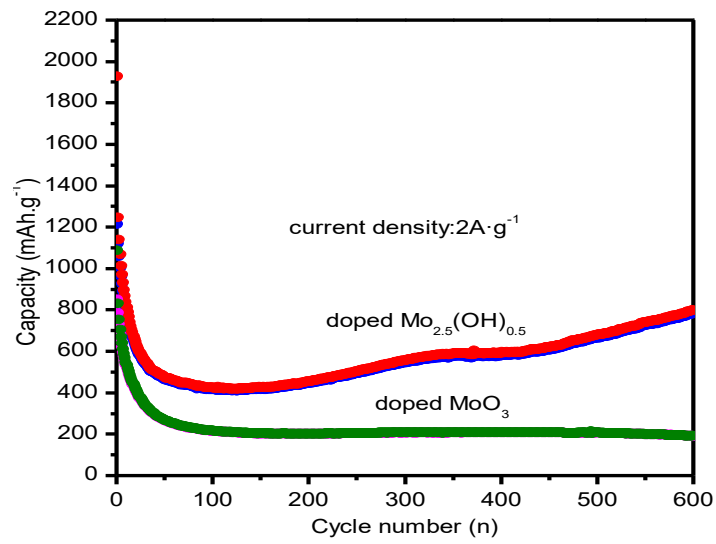


Figure 3: Cycling performances of doped MoO_3 and doped $\text{MoO}_{2.5}(\text{OH})_{0.5}$ at 2A g^{-1} .

Presenting Author: Kai Liu, Hao Luo

School of Materials Science and Engineering, Tsinghua, Beijing, China

Contact: liuk@tsinghua.edu.cn

Probing and Modulating Interface Interactions in 2-Dimensional Materials and Their Heterostructures

Abstract

2-dimensional (2D) van der Waals structures built up from layered materials, such as graphene, MoS₂, and their heterostructures, have received growing attention owing to their simple fabrication by straightforward stacking and various types of band alignments. Interface interactions in 2D materials and their heterostructures are of vital importance to determine the properties of the 2D layers. In this talk, I will introduce some efforts in my group on probing and modulating interface interactions in 2D systems, including mechanically characterizing their interlayer interactions, employing surface enhanced Raman technique to probe local strains, and inducing interlayer connections by defect engineering. Lastly, I will present an example of modulating properties of a 2D semiconductor by interfacing it with an active, phase-transition material. Our results not only provide an insight to understand interface interactions in 2D van der Waals structures, but also potentially allow engineering of their properties as desired.

Keywords: 2D materials, heterostructure, interface interaction, phase transition

References

- [1] S. Tongay, H. Sahin, C. Ko, A. Luce, W. Fan, et al. **Nat. Commun.** 2014, 5, 3252.
- [2] S. Tongay, W. Fan, J. Kang, J. Park, U. Koldemir, et al. **Nano Lett.** 2014, 14, 3185.
- [3] K. Liu, Q. Yan, M. Chen, W. Fan, J. Wu, et al. **Nano Lett.** 2014, 14, 5097. (Arial Narrow 11)
- [4] Y. Sun#, K. Liu#, X. Hong, M. Chen, F. Wang, et al. **Nano Lett.** 2014, 14, 5329.
- [5] K. Liu, C.-L. Hsin, D. Fu, J. Suh, S. Tongay, et al. **Adv. Mater.** 2015, 27, 6841.
- [6] S. Lee, F. Yang, J. Suh, J. Wu*, et al. **Nat. Commun.** 2015, 6, 8573.
- [7] J. Hou, X. Wang, K. Liu*, et al. **Small** 2016, 12, 3976.
- [8] J. Zhang, Y. Wei*, F. Yao, et al. **Adv. Mater.** 2017, 29, 1604469.
- [9] Y. Sun, R. Wang, K. Liu*. **Appl. Phys. Rev.** 2017, 011301.
- [10] X. Wang, W. Fan, K. Liu*, et al. **Nanoscale** 2018, in press.

Ruisong Ma

Qing Huan, Lihong Bao, Hong-Jun Gao*

Institute of Physics & University of Chinese Academy of Sciences, Chinese Academy of Sciences, P.O. Box 603, Beijing 100190, P. R. China

hjgao@iphy.ac.cn

Direct Four-Probe Measurement of Grain-Boundary Resistivity and Mobility in Millimeter-Sized Graphene

Abstract

Grain boundaries (GBs) in polycrystalline graphene scatter charge carriers, which reduces carrier mobility and limits graphene applications in high-speed electronics. Here we report the extraction of the resistivity of GBs and the effect of GBs on carrier mobility by direct four-probe measurements on millimeter-sized graphene bicrystals grown by chemical vapor deposition (CVD). To extract the GB resistivity and carrier mobility from direct four-probe intragrain and intergrain measurements, an electronically equivalent extended 2D GB region is defined based on Ohm's law. Measurements on seven representative GBs find that the maximum resistivities are in the range of several $\text{k}\Omega\cdot\mu\text{m}$ to more than $100 \text{ k}\Omega\cdot\mu\text{m}$. Furthermore, the mobility in these defective regions is reduced to 0.4–5.9 % of the mobility of single-crystal, pristine graphene. Similarly, the effect of wrinkles on carrier transport can also be derived. The present approach provides a reliable way to directly probe charge-carrier scattering at GBs and can be further applied to evaluate the GB effect of other two-dimensional polycrystalline materials, such as transition metal dichalcogenides (TMDCs).

References

- [1] Ma, R. S., Huan, Q., Wu, L. M. et al. Nano Lett., 17 (2017) 5291- 5296
- [2] Ma, R. S., Huan, Q., Wu, L. M. et al. Rev. Sci. Instrum., 88 (2017) 063704
- [3] Ma, R. S., Huan, Q., Wu, L. M. et al. Chin. Phys. B 26 (2017) 066801

Figures

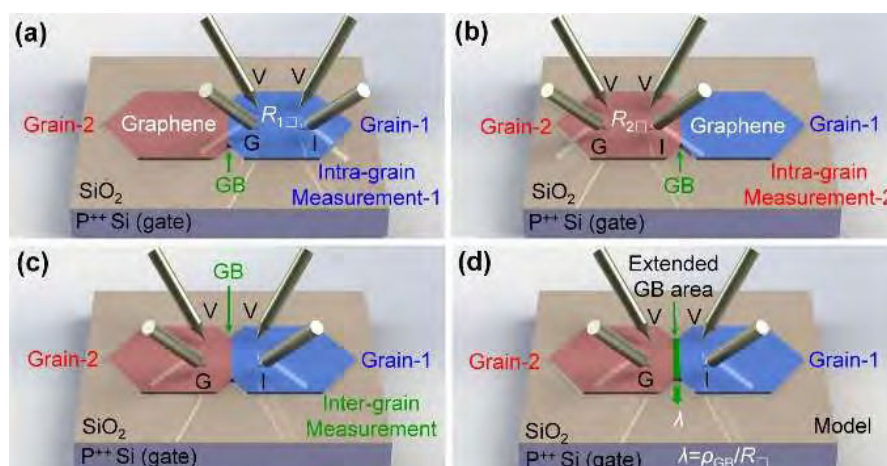


Figure 1: Schematic diagrams of four-probe measurements on graphene bicrystals.

Inyong Moon¹

Sungwon Lee¹, Myeongjin Lee¹, Changsik Kim¹, Daehee Seol², Yunseok Kim², Ki Hyun Kim², Geun Young Yeom^{1,2} and Won Jong Yoo¹

¹SKKU Advanced Institute of Nano-Technology (SAINT), Sungkyunkwan University, 2066 Seobu-ro, Jangang-gu, Suwon, Gyeonggi-do, 16419 Korea

²School of Advanced Materials Science and Engineering, Sungkyunkwan University, 2066 Seobu-ro, Jangang-gu, Suwon, Gyeonggi-do, 16419 Korea

yoowj@skku.edu

Measurements of Fermi Level and Doping Concentration of 2D Transition Metal Dichalcogenide Using Kelvin Probe Force Microscopy

Some of atomically thin two-dimensional (2D) materials show good electrical performances. Many of the interesting electrical properties can be realized more diversely by controlling dopant concentration. In this work, we used plasma techniques to control the Fermi level of 2D transition metal dichalcogenide (TMDC), which can be strongly related to dopant concentration (or it can be understood as carrier concentration many cases). As 2D TMDC, we found that semiconducting WSe₂ and MoTe₂ were effectively doped as p-type, attributed to surface oxidation induced by N₂ and O₂ plasma. To make the quantitative analysis of the plasma doping effects, the Kelvin probe force microscopy (KPFM) was employed in this work and we confirmed the Fermi level shifts, strongly related to the doping concentrations of 2D TMDC. The validity of the KPFM results were confirmed by measuring electrical characteristics of FET devices fabricated from the 2D TMDC.

ACKNOWLEDGMENTS

This work was supported by Basic Science Research Program through the National Research Foundation of Korea (NRF) funded by the Ministry of Education (2018R1D1A1B07044712), and the Global Research Laboratory (GRL) Program (2016K1A1A2912707) and Global Frontier R&D Program (2013M3A6B1078873), both funded both the Ministry of Science, ICT & Future Planning via National Research Foundation of Korea (NRF).

Quantum Capacitance Effect in Graphene-Metal-Oxide-Semiconductor Field Effect Transistor with Large Area Graphene Channel

This paper presents a physics-based quasianalytic modeling for graphene–metal-oxide-semiconductor field effect transistor (GFETs) with large area graphene based on energy-balance equation solver using two-dimensional density of states for the calculation of drain current. This model felicitates the reader with analysis of quantum capacitance effect and velocity saturation in GFETs. Formulation of the current velocity saturation equations at the steady state for determining energy of graphene phonon and their scattering rate is done by Monte Carlo simulation method. Estimated various quantum capacitance values, and the result are compared with the exiting methods. The proposed method gives the better results as compared with the state of art methods available in the literature.

References

- [1] I. Meric, M. Y. Han, A. F. Young, B. Ozyilmaz, P. Kim, and K. L. Shepard, *Nat. Nanotechnol.*, vol. 3, no. 11, pp. 654–659, 2008.
- [2] B. N. Szafrank, G. Fiori, D. Schall, D. Neumaier, and H. Kurz, pp. 1324–1328, 2012.
- [3] J. S. Moon et al., *IEEE Electron Device Le3.*, vol. 34, no. 9, pp. 1190–1192, 2013.

Figures

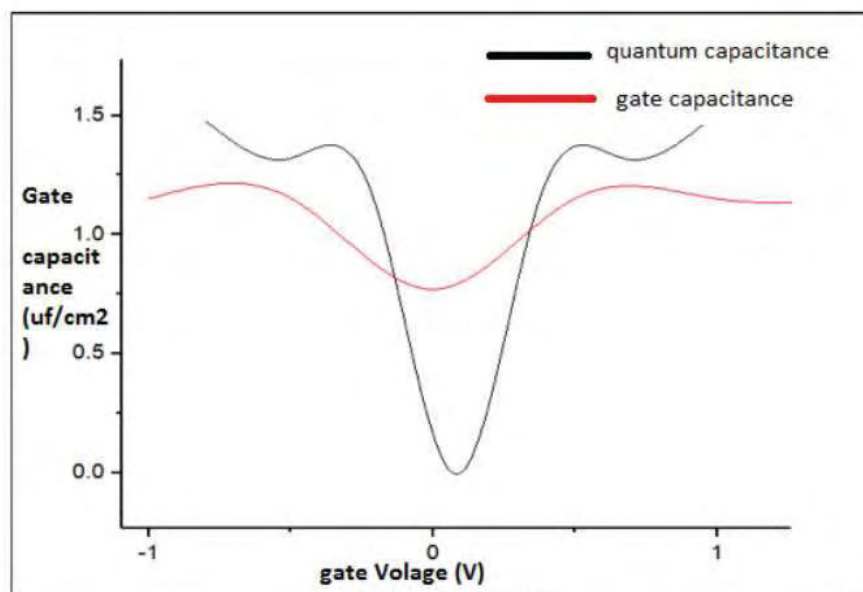


Figure 1: Iquantum capacitance vs gate voltage

Hamin Park

Sung-Yool Choi

School of Electrical Engineering, Center for Advanced Materials Discovery towards 3D Display, KAIST,
Daejeon, Korea

parkhamin@kaist.ac.kr

Interlayer interaction in a van der Waals heterostructure of transition metal dichalcogenide and hexagonal boron nitride

Two dimensional (2D) van der Waals (vdW) heterostructures have attracted explosive interest because of their potential ability to exhibit novel quantum phenomena based on condensed matter physics.[1] The 2D vdW heterostructures are formed by stacking different types of 2D materials, including graphene, transition metal dichalcogenide (TMD) and hexagonal boron nitride (h-BN).[2,3] Each layers are dangling-bond-free and weakly bound to neighboring layers by vdW interactions. The 2D vdW heterostructures have exhibited novel quantum phenomena emerging from layer-layer interaction, such as electron-electron interaction and electron-phonon interaction. As a template for an application to electronic device, the layer-layer interaction between TMD and h-BN layer needs to be significantly investigated, because the TMD and h-BN exhibit a semiconducting and insulating characteristic, respectively. In this study, we investigate the interlayer interaction between TMD and h-BN by observing spectroscopic characteristics from the 2D vdW heterostructures. We fabricated the heterostructures by transferring a top-layer flake onto bottom-layer flake using a pick-up transfer technique based on polydimethylsiloxane (PDMS)/ polypropylene carbonate (PPC) stamp. The investigation of Raman scattering and photoluminescence (PL) reveals the nature of phonon vibration and excitonic transition of the heterostructures. We expect that the fundamental understanding of the layer-layer interaction in the 2D vdW heterostructures play a key role for future applications to electronic devices based on 2D materials.

References

- [1] Geim, A., et al., Nature, 499 (2013) 419
- [2] Novoselov, K. S., et al., Science, 353 (2016) aac9439
- [3] Pizzocchero, F., et al., Nature Communications, 7 (2016) 11894

Figures

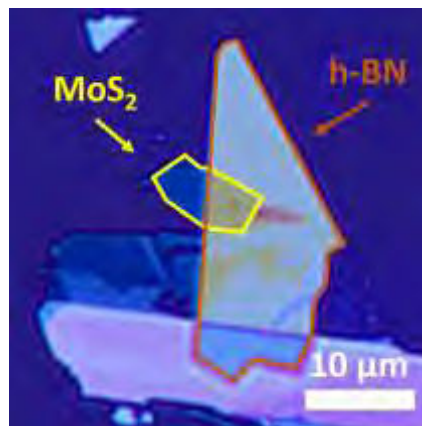


Figure 1: Optical image of heterostructure composed of molybdenum disulfide and hexagonal boron nitride.

Jiang Pu

W. Zhang, Y. Kobayashi, Y. Takaguchi, Y. Miyata, K. Matsuda, Y. Miyauchi, T. Takenobu
Dept. of Applied Physics, Nagoya Univ., Bldg.3 Room 262, Furo-cho, Chikusa-ku, Nagoya 464-8603, Japan

Contact : jiang.pu@nagoya-u.jp

Room Temperature Valley Polarized Light-Emitting Diodes of Monolayer Transition Metal Dichalcogenides

Owing to broken spatial inversion symmetry and spin-orbit interaction in monolayer transition metal dichalcogenides (TMDCs), their electronic properties at the band edge are associated with the two inequivalent (K and -K) valleys, resulting in the interband transition coupled with optical helicity [1,2]. Indeed, the valley polarization have been exclusively controlled by circularly polarized light pumping [2]. These features motivate us to develop valley-polarized light-emitting diodes (LEDs) that can electrically generate circularly polarized light emission. Although several researches have reported chiral electroluminescence (EL) from TMDCs, the solid manner for electrical control valley polarized EL have remained unclear [3,4]. This lead to the limited utility of relevant valley polarized LEDs, for instance, circularly polarized EL have mostly observed at low temperature (< 80 K). Therefore, establishing the approach to produce valley polarized LEDs operated at room temperature is highly required for the development of TMDC-based valley functional device applications.

To understand operational mechanism for circularly polarized EL, the detailed evaluations in terms of electric field dependence, temperature dependence, and importantly, spatial imaging of polarized light emission should be addressed. However, current methods for fabricating TMDC LEDs have adopted complicated device configurations such as transistors and heterostructures using tiny exfoliated samples, and thus, this fundamental barrier has made investigating circularly polarized EL properties of TMDCs inevitably difficult [3,4]. Here, we newly propose a versatile and simple approach to generate light emission in TMDCs [5,6]. The proposed device only needs two electrodes deposited onto TMDCs, followed by spin-coating ion gels, a mixture of ionic liquid and triblock co-polymer (Fig. 1). We apply this method to chemical vapor deposition (CVD)-grown single-crystalline WSe₂ and WS₂ monolayers to achieve polarized EL imaging and spectroscopy.

Figures 2a and 2b shows optical micrograph and EL image obtained in WS₂ LEDs near room temperature (280 K). We observed clear light emission between two electrodes, resulting in EL generation due to electrolyte-induced p-i-n junctions (Fig.1). Owing to direct EL observations, we performed spatial polarization-resolved EL spectroscopy. Figures 2c and 2d exhibit polarization-resolved EL spectra obtained at two different positions of WS₂ flake, in which each spectrum was recorded inside crystal and crystal edge regions, respectively. Only small EL polarization was obtained at lower temperature (< 40 K) inside crystal regions (Fig. 2d). In contrast, larger EL polarization was observed at higher temperature (> 100 K) at crystal edge regions (Fig. 2c). Most importantly, this large EL polarization was robustly remained up to 280 K. These results suggest the position-dependent distinct EL polarization mechanism in TMDCs. In order to examine the origin of robust circularly polarized EL, furthermore, we compare these EL results with photoluminescence mapping done in same crystal. As a result, we found out that the local strain induced at crystal edge regions due to lattice mismatch would play a significant role to create robust EL polarization in TMDCs. Our observations provide possible ability to construct practical TMDC-based atomically thin chiral light sources for future opto-valleytronic applications.

References

- [1] D. Xiao *et al.*, *Phys. Rev. Lett.* 108, 196802 (2012)
- [2] X. Xu *et al.*, *Nat. Phys.* 10, 343 (2014)
- [3] Y. J. Zhang *et al.*, *Science* 344, 725 (2014)
- [4] W. Yang *et al.*, *Nano Lett.* 16, 1560 (2016)
- [5] J. Pu *et al.*, *Adv. Mater* 29, 1606918 (2017)
- [6] J. Pu and T. Takenobu *Adv. Mater.* 1707627 (2018)

Figures

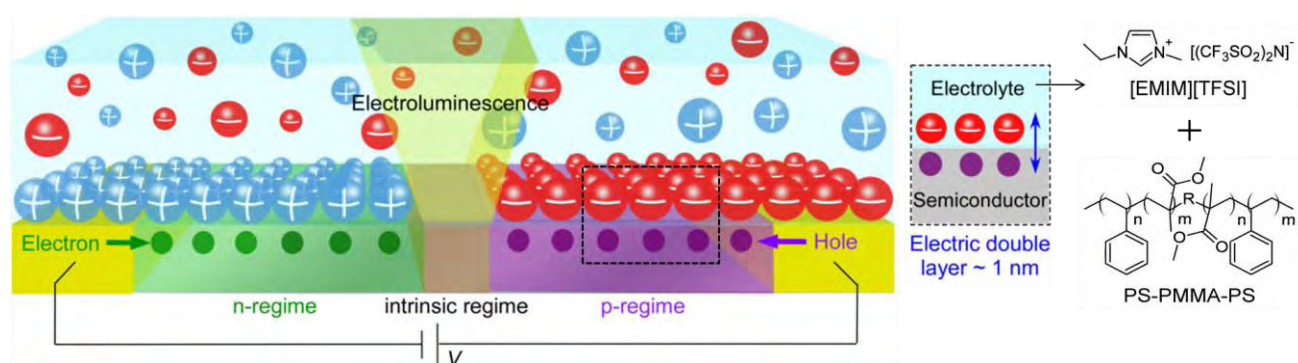


Figure 1: Schematic illustrations of a proposed light-emitting device, an ionic liquid, and a triblock copolymer.

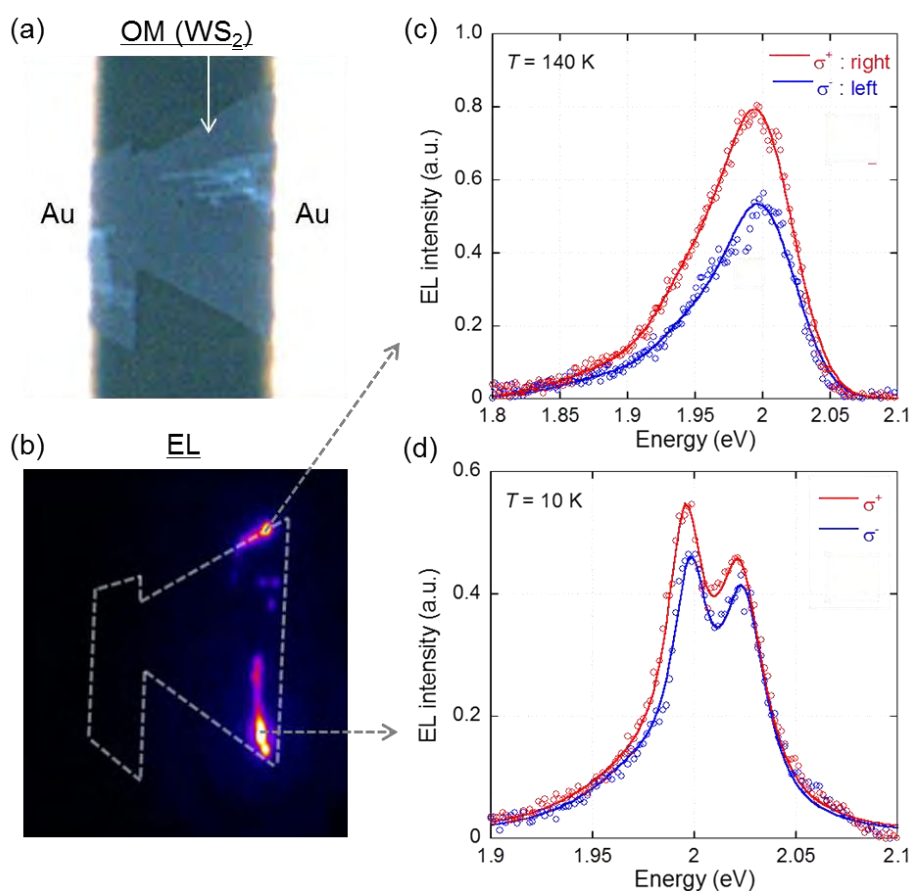


Figure 2: (a) Optical micrograph and (b) EL image of a CVD-grown single-crystalline monolayer WS₂ light-emitting diode. Polarization-resolved EL spectra measured at temperature of (c) 140 K and (d) 10 K, in which each spectrum is recorded at different positions of a WS₂ flake.

Cryogenic near-field imaging and spectroscopy at the 10-nanometer-scale

Two-dimensional materials like graphene, boron-nitride or transition-metal dichalcogenides are of rising interest for novel plasmonic and opto-electronic applications due to their unique characteristics and their broad application range. However, being highly sensitive to the local environment, their properties can strongly vary on the nanometer length scale, severely limiting the macroscopic performance of such novel devices. Scattering-type scanning near-field optical microscopy (s-SNOM) and nanoscale FTIR spectroscopy (nano-FTIR) systems have become the key technology to understand and resolve these limitations by measuring the optical and electronic properties of such nanostructures down to the 10-nanometer length scale.

SNOM [1-8] and nano-FTIR [1,2] have already proven themselves vital for modern nanoscopy and have been used in applications such as chemical identification [2], free-carrier profiling [3], or the direct mapping of propagating plasmons [4,5,8] and polaritons [6]. It enables extraction of key information such as the local conductivity, intrinsic electron-doping, absorption or the complex-valued refractive index, all at the nanoscale.

Within this talk we will introduce the newest technological breakthrough in the field of near-field optics - Cryogenic near-field imaging and spectroscopy. Pioneered by the group of Dimitri Basov [7,8], this novel approach extends ambient near-field measurements to the cryogenic temperature range (<10-300 Kelvin, [1]) and opens a complete new world for nanoscale optical microscopy and spectroscopy. This technology enables for example the direct mapping of phase-transitions in strongly correlated materials [7,9] or the detection of low-energy elementary excitations at the surface of solid-state systems such as graphene [8].

References

- [1] www.neaspec.com
- [2] F. Huth et al., Nano Letters 12, 3973 (2012)
- [3] J. M. Stiegler et al., Nano Letters 10, 1387 (2010)
- [4] J. Chen et al., Nature 487, 77 (2012)
- [5] Z. Fei et al., Nature 487, 82 (2012)
- [6] E. Yoxall et al., Nature Photonics 9, 674 (2015)
- [7] A. S. McLeod et al., Nature Phys. 13, 80 (2017)
- [8] G. X. Ni et al., Nature 557, 530–533 (2018)
- [9] H.T. Stinson et al., arXiv:1711.05242v1

Figures

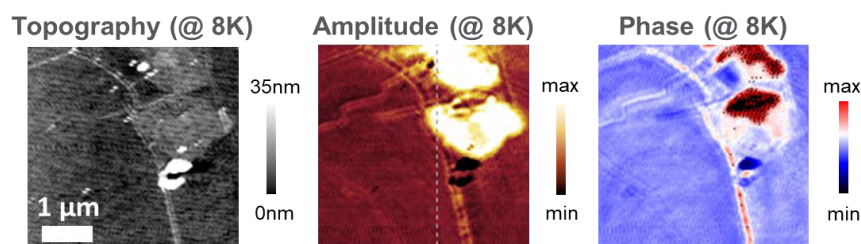


Figure 1: Cryogenic near-field optical microscopy. Topography, near-field amplitude, and near-field phase image of an epitaxial graphene sample measured at an excitation wavelength of $9.7\mu\text{m}$. The sample temperature for these measurements is set to 8.0 Kelvin. Clear interference pattern of propagating surface-plasmon polaritons are visible at grain boundaries and defect sites [3,4].

Valentino Romano¹

Sebastiano Bellani², Beatriz-Martin Garcia², Leyla Najafi², Antonio Esau Del Rio Castillo², Mirko Prato³, Giovanna D'Angelo¹ and Francesco Bonaccorso^{2,4}

¹ Dipartimento di Scienze Matematiche ed Informatiche, Scienze Fisiche e Scienze della Terra, Università di Messina, Viale F. Stagno D'Alcontres 31, S. Agata, 98166 Messina, Italy.

² Graphene Labs, Istituto Italiano di Tecnologia, via Morego 30, 16163 Genova, Italy.

³ Materials Characterisation Facility, Istituto Italiano di Tecnologia, via Morego 30, 16163 Genova, Italy.

⁴ BeDimensional Srl, via Albisola 120, 16163 Genova, Italy.

vromano@unime.it

An industrial scalable approach for graphene/carbon nanotubes hybrid flexible supercapacitors

Flexible electronic devices are the forefront of research activity for their multiple uses. [1, 2] One of the major challenges in this research area is the fabrication of flexible energy storage systems (ESSs) since they can be used in wearable electronic applications such as medical devices, portable antennas, etc. [1, 2] Nowadays, batteries and conventional capacitors are prototypical ESSs but they suffer from some limitations. On the one hand, batteries have low power density, slow recharge time and limited cyclability [3]. On the other hand, conventional capacitors show high power density and life-cycles stability, but with the downside of lower energy density compared to batteries. The development of electrochemical double layer capacitors (EDLCs or supercapacitors) is bridging the gap between these two ESSs technologies. In fact, supercapacitors show higher energy density than conventional capacitors and higher charge/discharge rates, life – time and power density than batteries. [4] These performances are achieved thanks to the materials used in the electrodes for supercapacitors: high porous/specific surface area carbon based materials, e.g., activated carbon (AC) [4]. However, AC suffers from a major drawback: its surface area is not entirely accessible to the ions of the electrolyte due to the presence of micro-pores that hinder the adsorption of ions. Moreover, AC based electrodes require the use of binder that wrap together the AC particles, but cause an increase in the electrical resistivity of the electrodes. [5] To overcome these drawbacks, many other carbon-based materials have been suggested as possible active material alternatives , including carbon nanotubes (CNTs) and graphene. [6] Nevertheless, electrodes fabricated by using either CNTs or graphene suffer from re-aggregation effects (such as the bundling of CNTs and the restacking of graphene flakes) which cause a reduction of the specific surface area and consequently of the electrochemical performance of the device. [7] To tackle these issues, hybrid compounds (graphene/CNTs mixtures) were proposed as possible solutions. [7] Herein, we introduce a scalable approach for the production of this type of devices. Our starting materials are commercial CNTs and graphite, dispersed in a solvent (N-methyl-2-pyrrolidon). The CNTs are de-bundled by means of ultrasonication techniques [8], while graphene is produced by wet-jet milling exfoliation of pristine graphite [9, 10]. The wet-jet milling is a high-yield (~ 100 %) procedure that allows the production of large quantities of graphene (> 20 g h⁻¹). [9, 10] These features are compatible with industrial requirements and avoid time-consuming solution-based processes. [11] By mixing the CNTs and graphene dispersions in a 1:1 weight ratio, the final functional ink is obtained and can be used for scalable manufacturing of supercapacitors through methods such as printing and vacuum filtration. [12] The as produced electrodes are flexible and self-standing (no binder is used) and the devices, fabricated without the need of any metal, show areal capacitances > 150 mF cm⁻².

References

- [1] Nathan A., Ahnood A., Cole M.T., Lee S., Suzuki Y., Hiralal P., Bonaccorso F., Hasan T., Garcia-Gancedo L., Dyadyusha A. and Haque S., *Proceedings of the IEEE*, 100(Special Centennial Issue) (2012), pp. 1486-1517.
- [2] Bonaccorso F., Colombo L., Yu G., Stoller M., Tozzini V., Ferrari A.C., Ruoff R.S. and Pellegrini V., *Science*, 6217 (2015), pp. 1246501.
- [3] Bruce P.G., Freunberger S.A., Hardwick L.J. and Tarascon J.M., *Nature materials*, 11(2012), pp. 19-29.
- [4] González A., Goikolea E., Barrena J.A. and Mysyk R., *Renewable and Sustainable Energy Reviews*, 58 (2016), pp. 1189-1206.
- [5] Pandolfo A.G., Hollenkamp A.F., *Journal of Power Sources*, 157 (2006), pp. 11-27
- [6] Burke A., *Journal of power sources*, 91(2000), pp. 37-50.
- [7] Ansaldo A., Bondavalli P., Bellani S., Del Rio Castillo A.E., Prato M., Pellegrini V., Pognon G. and Bonaccorso F., *ChemNanoMat*, 3(2017), pp. 436-446.
- [8] Bonaccorso F., Hasan T., Tan P.H., Sciascia C., Privitera G., Di Marco G., Gucciardi P.G. and Ferrari A.C., *The Journal of Physical Chemistry C*, 114(2010), pp. 17267-17285.
- [9] Patent number: UB2015A005920.
- [10] Castillo A.E.D.R., Pellegrini V., Ansaldo A., Ricciardella F., Sun H., Marasco L., Buha J., Dang Z., Gagliani L., Lago E. and Curreli N., Gentiluomo S., Palazon F., Toth P., Mantero E., Crugliano M., Gamucci A., Tomadin A., Polini M. and Bonaccorso F. *arXiv preprint arXiv:1804.10688* (2018).
- [11] Bonaccorso F., Lombardo A., Hasan T., Sun Z., Colombo L. and Ferrari A.C., *Materials today*, 15(2012), pp. 564-589.
- [12] Bonaccorso F., Bartolotta A., Coleman J.N. and Backes C., *Advanced Materials*, 28(2016), pp. 6136-6166.

Magneto-transport Properties of Graphene Foam

Large area single crystal two dimensional (2D) graphene is not realized to the date, which is the biggest hurdle for the utilization of graphene in practical electronic gadgets.¹ According to the roadmap of Novoselov et al.,² high-quality large area 2D graphene may be available in 2035, indicating unavailability of large area single crystal graphene in the present days. However, hierarchy of 3D structure of 2D graphene such as graphene foam (GF) for graphene-based practical devices could turn as an alternate.³ To the best of our knowledge, magneto-transport properties of bulk GF have not been explored so far. Magneto-transport properties of GF could be different in comparison to 2D graphene due to the presence of different sizes of graphene flakes and more crucially the types of connection between these flakes, presence of edge boundaries,⁵ geometry of graphene edges,⁶ difference in the stacking of graphene layers and different number of graphene layers.⁷⁻⁹ Therefore, graphene morphology may influence on the motion and trajectories of the charge carriers under the applied magnetic field, thus, interesting electro/magneto transport properties can be observed. However, metal electrode deposition on the top of GF is a big challenge for studying electro/magneto transport properties.¹⁰ Herein, we present the first observation of magneto-transport properties of GF composed of a few layers in a wide temperature range of 2 – 300 K. The multilayer polycrystalline GF was fabricated with the help of Chemical Vapor Deposition (CVD) (Fig. 1a-f). Large room temperature linear positive magnetoresistance (PMR ~ 171 % at B ~ 9 T) has been detected.¹¹ The largest PMR ~ 213 % has been achieved at 2 K under a magnetic field of 9 T, which can be tuned by the addition of poly-(methyl methacrylate) to the porous structure of the foam. The excellent magneto-transport properties of GF open a way towards three-dimensional graphene-based magnetoelectronic devices. Magnetoresistance (MR) of graphene is fixed under a particular magnetic field and temperature but can be further improved or controlled by introducing artificial defect states. These artificial defects can be introduced via fluorination that is a conventional method to control the magnitude of MR required for magnetoelectronic applications. One of the main benefits of fluorination is the de-fluorination, which takes place within few days resulting in doping-free defects. Herein, tunable and temperature-independent magnetotransport of GF is achieved by controlled fluorination process for the first time. The magnitude of MR decreases with the increasing fluorination time (i.e. 30, 60 and 90 min), indicating defects induced scattering plays a major role in magnetotransport properties of fluorinated GF (FGF). The magnitude of MR in FGF specimens at room temperature (under a magnetic field strength of 5 T) was observed for three months, a particular value of MR (FGF-30 ~ 59%, FGF-60 ~ 58%, FGF-90 ~ 37%) is observed that is higher in magnitude than the first day of fluorination. In this way, fluorination of GF can provide a pathway to tune magnetotransport properties being very useful for magnetoelectronics devices especially highly sensitive magnetic sensors.

References

1. Y. Hao, L. Wang, Y. Liu, H. Chen, X. Wang, C. Tan, S. Nie, J. W. Suk, T. Jiang, T. Liang, J. Xiao, W. Ye, C. R. Dean, B. I. Yakobson, K. F. McCarty, P. Kim, J. Hone, L. Colombo and R. S. Ruoff, *Nat Nanotechnol* 11 (5), 426-431 (2016).
2. K. S. Novoselov, V. I. Falko, L. Colombo, P. R. Gellert, M. G. Schwab and K. Kim, *Nature* 490 (7419), 192-200 (2012).
3. K. Shehzad, Y. Xu, C. Gao and X. Duan, *Chem Soc Rev* 45 (20), 5541-5588 (2016).
4. P. Li, Q. Zhang, X. He, W. Ren, H.-M. Cheng and X.-x. Zhang, *Phys Rev B* 94 (4), 045402 (2016).
5. G. Xu, C. M. Torres, J. Tang, J. Bai, E. B. Song, Y. Huang, X. Duan, Y. Zhang and K. L. Wang, *Nano Lett* 11 (3), 1082-1086 (2011).
6. A. T. Murdock, A. Koos, T. B. Britton, L. Houben, T. Batten, T. Zhang, A. J. Wilkinson, R. E. Dunin-Borkowski, C. E. Lekka and N. Grobert, *Acs Nano* 7 (2), 1351-1359 (2013).

7. Y. Zhang, T. T. Tang, C. Girit, Z. Hao, M. C. Martin, A. Zettl, M. F. Crommie, Y. R. Shen and F. Wang, *Nature* 459 (7248), 820-823 (2009).
8. R. U. R. Sagar, X. Zhang and C. Xiong, *Mater Res Innov* 18 (S4), S4-706-S704-710 (2014).
9. C. H. Lui, Z. Li, K. F. Mak, E. Cappelluti and T. F. Heinz, *Nat Phys* 7 (12), 944-947 (2011).
10. A. Allain, J. Kang, K. Banerjee and A. Kis, *Nat Mater* 14 (12), 1195-1205 (2015).
11. R. U. R. Sagar, M. Galluzzi, C. Wan, K. Shehzad, S. T. Navale, T. Anwar, R. S. Mane, H. G. Piao, A. Ali and F. J. Stadler, *ACS Appl Mater Interfaces* 9 (2), 1891-1898 (2017).

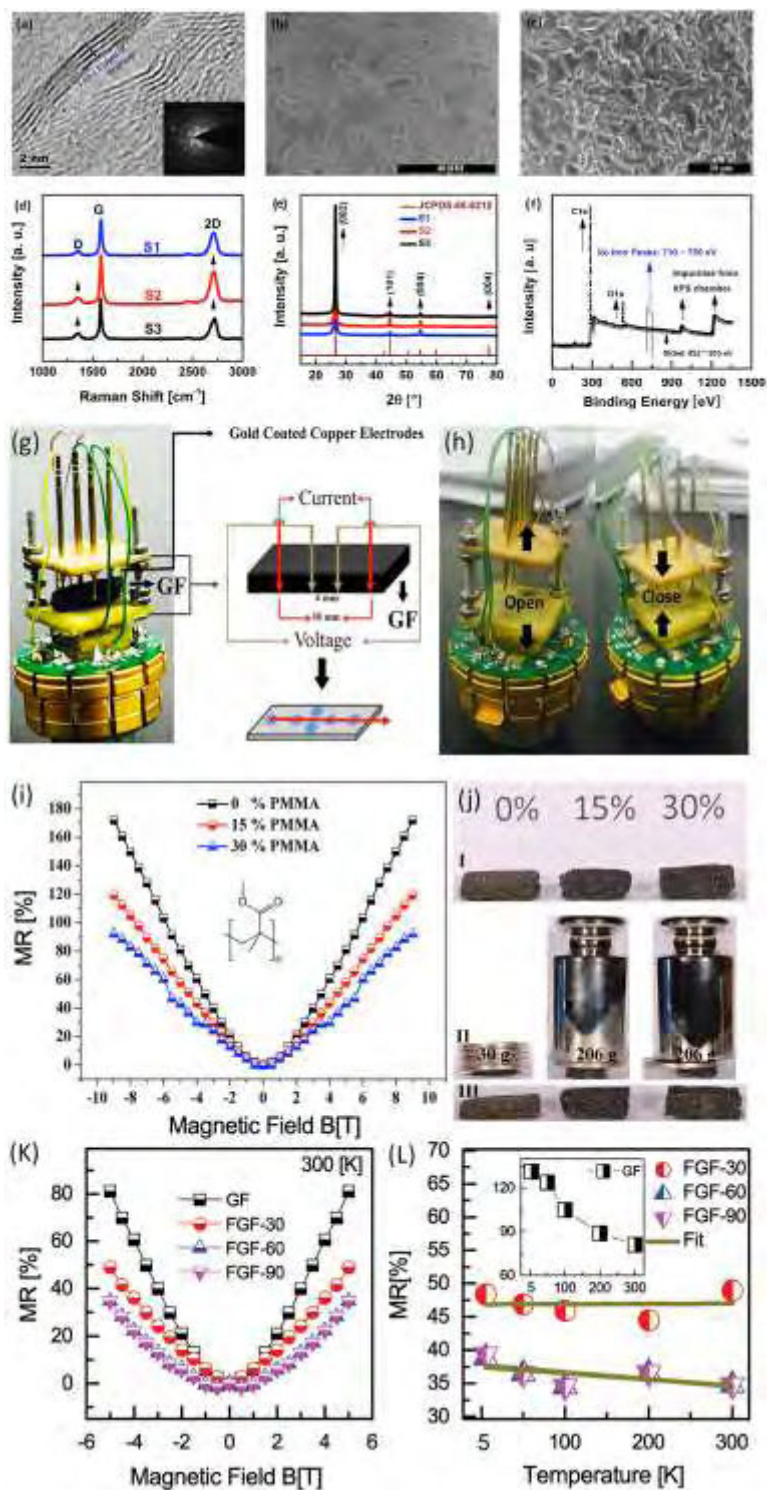


Figure 1: Characterization of Chemical Vapor Deposition (CVD) grown graphene foam (GF) (a-f). Electrode assembly for magnetotransport properties of GF (g-h). Magnetoresistance (MR) of GF and GF/Polymethyl-methacrylate (PMMA) specimen (i) Mechanical stability of GF *via* PMMA infiltration. MR of fluorinated GF (FGF) under 30, 60 and 90 mins.

Suyan Shan

Yong Liu*

Laboratory of Nanoscale Biosensing and Bioimaging,
School of Ophthalmology and Optometry, School of Biomedical Engineering,
State key Laboratory of Ophthalmology, Optometry and Vision Science
Wenzhou Medical University, Wenzhou, Zhejiang 325027, China

yongliu@wmu.edu.cn

The fibroblast growth factor modified nitrogen-containing graphene for regeneration of photo-damaged retinal pigment epithelial cells

Abstract:

Age-related macular degeneration (AMD) is one of the most common ocular diseases which may cause irreversible blindness, particularly among people who are aged more than 65 years. AMD is mainly caused by the apoptosis of retinal pigment epithelial (RPE) cells. RPE cells contain lipofuscin and rich long-chain unsaturated fatty acids which are sensitive to reactive oxygen species (ROS). Presence of excessive ROS inside cells always results in the damage or apoptosis of cells. Thus, it is a big challenge for both scientists and clinicians on how to decrease the level of ROS inside damaged RPE cells and realize the regeneration of RPE cells, for the treatment of AMD related diseases.

In this work, we synthesized nanocomposites from the basic fibroblast growth factor (bFGF) and graphene which could efficiently facilitate the reduction of ROS. Our recent study discovered that nitrogen-doped graphene (NG) exhibited superb catalytic activity for reduction of oxygen [1]. It is thus interesting to investigate the capability of NG on the reduction of ROS inside cells. This work presents a facile way to prepare nitrogen containing molecules (such as bFGF) modified graphene (bFGF-NG) via a self-discovered edge-functionalized ball milling method [2, 3]. The capability of the resulting bFGF-NG to eliminate the ROS inside photo-damaged RPE cells will be discussed. Presence of bFGF can further inhibit the oxidative stress of cells by enhancing the activity of signal pathways such as PI3K/AKT and Nrf₂. Incorporation of graphene with bFGF is also beneficial for improving the poor stability and half-life period of bFGF inside cells. Our preliminary results support that the ROS level of photo-damaged RPE cells could be significantly reduced by the utilization of the as-synthesized bFGF-NG nanocomposites, suggesting possibility for the regeneration of ROS induced apoptotic cells.

References

- [1] L. Qu, Y. Liu, J. Baek, L. Dai. ACS Nano. (2010) 4, 1321.
- [2] L. Yan, M. Lin, C. Zeng, et al. J. Mater. Chem. (2012) 2, 8367.
- [3] M. Lin, S. Shan, P. Liu, et al. J. Biomed. Nanotechnol. (2018) 14, 1-10.

Figures

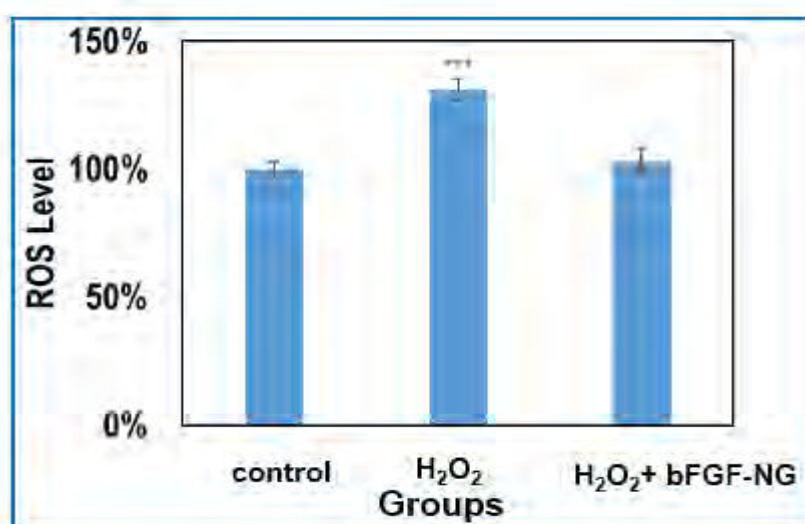


Figure 1: The ROS level of ARPE-19 after cultured with H_2O_2 and H_2O_2 + bFGF-NG. The ROS level is reduced near to 40% by bFGF-NG.

Gwang Hyuk Shin

Junghoon Park, Khang June Lee, Geon-Beom Lee, Hyun Bae Jeon, Yang-Kyu Choi, Kyoungsik Yu and Sung-Yool Choi

School of Electrical Engineering, Center for Advanced Materials Discovery towards 3D Display, KAIST, Daejeon, Korea

skh89@kaist.ac.kr

Si-MoS₂ Vertical Heterostructure for High Responsivity Photodetector

We demonstrate the photodiode characteristics based on mechanically exfoliated multilayer MoS₂/p-type silicon heterojunction by optimizing the thickness of the MoS₂ layer. Among devices, 48-nm thickness MoS₂ device showed the best performance with the responsivity (R) of 76.1 A/W, the detectivity (D^*) of 1.6×10^{12} Jones, and the noise equivalent power (NEP) of 7.82×10^{-15} A/Hz^{1/2} at an external reverse bias, which is approximately 100-fold improvement of the R compared to the commercial Si p-i-n photodiode with the R below 1 A/W. In addition, the device exhibited zero bias operation (photovoltaic characteristic) with the open-circuit voltage (V_{oc}) of 0.5 V and the short-circuit current density (J_{sc}) of 161 mA/cm². Indeed, this p-n vertical van der Waals heterojunction exhibited good photoresponse characteristics. These results could contribute to the application of MoS₂/Silicon heterojunction toward optoelectronics such as photodetectors [1] and solar cells [2].

References

- [1] Wang, L. et al., Adv. Funct. Mater., 25 (2015) 2910-2919
- [2] Tsai, M.-L. et al., ACS Nano, 8 (2014) 8317-8322

Figures

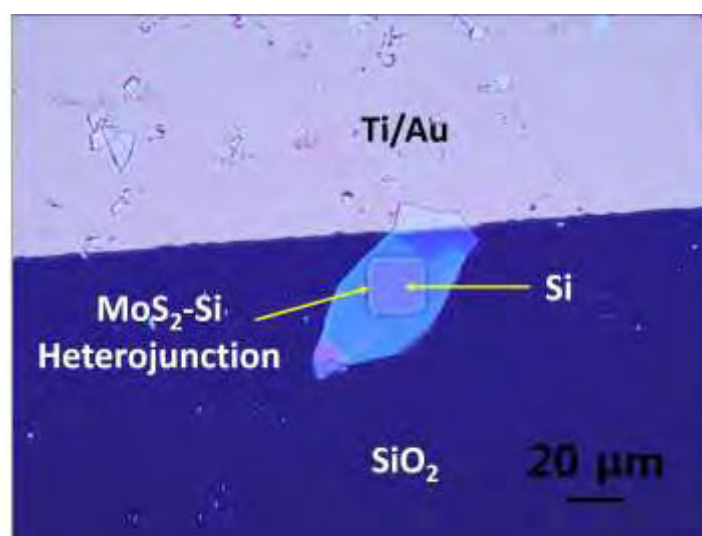


Figure 1: Optical microscope image of the photodetector.

Jinhua Sun¹

Vincenzo Palermo^{1,2}

¹ Department of Industrial and Materials Science, Chalmers University of Technology, Gothenburg, Sweden

² Institute of Organic Synthesis and Photoreactivity (ISOF), National Research Council of Italy (CNR), Via P. Gobetti 101, I-40129 Bologna, Italy

jinhua@chalmers.se

Molecular pillar approach to construct functionalized graphene for energy storage

The rich and numerous oxygen-containing functional groups decorated on graphene oxide (GO) provide a possibility to chemically modify GO for various applications. In my talk, I will first introduce our research progress in tuning the interlayer distance of GO in the precision of angstrom by swelling in different solvents and using intercalation of differently sized organic molecular pillars, with the focus on using rigid molecule (Tetrakis(4-aminophenyl)methane (TKAm)) to make inter-linking of GO planes (Figure 1a).[1] The 3D shape of this rigid molecule could be of advantage for stability of pillared structures. The synthesized GO pillared with TKAm shows an expansion of inter-layer distance of GO from $\sim 7.5\text{\AA}$ to $13\text{-}14\text{\AA}$. The intercalated TKAm as molecular pillars expand the GO structure resulting in high surface area up to $660\text{ m}^2\text{ g}^{-1}$. Besides 3D molecules, a simple molecule 4-benzene diboronic acid (DBA) as an idealized linker was reported to be efficient for linking GO.[2] However, our previous studies have demonstrated that the DBA molecules are likely to attach only on one side of inter-layer. Instead of using it to prepare graphene pillared structure, our alternative idea is to develop a molecular pillar approach to construct 2D-2D hybrid materials by using DBA pillars on GO. I will introduce how we utilize the chemically attached DBA as molecular pillars to directing grow ultrathin covalent organic frameworks (COF) nanosheets (v-COF-GO) (Figure 1b).[3] The hybrid material shows forest of COF-1 nanosheets with thickness of ~ 3 to 15 nm vertically grafting on the surface of GO via DBA linker. To emphasize the important role of DBA pillars on vertical growth of COF-1, the same reaction in absence of molecular pillars was performed and resulted in uncontrollable growth of thick COF-1 platelets parallel to the surface of GO. The v-COF-GO was converted into conductive carbon material with ultrathin porous carbon nanosheets grafted to graphene in edge-on orientation. It was demonstrated as a high-performance electrode material for supercapacitors. Controlling nucleation of 2D COF sheets and their growth direction by using molecular pillars covalently attached to graphene as structure-directing agent provides very promising route for preparation of new family hybrid materials.

References

- [1] J. H. Sun, F. Morales-Lara, A. V. Talyzin, et al., *Carbon* 120 (2017) 145-156.
- [2] J. W. Burrell, S. Gadipelli, J. Ford, et al., *Angew. Chem. Int. Ed.* 49 (2010) 8902-8904.
- [3] J. H. Sun, A. Klechikov, A. V. Talyzin, et al., *Angew. Chem. Int. Ed.* 57 (2018) 1034-1038.

Figures

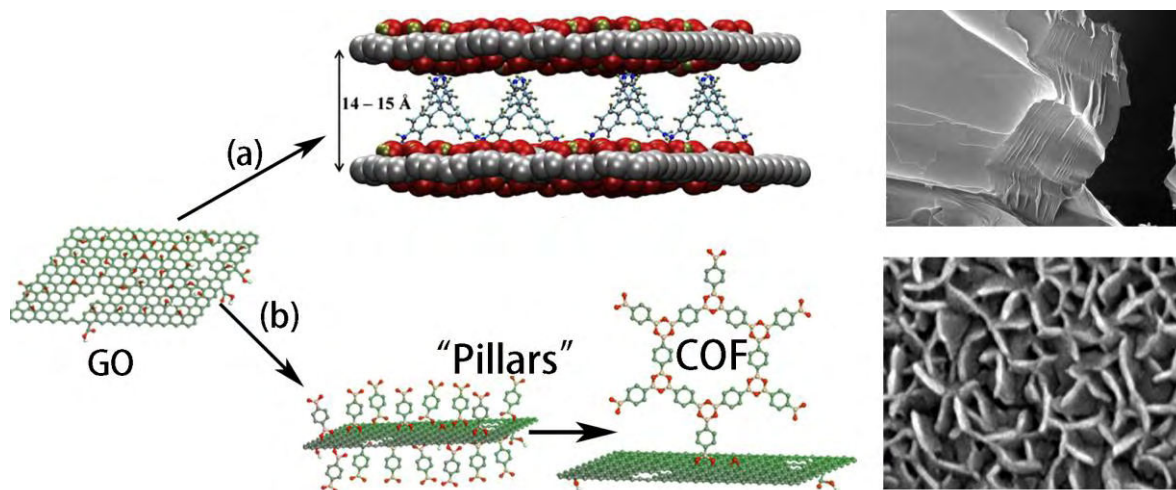


Figure 1: (a) Intercalation of rigid 3D molecules into interlayers of graphene for the synthesis of pillared graphene. (b) Growth of vertical COF-1 nanosheets using DBA as molecular nucleation sites grafted on GO.

Xiao Sun

Hailin Peng and Zhongfan Liu

Peking University, 202 Chengfu Road, Haidian District, Beijing 100871, P. R. China

sunxiao-cnc@pku.edu.cn

Rapid Growth of Large Single-Crystalline Graphene with Ethane

Many studies are conducted based on large single-crystalline graphene for its promising application prospects. Contemporary growth conditions of large domain size graphene not only requiring a fastidious condition, but also suffering from a slow growth^[1, 2]. Thus, it led to a high energy consumption in large-scale production. Herein, we report a rapid growth method of large single-crystalline graphene using ethane as carbon feedstock. Experimental results have shown ethane as a carbon source could trigger the growth of high-quality graphene 4 times faster than using methane. Sub-centimeter single-crystalline graphene at 1000 °C by using ethane was achieved, with a remarkable growth rate 420 $\mu\text{m min}^{-1}$. In addition, for rapid growth of large single-crystalline graphene we proposed a method by making good use of thermal decomposition of carbon source which has lower decomposition energy barrier.

References

- [1] Han, G. H.; Gunes, F.; Bae, J. J.; Kim, E. S.; Nano Lett. 11 (2011), 4144.
- [2] Zhou, H.; Yu, W. J.; Liu, L.; Cheng, R.; Nat. Commun. 4 (2013), 2096.

Figures

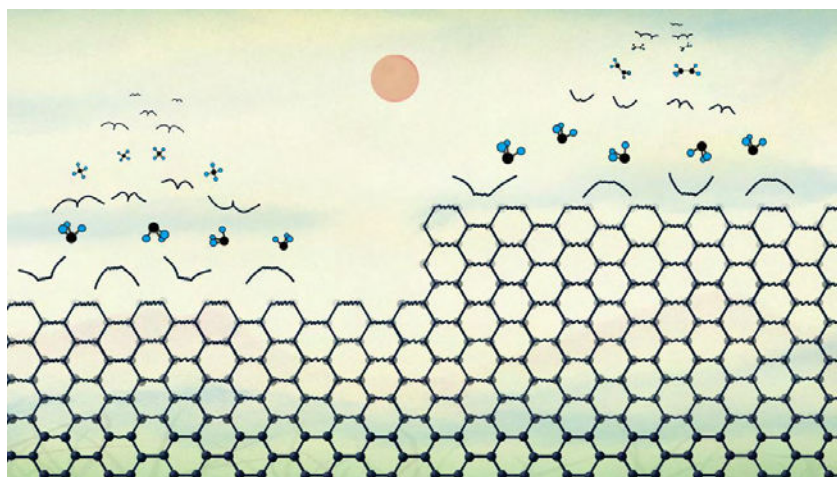


Figure 1: Comparison of graphene growth with methane (left) and ethane (right).

Haihua Tao

Shubin Su, Hao Li, Yixuan Wu, Huan Yue, Xianfeng Chen

Institute of Physics and Astronomy, Shanghai Jiao Tong University, Shanghai 200240, China

tao.haihua@sjtu.edu.cn

Patterning Graphene Film by Magnetic-assisted UV Photochemical Oxidation

Patterning graphene film is a significant step in fabricating graphene-based elements in optoelectronics. In this talk, I will present a feasible solution, including our recent breakthrough progress, to make graphene patterns by magnetic-assisted UV photochemical oxidation that overcomes the obstacles of organic contamination, linewidth resolution, and substrate damaging [1-4]. During this process, the photodissociated paramagnetic oxidative radicals are magnetized and they form directional motions in an inhomogeneous external magnetic field. As a consequence, the directional and enhanced oxidation of these radicals facilitate graphene patterning. Using a ferromagnetic steel mask, a certain inhomogeneous vertical magnetic-field-assisted UV photochemical oxidation has a capability of patterning graphene microstructure with a line width of 20 μm and lateral under-oxidation less than 1 μm . This approach can be applied to fabricate graphene field-effect transistor and photodetector arrays. Magnetic-assisted UV photochemical oxidation should be a promising solution toward resist-free, substrate non-damaging, and cost-effective fabrication of graphene microstructures.

References

- [1] Y. Wu, H. Tao*, S. Su, H. Yue, H. Li, Z. Zhang, Z. Ni, and X. Chen*. *Sci. Rep.* 7, 46583, 2017.
- [2] H. Yue, H. Tao*, Y. Wu, S. Su, H. Li, Z. Ni, and X. Chen*. *Phys. Chem. Chem. Phys.* 19, 27353, 2017.
- [3] Z. Zhang, H. Tao*, H. Li, G. Ding, Z. Ni, and X. Chen*. *Opt. Mater. Express* 6, 3527, 2016.
- [4] N. Leconte, J. Moser, P. Ordejon, H. Tao, A. Lherbier, A. Bachtold, F. Alsina, C. M. S. Torres, J. C. Charlier and S. Roche, *ACS Nano* 4, 4033, 2010.

Figures

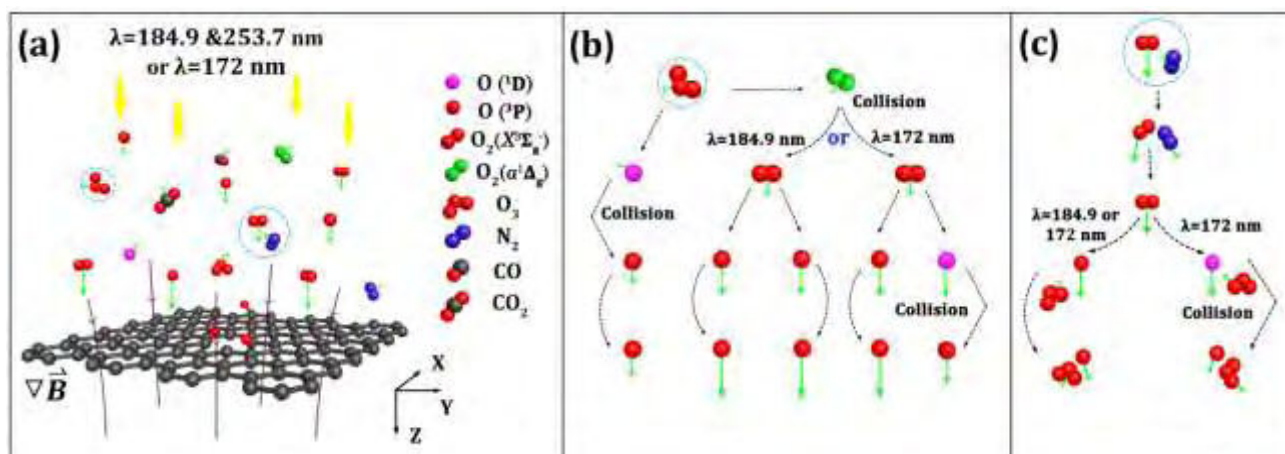


Figure 1: Dynamic photochemical reaction in the magnetic-assisted UV photochemical oxidation ($B_z=0.31$ T, $\nabla B_z=90$ T·m⁻¹) under irradiation of the ultraviolet lamp. (a) Dynamic motion of various molecules with green arrows denoting the velocity. (b) Photodissociation of ozone and oxygen molecule under different UV excitations in the magnetic field. (c) Collisions between the oxygen molecule/atoms and the diamagnetic molecules. The diamagnetic singlet oxygen molecule ($\alpha^1\Delta_g$) and atom (O(¹D)) deactivate individually to their ground states via collisions.

Lei Tao (陶蕾)^{1,2}

Yu-Yang Zhang (张余洋)^{1,2,3}, Jiatao Sun (孙家涛)^{1,2}, Shixuan Du (杜世萱)^{1,2,3†}

and Hong-Jun Gao (高鸿钧)^{1,2,3}

¹Institute of Physics, Chinese Academy of Sciences, Beijing 100190, China

²University of Chinese Academy of Sciences, Beijing 100190, China

³CAS Center for Excellence in Topological Quantum Computation, Chinese Academy of Sciences, Beijing 100190, China

ltao@iphy.ac.cn

Band engineering of double-wall Mo-based hybrid nanotubes

Hybrid transition-metal dichalcogenides (TMDs) with different chalcogens on each side (X-TM-Y) have attracted attentions because of the unique properties. Nanotubes based on hybrid TMD materials have advantages in flexibility over conventional TMD nanotubes. Here we predict the wide band gap tunability of hybrid TMD double-wall nanotubes (DWNTs) from metal to semiconductor. Using density-function theory (DFT) with HSE06 hybrid functional, we find that the electronic property of X-Mo-Y DWNTs (X = O and S, inside a tube. Y = S and Se, outside a tube) depends both on electronegativity difference and diameter difference. If there is no difference in electron negativity between inner atoms (X) of outer tube and outer atoms (Y) of inner tube, the band gap of DWNTs is the same as that of the inner one. If there is a significant electronegativity difference, the electronic property of DWNTs ranges from metallic to semiconducting, depending on diameter differences. Our results provide alternative ways for the band gap engineering of TMD nanotubes.

References

[1] Lei Tao, Yu-Yang Zhang, Jiatao Sun, Shixuan Du, Hong-Jun Gao, Band engineering of double-wall Mo-based hybrid nanotubes, Chinese Physics B, Vol. 27, No. 7, 2018.

He Tian

Tsinghua University, Beijing, China

tianhe88@tsinghua.edu.cn

Novel 2D devices based on graphene, BP and perovskite

In this talk, I will introduce several novel 2D devices beyond graphene. The first part is related to graphene devices. Tunable graphene LED [1] and graphene artificial throat [2] has been demonstrated. The second part is related to 2D perovskite devices. Record low operation current 2D perovskite-RRAM has been demonstrated [3]. Great stability has also been demonstrated via hBN-2D perovskite stacking [4]. The third part is related to BP devices. Reconfigurable BP-SnSe synapse has been demonstrated [5]. Moreover, the reconfigurable BP p-n junctions have been demonstrated with ideality factor close to 1 [6].

References

- [1] X. Wang+, **H. Tian+**, et al., Nature Communications, 6 (2015) 7767.
- [2] L. Tao+, **H. Tian+**, et al., Nature Communications, 8 (2017) 14579.
- [3] **H. Tian***, et al., ACS Nano, 11 (2017) 12247.
- [4] L. Zhao+, **H. Tian+***, et al., Joule, In press (2018).
- [5] **H. Tian**, et al., ACS Nano, 11 (2017) 7156.
- [6] **H. Tian***, et al., IEEE Transactions on Electron Devices, In press (2018).

Hai Wang

Mischa Bonn

Molecular Spectroscopy Group, Max Planck Institute for Polymer Research,

Ackermannweg 10, 55128 Mainz, Germany

wanghai@mpip-mainz.mpg.de

Tailoring Graphene: from optical control of carrier density to bandgap engineering in graphene nanoribbons

Abstract

Owing to their massless nature, charge carriers in graphene possess record mobilities up to $350,000 \text{ cm}^2\text{-V}^{-1}\text{-s}^{-1}$.^[1] The application of graphene for high mobility devices requires switching the conducting states in graphene, so that control of the carrier density or Fermi level is critical. Control of the Fermi level is conventionally achieved by electrostatic or electrochemical gating.^[2] Such Fermi energy tuning schemes are effective, but typically require elaborate clean room fabrication, especially when sub-micron local gating structures are required. Here, I will present two examples of effectively modulating the doping structures in graphene in a convenient and reversible manner, by: (1) optically controlling the adsorption-desorption equilibrium of molecular oxygen (a p-dopant) by laser excitation to dynamically modify the doping concentration in graphene;^[3] and (2) tuning the photo-induced structural change and charge transfer dynamics between the grafted molecules and graphene.^[4] Additionally, we demonstrate that the optical control of Fermi energy in graphene allows one to optically write doping structure with spatial control, opening new opportunities for creating complex doping features in a convenient way.

The second part of the talk will deal with graphene nanoribbons. Due to its semimetal characteristics of graphene's band structure, the on-off ratio in the graphene-based transistor is too low to be useful for practical applications. It has been a long-standing pursuit, to open up and control the bandgap in graphene, by tailoring the graphene into its nanoribbons with atomic precision. Recent advances in bottom-up synthesis in Mainz (in the group of Dr. Akimitsu Narita, Prof. Xinliang Feng and Prof. Klaus Muellen) now allow atomic control of graphene nanoribbons (GNRs) with well-defined bandgap and optical properties. I will present some of our recent optical ultrafast conductivity studies on graphene nanoribbons using THz spectroscopy, and show how the conductivity varies with the precise structure of the nanoribbons (e.g. the width, and edge structure).^[5-7]

References

- [1] Banszerus Luca et al., Ultrahigh-mobility graphene devices from chemical vapor deposition on reusable copper, *Science Advances* **2015** 1(6), e1500222;
- [2] Kostya S Novoselov et al., Electric field effect in atomically thin carbon films, *Science* **2004** 306 (5696), 666-669;
- [3] Hai I Wang et al., Reversible Photochemical Control of Doping Levels in Supported Graphene, *The Journal of Physical Chemistry C* **2017**, 121 (7), 4083–4091;
- [4] Zhaoyang Liu, Hai I Wang et al., Photoswitchable Micro-Supercapacitor Based on a Diarylethene-Graphene Composite Film, *Journal of the American Chemical Society* **2017**, 139 (28), 9443–9446;
- [5] Zongping Chen, Hai I Wang et al., Lateral Fusion of Chemical Vapor Deposited N = 5 Armchair Graphene Nanoribbons, *Journal of the American Chemical Society* **2017**, 139 (28), 9483–9486;

[6] Zongping Chen, Hai I Wang et al., Chemical Vapor Deposition Synthesis and Terahertz Photoconductivity of Low-Band-Gap N = 9 Armchair Graphene Nanoribbons, *Journal of the American Chemical Society* **2017**, 139 (10), 3635–3638;

[7] Ivan Ivanov et al., Role of Edge Engineering in Photoconductivity of Graphene Nano-ribbons, *Journal of the American Chemical Society* **2017**, 139 (23), 7982–7988;

Hai Wang

Caihong Yang

Ministry-Province Jointly-Constructed Cultivation Base for State Key Laboratory of Processing for Non-ferrous Metal and Featured Materials, Guangxi Zhuang Autonomous Region, Guilin, China.

hbwanghai@gmail.com

Consideration on the structure of Mo-based anode materials for improving lithium storage performance

Abstract: Mo-based compounds have drawn increasing interest because of their high theoretical specific capacity and cyclic stability. Our research group had synthesized several kinds of Mo-based compounds, such as H_xMoO_3 , $MoO_{2.5}(OH)_{0.5}$, MoO_{3-x} in recent years, and explored their electrochemical properties. In the process, we noticed that the structure of Mo-based compounds is wide in tunability. There is no doubt that this offers us a lot of opportunities, for example, heteroatom doping and hybridization with carbon-based compounds, in the hope of changing the defects of the electrode material itself, such as their poor electrical conductivity and pulverization during charge-discharge, so as to improve the battery performance.

References

- [1] H. Wang, Y. Su, RSC Adv., 6(2016), 97749-97758.
- [2] Y. Song, H. Wang, Z. Li, N. Ye, L. Wang, Y. Liu, Int. J. Hydrogen Energy, 9 (2015), 3613-3623.
- [3] Y. Song, H. Wang, Z. Li, N. Ye, L. Wang, Y. Liu, RSC Adv., 5(2015), 16386-16393.

Figures

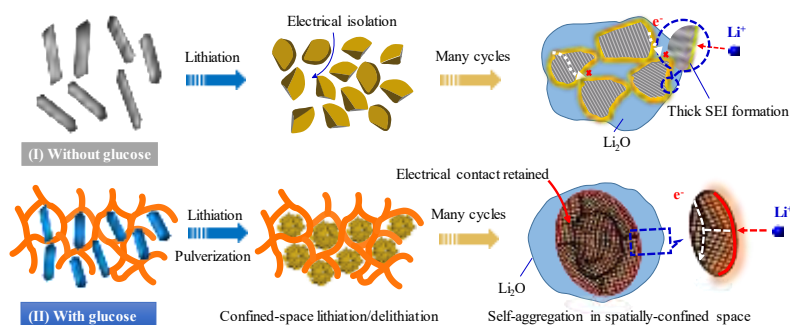


Figure 1: Spatially-confined electrochemical reactions of MoO₃ nanobelts were designed rationally for reversible high capacity by a green and simple vacuum drying method.

Co-synthesis of atomic Fe and few-layer graphene towards superior electrocatalysts of O₂ and CO₂

Abstract Large-scale synthesis of either single-metal atom catalyst or graphene from graphite direct exfoliation at high yield is quite challenging. Here we demonstrate a scalable electrochemical approach to synthesize few-layer graphene flakes and isolated Fe atoms at the same time. It is found that graphite could be expanded in FeCl₄⁻ ionic liquid at a low potential of 2 V. Fe isolated onto graphene results from electrochemical reactions of FeCl₄⁻-based intercalates. After annealing at the presence of nitrogen source, atomic Fe isolation is kept and coordinated with nitrogen. The paintable atomic layer material exhibits superior oxygen reduction reaction performance to Pt/C. The catalytic activity could be enhanced 30 times per gram and 100 times per metal atom, if Fe-Nx/graphene is compared with Pt/C (20 wt.% Pt) on the basis of metal content. After changing the synthesis conditions, atomic irons embedded in a new hierarchical carbon matrix were prepared which exhibits superior properties in CO₂ electroreduction. A highly selective conversion of CO₂ to CO at low overpotential with maximum Faradaic efficiency of ~95% for 12 h was achieved.

References

- [1] J. Wang, H. Zhang, C. Wang, Y. Zhang, J. Wang, H. Zhao, M. Cheng, A. Li, J. Wang, Energy Storage Mater. 2018, 1, 1.
- [2] H. Zhang, J. Wang, Z. Zhao, H. Zhao, M. Cheng, A. Li, Y. Zhang, C. Wang, J. Wang, J. Wang, Green Chem. 2018, 20, 3521.

Figures

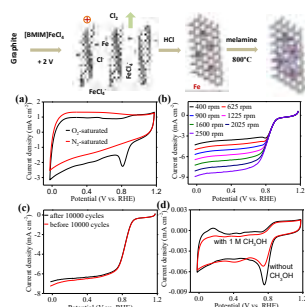


Figure 1: Co-synthesis of few-layer graphene and atomic Fe through electrochemical exfoliation of graphite in FeCl₄⁻ ionic liquid. Electrochemical performances in O₂-saturated 0.10 M KOH solution of N-Fe/G. (a) CV curves, (b) Rotating-disk voltammograms at the different rotation rates. (c) Endurance tests. (d) CV curves without and with 1.0 M CH₃OH.

Presenting Author (Lin Wang)

Co-Authors (Jin Wang, Cheng Guo, Xiaoshuang Chen)

Shanghai Institute of Technical Physics, Chinese Academy of Sciences, 500 Yu-Tian Road, Shanghai, China

wanglin@mail.sitp.ac.cn

Toward Sensitive Terahertz Detection Based on Two-dimensional Materials

Abstract

Terahertz band, routinely defined with frequency ranged from 0.1THz to 10THz, has find its unique advantage for extensive applications like remote sensing, biomedical imaging, security due to its non-invasive nature, and located with the same energy as the rotational and vibrational modes in biomolecules. Even if it has been lightened by the explosion of science and technological knowledge since the last decade, the terahertz band is still considered as a "black hole" going from basic technological weakness, due to the scarcity of reliable source as well as sensitive detectors. Photon detector reported to date has been rendered to be impossible to work at wavelength far below the bandgap, and the efficiency decreased evidently when the wavelength is extended. Therefore, it is still formidable challenge to achieve sensitive terahertz detection following the formerly well-established rules. This work will introduce the interdisciplinary study of material science and terahertz photonics recently in our group. Here, we review our recent outcomes of graphene-like two-dimensional materials with peculiar properties being well suited to THz-oriented applications. Graphene, and transition-metal dichalcogenides(TMDs) exhibiting novel quantum state of matter, due to their novel two-dimensional nature. We have achieved antenna-integrated structure, allowing for both the electromagnetic coupling and electrical interconnection. As benefitting from its small electronic heat capacity, the hot electron stays with high kinetic energy leading to the prominent phenomenon of photoconductive. Photogalvanic effect of Bi₂Se₃ compound is observed at THz band, allowing the efficient direct photocurrent generation. All these results open up new opportunities to achieve flexible detectors with high responsivity as well as fast response.

References

- [1] Weiwei Tang, Antonio Politano, Cheng Guo, Wanlong Guo, Changlong Liu, Lin Wang, Xiaoshuang Chen, Wei Lu. Ultrasensitive room-temperature terahertz direct detection based on a bismuth selenide topological insulator. *Adv. Funct. Mater.* 1801786 (2018).
- [2] Changlong Liu, Lin Wang, Xiaoshuang Chen, Jing Zhou, Weida Hu, Xinran Wang, Jinhua Li, Zhiming Huang, Wei Zhou, Weiwei Tang, Gangyi Xu, Shao-Wei Wang, Wei Lu. Room-temperature photoconduction assisted by hot-carriers in graphene for sub-terahertz detection. *Carbon*, 130, 233-240(2018).
- [3] Changlong Liu, Lei Du, Weiwei Tang, Dacheng Wei, Jinhua Li, Lin Wang, Gang Chen, Xiaoshuang Chen, Wei Lu. Towards sensitive terahertz detection via thermoelectric manipulation using graphene transistors. *NPG Asia Materials*, 10, 318-327 (2018).
- [4] Lin Wang, Changlong Liu, Xiaoshuang Chen, Jing Zhou, Weida Hu, Xiaofang Wang, Jinhua Li, Weiwei Tang, Anqi Yu, Shao-Wei Wang, Wei Lu. Toward sensitive room-temperature broadband detection from infrared to terahertz with antenna-integrated black phosphorus photoconductor. *Adv. Funct. Mater.* 27, 1604414 (2017)

Figures

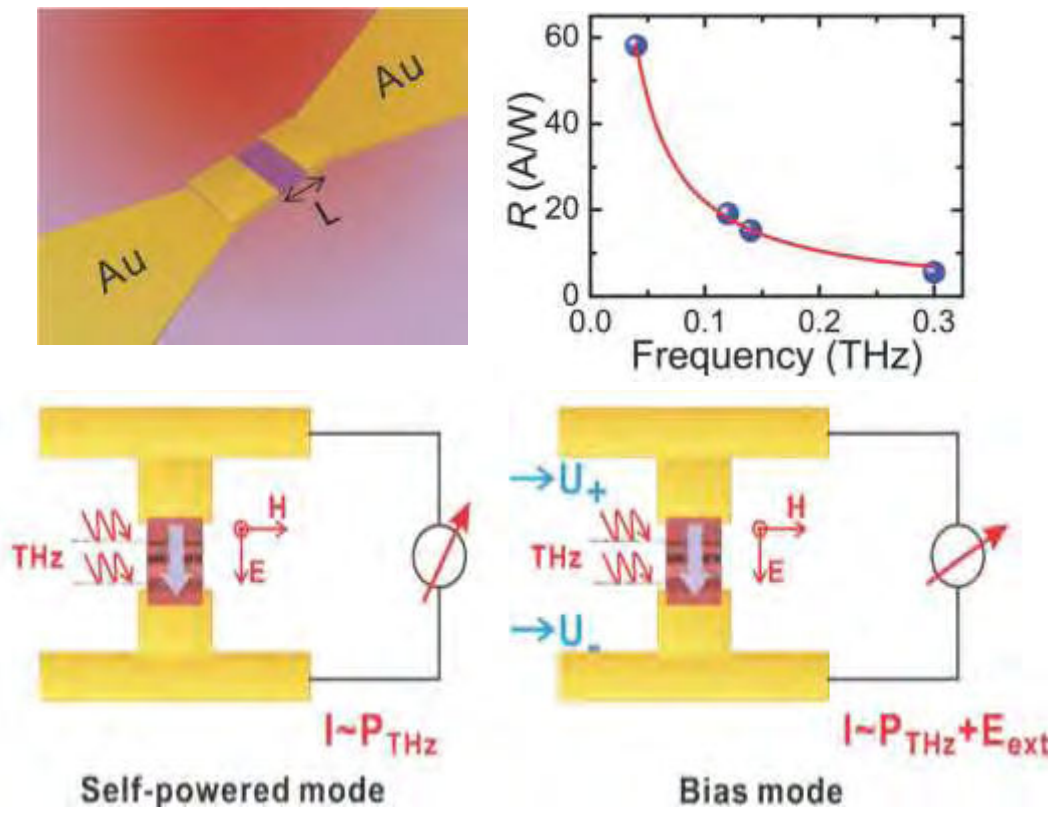


Figure 1: Schematic of MTM (metal-topological insulator-metal) terahertz detector, and frequency dependent response for self-powered and bias modes.

Low-temperature superlubricity of suspended graphene

We study the superlubric sliding of a nanometer-sized diamond-like-carbon tip over a suspended graphene layer at different temperatures using molecular dynamics [1-5]. Dramatic effects of thermally- and mechanically-induced rippling are demonstrated on the frictional properties of free-standing graphene. The tensile deformation of graphene in response to the normal load is found to be beneficial for achieving low friction at most of the studied temperatures. However, graphene at liquid-helium temperature exhibits an inverse trend, the friction is even found to be negative at low-load. This abnormal behavior arises from the oscillation of graphene in favor of superlubricity. The breakdown of superlubricity in suspended graphene is found to be strongly correlated to the competition between the rippling and oscillation mechanisms.

References

- [1] Z. Wang, to be published.
- [2] Z. Wang and M. Devel, Phys. Rev. B 83 (2011) 125422.
- [3] Z. Wang, Carbon 47 (2009) 3050.
- [4] Z. Wang, W. Mook, C. Niederberger, R. Ghisleni, L. Philippe and J. Michler, Nano Lett. 12 (2012) 2289.
- [5] W. Guo, Z. Wang and J. Li, Nano Lett. 15 (2015) 6582.

Figures

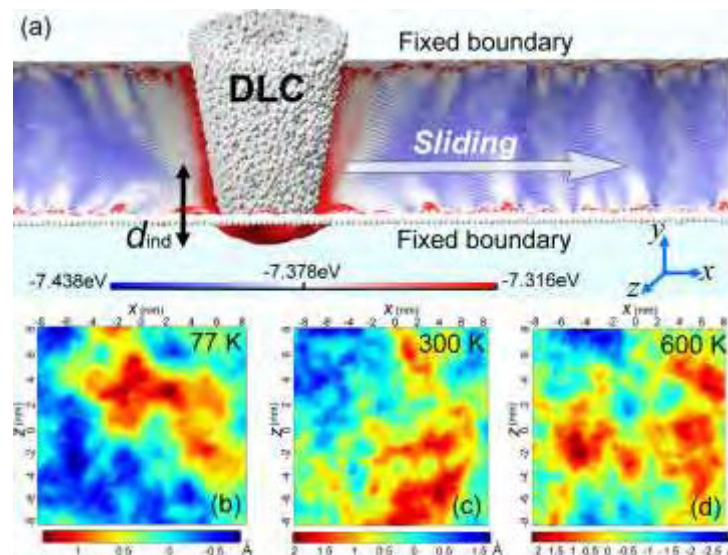


Figure 1: (a) Model setup for a DLC tip sliding over an infinite graphene layer that is suspended between two parallel hypothetical supports. (b-d) Morphology of suspended graphene at different temperatures.

Qinwei Wei

Songfeng Pei, Wencai Ren, Hui-Ming Cheng

1. Shenyang National Laboratory for Materials Science, Institute of Metal Research, Chinese Academy of Sciences, Shenyang 110016, P. R. China

2. School of Materials Science and Engineering, University of Science and Technology of China, 96 Jinzhai Road, Hefei 230026, P. R. China

Contact: qwwwei15s@imr.ac.cn

Green Controlled Synthesis of Graphene Oxide by Water Electrolytic Oxidation

Graphene oxide (GO), as an important graphene derivative, has many unique properties and interesting applications based on the chemical and physical properties of GO.[1] GO sheets are usually synthesized by oxidizing graphite with mixtures containing strong oxidizing agents, acid solvent and other chemical reagent.[2] However, the chemical oxidation encounter problems such as a complex preparing process, a long reaction time, involving explosive chemicals and toxic gas, a large amount of heavy metal waste water, which are obstacle for industrial preparation of graphene oxide. The electrochemical exfoliation of graphene has attracted attention due to easy, fast and environmentally friendly nature for producing graphene.[3] However, the electrochemical route of the synthesis of GO is not obtained so successful. We report a scalable, safe, ultrafast and green electrochemical method to synthesize GO sheets, which involves electrochemical intercalation of graphite by sulfur acid and subsequent water electrolytic oxidation. The pre-intercalation of graphite efficiently inhibits oxygen evolution and consequently enables ultrafast water electrolytic oxidation of graphite within a few seconds and the graphene oxide prepared is similar to those achieved by the chemical oxidation methods. We also discuss the mechanism of controlled synthesis of graphene oxide and its application.[4] In addition, we will report a one-step electrolytic method for synthesis of graphene quantum dots with blue fluorescent characteristics in aqueous solution.

References

- [1] D. R. Dreyer, S. Park, C. W. Bielawski, R. S. Ruoff, *Chemical Society Reviews*, 39(2010)228
- [2] C. Galande, W. Gao, A. Mathkar, A. M. Dattelbaum, et al., *Particle & Particle Systems Characterization*, 31(2014)619
- [3] S. Yang, M. R. Lohe, K. Müllen, et al., *Advanced Materials*, 28(2016)6213
- [4] S. Pei, Q. Wei, K. Huang, et al., *Nature Communications*, 9(2018)145

Figures

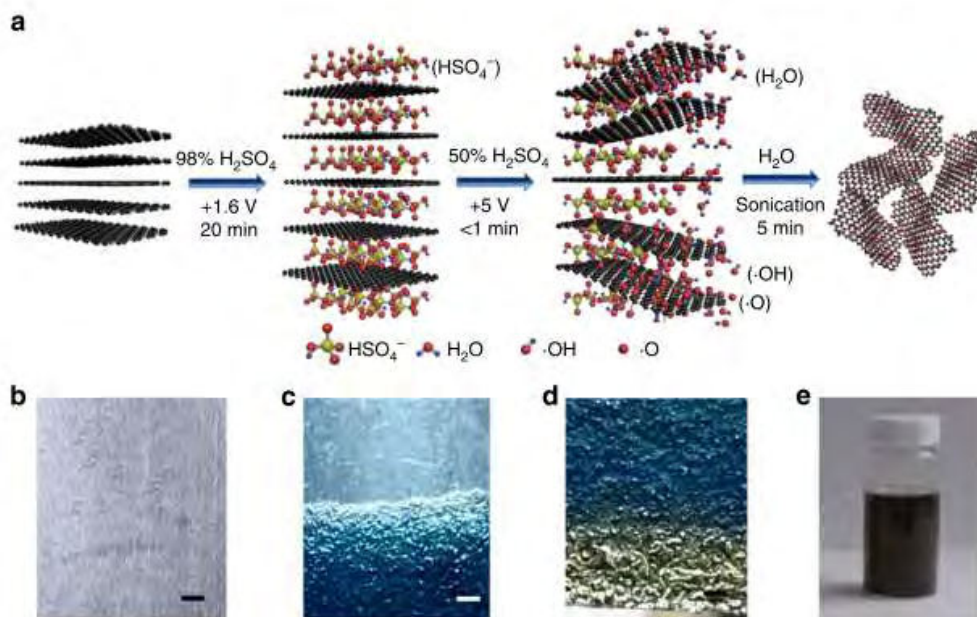


Figure 1: Synthesis of EGO by water electrolytic oxidation. a, Schematic illustration of the synthesis process of EGO by water electrolytic oxidation. b–e, Photos of the raw material and the products obtained at each step. b, FGP. c, GICP (blue area) obtained after EC intercalation of FGP in 98 wt.% H_2SO_4 at 1.6 V for 20 min. d, Graphite oxide (yellow area) obtained by water electrolytic oxidation of the GICP in 50 wt.% H_2SO_4 at 5 V for 30 s. e, Well-dispersed EGO aqueous solution ($5 \text{ mg}\cdot\text{mL}^{-1}$) obtained by sonication of the graphite oxide in water for 5 min. Scale bars in b-d: 1mm

ZhengMing Wu²

Colin Rawlings², Simon Bonanni², Martin Spieser², Philipp Mensch¹, Siegfried Kang¹, Heiko Wolf¹, Armin Knoll¹

¹IBM Research – Zurich, Saeumerstrasse 4, 8803 Rueschlikon, Switzerland

²SwissLitho AG, Technoparkstrasse 1, 8005 Zurich, Switzerland

wu@swisslitho.com

Fabrication of sub-20 nm Metal Electrodes on 2D Materials without a Charged Particle Beam

Abstract

Charged particle beams for the fabrication of devices comprising sensitive nanowires or 2D materials often lead to unwanted influence or damage of electronic properties of the device [1]. Still, electron beam lithography (EBL) in combination with lift-off is the most commonly used method to fabricate prototypes of such devices.

Thermal Scanning Probe Lithography (t-SPL) [2, 3] is an alternative mask-less lithography technique which is also commercially available since 2014. It provides similar speed (up to 20 mm/s) and resolution (10 nm half-pitch) as EBL, but without charged particles involved. Here, we present two recently developed lift-off techniques for t-SPL that have enabled the creation of complex sub-20 nm Au, Pt and Ni structures and devices without the usage of high energy charged particle beams [4].

Thermal Scanning Probe Lithography (t-SPL) uses a heated silicon tip to locally decompose and evaporate a thermally responsive resist [5], usually PPA (polyphthalaldehyde). A two-layer or three-layer process in combination with wet or dry etching is demonstrated to create a suitable under-cut for lift-off, respectively. During the t-SPL process the heated tip only influences the top PPA layer and leaves the underlying substrate unharmed. This is in contrast to beam based technologies like EBL or Focused Ion Beam (FIB) where most of the energy is actually deposited in the substrate and vacancies in graphene or other 2D materials can be created.

We demonstrate the capabilities of the new t-SPL lift-off processes by fabrication of transistors with improved performance (See Figure1). 50 nm wide fingered top gates have been fabricated with nanometer overlay accuracy. The superb switching behavior of the transistor shows the absence of trapped charge in the gate oxide, which usually occurs during EBL fabrication of such devices and prevents proper device operation.

ACKNOWLEDGMENTS:

We thank P. Mensch and S. Karg for providing InAs nanowires and performing the transport measurements, U. Drechsler for cantilever fabrication, and R. Allenspach and W. Riess for fruitful discussions. The research leading to these results received funding from European Union's Seventh Framework Program FP7/2007-2013 under Grant Agreement No. 318804 (SNM).

References

- [1] S. F. Karg, V. Troncale, U. Drechsler, P. Mensch, P. Das Kanungo, H. Schmid, V. Schmidt, L. Gignac, H. Riel, B. Gotsmann, *Nanotechnology* 25 (2014), 305702.
- [2] D. Pires, J.L. Hedrick, A. de Silva, J. Frommer, B. Gotsmann, H. Wolf, M. Despont, U. Duerig, A.W. Knoll, *Science* 328 (2010), 732-735
- [3] P.C. Paul, A.W. Knoll, F. Holzner, M. Despont, U. Duerig, *Nanotechnology* 22 (2011), 275306.
- [4] H. Wolf, C. Rawlings, P. Mensch, J.L. Hedrick, D.J. Coady, U. Duerig and A. Knoll, *J. Vac. Sci. Technol. B* 33 (2015), 02B102.

Figures

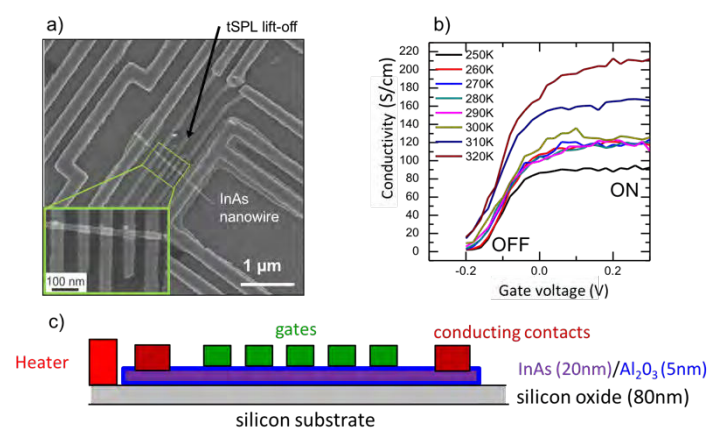


Figure 1: a) The gate electrodes of InAs nanowire transistor fabricated using the tSPL and lift-off. b) Switching behavior of the transistor. c) Schematic of the InAs nanowire transistor.

Zhenyuan Xia^{1,2}

Catia Arbizzani³, Meganne Christian⁴, Vittorio Morandi⁴, Massimo Gazzano¹,
Vincenzo Palermo^{1,2}

¹ Istituto per la Sintesi Organica e la Fotoreattività - Consiglio Nazionale delle Ricerche, via Gobetti 101, 40129 Bologna, Italy

² Industrial and Materials Science, Chalmers University of Technology, Hörsalsvägen 7B, 41258 Goteborg, Sweden

³ Dipartimento di Chimica "Giacomo Ciamician", University of Bologna, via Selmi 2, Bologna, 40126, Italy

⁴ Istituto per la Microelettronica e Microsistemi - Consiglio Nazionale delle Ricerche, via Gobetti 101, 40129 Bologna, Italy

zhenyuan@chalmers.se

Three-Dimensional Multilayer Graphene-Fe₂O₃ Foam Composites and Their Application in Energy Storage

The use of electrochemistry for the preparation of graphene and its derivatives has been intensively studied over the past decade. [1-4] In this work, we demonstrate a unique strategy for the fabrication of multilayer nano-porous iron oxide and graphene structure on three-dimensional graphene foam (GF). The combination of Fe₂O₃ and GF takes the advantage of the high energy storage capacity of the former and the good conductivity of the former structure. Precise control of the Fe₂O₃ mass loading was achieved by an electrodeposition approach, which produced nano-wall arrays. The favorable attraction of electrochemically exfoliated graphene oxide (EGO) to Fe₂O₃ facilitates the uniform coating of EGO on the surface of iron oxide. Alternating multilayer structures of EGO and Fe₂O₃ were realized thanks to the unique properties of EGO as both a spacer and current collector (figure 1). The composite could be used directly as a binder-free anode in Li-ion batteries, demonstrating the viability of this approach for high yield and scalable production of graphene/metal oxide composites.

References

- [1] S. Yang, et al., *Adv. mater*, 28 (2016) 6213
- [2] Y. Xia, V. Morandi, V. Palermo, et al., *Ad. Funct. Mater*, 23 (2013) 4684
- [3] Z. Y. Xia, V. Palermo et al., *Carbon*, 84 (2015) 254
- [4] Z. Y. Xia, V. Palermo et al., *FlatChem*, 3 (2017) 8

Figures

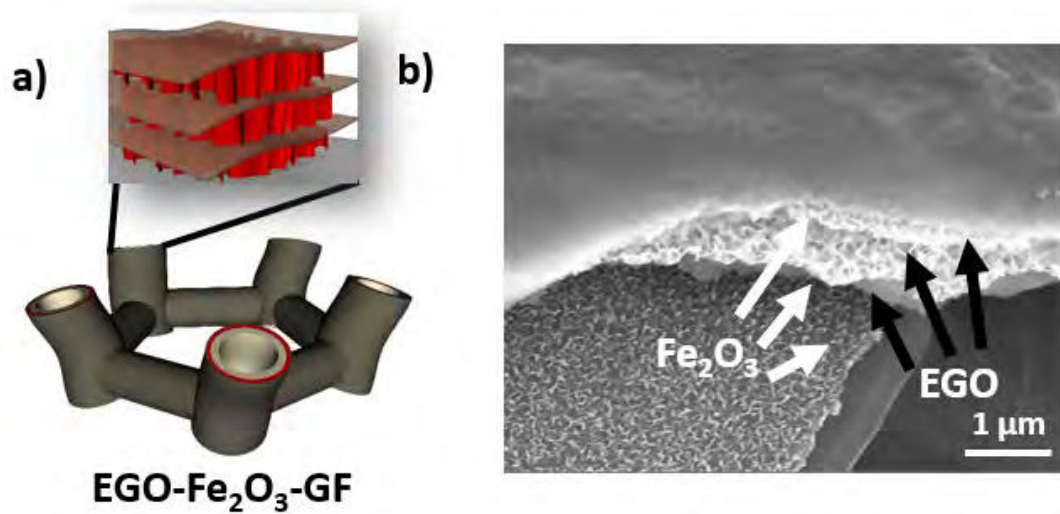


Figure 1: a) Schematic illustration of the multilayer EGO-Fe₂O₃-GF architecture; b) SEM image of the corresponding EGO-Fe₂O₃-GF sample

Xing Xin

Zeyuan Fei, Teng Ma, Long Chen, Mao-Lin Chen, Chuan Xu, Xitang Qian, Dong-Ming Sun, Xiu-Liang Ma, Hui-Ming Cheng, Wencai Ren

1. Shenyang National Laboratory for Materials Science, Institute of Metal Research, Chinese Academy of Sciences, Shenyang 110016, P. R. China

2. University of Chinese Academy of Sciences, Shenyang 110016, P. R. China.

Contact: xxin13b@imr.ac.cn

Circular Graphene Platelets with Grain Size and Orientation Gradients Grown by Chemical Vapor Deposition

Abstract

Materials that have a continuous structure gradient have unique properties and promising applications that are different from conventional homogenous materials. For instance, the structure gradient in bamboo makes it an interesting material with a hard surface but a soft interior. The gradient chemical composition makes the beak of the squid one of the hardest and stiffest organic materials.^[1] Learning from nature, many materials with unique properties have been developed by designing a structure or composition gradient.^[2,3] Although many such three-dimensional bulk materials have been developed, no two-dimensional (2D) materials have been achieved. Graphene as a typical representative of two-dimensional (2D) materials has attracted great attention.^[4,5] Recent extensive studies show that grain boundary has important influences on the electrical, mechanical, thermal and chemical properties of graphene.^[6-9] Therefore, the graphene platelets with grain structure gradient are expected to have gradient properties, and therefore some potential interesting applications as the cases in 3D materials. Here, we have developed a chemical vapor deposition (CVD) method, using a tungsten (W) foil on which was deposited a very thin layer of copper (Cu) as a substrate, to grow circular graphene platelets with gradients in grain size and orientation distribution in the radial direction.^[10] It was found that the substrate undergoes continuous loss of Cu and the formation of a huge number of small tungsten carbides crystals with different orientations during growth. Because of the different interactions and growth behaviors of graphene on Cu and tungsten carbide, such substrates cause the formation of grain size and orientation gradients through the competition of Cu and tungsten carbide in the dominant role in graphene growth. Our findings not only add a new member to the large family of 2D materials but also provide a general strategy to synthesize other 2D materials with a grain structure gradient by substrate design, which opens up possibilities for investigating the unique properties and applications of such materials.

References

- [1] A. Miserez, T. Schneberk, C. Sun, F. W. Zok, J. H. Waite, *Science*, 319 (2008) 1816-1819.
- [2] T. Ishikawa, H. Yamaoka, Y. Harada, T. Fujii, T. Nagasawa, *Nature*, 416 (2002) 64-67.
- [3] T. H. Fang, W. L. Li, N. R. Tao, K. Lu, *Science*, 331 (2011) 1587-1590.
- [4] K. S. Novoselov, A. K. Geim, S. V. Morozov, D. Jiang, Y. Zhang, S. V. Dubonos, I. V. Grigorieva, A. A. Firsov, *Science*, 306 (2004) 666-669.
- [5] A. K. Geim, *Science*, 324 (2009) 1530-1534.
- [6] R. Grantab, V. B. Shenoy, R. S. Ruoff, *Science*, 330 (2010) 946-948.
- [7] A. Bagri, S. P. Kim, R. S. Ruoff, V. B. Shenoy, *Nano Lett.*, 11 (2011) 3917-3921.
- [8] Q. Yu, L. A. Jauregui, W. Wu, R. Colby, J. Tian, Z. Su, H. Cao, Z. Liu, D. Pandey, D. Wei, T. F. Chung, P. Peng, N. P. Guisinger, E. A. Stach, J. Bao, S.-S. Pei, Y. P. Chen, *Nat. Mater.*, 10 (2011) 443-449.

- [9] K. Kim, H.-B.-R. Lee, R. W. Johnson, J. T. Tanskanen, N. Liu, M.-G. Kim, C. Pang, C. Ahn, S. F. Bent, Z. Bao, Nat. Commun., 5 (2014) 4781.
- [10] X. Xin, Z. Fei, T. Ma, L. Chen, M.-L. Chen, C. Xu, X. Qian, D.-M. Sun, X.-L. Ma, H.-M. Cheng, W. Ren, Adv. Mater., 29 (2017) 1605451.

Figures

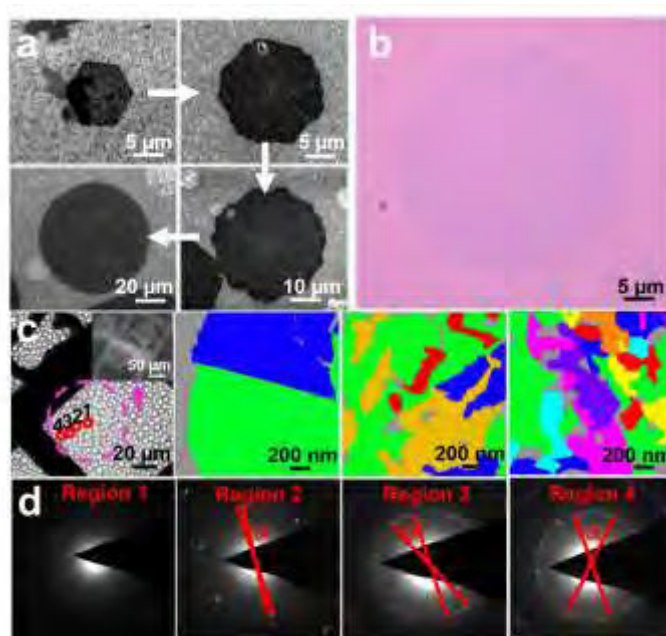


Figure 1: Growth of circular graphene platelets with grain size and orientation gradients. (a) Typical scanning electron microscopy images of graphene islands grown on a W-Cu substrate with a flow rate of 5.0 sccm CH₄ and 300 sccm H₂ for 20, 40, 60, and 90 min, showing the morphology evolution of the islands from hexagonal to circular. (b) Optical image of a circular graphene island transferred onto an SiO₂/Si substrate. (c) A transmission electron microscopy (TEM) image of a circular graphene island and the false-color, superimposed dark-field TEM images of regions 2-4. (d) Selected area electron diffraction patterns taken from the four regions 1-4 in (c). The regions marked 1 to 4 were selected from the center to the edge of a circular graphene island. The above results indicate that the graphene island has a grain size and an orientation-dispersed angle gradient from the center to the periphery.

Chuan Xu

Zhibo Liu, Ning Kang, Hui-Ming Cheng, Wencai Ren

Shenyang National Laboratory for Materials Science, Institute of Metal Research, Chinese Academy of Sciences, Shenyang 110016, China

cxu11s@imr.ac.cn

CVD-Grown High-Quality Ultrathin Mo₂C Crystals and Their Vertical Heterostructures with Graphene

Transition metal carbides (TMCs) are a large family of materials that combine the properties of ceramics and metals. High-quality 2D TMCs are essential for investigating new physics and properties in 2D limit. However, the commonly used chemical etching method can only produce functionalized 2D TMC nanosheets with abundant defects and functional groups, known as MXenes. Recently, we developed a universal CVD method [1] to fabricate large-area high-quality ultrathin 2D TMC crystals. The obtained α -Mo₂C crystals are a few nanometres thick and over 100 μm in size. They show 2D characteristics of superconducting transitions; moreover, the superconductivity is also strongly dependent on the crystal thickness. Further studies show that 2D α -Mo₂C crystals have unique domain structure with rotational-symmetry and well-defined line-shaped domain boundaries, and the domain boundaries have a significant influence on 2D superconductivity [2]. We also realized the direct growth of high-quality graphene/2D superconducting α -Mo₂C vertical heterostructures with uniformly well-aligned lattice orientation and strong interface coupling by a two-step CVD process [3]. The strong interface coupling leads to a phase diagram of superconducting transition with multiple voltage steps being observed in the transition regime. Furthermore, we demonstrated the realization of highly transparent Josephson junction devices based on these heterostructures.

References

- [1] C. Xu, et al., *Nature Materials*, 11 (2015) 1135-1141
- [2] Z. Liu, et al., *Nano Letters*, 7 (2016) 4243-4250
- [3] C. Xu, et al., *ACS Nano*, 6 (2017) 5906-5914

Figures

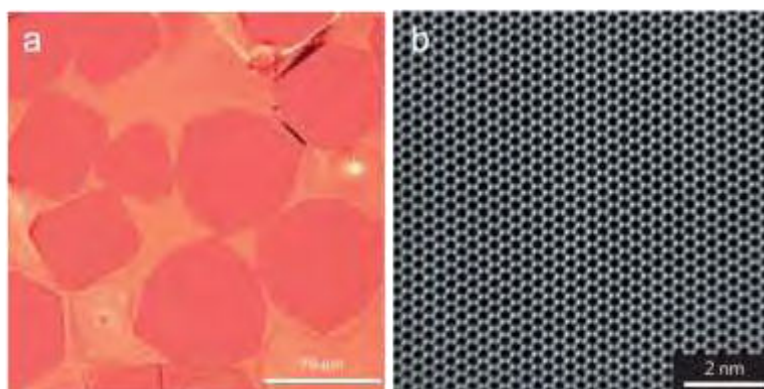


Figure 1: (a) Typical optical image of ultrathin α -Mo₂C crystals on a Cu/Mo substrate, showing different regular shapes. (b) Atomic-level HAADF-STEM image of an α -Mo₂C sheet, showing highly crystalline quality.

Dewu Yue

Won Jong Yoo

SKKU Advanced Institute of Nano-Technology(SAINT), Sungkyunkwan University(SKKU), 2066 Seobu-ro, Jangan-gu, Suwon, Gyeonggi-do, 16419 Korea.

yoowj@skku.edu

High Performance Two-dimensional Semiconductors established by using a Benzyl Viologen Interlayer

Abstract

Electrical performance of two-dimensional (2D) semiconductor devices are limited by the properties of the electrical contact between the electrode and the semiconductor surface, requiring good Ohmic contact^{[1][2]}. Solution processed polymeric contacts have been widely used in organic semiconductors, but not in 2D semiconductors until now. We demonstrated the fabrication of solution-processed polymeric contacts for the preparation of high mobility MoS₂, MoTe₂, and BP (black phosphorous) FETs with significantly lowered contact resistance. Ohmic contacts were achieved and produced 4-, 16-, and 13-fold increases in the effective mobilities, respectively, compared to the respective materials alone. Our devices exhibit excellent stability in both ambient and vacuum. Our strategy provides a promising method for obtaining Ohmic-contact 2D semiconductor devices as well as 2D logical integrated circuits.

References

- [1] Yue, D. W.; Ra, C. H.; Liu, X. C.; Lee, D. Y.; Yoo, W. J., *Nanoscale*, 7(2015) 825-831(Arial Narrow 11)
- [2] Yue, D.; Lee, D.; Jang, Y. D.; Choi, M. S.; Nam, H. J.; Jung, D. Y.; Yoo, W. J., *Nanoscale*, 8 (2016) 12773-12779

Muhammad Zahid¹

Francesco Bonaccorso², Antonio Esau Del Rio Castillo², Athanassia Athanassiou¹

¹Smart Materials group, Istituto Italiano di Tecnologia, Via Morego 30 16163, Genova, Italy

²Graphene labs, Istituto Italiano di Tecnologia, Via Morego 30 16163, Genova, Italy

muhammad.zahid@iit.it

francesco.bonaccorso@iit.it

athanassia.athanassiou@iit.it

Effect of 2D Nanomaterials on Gas Permeability and Mechanical Properties of Thermoplastic Polyurethane Nanocomposites

Abstract: Thermoplastic polyurethanes (TPU) are highly versatile polymers as they close the gap between rubber and hard thermoplastics. They possess a unique combination of properties, such as, high wear resistance, good resistance to oils, greases and solvents, and extremely good weather stability, combined with high elasticity. However, in their neat forms, they are unsuitable for packaging and storage applications due to their high gas permeability. In the past, many efforts have been dedicated to improve gas barrier properties in TPU nanocomposites by incorporating different 2D nanomaterials such as nanoclays [1], graphene oxides [2] and graphene nanoribbons [3]. The incorporated 2D nanofillers create a tortuous path for gas molecules within the polymer matrix [4], thus making it difficult for gas to diffuse and get transported across the membranes, as illustrated in Figure 1. In particular, graphene filled TPU nanocomposites exhibit substantial improvements in gas barrier properties as well as mechanical, electrical and thermal properties. Graphene, with impermeable 2D structure and high aspect ratio, provides superior gas barrier properties in the prepared nanocomposites as compared to its spherical counterparts (like nanoparticles) [4]. In this study, we investigate the effect of different aspect ratios of graphene on the gas barrier properties of the TPU nanocomposites, where the nanofillers have been incorporated. TPU nanocomposites were prepared by solvent casting technique, using different types of graphene powders dispersed into chloroform, with the help of sonication. The as prepared TPU nanocomposites demonstrated significant improvements in the gas barrier properties with respect to the pure polymer matrix, which depend on their aspect ratios. In particular, a reduction of 70 % in the gas permeability was observed at 6.0 wt.% concentration of graphene having lateral size and thickness of 415 nm and 5.3 nm, respectively. Their corresponding aspect ratio is 78.30. The normalized gas permeability rate was reduced from 144,846.44 mL.micron/m²/day for the neat TPU films, to 42,508.53 mL.micron/m²/day at 6.0 wt.% graphene mass loading. This can be attributed to the good dispersion of the graphene flakes into chloroform solvent [5] and packing of the graphene flakes into TPU nanocomposites. Likewise, mechanical properties (Young's modulus) of the as prepared nanocomposites were improved at similar mass fractions. In particular the Young's modulus was increased from 5.16 MPa (for neat TPU) to 11.84 MPa making the TPU nanocomposites more resistant to deformations. The prepared nanocomposites have been also characterized using SEM, TEM and Raman spectroscopy. Future work will involve preparation of solvent-free TPU/graphene nanocomposites with enhanced properties using twin screw extruder and a pelletizer.

References

- [1] S. Pandey, K. K. Jana, V. K. Aswal, D. Rana and P. Maiti, *Applied Clay Science*, **146** (2017) 468-474.
- [2] H. Kim, Y. Miura and C. W. Macosko, *Chemistry of Materials*, **22** (2010) 3441-3450.
- [3] C. Xiang, P. J. Cox, A. Kukovecz, B. Genorio and *et al.*, *ACS Nano*, **7** (2013) 10380-10386.
- [4] Y. Cui, S.I. Kundalwal, S. Kumar, *Carbon*, **98** (2016) 313-333.
- [5] D. W. Johnson, B. P. Dobson and K. S. Coleman, *Current Opinion in Colloid and Interface Science*, **5** (2015) 367-382.

Figures

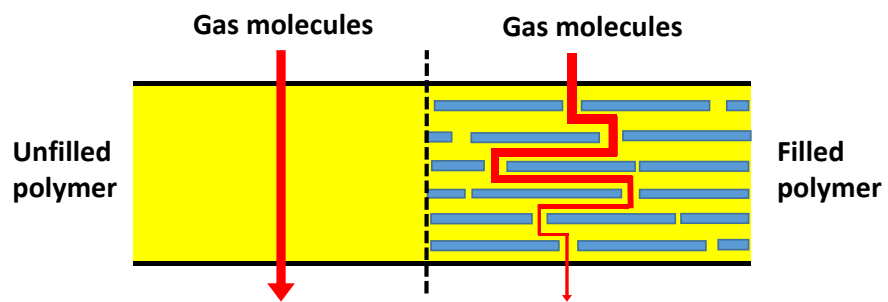


Figure 1: Mechanism of gas molecule's absorption and transportation through a neat polymer film and graphene filled polymer nanocomposite.

Jian Zhang

Zheling Zhang, Yong Hu, Cong Xu, Shuyao Zhang

College of Material Science & Engineering, Guilin University of Electrical Technology, Guilin 541004, China

jianzhang@guet.edu.cn

Graphene quantum dots as interface materials for organic photovoltaic cells

Organic photovoltaic cells (OPVs) represent an exciting class of renewable energy technology, and are under intensive investigation in both academic institutions and industrial companies due to their potential to enable mass production of flexible and cost-effective devices through roll-to-roll techniques. The proper choice of interface materials is a must for highly efficient and stable OPV devices and has become a significant part of the OPV research today. Interface materials are either non-conducting, semiconducting or conducting layers which not only provide selective contacts for carriers of one sort, but can also determine the polarity of OPV devices, affect the open-circuit voltage, and act as optical spacers or protective layers.

Owing to their unique two-dimensional structure, and functionalization-induced tunable electronic structures, graphene and its derivatives have been used as a new class of efficient interface materials in OPVs. Highly efficient and stable OPVs have been fabricated with graphene and its derivatives as interface materials. After a brief introduction of OPVs, the progress in interface materials and interface engineering at the both anode and cathode in OPVs and PSCs in my group will be introduced. At anode interface, the work function of graphene oxide (GO) is improved by O₂ plasma treatment or photochemical chlorination. Due to high transparency and high work function of GO derivatives, the power conversion efficiency of OPVs was improved significantly when the GO derivatives with higher work function was used as anode interfacial materials.

Acknowledgement: This research was financially supported by the National Natural Science Foundation of China (61564003), and the Guangxi Natural Science Foundation (2015GXNSFGA139002), and the Guangxi Bagui Scholar program.

References

- [1] Zhou, L.; Xu, Y.; Yu, W.; Guo, X.; Yu, S.; Zhang, J.; Li C.* J. Mater. Chem. A, 2016, 4, 8000.
- [2] Fu, P.; Huang, L.; Yu, W.; Yang, D.; Liu, G.; Zhou, L.; Zhang, J.;* Li, C.* Nano Energy 2015, 13, 275.
- [3] Yang, D.; Fu, P.; Zhang, F.; Wang, N.; Zhang, J.;* Li, C.* J. Mater. Chem. A 2014, 2, 17281.
- [4] Yang, D.; Yu, W.; Zhou, L.; Zhang, J.;* Li, C.* Adv. Energy Mater. 2014, 4, 1400591.
- [5] Yang, D.; Zhou, L.; Chen, L.; Zhao, B.; Zhang, J.;* Li, C.* Chem. Comm. 2012, 48, 8078.

Figures

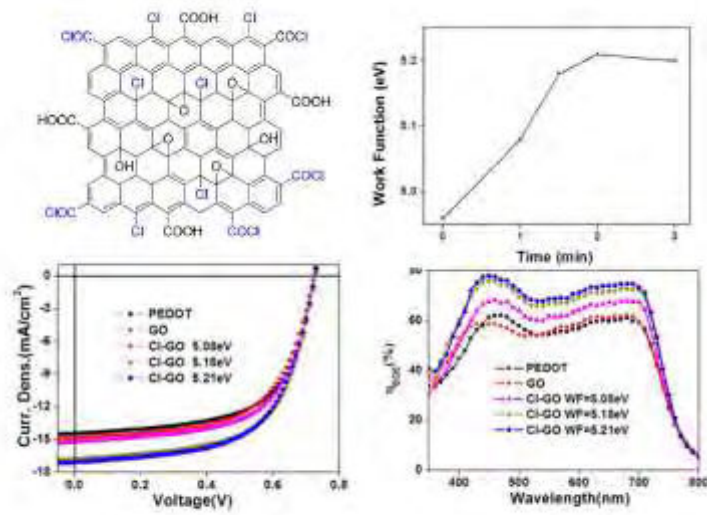


Figure 1: Chlorinated GO and the performance of organic solar cells

1,2 Shaolin Zhang

²Thuy Hang Nguyen, ²Woochul Yang

¹Advanced Institute of Engineering Science for Intelligent Manufacturing, Guangzhou University, Guangzhou 510006, China

²Department of Physics, Dongguk University, Seoul 04620, Korea

wyang@dongguk.edu

Preparation and mechanism of molybdenum diselenide nanosheets for ethanol detection

Two-dimensional (2D) transition metal dichalcogenides (TMDCs) as alternative sensor materials of conventional metal oxides have attracted much attention recently [1,2]. These materials present enormous surface/volume ratio and unusual electronic, optical, and magnetic properties in the form of single- or few-layer, and have accelerated the development of a diverse range of applications including gas sensor [3]. Among TMDCs, molybdenum diselenide (MoSe₂), as an emerging semiconducting material has rarely been investigated for sensor application. Late et al. firstly investigated the mechanically exfoliated single-layer MoSe₂ and demonstrated its high sensing performance to ppm-level NH₃ gas [4]. Very recently Baek et al. also developed a MoSe₂ multilayer based field-effect transistor (FET) for detecting NO₂ gas [5]. However, the sensing mechanism of ultrathin MoSe₂ is still ambiguous to date.

In this study, MoSe₂ nanosheets thin film gas sensor was firstly fabricated and its sensing potential to ppm-level ethanol vapor at low operating temperature was investigated. Ultrathin MoSe₂ nanosheets were prepared in large scale through a facile liquid-phase exfoliation method using low boiling temperature solvent. The exfoliated MoSe₂ nanosheets exhibited high purity and crystallinity with few atomic layer thickness. Systematical gas sensing tests demonstrated that MoSe₂ nanosheets based thin film could be utilized as ethanol gas sensor with linear response, quick recovery, and good repeatability at 90°C, as shown in Figure 1. The sensing mechanism of MoSe₂ toward ethanol was investigated based on first principle calculation. The adsorption behavior of ethanol molecule on MoSe₂ surface was revealed in light of adsorption orientation, adsorption energy, charge transfer, projected electronic density of state, and molecular orbital. The calculation well matched with experimental results. It is found the quick and complete recovery of MoSe₂ nanosheets sensor were benefited by the appropriate physical interaction between ethanol and MoSe₂ surface. This finding offers a competitive option instead of conventional graphene sensor for ethanol gas detection at low temperature.

References

- [1] B. L. Li, J. P. Wang, H. L. Zou, S. Garaj, C. T. Lim, J. P. Xie, N. B. Li, and D. T. Leong, *Adv. Funct. Mater.*, 26 (2016) 7034.
- [2] J. H. Cha, S. J. Choi, S. Yu, and I. D. Kim, *J. Mater. Chem. A*, 5 (2017) 8725.
- [3] W. Choi, N. Choudhary, G. H. Han, J. Park, D. Akinwande, and Y. H. Lee, *Mater. Today*, 20 (2017) 116.
- [4] D. J. Late, T. Doneux, and M. Bougouma, *Appl. Phys. Lett.*, 105 (2014) 233103.
- [5] J. Baek, D. Yin, N. Liu, I. Omkaram, C. Jung, H. Im, S. Hong, S. M. Kim, Y. K. Hong, J. Hur, Y. Yoon, and S. Kim, *Nano Res.*, 10 (2017) 1861.

Figures

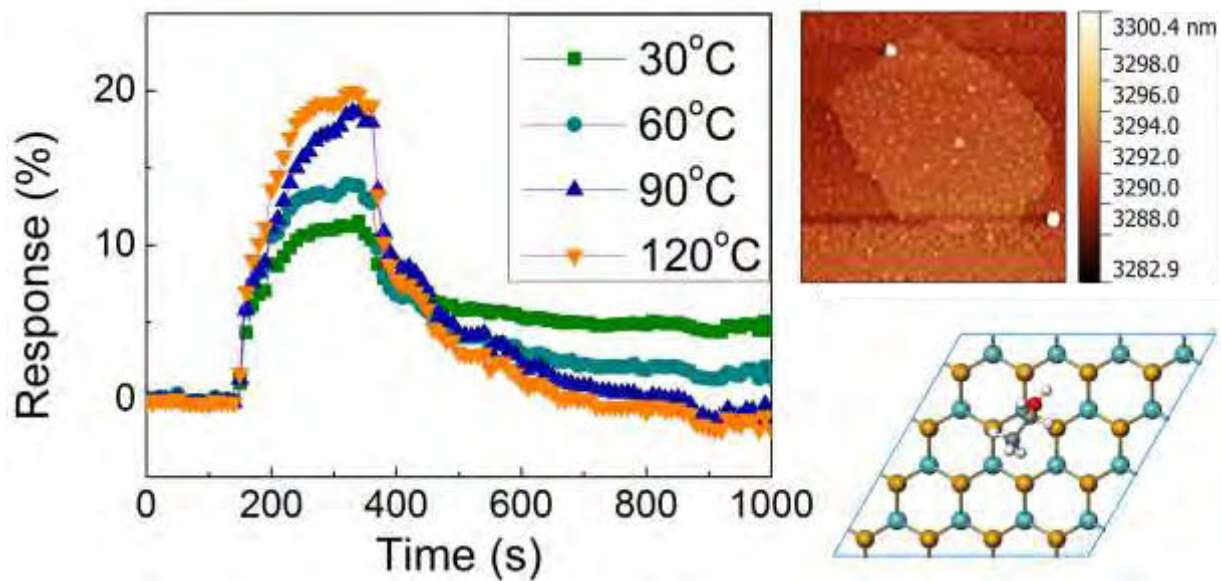


Figure 1: Typical sensing response curves of MoSe₂ nanosheets sensor toward 20 ppm ethanol with different operating temperatures (left). AFM image of as-prepared MoSe₂ nanosheet (upper right). Adsorption model of ethanol molecule on MoSe₂ surface (lower right).

Defects engineering for monolayer MoS₂ homojunction construction

Due to its reduced dimensions, chemical stability, proper direct band gap, highly efficient light absorption and piezoelectricity¹, two-dimensional (2D) molybdenum disulfide (MoS₂) has the potential in developing next-generation flexible, transparent and wearable nanodevices. As an example, many researchers have focused on creating MoS₂ homojunction, the fundamental building block of modern electronics. Due to its identical crystal structure and continuous band alignments in the interface, the MoS₂ homojunctions display ideal current rectifying behavior and highly efficient photoresponse than those of heterojunctions. In the homojunction construction, it is the key issue to control the carrier concentration and work function in MoS₂. However, by utilizing the conventional methods of chemical doping and thermal annealing, the monolayer MoS₂ homojunction shows instability and poor performance^{2,3,4}.

Here, a novel homojunction construction strategy is proposed, in which the sulfur vacancies are healed spontaneously by the sulfur adatom clusters on MoS₂ surface through a poly(styrenesulfonate) (PSS)-induced hydrogenation process. The electron concentration of the as-healed MoS₂ dramatically decreased, leading to work function enhancement up to ~58 meV. This strategy is then employed to fabricate a high performance lateral monolayer MoS₂ homojunction, which presents an ideal current rectifying behavior. Distinguished with previous unstable chemical doping, the lattice defects induced local fields are eliminated during the process of the sulfur vacancy self-healing, which largely improve the performance of MoS₂ homojunction. These claims are all supported by the experimental results, including Kelvin probe force microscopy (KPFM) and the photodetection performance. Our findings demonstrate a promising strategy in 2D materials electronic structure modulation for the development of the next-generation electronics and optoelectronics.

References

- [1] Qi J, et al. Piezoelectric effect in chemical vapour deposition-grown atomic-monolayer triangular molybdenum disulfide piezotronics. *Nat. Commun.* 6, 7430 (2015).
- [2] Li HM, et al. Ultimate thin vertical p-n junction composed of two-dimensional layered molybdenum disulfide. *Nat. Commun.* 6, 6564 (2015).
- [3] Choi MS, et al. Lateral MoS₂ p-n junction formed by chemical doping for use in high-performance optoelectronics. *ACS nano* 8, 9332-9340 (2014).
- [4] Jin Y, Keum DH, An SJ, Kim J, Lee HS, Lee YH. A Van Der Waals Homojunction: Ideal p-n Diode Behavior in MoSe₂. *Adv. Mater.* 27, 5534-5540 (2015).

Figures

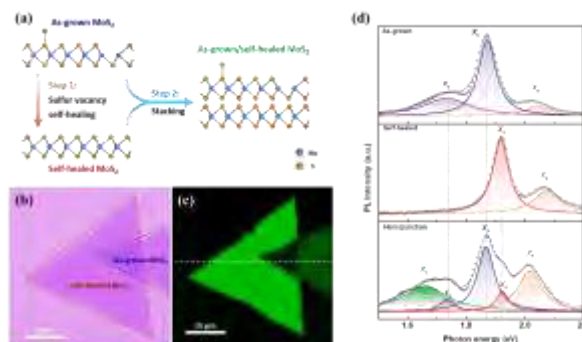


Figure (a) schematic diagram of the stacked bilayer homojunction, (b) optical image, (c) PL mapping, (d) low temperature PL spectrum.

Single Layer TMD Fabrication and Rolling up into Nanoscrolls

Transition metal dichalcogenides like molybdenum disulphide have attracted great interest as two-dimensional materials beyond graphene due to their unique electronic and optical properties. The scalable fabrication of atomically thin transition metal dichalcogenides is vital for industrial applications. We demonstrated a high-yield exfoliation process using lithium, potassium and sodium naphthalenide where an intermediate ternary Li_xMX_n crystalline phase (X=selenium, sulphur, and so on) is produced. Using a two-step expansion and intercalation method, we produce high-quality single-layer molybdenum disulphide sheets with unprecedentedly large flake size, that is up to 400 mm^2 . Single-layer dichalcogenide inks prepared by this method may be directly inkjet-printed on a wide range of substrates.

The self-assembly of transition metal dichalcogenides flakes, as an emerging area, is largely unexplored. High-quality nanoscrolls rolled up from chemical vapour deposition-grown transition metal dichalcogenides flakes were demonstrated. Based on the internal open topology, nanoscrolls hybridized with a variety of functional materials have been fabricated, which is expected to confer transition metal dichalcogenides nanoscrolls with additional properties and functions attractive for potential application.

References

- [1] Jian Zheng, et al, Nat.Comm., 5 (2014) 2995.
- [2] Jian Zheng, et al, Nat.Comm., 9 (2018) 1301

Figures

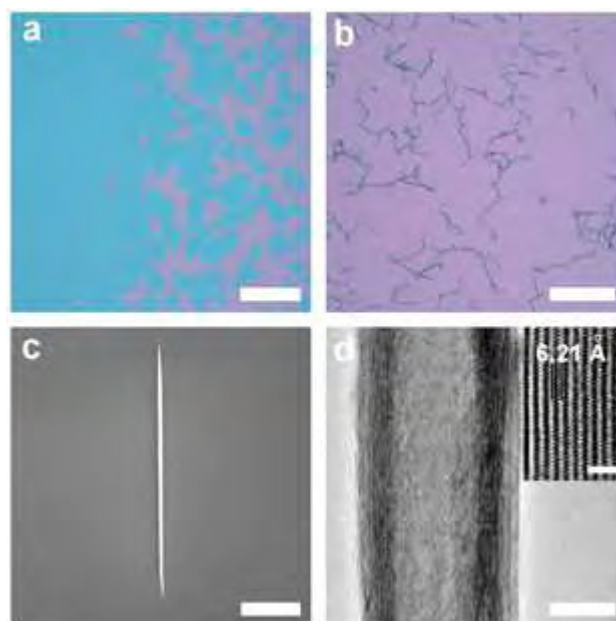


Figure 1: a, Optical image of CVD-grown MoS₂ monolayer flakes on a SiO₂/Si substrate. b, Optical image of MoS₂ nanoscrolls on a SiO₂/Si substrate. c, SEM images of MoS₂ nanoscrolls. d, TEM images of MoS₂ nanoscrolls. Inset: High-magnification images of sidewalls of MoS₂ nanoscrolls. (Scale bars, 500 μm in a, 100 μm in b, 5 μm in f and 2 nm for the inset).

Electric-field control of magnetism in a few-layered van der Waals ferromagnetic semiconductor

Manipulating a quantum state via electrostatic gating has been of great importance for many model systems in nanoelectronics. Until now, however, controlling the electron spins or, more specifically, the magnetism of a system by electric field tuning has proven challenging^{1–4}. Recently, atomically thin magnetic semiconductors have attracted significant attention due to their emerging new physical phenomena^{5–13}. However, many issues are yet to be resolved to convincingly demonstrate gate-controllable magnetism in these two-dimensional materials. Here, we show that, via electrostatic gating, a strong field effect can be observed in devices based on few-layered ferromagnetic semiconducting Cr₂Ge₂Te₆. At different gate doping, micro-area Kerr measurements in the studied devices demonstrate bipolar tunable magnetization loops below the Curie temperature, which is tentatively attributed to the moment rebalance in the spin-polarized band structure. Our findings of electric-field-controlled magnetism in van der Waals magnets show possibilities for potential applications in new-generation magnetic memory storage, sensors and spintronics.

References

- [1] 1. Chappert, C., Fert, A. & Nguyen Van Dau, F. *Nat. Mater.* 6, 813–823 (2007).
- [2] 2. Matsukura, F., Tokura, Y. & Ohno, H. *Nat. Nanotech.* 10, 209–220 (2015).
- [3] 3. Lin, M.W. et al. *J. Mater. Chem. C* 4, 315–322 (2016).
- [4] 4. Xing, W. et al. *2D Mater.* 4, 024009 (2017).
- [5] 5. Huang, B. et al. *Nature* 546, 270–273 (2017).
- [6] 6. Gong, C. et al. *Nature* 546, 265–269 (2017).
- [7] 7. Wang, Z. et al. Preprint at <https://arxiv.org/abs/1801.08188> (2018).
- [8] 8. Klein, D. R. et al. *Science* 360, 1218–1222 (2018).
- [9] 9. Song, T. C. et al. *Science* 360, 1214–1218 (2018).
- [10] 10. Sivadas, N., Daniels, M. W., Swendsen, R. H., Okamoto, S. & Xiao, D. *Phys. Rev. B* 91, 235425 (2015).
- [11] 11. Mounet, N. et al. *Nat. Nanotech.* 13, 246–252 (2018).
- [12] 12. Bonilla, M. et al. *Nat. Nanotech.* 13, 289–293 (2018).
- [13] 13. Arai, M. et al. *Appl. Phys. Lett.* 107, 103107 (2015)

Figures

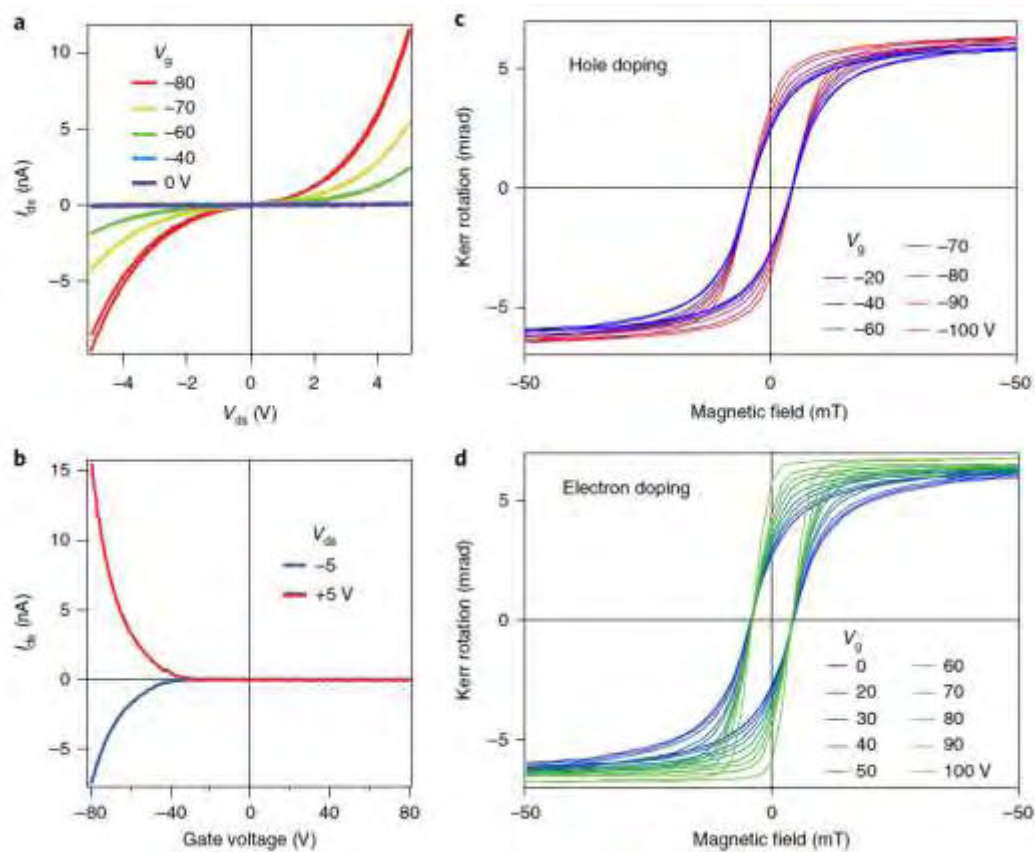


Figure 1: Kerr measurement of BN-encapsulated 3.5 nm $\text{Cr}_2\text{Ge}_2\text{Te}_6$ sample with solid Si gate. a, I-V characteristics of the same device with five different fixed Si gate voltages measured at 40 K. b, Field-effect curves at 40 K with $V_{ds} = -5$ and $+5$ V (blue and red, respectively). c, d, Kerr angle measured at 40 K for negative (c) and positive (d) gate voltages respectively.



POSTER CONTRIBUTIONS

Jong-Guk Ahn

Younghee Park, Hyunseob Lim

Department of Chemistry, Chonnam National University (CNU), Gwangju 61186, Republic of Korea

Jongguk.ahn@gmail.com

Surface Enhanced Raman Spectroscopy at Nanogap between Au Nanoparticles Separated by 2D hexagonal Boron Nitride

The controlled formation of hot spot formed at nanogap between metal nanoparticles in surface enhanced Raman spectroscopy (SERS), since it can enhance the Raman signal of target molecule dramatically. Therefore, various methods have been attempted to produce the nanogap, and several approaches even enable the single molecule level detection by SERS. Nevertheless, the precise control of nanogap is not only technically difficult, but also the reproducibility is not good. In addition, the most of approaches is not appropriate to practical applications. Herein, we present a new approach to produce nanogaps between Au nanoparticles (Au NPs) separated with hexagonal boron nitride (h-BN) by making a Au NPs/h-BN/Au NPs heterostructure. In previous study, we have demonstrated that h-BN can be a good wrapping layer for SERS nanoparticle, which is used as a two-dimensional insulator material. The Au NPs/h-BN/Au NPs heterostructure can be manufactured by introducing additional Au NPs onto h-BN/Au NP substrate. The theoretical simulation has been carried out by using Finite-Difference Time-Domain (FDTD) method to visualize the electromagnetic field amplification at Au NPs/h-BN/Au NPs nanogap, which reveals that the stronger electromagnetic field can be generated at the nanogap structure of AuNP/h-BN/AuNPs. We believe that our results provide the critical insight for the nanogap based SERS applications by using the heterostructures of two-dimensional insulators and metal nanoparticles.

References

- [1] Katrin Kneipp, *et al.* Phys. Rev. Lett., **78** (1997) 1667
- [2] Jian-Feng Li, *et al.* Nature, **464** (2010) 392
- [3] Gwangwoo Kim, *et al.* ACS Nano, **10** (2016) 11156

Figures

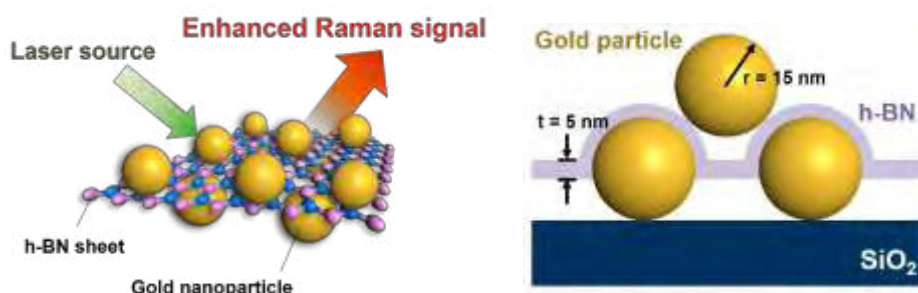


Figure 1. Schematic illustration of Au nanoparticles/h-BN/Au nanoparticles heterostructure

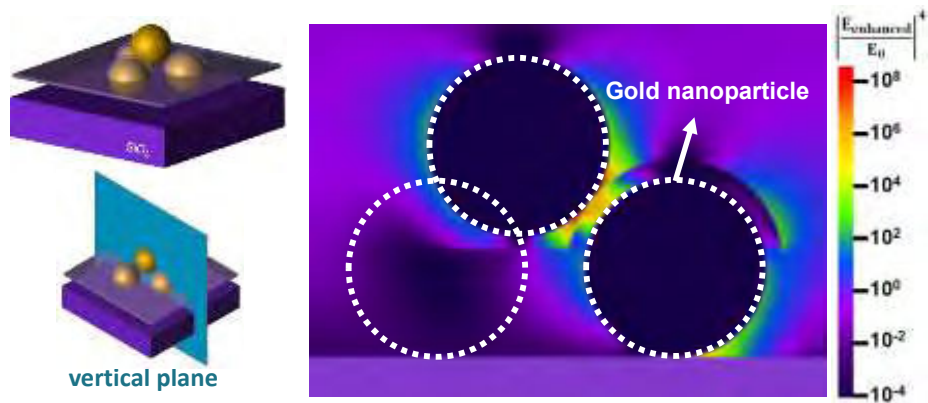


Figure 2. Finite-Difference Time-Domain simulation results of Au nanoparticles/h-BN/Au nanoparticles structure.

BNNS@Ti₃C₂ Intercalation Electrocatalyst for Hydrogen Evolution Reaction

Electrocatalysts with advantages of stability, high efficiency and noble-metal-free feature are in urgent need for water splitting [1-2]. Herein, we firstly utilized the intercalation method to incorporate Ti₃C₂ into interlayers of boron nitride nanosheet (BNNS) and fabricated a novel BNNS@Ti₃C₂ intercalation electrocatalyst. Theoretical calculation proves that the interface has transformed from semiconducting property to metallicity in the unique intercalation structure. The rich active sites of Ti₃C₂ are better protected as well as serve as a bridge to connect different layers of BNNS [3]. The as-obtained composite possesses the improved conductivity and abundant catalytic active sites which are useful for enhancing electrocatalytic performance. As a non-noble-metal electrocatalyst, the sample shows an outstanding electrocatalytic activity and excellent long-term durability. BNNS@Ti₃C₂ is used as the electrocatalyst for the first time without noble-metal assistance. This work demonstrates that the layered 2D materials can serve as a promising electrocatalyst by forming intercalation structure.

References

- [1] D. Merki, X. Hu, *Energy Environ. Sci.* 4 (2011) 3878–3888.
- [2] J. Yang, H.S. Shin, *J. Mater. Chem. A* 2 (2014) 5979–5985.
- [3] X. Li, X. Hao, M. Zhao, Y. Wu, J. Yang, Y. Tian, G. Qian, *Adv. Mater.* 25 (2013) 2200-2204.

Figure 1

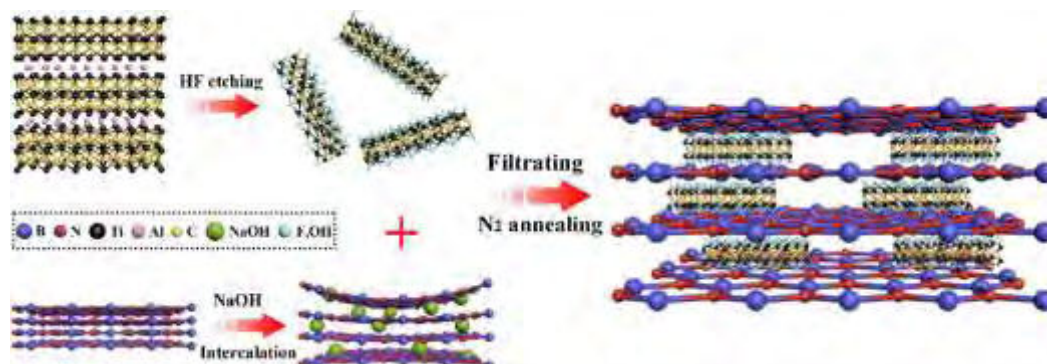


Figure 1: Schematic illustration for the synthesis of BNNS@Ti₃C₂.

Morphology and electrical studies on NaCl-assisted CVD synthesis of WS₂

Atomically thin two-dimensional materials such as transition metal dichalcogenides (TMDC), have been attracted a great deal of attention due to their electronic properties [1]. For the applications of various sensors and low power field effect transistors (FETs), thin films growth of TMDC with large area and uniformity is essential. Recently, alkali-metal halide assisted chemical vapor deposition (CVD) growth of TMDC have been attracted attention because alkali metal halide can reduce the density of nuclei and promote two-dimensional lateral growth [2]. In this work, I report a CVD growth of WS₂ with the assistant of NaCl and investigate the morphology and electrical characteristics of the CVD-grown WS₂.

The NaCl-assisted CVD experimental setup is shown in Fig. 1(a). WO₃ (99.99 %) precursor (~0.02 g) with one drop of 2N NaCl (~0.04 g) was put in the center of the one-zone CVD furnace. Sulfur (99.99 %) precursor (~0.5 g) was put 5 cm away from the end of the furnace and was heated with a heating tape independently. Two 285 nm SiO₂ / p⁺⁺-Si (100) substrates with SiO₂ surfaces facing each other were placed about ~1 cm downstream from the WO₃ precursor. One 285 nm SiO₂ / p⁺⁺-Si (100) substrates with SiO₂ surfaces facing down was also placed just above the WO₃ precursor. The CVD growth was performed at atmospheric pressure using 35-40 sccm 3% H₂/Ar as the carrier gas. Typical temperature programming process of WO₃ and S precursors during WS₂ growth is shown in Fig. 1(b).

The size of the CVD-grown WS₂ was estimated by optical microscope images (Fig. 2(a)). Thickness and surface morphology of the WS₂ were measured by atomic force microscope (AFM: Digital Instruments, Nanoscope IIIa) measurements (Figs. 2(b) and 2(c)). The quality of the WS₂ was evaluated by Raman spectra compared to mechanically exfoliated bulk WS₂ (Fig. 3(a)). Two different types of WS₂ deposition were observed: one was normal triangular shape WS₂ and another was WS₂ in a etched pit. The existence of the pits suggests that etching of SiO₂ occurred during the WS₂ formation process [3].

For electrical characterizations, source and drain electrodes were formed on the as-grown WS₂ by the standard photolithography process with AZ5214E photoresist (Clariant). Cr/Au (10/50 nm), Ti/Au (10/50 nm) and Au (60 nm) metal electrodes were examined. Before metal depositions, the surfaces of the WS₂ were modified by O₂ plasma treatment (5 s) performed with a resist strip system (Diener electronics, Nano). The device channel lengths were 2000-6000 nm. Figure 3(b) shows an optical microscope image of a fabricated FET with Ti/Au (10/50 nm) source and drain electrodes. Thickness and surface morphology of the WS₂ channel were estimated by AFM measurements (Figs. 3(c) and 3(d)). Electrical characterization of the WS₂ FETs was performed with a semiconductor parameter analyzer (Keithley 4200-SCS) in room temperature and under ambient conditions. Figure 4 shows drain-source (I_d-V_d) characteristics at various gate voltages (V_g) for (a) pristine WS₂ FET as shown in Fig. 3, (b) the same WS₂ FET annealing at 225 °C under a 300 sccm 3% H₂/Ar gas flow for 3.5 h, (c) the same WS₂ FET additionally annealing at 225 °C under a 300 sccm 3% H₂/Ar gas flow for 2 h (Total 5.5 h). Annealing process in 3% H₂/Ar gas flow is effective for improvement of electrical contacts at metal-WS₂ interfaces. The detailed results will be discussed at the presentation.

References

- [1] B. Radisavljevic, A. Radenovic, J. Brivio, V. Giacometti and A. Kis, *Nature Nanotech.*, **6** (2011) 147.
- [2] S. Li, S. Wang, D. M. Tang, W. Zhao, H. Xu, L. Chu, Y. Bando, D. Golberg and G. Eda, *Appl. Mater. Today*, **1** (2015) 60.
- [3] K. N. Kang, K. Godin and E.-H. Yang, *Sci Rep.*, **5** (2015) 13205.

Figures

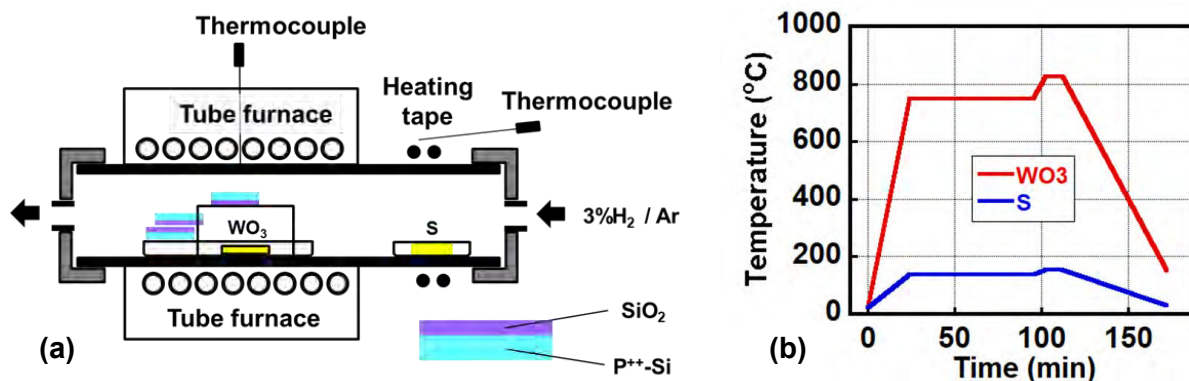


Figure 1: (a) Schematic illustration of the CVD experimental setup. (b) Temperature programming process of WO₃ and S precursors.

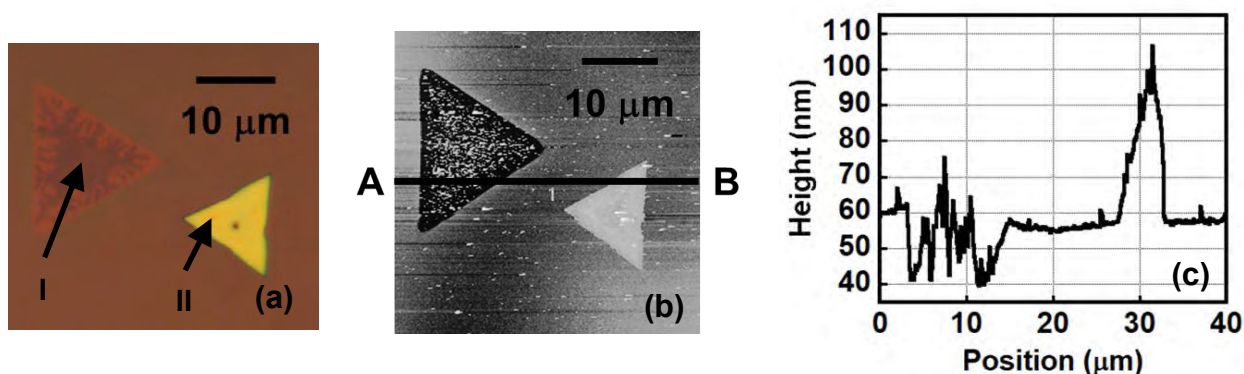


Figure 2: (a) Optical microscope image of the CVD-grown WS₂. (b) AFM image of the WS₂ at the same area in (a). (c) Cross-section profile between A and B in (b).

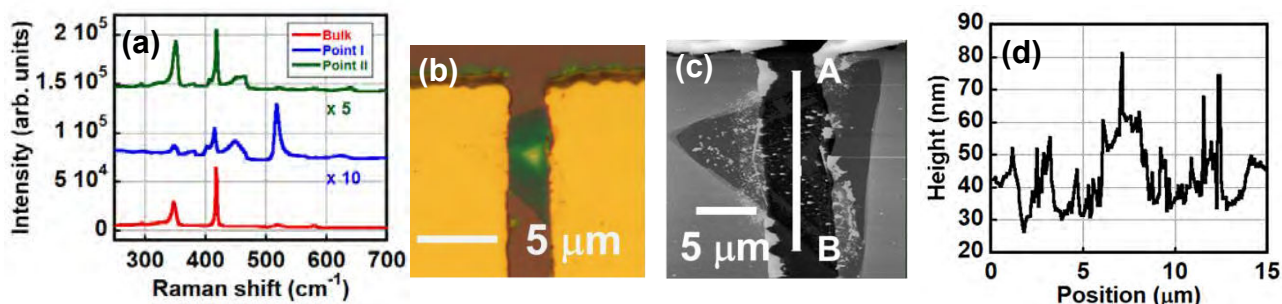


Figure 3: (a) Raman spectra of the bulk WS₂ and the CVD-grown WS₂ on SiO₂ measured at different points (I and II in Fig. 2(a)). (b) Optical microscope image of the CVD-grown WS₂ FET. (c) AFM image of the WS₂ at the same FET in (b). (d) Cross-section profile between A and B in (c).

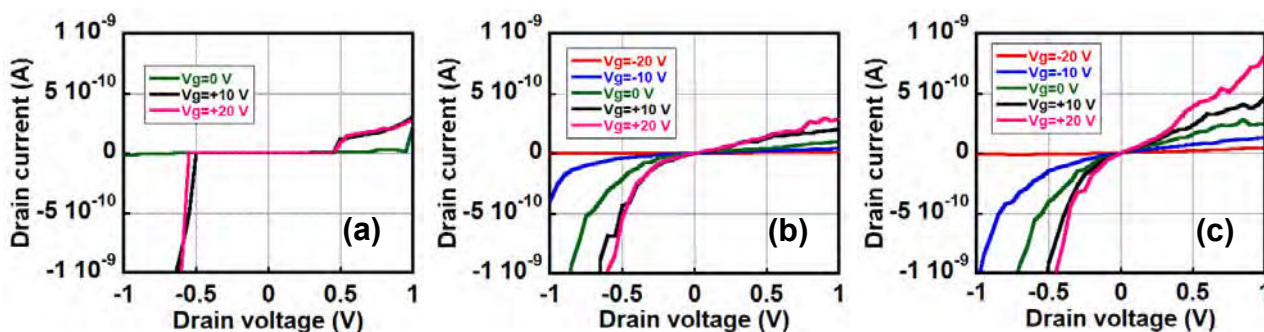


Figure 4: Drain-source (I_d - V_d) characteristics at various gate voltages V_g for (a) pristine WS₂ FET as shown in Fig. 3, (b) the same WS₂ FET after annealing at 225 °C under a 300 sccm 3% H₂/Ar gas flow for 3.5 h, (c) the same WS₂ FET after additionally annealing at 225 °C under a 300 sccm 3% H₂/Ar gas flow for 2 h (Total 5.5 h).

Presenting Author: Maya Narayanan Kutty^{1*}

Co-Authors: Ozhan Koybasi², Øystein Dahl³, Amin S. Azar³, T. Taniguchi⁴, K. Watanabe⁴, Edouard Monakhov¹, and Branson D. Belle²

¹Centre for Materials Science and Nanotechnology, Department of Physics, University of Oslo, P.O. Box 1048, Blindern, N-0316 Oslo, Norway.

²SINTEF DIGITAL, Forskeningsveien 1, NO-0314 Oslo, Norway.

³SINTEF INDUSTRY, Forskeningsveien 1, NO-0314 Oslo, Norway.

⁴Advanced Nanomaterials Laboratory, High Pressure Group, National Institute for Materials Science, 1-1 Namiki, Tsukuba, Ibaraki 305-0044, Japan.

*m.n.kutty@smn.uio.no

Gamma ray radiation effects on hBN encapsulated Graphene Field Effect Transistors

In the advent of emerging technologies graphene with its unique properties of flexibility, high mechanical strength, high thermal conductivity, structural stability along with high mobility, and optical transparency provides a foundation for boundless applications especially in the development of X-Ray-, THz- IR-, UV-, visible light-, chemical/ bio-sensors. It is then imperative to study the mechanisms that arise in graphene-based composite/hybrid devices under various radiation harsh environments. Radiation on graphene can cause formation of defects, displacement of its tightly packed stable structure. However, most damage under high energy radiation occurs in the substrate creating defects at the interface of graphene and substrate such as traps, tunneling sites, generation/ recombination sites, and compensators [1].

Graphene field effect transistors (GFETs) provide an adept vehicle for investigation of radiation effects as the field effect mobility and charge neutrality (Dirac) point are highly sensitive to unintentional doping from surrounding environment traps, fixed charges at oxide/substrate interface. Prior studies have shown that Gamma radiation in GFETs can cause electrically active defects in the substrate, increase trap density at the interfaces [2] while affecting the lattice of graphene itself exhibiting p-doped behavior. Encapsulation of graphene in 2D material such as hexagonal boron nitride (hBN) can isolate it from moisture rich ambient air, provide supporting substrate, passivating dielectric and due to the relatively inert nature of the hBN/graphene interface there are less dangling bonds or charged surface traps. But under X-ray irradiation, charge trapping is observed at or near hBN/graphene interface [3] wherein OH⁻ and H⁺ species can act as acceptor or donor defects [4].

In our study we delve deeper into understanding radiation induced defects by evaluating the material and electrical response of hBN encapsulated exfoliated GFETs and non-encapsulated CVD grown GFETs under un-irradiation and irradiation by Co₆₀ (Gamma rays) conditions. The Raman spectra (at 532nm) of non-encapsulated CVD grown graphene and hBN encapsulated exfoliated graphene before and after gamma irradiation (total dose of 5kGy) shows an upshift of both G and 2D peaks by about 5cm⁻¹ in non-encapsulated CVD grown graphene. This is in contrast to hBN

encapsulated exfoliated graphene which showed no change at the D peak under 5kGy gamma irradiation but a small upshift in 2D peak by 1cm^{-1} as shown in Fig.1 and this slight upshift can be attributed to an increase in doping. The transport characteristics measured at 300K of hBN encapsulated exfoliated GFETs show shift in the Dirac voltage from -2.72V pre-irradiation to $+4\text{V}$ post irradiation as shown in Fig.2 along with degradation of mobilities from $36\times 10^3\text{cm}^2/\text{V.s}$ pre-irradiation to $21\times 10^3\text{cm}^2/\text{V.s}$ post-irradiation. We infer that the energy deposited by radiation creates electrically charged defects in the substrate and substrate/oxide interfaces negatively affecting device performance. Furthermore we will present the electrical and material study of the effects of increasing total dosage of gamma ray radiation on hBN encapsulated exfoliated GFETs in contrast to the non-encapsulated CVD grown graphene providing further insight into creating radiation hardened graphene sensors.

References

- [1] R.C. Walker II, T. Shi, E.C. Silva, I. Jovanovic, and J.A. Robinson, 'Radiation Effects on two dimensional materials', Phys. Status Solidi A, 213 (12), 3057-3268 (2016).
- [2] K. Alexandrou, A. Masurkar, H. Edrees, J.F. Wishart, Y. Hao, N. Petrone, J. Hone, and I. Kymissis, Appl. Phys. Lett., 109, (2016) 153108.
- [3] C.X. Zhang, B. Wang, G.X. Duan, E. X. Zhang, D. M. Fleetwood, M.L. Alles, R.D. Schrimpf, A. P. Rooney, E. Khestanova, G. Auton, R. V. Gorbachev, S.J. Haigh, and S.T. Pantelides, IEEE TRANSACTIONS ON NUCLEAR SCIENCE, Vol.61, No.6, 2868 (2014).
- [4] P. Wang, C. Perini, A. O'Hara, B.R. Tuttle, E. X. Zhang, H. Gong, C. Liang, R. Jiang, W. Liao, D. M. Fleetwood, R.D. Schrimpf, E.M. Vogel, and S.T. Pantelides, IEEE TRANSACTIONS ON NUCLEAR SCIENCE, Vol.65, No.1, 156 (2018).

Figures

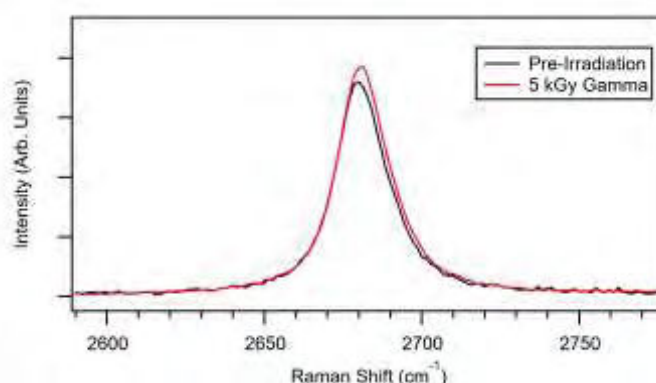


Figure 1: 2D peak of the Raman Spectrum for hBN encapsulated GFETs for pre-irradiation and post-irradiation of 5kGy Gamma rays.

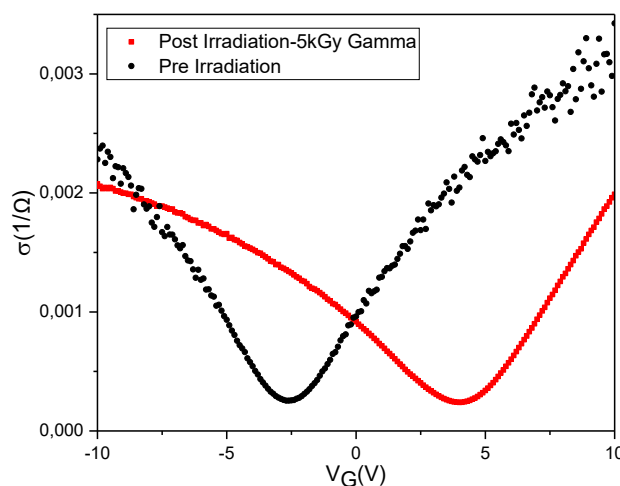


Figure 2: Conductivity versus Gate Voltage plot of hBN encapsulated GFETs comparing pre-irradiation and post-irradiation of 5kGy Gamma rays.

Milan Blaskovic

Slaven Garaj

National University of Singapore, Centre for Advanced 2D Materials, 6 Science Drive 2, 117542 Singapore, Singapore

a0129484@u.nus.edu/mblaskovic1989@gmail.com

Tunable interaction between graphene and a DNA molecule

CVD grown monolayer graphene has shown significant potential in bio-sensing and single-molecule detection applications due to its atomic thinness, mechanical robustness, excellent electronic properties, and functionalization possibilities [1, 2]. However, rational implementation of monolayer graphene has been hampered by the lack of understanding of the nature of its interactions with different biomolecules.

We investigated interaction of individual single-stranded DNA oligomers with the CVD grown monolayer graphene supported on SiO₂/Si surface, in a wide range chemical and physical liquid environments; and we fully identified and quantified all the relevant forces contributing to the total interactions.

Using atomic force microscopy (AFM), we measured force vs. distance curves for the interaction between a DNA tethered on a AFM tip and a graphene surface in aqueous environment. We observed characteristic plateaus in the curves, which are associated with unzipping of the DNA molecule from the surface (Fig 1). The single-molecule forces were measured at room temperature in a range of solutions with varying concentration of salts and various pH values. Lack of significant variation of the molecular forces in these solutions indicated that there is no electrostatic contribution to the force [3]. Further experiments in aqueous solution with inclusion of methanol, and experiments with varying temperature, demonstrated that hydrophobic hydration has dominating contribution to the overall force. With addition of an aromatic solvent (phenol) into the solution, we observe clear decrease in the overall interaction, due to disruption of pi-pi stacking interactions between graphene and aromatic DNA nucleobases.

The experiments identified that the overall DNA-graphene interaction is the combination of hydrophobic and pi-pi stacking forces. To understand the experiments, we proposed an elastic polymer chain model, which helped us quantifies all the relevant contributions to the force: pi-pi stacking interactions contribute around 20%; entropic-elastic forces contribute around 10%; and hydration (hydrophobic) forces contribute around 70% to total interaction. The insight obtained from our experiments can be used to modulate DNA-graphene interaction and possibly control to movement of individual biomolecule; to completely eliminate interactions for nanopore-based DNA sequencing; or to limit fouling of graphene membranes in desalination applications.

References

- [1] Yan, F., Zhang, M. & Li, J. Solution-Gated Graphene Transistors for Chemical and Biological Sensors. *Adv. Healthc. Mater.* **3**, 313–331 (2014).
- [2] Garaj, S., Liu, S., Golovchenko, J. A. & Branton, D. Molecule-hugging graphene nanopores. *Proc. Natl. Acad. Sci.* **110**, 12192–12196 (2013)
- [3] Iliafar, S., Wagner, K., Manohar, S., Jagota, A. & Vezenov, D. Quantifying Interactions between DNA Oligomers and Graphite Surface Using Single Molecule Force Spectroscopy. *J. Phys. Chem. C* **116**, 13896–13903 (2012)

Figures

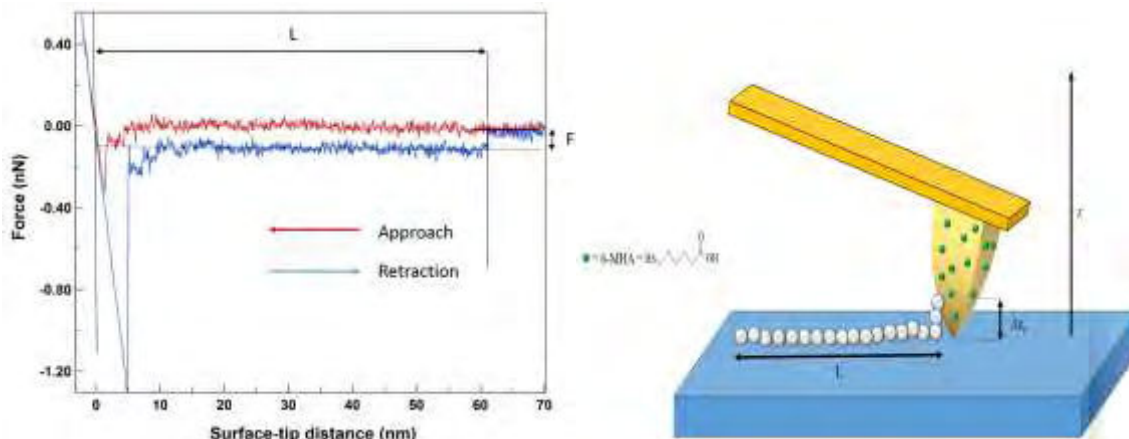


Figure 1. Characteristic force vs. distance curve (left), and force curve collection schematics (right)

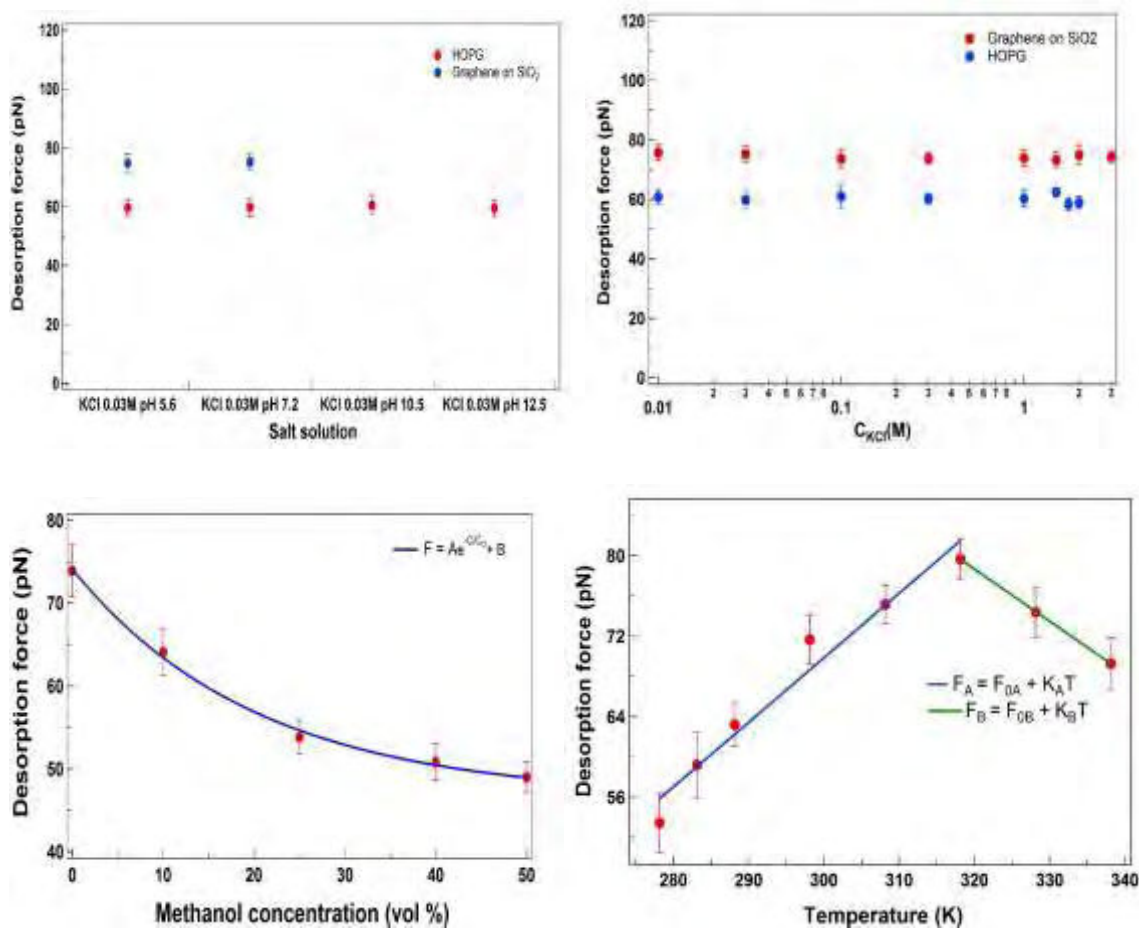


Figure 2. pH and molarity dependence of ssDNA interaction with graphene (upper left and right, respectively), dependence of interaction on methanol addition (lower left), and temperature of liquid environment (lower right)

Yichao Cai

Xiaofei Hu, Jianchao Sun, Zifan Li, Yong Lu, Hao Yang, Jun Chen*

Key Laboratory of Advanced Energy Materials Chemistry (Ministry of Education), Nankai University, Tianjin, China

chenabc@nankai.edu.cn

Graphene and Carbon Nanotube in Na-CO₂ Battery

Abstract

Sharing the similar structure of 3-dimensional tri-continuous porous structure, multidimensional continuous electron-transport pathways and excellent mechanical strength, graphene and carbon nanotube have attracted enormous interest and been widely applied in metal-air battery. However, during the past decades, all reported Na-CO₂ batteries are non-rechargeable at room temperature in pure CO₂ atmosphere, which was caused by gas channel blockage, electro-conductivity decrease, and insufficient cathode wettability to electrolyte. In order to solve this leftover problem and to take the full advantages of those two carbon materials, we introduced the multi-wall carbon nanotube as the cathode of Na-CO₂ battery, and achieved the first rechargeable Na-CO₂ battery at room temperature. And with the help of a novel rGO-Na anode, a better electrochemical performance Na-CO₂ battery with higher safety has been able to be published. The introduction of multi-wall carbon nanotube could bring numerous advantages in CO₂ battery system. First, this 3-dimentional tri-continuous porous structure cathode could avoid the unwanted product clogging. Second, the high specific surface area and better electrolyte wettability contributed to an increased triple-phase boundary for discharging reaction. Third, the high electro-conductivity of multi-wall carbon nanotube could minimize the polarization during charge. Moreover, the amorphous carbon on the surface of multi-wall carbon nanotube is exactly the same product during the discharge, this reactive-carbon-rich cathode promised the easier charge progress for Na-CO₂ battery.^[1,2] To replace the unstable Na metal anode, we proposed the rGO-Na composite anode for the first time, and applying to a high safty Na-CO₂ battey system.^[3] Thanks to the unique structure and excellent physical property of graphene, the rGO-Na anode represented faster Na⁺ diffusion rate and depressed Na dendrite growth. With the help of graphene and carbon nanotube, so many remarkable progresses have been made in Na-CO₂ battery, and they also hold a broad prospect of application in other metal-air batteries and commercial battery systems.

References

- [1] X. Hu, J. Sun, Z. Li, Q. Zhao, C. Chen, J. Chen, *Angew. Chem. Int. Ed.*, 55, (2016), 6482 - 6486
- [2] J. Sun, Y. Lu, H. Yang, M. Han, L. Shao, J. Chen, *Research*, DOI: 10.1155/2018/6914626
- [3] X. Hu, Z. Li, Y. Zhao, J. Sun, Q. Zhao, J. Wang, Z. Tao, J. Chen, *Sci. Adv.* 3, (2017), e1602396

Figures

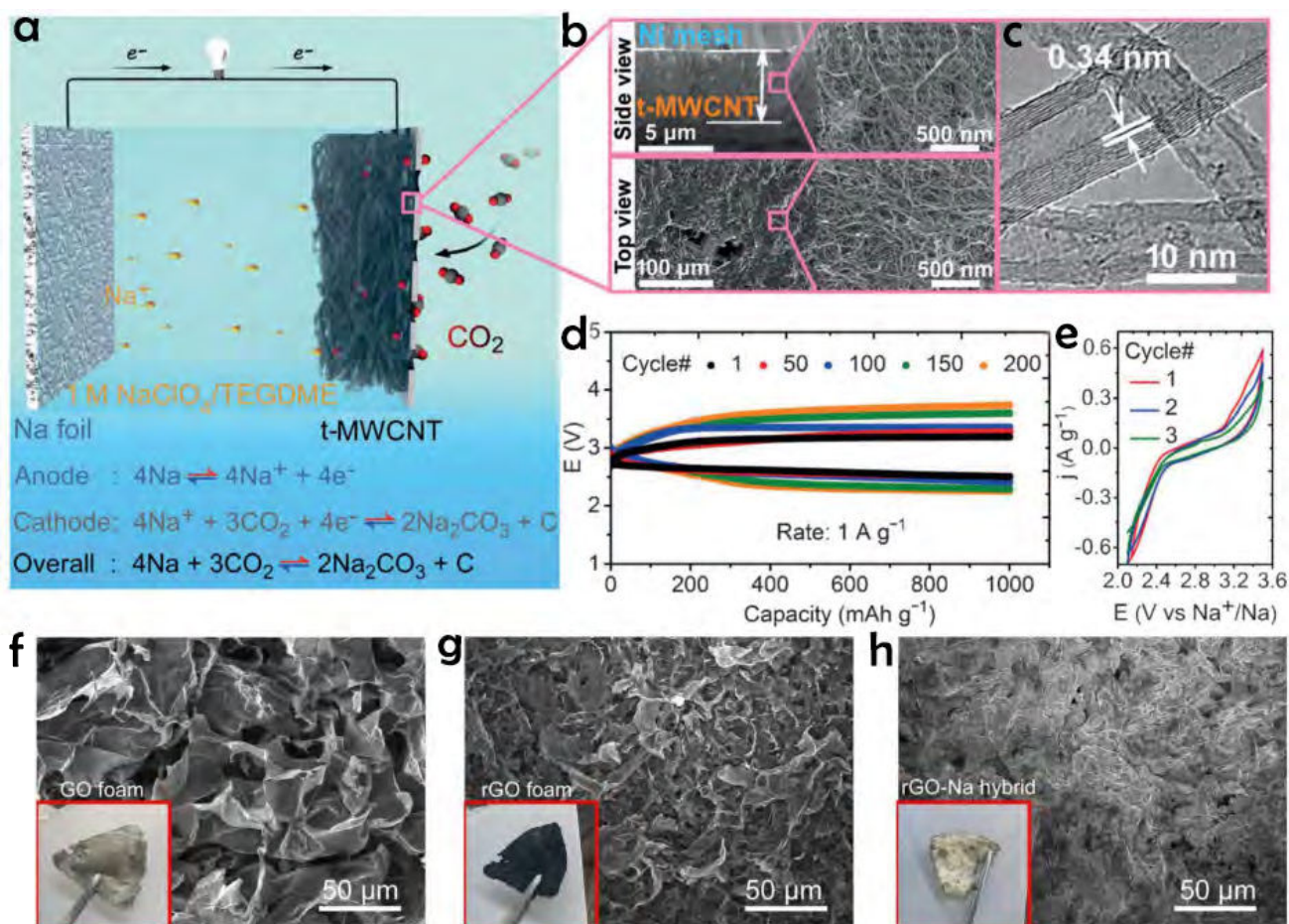


Figure 1: (a) Structure of Na-CO₂ batteries with metal Na foil anode, ether-based electrolyte, and t-MWCNT cathode. (b) SEM images of cathode from top and side views. (c) HRTEM image of t-MWCNT. (d) Discharge and charge profiles of Na-CO₂ batteries at 1 A/g (e) CV curves of Na-CO₂ batteries with scan rate of 0.1 mV/s. SEM images with corresponding inset photographs of (f) GO foam, (g) rGO foam reduced by molten Na, and (h) rGO-Na anode surface

Tunable Band Gap Energy from WS_xSe_y Monolayer

The transition metal dichalcogenides (TMDs) have attracted much attention because its unique characteristics and potential application in the low-power and optoelectronic devices. Recent reports have successfully demonstrated the growth of 2-dimensional MoS_xSe_y , $Mo_xW_yS_2$ and $Mo_xW_ySe_2$ alloys, where these materials exhibit tunable band gap energies. However, WS_xSe_y alloys are not available via CVD process until now. In the study, we report that WS_xSe_y monolayer alloys were synthesized using tungsten oxides, selenium and sulfur powders as the sources in the CVD process, where different heating temperatures of selenium and sulfur powders are applied respectively to control the ratio of S to Se. The optical band gap of the as-grown WS_xSe_y monolayer alloys is precisely tunable from 2.0 eV to 1.64 eV via modulating the ratio of S to Se. With the increase of selenium in WS_xSe_y monolayers, apparent electronic state transformation from p-type to n-type were recorded through energy band diagrams, beneficial for the future optical design.

References

- [1] Yung-Huang Chang, Wenjing Zhang, Yihan Zhu, Yu Han, Jiang Pu, Jan-Kai Chang, Wei-Ting Hsu, Jing-Kai Huang, Chang-Lung Hsu, Ming-Hui Chiu, Taishi Takenobu, Henan Li, Chih-I Wu, Wen-Hao Chang, Andrew Thye Shen Wee, Lain-Jong Li, *ACS Nano* **2014**, 8, 8582–8590.
- [2] Jing-Kai Huang, Jiang Pu, Chang-Lung Hsu, Ming-Hui Chiu, Zhen-Yu Juang, Yung-Huang Chang, Wen-Hao Chang, Yoshihiro Iwasa, Taishi Takenobu, Lain-Jong Li, *ACS Nano* **2014**, 8, 923–930.

Figures

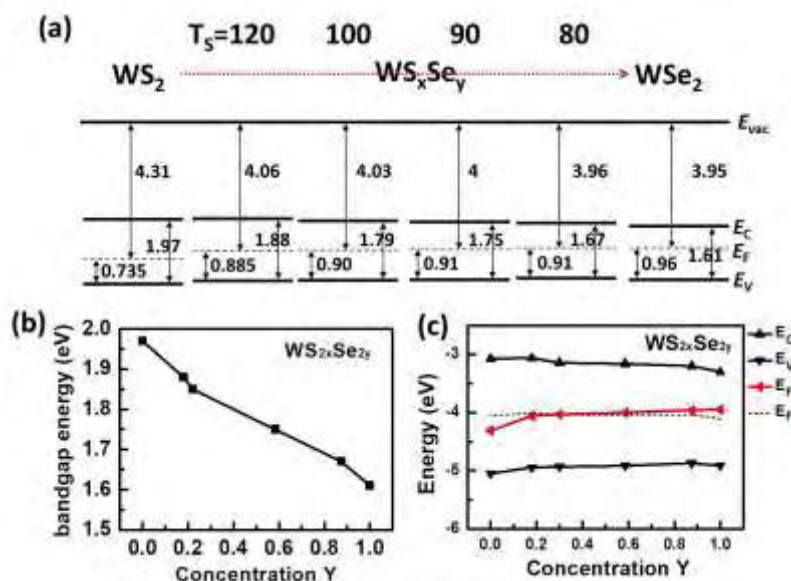


Figure 1: (a) The energy band diagram of pristine WS_2 , WSe_2 and as-grown WS_xSe_y monolayers acquiring from UPS examination. (b) The band-gap energy of WS_xSe_y monolayers as a function of Se concentration, showing a well linear relationship. (c) The conduction band minimum (CBM), valence band maximum (VBM) and Fermi level positions of WS_xSe_y monolayers as a function of Se concentration. The vacuum energy is taken as zero for reference.

Chang-Hsiao Chen^{1,*}

Han-Ching Chang¹, Chien-Liang Tu¹, Kuang-I Lin², Jiang Pu³, Taishi Takenobu³,
Chien-Nan Hsiao⁴

¹Department of Automatic Control Engineering, Feng Chia University, Taichung, Taiwan

²Center for Micro/Nano Science and Technology, National Cheng Kung University, Tainan, Taiwan

³Department of Applied Physics, Nagoya University, Nagoya, Japan

⁴Instrument Technology Research Center, National Applied Research Laboratories, Hsinchu, Taiwan

chsiaoc@fcu.edu.tw

Chemical Vapor Deposition Synthesis of Large-Area Monolayer InSe

Recently, two-dimensional materials of indium selenide (InSe) layers have attracted much attention from scientific community due to their high mobility transport and fascinating physical properties.[1-3] To date, reports on synthesis of high quality and scalable InSe atomic films have been limited. Here, we report that a synthesis of InSe atomic layers by vapor phase selenization of In_2O_3 in a chemical vapor deposition (CVD) system, resulting in large-area monolayer flakes or thin films.[4] The atomic films are continuous and uniform over a large area of $1 \times 1 \text{ cm}^2$, comprising of primarily InSe monolayers. Spectroscopic and microscopic measurements reveal the highly crystalline nature of the synthesized InSe monolayers. The ion-gel-gated field-effect transistors based on CVD InSe monolayers exhibited n-type channel behaviors, where the field effect electron mobility values can be up to $\sim 30 \text{ cm}^2/\text{Vs}$ along with an on/off current ratio, of $>10^4$ at room temperature. In addition, the graphene can serve as a protection layer to prevent the oxidation between InSe and the ambient environment. Meanwhile, the synthesized InSe films can be transferred to arbitrary substrates, enabling possibility of reassembly of various two-dimensional materials into vertically stacked heterostructures, prompting research efforts to probe its characteristics and applications.

References

- [1] Denis A. Bandurin et al., Nature Nanotechnology, 12 (2016) pp 223-227
- [2] Po-Hsun Ho et al., Acs Nano, 11 (2017) pp 7362-7370
- [3] Sukrit Sucharitakul et al., Nano Letters, 15 (2015) pp 3815-3819
- [4] Han-Ching Chang et al., Small, (2018) doi: 10.1002/smll.201802351

Figures

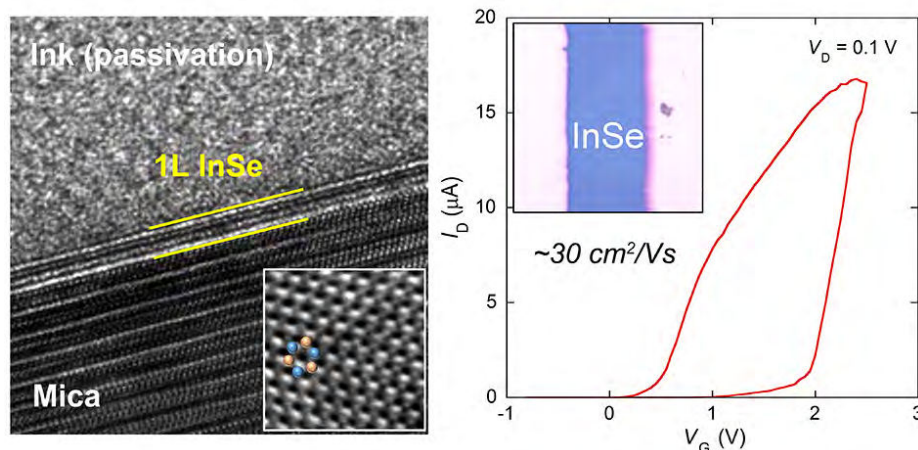


Figure 1: (Left) Cross-section TEM image of a monolayer InSe film, (Right) Linear scale transfer curve of the InSe FET.

Ah-Jin Cho

and Jang-Yeon Kwon

School of Integrated Technology, Yonsei University, Songdogwahak-ro 85, Incheon, South Korea

Yonsei Institute of Convergence Technology, Songdogwahak-ro 85, Incheon, South Korea

ahjincho@yonsei.ac.kr

Evaluation of a WSe₂/MoS₂ Heterojunction in the Perspective of a Transparent Thin-film Solar Cell

Solar energy is one of the most powerful and reliable renewable energy sources, but its wide-use is often hampered by the limited installation space. As conventional c-Si solar cell is very bulky and heavy, it requires large extra space to be installed. As a means to overcome such limitation, a transparent and light-weighted thin-film solar cell, which can be installed at the exterior of the buildings, has been studied [1-3]. In order to achieve transparency and photon-electron conversion at the same time, special structure or material is needed. We are suggesting a p-n heterojunction of 2D semiconductors as a candidate material to realize a transparent thin-film solar cell. In that few layers of a 2D semiconductor is highly transparent due to its thinness, but still maintain its photovoltaic effect and show relatively high light-matter interaction, it can meet those two contradictory requirements of a transparent solar cell [4]. Here, we fabricated a transparent thin-film solar cell with a p-n heterojunction of WSe₂/MoS₂ and evaluated its performance. By utilizing a glass substrate, a 2D p-n heterojunction, ITO electrodes and a CYTOP encapsulation, we achieved a highly transparent (~80 %) and stable solar cell. Our WSe₂/MoS₂ heterojunction device showed clear current rectification under dark state, and photovoltaic effect with sizable open circuit voltage (Voc) and short circuit current (Isc) under illumination. 2D materials are usually vulnerable to the environmental factors and easily degraded under ambient condition. However, by simply spin coating CYTOP as an encapsulation layer, the device properties were maintained stable for ~2 months. Especially, the standard deviation of Voc values throughout the measurement was less than 3% of the initial Voc value, which indicates how stable the devices are. In order to evaluate the real performance of the 2D solar cell under sunlight, I-V characteristic of a WSe₂/MoS₂ heterojunction under AM1.5G illumination was conducted. It turned out to show power conversion efficiency of 0.84 % under solar spectrum. In addition, the photovoltaic characteristics under monochromatic light representing red, green and blue were measured. The Isc and Voc of our solar cell showed fast response to the light pulse repeating on and off with the interval of 1.5 and 3 seconds, respectively. Good dynamic performance with consistent current or voltage level at light 'on' stage during repetitive measurement indicates small interface trap density of our device. We believe that our result exhibits great potential of a 2D heterojunction to be utilized as a transparent thin-film solar cell.

References

- [1] R. R. Lunt and V. Bulovic, *Appl. Phys. Lett.*, 98 (2011), 113305.
- [2] Y. Zhao and R. R. Lunt, *Adv. Energy Mater.*, 3 (2013), 1143-1148.
- [3] J. L. H. Chau, R. T. Chen, G. L. Hwang, P. Y. Tsai and C. C. Lin, *Sol. Energy Mater. Sol. Cells*, 94 (2010), 588–591.
- [4] M. L. Tsai, M. Y. Li, J. R. D. Retamal, K. T. Lam, Y. C. Lin, K. Suenaga, L. J. Chen, G. Liang, L. J. Li, H. He Jr, *Adv. Mater.*, 29 (2017), 1701168.

Figures

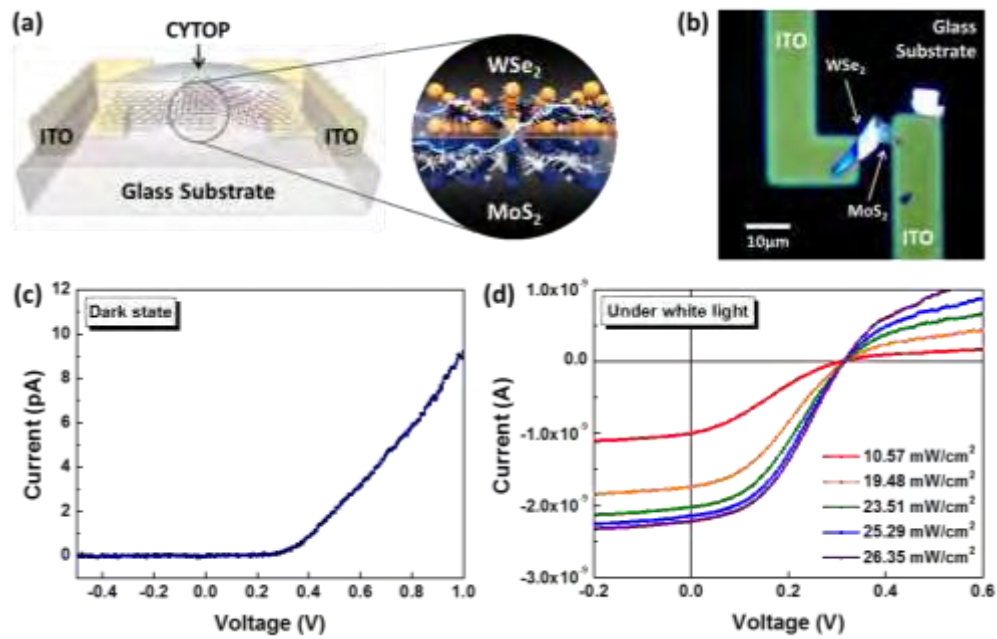


Figure 1: (a) A schematic and (b) an optical microscope image of a $\text{WSe}_2/\text{MoS}_2$ heterojunction device and its I-V characteristics under (c) dark state and (d) illumination (halogen lamp).

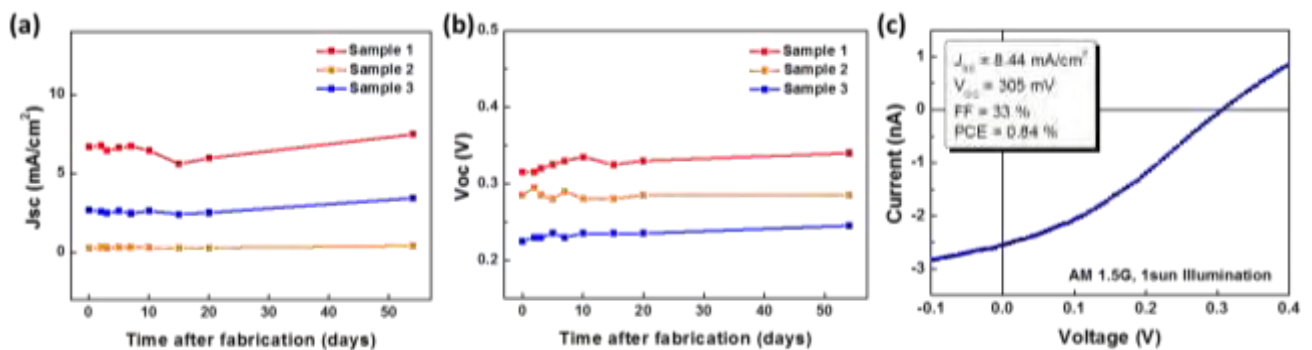


Figure 2: Variation of (a) J_{sc} and (b) V_{oc} values as time goes on after fabrication. (c) I-V characteristic of the 2D solar cell under AM 1.5G illumination (1sun) and related parameters.

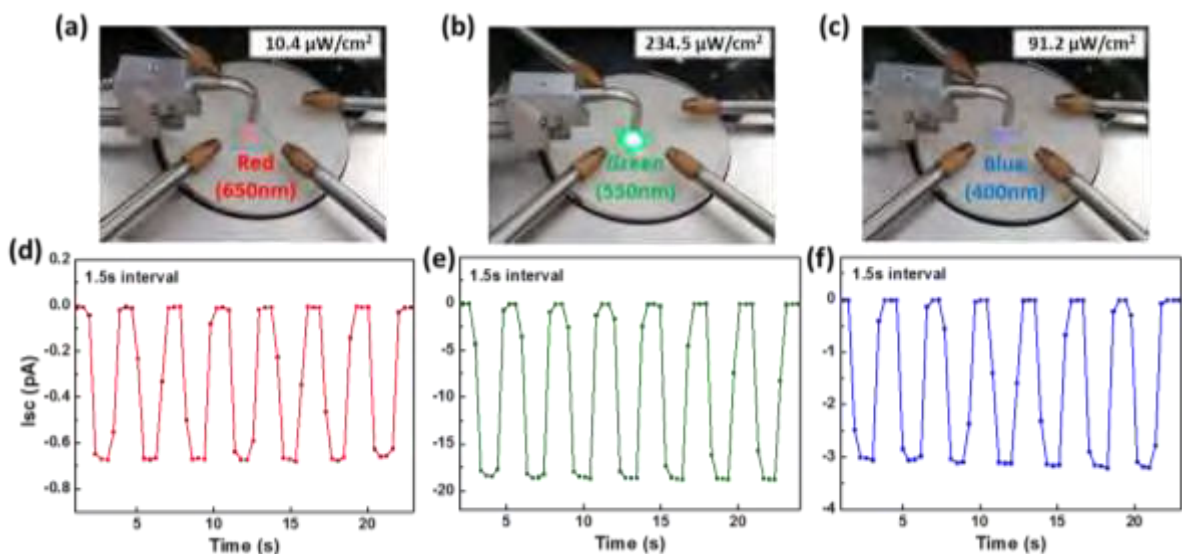


Figure 3: Photograph of measurement setup for (a) red, (b) green and (c) blue light response. I_{sc} -time plot of our device, measured under (d) red, (e) green and (f) blue light pulse repeating on and off for 1.5 seconds.

Hailiang Chu

Errui Wang, Tingting Fang, Shujun Qiu, Yongjin Zou, Cuili Xiang, Huangzhi Zhang, Erhu Yan, Fen Xu, Lixian Sun

Guangxi Key Laboratory of Information Materials, Guangxi Collaborative Innovation Center of Structure and Property for New Energy and Materials and School of Materials Science and Engineering, Guilin University of Electronic Technology, No.1 Jinji Road, Qixing District, Guilin 541004, PR China

chuhailiang@guet.edu.cn (H.C.); sunlx@guet.edu.cn (L.S.)

Effect of Reduced Graphene Oxide on the Electrochemical Properties of Overlithiated Oxide Cathode Materials for Li-Ion Batteries

Lithium-ion batteries (LIBs) have been used in many fields such as military power supply, electric vehicles (EVs), and portable electronic products. Cathode material is one of the key factors of LIBs, which is now becoming a technological bottleneck to achieve a high powder/energy density.^[1-4] In this contribution, we successfully prepared nano-particles overlithiated oxide cathode material $\text{Li}_{1.2}\text{Mn}_{0.6}\text{Ni}_{0.2}\text{O}_2$ by solid phase method through ball milling. Reduced graphene oxide was introduced into nano-particles $\text{Li}_{1.2}\text{Mn}_{0.6}\text{Ni}_{0.2}\text{O}_2$ through hydrothermal method. Structure characterization and performance testing show that the addition of 3 wt% graphene gives rise to the improved electrochemical properties (Figure 1).

References

- [1] Li Biao, Xia Dingguo, *Advanced Materials*, 29 (2017) 1701054.
- [2] Wang Lin, Shi Ji-Lei, Su Heng, Li Guangyin, Zubair Muhammad, Guo Yu-Guo, Yu Haijun, *Small*, 14 (2018) 1800887.
- [3] Li Wangda, Song Bohang, Manthiram Arumugam, *Chemical Society Reviews*, 46 (2017) 3006.
- [4] Wang Errui, Shao Chunfeng, Qiu Shujun, Chu Hailiang, Zou Yongjin, Xiang Cuili, Xu Fen, Sun Lixian, *RSC Advances*, 7 (2017) 1561.

Figures

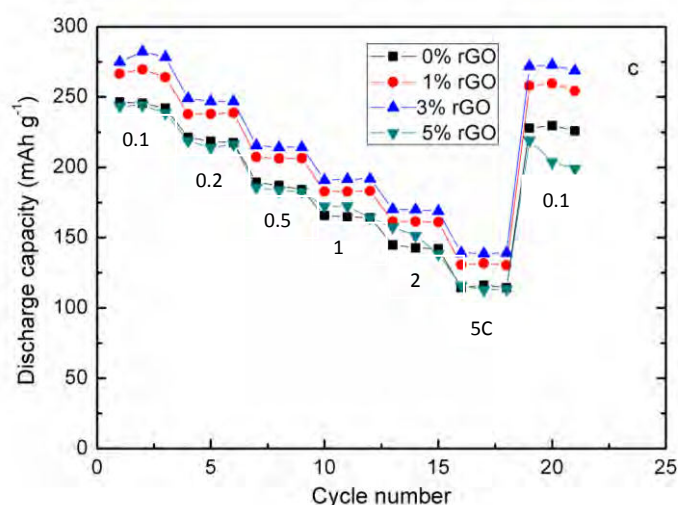


Figure 1: Rate performance of $\text{Li}_{1.2}\text{Mn}_{0.6}\text{Ni}_{0.2}\text{O}_2$ with addition of different amounts of reduced graphene oxide

Vertically-oriented Graphene Growth at Low Temperature for Solarthermal Applications

Abstract

Compared with the conventional two-dimensional graphene, vertically-oriented graphene (VG) nanosheets [1], composed by few-layer graphene, have also been synthesized via a plasma-enhanced chemical vapor deposition (PECVD) route on metal or dielectric substrates. Many unique properties, including large amount of exposed edges, non-stacking geometry, and a large surface-to-volume ratio were detected for such graphene nanosheets. In particular, different application aspects with regard to their 2D counterparts have been developed [2]. By a direct-current -PECVD system at 580 °C, the direct synthesis of VG nanosheets on traditional soda-lime glass or other glass substrates can be achieved, which is right below the softening point of normal glass, and featured a scale-up size ~6 inches. Particularly, the fabricated VG nanosheets-glass hybrid materials at a transmittance range of 97%–34% exhibited excellent solarthermal performances, reflected by a 70%–130% increase in the surface temperature under simulated sunlight irradiation. We believe that the graphene glass hybrid materials have great potential for use in future transparent “green-warmth” construction materials.

References

- [1] Bo, Z.; Yang, Y.; Chen, J. H.; Yu, K. H.; Yan, J. H.; Cen, K. F. *Nanoscale*, 5 (2013) 5180–5204.
- [2] Zhang, Z; Lee, C. S.; Zhang, W. *Advanced Energy Materials*, 7 (2017) 1700678.

Figures

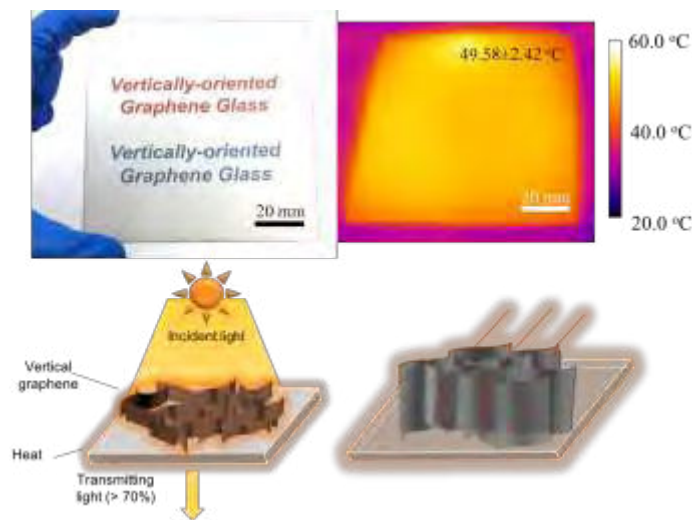


Figure 1: The schematic illustration of VG-glass materials for solarthermal applications

Lingzhi Cui

Xudong Chen,¹ Bingzhi Liu,¹ Ke Chen,¹ Zhaolong Chen,¹ Yue Qi,¹ Huanhuan Xie,¹ Fan Zhou,¹ Mark H. Rummeli,⁴ Yanfeng Zhang,^{*,1,2,3} and Zhongfan Liu^{*,1,3}

¹ Center for Nanochemistry (CNC), Beijing National Laboratory for Molecular Sciences, College of Chemistry and Molecular Engineering, Academy for Advanced Interdisciplinary Studies, Peking University, Beijing 100871, People's Republic of China

² Department of Materials Science and Engineering, College of Engineering, Peking University, Beijing 100871, People's Republic of China

³ Beijing Graphene Institute, Beijing 100091, People's Republic of China

⁴ Soochow Institute for Energy and Materials Innovations (SIEMIS), Key Laboratory of Advanced Carbon Materials and Wearable Energy Technologies of Jiangsu Province, Soochow University, Suzhou 215006, P.R. China.

cuilz-cnc@pku.edu.cn

Highly Conductive Nitrogen-doped Graphene Grown on Glass Towards Electrochromic Applications

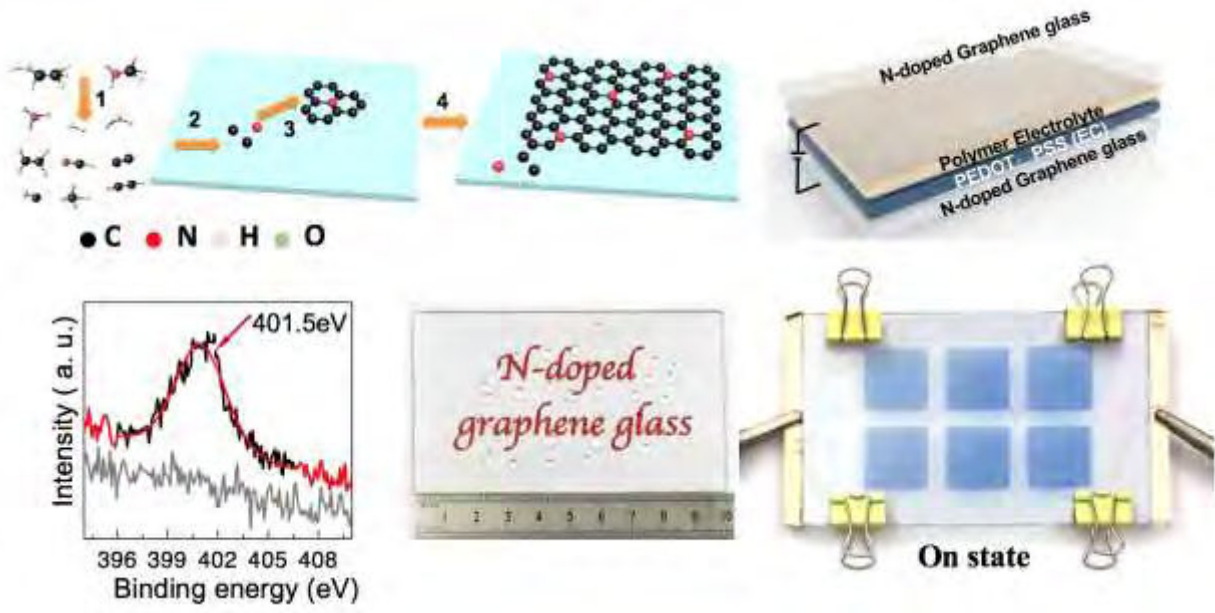
Abstract

The direct synthesis of low sheet resistance graphene on glass can promote the applications of such intriguing hybrid materials in transparent electronics and energy related fields. Chemical doping is efficient for tailoring the carrier concentration and the electronic properties of graphene that previously derived from metal substrates. Herein, we report the direct synthesis of 5-inch uniform nitrogen-doped (N-doped) graphene on the quartz glass, through a designed low- pressure chemical vapor deposition (LPCVD) route. Ethanol and methylamine were selected respectively as precursor and dopant for acquiring predominantly graphitic-N doped graphene. We reveal that, by a precise control of growth temperature and thus the doping level, the sheet resistance of graphene on glass can be as low as one half that of non-doped graphene, accompanied with relative high crystal quality and transparency. Significantly, we demonstrate that, this scalable, 5-inch uniform N-doped graphene glass can serve as excellent electrode materials for fabricating high performance electrochromic smart windows, featured with a much simplified device structure. This work should pave ways for the direct synthesis and application of the new type graphene- based hybrid material.

References

- [1] Lingzhi Cui, Xudong Chen, Bingzhi Liu, Ke Chen, Zhaolong Chen, Yue Qi, Huanhuan Xie, Fan Zhou, Mark H. Rummeli, Yanfeng Zhang, and Zhongfan Liu. Highly Conductive Nitrogen-Doped Graphene Grown on Glass toward Electrochromic Applications. *ACS Applied Materials & Interfaces* **Article ASAP**

Figures



Xueping Cui

(Jian Zheng)

Institute of Chemistry Chinese Academy of Sciences, Zhongguancun North First Street 2, 100190, Beijing, China

cuixueping@iccas.ac.cn

Fabrication of Transition Metal Dichalcogenides Nanoscrolls

Abstract

Atomically thin transition metal dichalcogenides (TMD) flakes were believed capable to scroll into nanoscrolls (NS) with distinct properties. However, limited by mechanical strength and chemical stability, production of high-quality transition metal dichalcogenides nanoscrolls remain challenging. Here, we demonstrated high-quality nanoscrolls made from chemical vapour deposition-grown transition metal dichalcogenides flakes. Based on the internal open topology, nanoscrolls hybridized with a variety of functional materials have been fabricated, which is expected to confer transition metal dichalcogenides nanoscrolls with additional properties and functions attractive for potential application.

References

- [1] Xueping Cui, Jian Zheng*, et al. Nature Commun. 9(2018),1301.

Figures

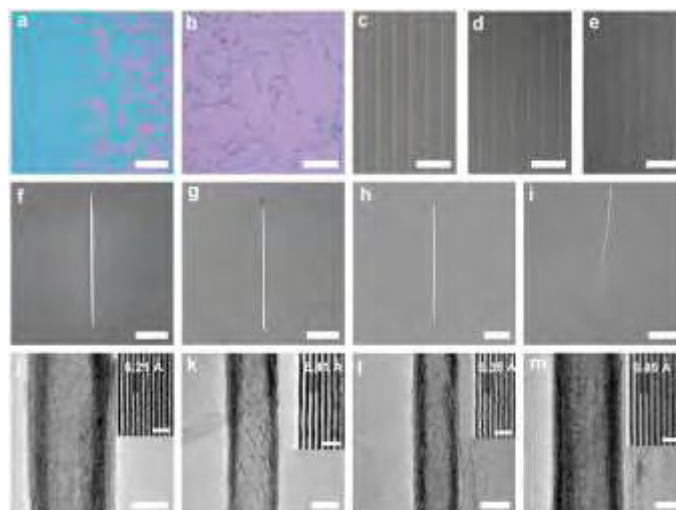


Figure 1: TMD-NSs from self-scrolling CVD-based TMD monolayer flakes. a, Optical image of CVD-grown MoS₂ monolayer flakes. b, Optical image of MoS₂-NSs. c-e, The fabrication process of a MoS₂-NS array. f-i, SEM images of typical TMD-NSs: MoS₂-NSs (f), WS₂-NSs (g), MoSe₂-NSs (h), and WSe₂-NSs (i). j-m, TEM images of typical TMD-NSs: MoS₂-NSs (j), WS₂-NSs (k), MoSe₂-NSs (l), and WSe₂-NSs (m). Inset: High-magnification images of sidewalls of TMD-NSs. (Scale bars, 500 μm in a; 100 μm in b; 50 μm in c-e; 5 μm in f, i; 10 μm in g, h; 20 nm in j-m; 2 nm in inset).

Xi Dai

Fang Wan, Linlin Zhang, Hongmei Cao, Zhiqiang Niu

Key Laboratory of Advanced Energy Materials Chemistry (Ministry of Education), College of Chemistry, Nankai University, Tianjin 300071, PR China

daixi@mail.nankai.edu.cn, zqniu@nankai.edu.cn

Freestanding graphene/VO₂ composite films for highly stable aqueous Zn-ion batteries with superior rate performance

Aqueous Zn-ion batteries (ZIBs) are promising energy storage systems owing to their high safety and low cost.^[1] However, their unsatisfactory energy and power densities as well as the cycling performance have hindered their practical application. Herein, we demonstrate a highly reversible zinc/vanadium dioxide system, where freestanding reduced graphene oxide/vanadium dioxide (RGO/VO₂) composite films are used as the cathodes. Owing to the synergistic effects from continuously porous network of RGO^[2] and the robust structure of VO₂, RGO/VO₂ composite films not only enhance the transport of electrons and ions, but also accommodate the considerable deformations caused by Zn²⁺ extraction/insertion. Therefore, the Zn/VO₂ batteries exhibit an energy density of 65 Wh kg⁻¹ even at a high power density of 7.8 kW kg⁻¹. More impressively, they deliver excellent capacity retention of 99% after 1000 cycles. In addition, the RGO/VO₂ composite films can serve as the electrodes of flexible ZIBs. Flexible soft-packaged Zn/VO₂ batteries demonstrated stable electrochemical performance at various bending states. Therefore, the rechargeable Zn/VO₂ battery can bridge the gap between conventional batteries and supercapacitors, opening new opportunities for powering portable electronic devices and hybrid electric vehicles.

References

- [1] Fang Wan, Linlin Zhang, Xi Dai, Xinyu Wang, Zhiqiang Niu & Jun Chen. *Nat. Commun.* 1 (2018).
[2] Zhiqiang Niu, Lili Liu, Li Zhang, Qi Shao, Weiya Zhou, Xiaodong Chen, Sishen Xie. *Adv. Mater.* 22 (2014).

Figure

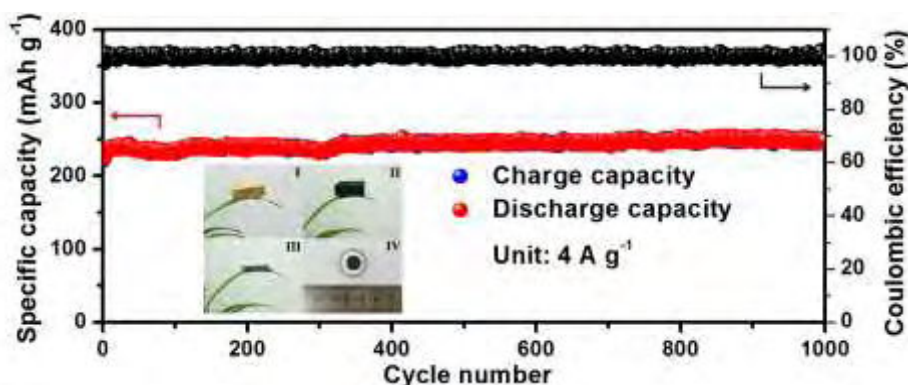


Figure: Long-term cycling performance with Coulombic efficiency of the RGO/VO₂ composite film at 4 A g⁻¹. The inset shows the optical images of corresponding samples. I: NH₃VO₄/GO foam through freeze-drying; II: RGO/VO₂ foam via calcination; III: freestanding RGO/VO₂ electrode film after mechanical compression; IV: the desirable piece of RGO/VO₂ composite film electrode for ZIBs.

Bing Deng

Zhongfan Liu, Hailin Peng

Peking University, Yiheyuan Road N0.5, Beijing, China

Beijing Graphene Institute, Sujiatuo Zhen Cui Hunan road 13, Beijing, China

hlpeng@pku.edu.cn, zfliu@pku.edu.cn

Graphene as Electronic Materials: Controlled Growth of Single-Crystal Graphene Wafer

Similar to silicon (Si) wafers as the cornerstone of modern Si based electronics, single-crystal graphene wafers are vital components in future high-performance graphene electronics. Two approaches have been employed for single-crystal graphene growth by chemical vapor deposition (CVD), that is, the single-nucleation approach enabled by reducing the nucleation density, and the multi-nucleation approach featured with oriented graphene growth on an epitaxial substrate. Cu(111) is a substrate enabling epitaxial growth of graphene. We fabricated single-crystal Cu(111) thin films free of in-plane twinning on sapphire by magnetron sputtering and solid state recrystallization process. 4 inch single-crystal graphene was grown on the Cu(111) by APCVD.^[1] The single-crystallinity was confirmed by multiscale characterization, including OM, SEM, Raman, LEED, and TEM. To improve the growth rate, single-crystal Cu₉₀Ni₁₀(111) thin films were fabricated. 4 inch single-crystal graphene was grown on the CuNi(111) within 10 min, 50 folds faster than that of Cu(111).^[2] Single-crystal graphene grown on Cu(111) and CuNi(111) can be free of wrinkles, which further improved the electrical and mechanical properties of graphene.^[3] One of the best benefits of graphene growth on the Metal(111) lies in the compatibility with wafer technology. A pilot-scale APCVD system is designed and built, and we are paving the way toward mass production of single-crystal graphene wafers.

References

- [1] Bing Deng, Zhongfan Liu, Hailin Peng, et al. *ACS Nano*, **2017**, 11, 12337.
- [2] Bing Deng, Zhongfan Liu, Hailin Peng, et al. *Advanced Materials*, **2018**, submitted.
- [3] Bing Deng, Zhongfan Liu, Hailin Peng, et al. *Small*, **2018**, 14, 1800725.

Figures

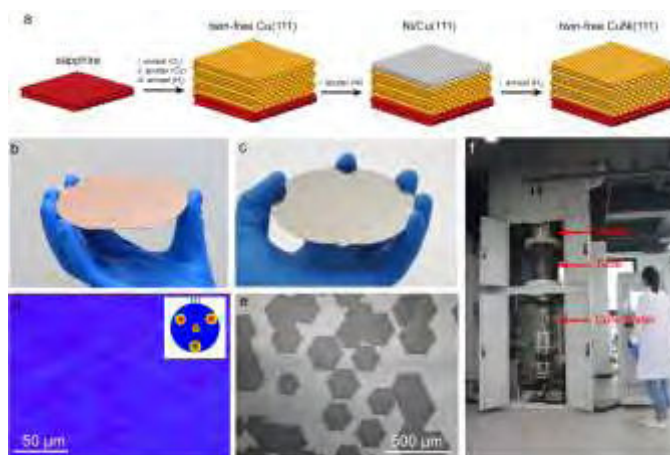


Figure 1: (a) Fabrication of single-crystal CuNi(111) thin films. (b) Photograph of a Cu(111) wafer. (c) Photograph of a CuNi(111) wafer. (d) EBSD of Cu(111). (e) SEM image of graphene grown on CuNi(111). (f) A homemade pilot-scale APCVD system for mass production of single-crystal graphene wafer.

Jianqiu Deng

Meng Li, Zonglin Zuo, Wen-Bin Luo, Qingrong Yao, Zhongmin Wang, Huaiying Zhou

School of Material Science and Engineering, Guilin University of Electronic Technology, Guangxi, Guilin 541004, China

jqdeng@guet.edu.cn

High-performance V-based electrode materials for sodium-ion batteries

Sodium ion batteries have been considered as one of the promising candidates for large-scale energy storage systems [1, 2]. From the application perspective of an integrated sodium ion full-cell system, it is important to develop a practical sodium-ion full-cell system with excellent cycling life, superior safety, and good rate capability to tolerate the frequent current impulses during the grid peak period [3]. Therefore, exploring appropriate electrode materials with excellent electrochemical properties is the key issue.

In this work, a series of high-performance V-based electrode materials for sodium-ion batteries have been synthesized by solvothermal and sol-gel methods. The microstructure and electrochemical properties of the materials are investigated by physical characterization and electrochemical measurement techniques. The electrode materials exhibit excellent electrochemical performance, including high capacity, superior rate capability, and remarkable cycling performance. $\text{Na}_3\text{V}_2(\text{PO}_4)_3/\text{C}/\text{CNT}$ anode delivers a reversible capacity of 60.2 mA h g^{-1} after 10000 cycles at 50 C. The fabricated symmetric full cell exhibits an initial discharge capacities of 89 mA h g^{-1} at a high current density of 20 C and can still maintain a capacity of 72.1 mA h g^{-1} over 5000 cycles, corresponding to a capacity retention of about 81%. In addition, micro-sized two-phase structured $\text{Li}_{2.6}\text{Na}_{0.4}\text{V}_2(\text{PO}_4)_3/\text{C}$ composite is comprised of numerous primary nanocrystals. It shows excellent long-term cycling stability with capacity retention of about 83 % and 100 % after 3000 cycles at 10 C, for the cathode and anode, respectively. Moreover, the symmetric sodium-ion full cells made of the $\text{Na}_2\text{LiV}_2(\text{PO}_4)_3/\text{C}$ nanocomposite have good rate capability and cycling stability, which verifies the feasibility for practical applications of the $\text{Na}_2\text{LiV}_2(\text{PO}_4)_3/\text{C}$ nanocomposite in sodium-ion batteries.

TWO pages abstract format: including figures and references.

Do not change the font sizes or line spacing to squeeze more text into a limited number of pages.

Please follow the model below.

Single-spaced and a single paragraph

Page margins are 2,00 cm top and down; 1,90 cm left and right.

Greek letters, sub- and superscripts should be formatted as such.

References

- [1] H. Pan, Y.-S. Hu, L. Chen, *Energ Environ Sci*, 2013, **6**, 2338-2360.
- [2] X. Xiang, K. Zhang, J. Chen, *Adv Mater*, 2015, **27**, 5343-5364.
- [3] J. Deng, W.-B. Luo, S.-L. Chou, H.-K. Liu, S.-X. Dou, *Adv. Energy Mater.*, 2018, **8**, 1701428.

Figures

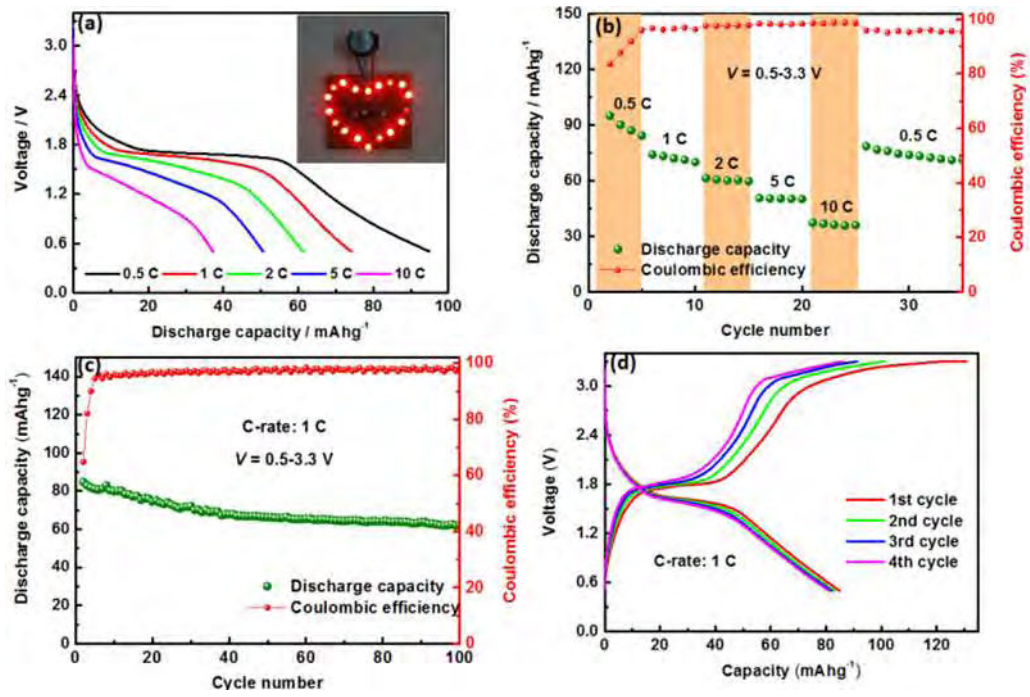


Figure 1: The electrochemical performance of symmetric full cells based on the NLVP/C.

Jie Gao

Guilin University of Electronic Technology, China

NextYearGJ@foxmail.com

Enhanced Thermoelectric Performance in Graphene Quantum Dots/Te Nanowires Flexible Hybrid Film

Graphene has been proved to be positive for reducing thermal conductivity in many thermoelectric nanocomposites. Here we prepared graphene quantum dots (GQDs) /Te nanowires flexible hybrid films on mica substrate through drop-cast method. After being annealed in H₂/Ar atmosphere, the hybrid films show enhanced thermoelectric performance due to the redox-reaction between GQDs and Te nanowires during annealing process. The thermoelectric performance of hybrid films can be further adjusted via changing size and percentage of GQDs in film. This work provides insights for the synthesis of graphene-based hybrid thermoelectric films.

Yunpeng Hou

Pengfei Zhou, Huanju Meng, Zhen Zhang, Zhanliang Tao* and Jun Chen*

Key Laboratory of Advanced Energy Materials Chemistry (Ministry of Education), College of Chemistry, Nankai University, Tianjin, China

chenabc@nankai.edu.cn

High-performance layered Ni-rich $\text{LiNi}_{1-x-y}\text{Co}_x\text{Al}_y\text{O}_2$ cathode materials for lithium ion batteries

Lithium ion batteries (LIBs) are expected to be used as energy storage technologies for electric vehicles, renewable power stations, and smart grids. One of the great challenges for LIBs is to develop advanced cathode materials in terms of high capacity, long cycling life, and high thermal stability. Among all kinds of cathode materials, layered Ni-rich $\text{LiNi}_{1-x-y}\text{Co}_x\text{Al}_y\text{O}_2$ materials are considered as promising candidates with advantages of high capacity and low cost. However, there still remain some crucial issues to be solved including unsatisfactory thermal stability and relatively rapid capacity fading during cycling. Optimizing synthesis process and surface coating are two major strategies to alleviate the above issues. Herein, on the one hand, we report an easy co-precipitation synthesis of microspherical $\text{Ni}_{1-x-y}\text{Co}_x\text{Al}_y(\text{OH})_2$ precursors employing AlO_2^- as the Al source to guarantee the co-precipitation of Ni^{2+} , Co^{2+} and Al^{3+} .^[1,2] As cathode materials for LIBs, both $\text{LiNi}_{0.8}\text{Co}_{0.15}\text{Al}_{0.05}\text{O}_2$ and $\text{LiNi}_{0.9}\text{Co}_{0.07}\text{Al}_{0.03}\text{O}_2$ exhibit high discharge capacity, good cycling performance and remarkable rate capability. The improved performance might be attributed to the combination of the high Ni component, well layered structure with low degree of $\text{Li}^+/\text{Ni}^{2+}$ mixing, and uniform microspheres with homogeneous distribution of Ni, Co, and Al. On the other hand, we report a one-step dry coating of amorphous SiO_2 or $\text{Zr}(\text{OH})_4$ on spherical $\text{LiNi}_{0.915}\text{Co}_{0.075}\text{Al}_{0.01}\text{O}_2$ (NCA) cathode materials.^[3,4] 0.2 wt% SiO_2 -coated NCA shows a specific capacity of $181.3 \text{ mA h g}^{-1}$ with a capacity retention of 90.7% after 50 cycles at 1 C. 0.5 wt% $\text{Zr}(\text{OH})_4$ -coated NCA delivers a capacity of $197.6 \text{ mA h g}^{-1}$ at the first cycle and $154.3 \text{ mA h g}^{-1}$ after 100 cycles with a capacity retention of 78.1% at 1 C. Such superior electrochemical performance is mainly ascribed to the surface coating layer of amorphous SiO_2 or $\text{Zr}(\text{OH})_4$, which effectively suppresses side reactions between NCA and electrolytes, decreases the SEI layer resistance, and retards the growth of charge-transfer resistance. All these works on the modification of layered Ni-rich cathode materials will further promote their commercial application in LIBs.

References

- [1] P. Zhou, H. Meng, Z. Zhang, C. Chen, Y. Lu, J. Cao, F. Cheng and J. Chen, *J. Mater. Chem. A*, 6, (2017), 2724-2731.
- [2] H. Meng, P. Zhou, Z. Zhang, Z. Tao and J. Chen, *Ceram. Int.*, 4, (2017), 3885-3892.
- [3] P. Zhou, Z. Zhang, H. Meng, Y. Lu, J. Cao, F. Cheng, Z. Tao and J. Chen, *Nanoscale*, 46, (2016), 19263-19269.
- [4] Z. Zhang, P. Zhou, H. Meng, C. Chen, F. Cheng, Z. Tao and J. Chen, *J. Energy Chem.*, 3, (2017), 481-487.

Figures

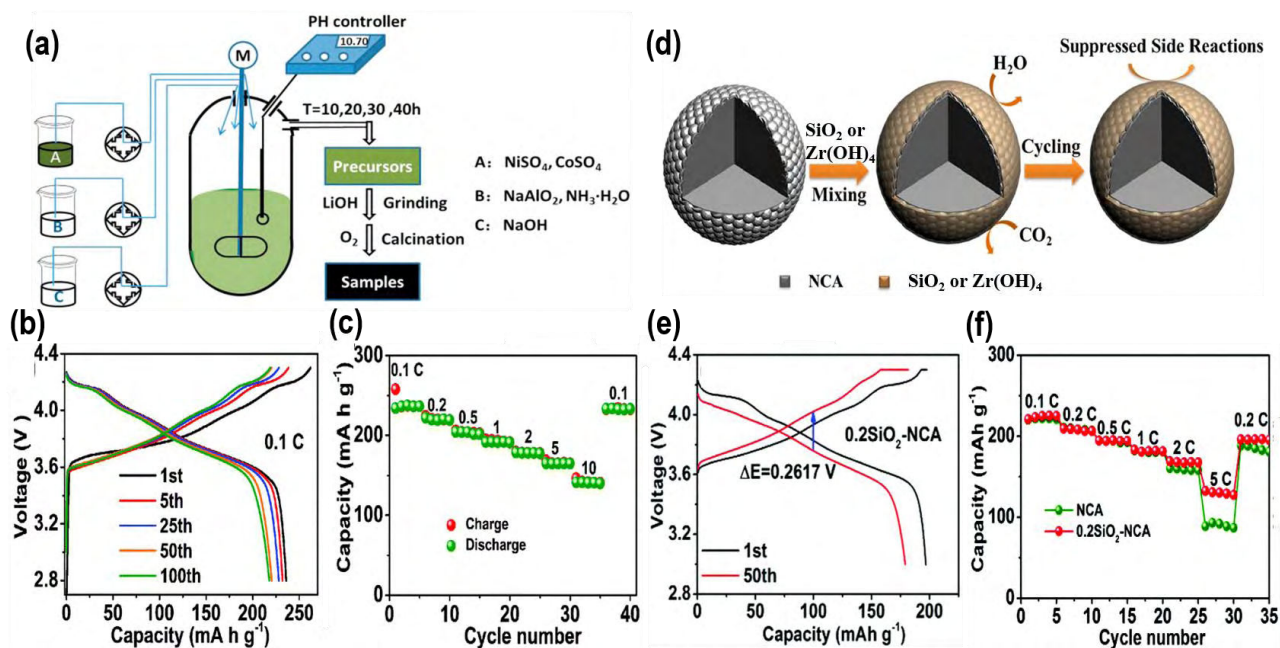


Figure 1: (a) Schematic illustration of the preparation process of spherical $\text{LiNi}_{1-x-y}\text{Co}_x\text{Al}_z\text{O}_2$. (b) Charge and discharge profiles at selected cycles at 0.1 C and (c) rate performance at various rates of the as-prepared $\text{LiNi}_{0.9}\text{Co}_{0.07}\text{Al}_{0.03}\text{O}_2$. (d) Schematic diagram for the effects of SiO_2 or Zr(OH)_4 coating layer on the surface of NCA. (e) Typical charge and discharge profiles of 0.2 wt% SiO_2 -coated NCA and (f) rate capability of pristine NCA and 0.2 wt% SiO_2 -coated NCA.

Keiichiro Ikeda¹

Ryo Nouchi^{1,2}

¹Department of Physics and Electronics, Osaka Prefecture University, Sakai 599-8570, Japan

²PRESTO, Japan Science Technology Agency, Kawaguchi 332-0012, Japan

r-nouchi@pe.osakafu-u.ac.jp

Chemical Modification of Graphene Controlled by Substrate Surface Treatment with Self-Assembled Monolayers

Graphene is a two-dimensional sheet in which carbon atoms are arranged in a honeycomb lattice form. Its ultimate thinness is one of the most prominent features in its structure. Owing to the thinness, it is possible to change its characteristics by chemical adsorption of foreign atoms or molecules. In addition, the ultimate thinness enables us to modulate an electron density in graphene by field-effect gating in a field-effect-transistor configuration. Therefore, it is expected that the surface chemical modification of graphene can be controlled by such gating method. We have demonstrated that the degree of surface chemical modification of graphene is indeed controllable by electron density modulation of graphene [1, 2]. In this study, we investigate on another methodology of field-effect gating, *i.e.*, molecular gating by means of modification of the supporting substrate surface with a self-assembled monolayer (SAM). The local electric field generated by the electric dipoles of the constituent molecules of the SAM [3] is found to control various chemical modification reactions of graphene.

We used two types of triethoxysilane molecules shown in Figure 1, which have antiparallel dipole moments. A SAM of these molecules was formed on a SiO₂ substrate (hereinafter, referred to as (a) F SAM and (b) CH₃ SAM). Graphene flakes were exfoliated on the SAM-treated substrate with adhesive tape. The degree of chemical modification was determined by the *D* band (~1350 cm⁻¹) in a Raman scattering spectrum.

We have performed molecular gate control on various chemical modifications of graphene. Among them, here we show results of photochemical reactions based on benzoyl peroxide (BPO) [4] deposited on graphene. Figure 2 displays Raman scattering spectra after ultraviolet irradiation to the BPO-covered graphene on (a) F SAM and (b) CH₃ SAM treated substrates. Even after the UV irradiation to induce the photochemical reaction, the *D* band is not seen from graphene on F SAM. On the other hand, it is clearly discernible in the spectrum of graphene on CH₃ SAM. The results indicate that the reactivity of graphene towards the photochemical reaction with BPO is higher on the CH₃-SAM treated substrate than on F-SAM treated one. Graphene on the CH₃ SAM should be more electron rich owing to the electrostatic effect (molecular gating effect) from the adjacent positive charge. Thus, graphene becomes more instable than the hole-rich one on the F SAM, leading to the higher reactivity. In the presentation, we will discuss other chemical modifications such as gas-phase photo-oxidation by atmospheric oxygen and liquid-phase modification by aryl diazonium salt.

References

- [1] X. Fan, R. Nouchi and K. Tanigaki: J. Phys. Chem. C **115** (2011) 12960
- [2] N. Mitoma and R. Nouchi: Appl. Phys. Lett. **103** (2013) 201605
- [3] K. Yokota, K. Takai and T. Enoki: Nano Lett. **11** (2011) 3669.
- [4] L. Haitao, R. Sunmin, C Zheyuan, M. L. Steigerwald, C Nuckolls and L. E. Brus: J. Am. Chem. Soc. **131** (2009) 17099.

Figures

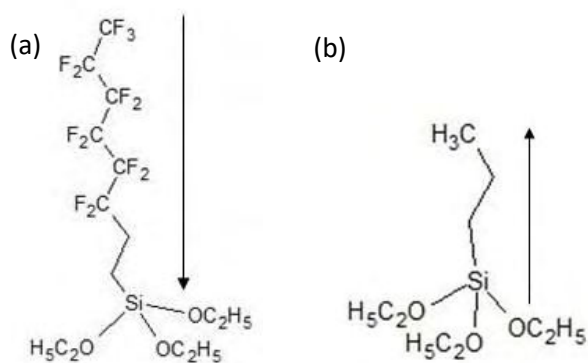


Figure 1: Chemical structure of triethoxysilane molecules used for (a) F-SAM and (b) CH_3 -SAM treatments of the substrate surface. The arrows indicate the direction of the electric dipole moment.

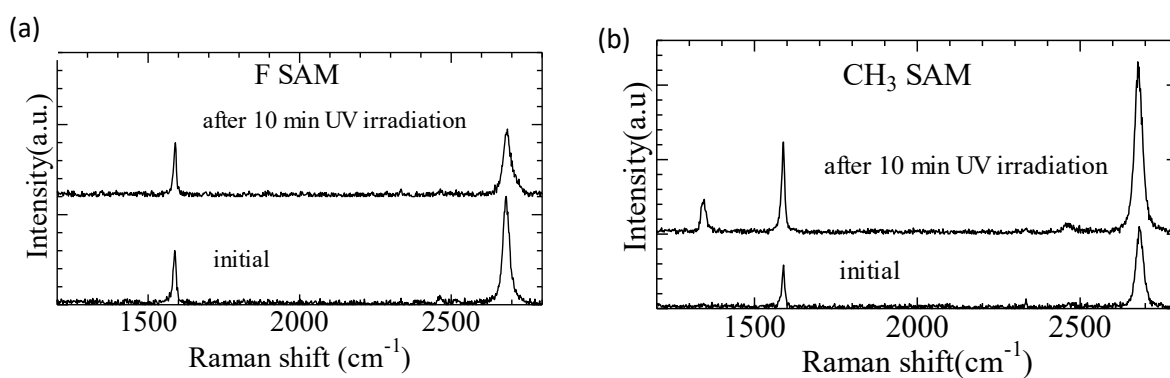


Figure 2: Raman scattering spectra after photo-oxidation of BPO-covered graphene on (a) F-SAM and (b) CH_3 -SAM treated substrates.

Flexible perovskite resistive random access memories employing graphene transparent conductive electrodes

Perovskite resistive random access memories (RRAMs) have received much attention due to their simple structure, high operation speed, low power consumption, and excellent scalability [1,2]. Perovskite materials are recognized as an attractive building block for RRAMs because perovskites exhibit novel dielectric, ferroelectric, semiconducting, and photosensitive functionalities. Recently, a device structure of Au/perovskites/ITO/polyethylene terephthalate (PET) has been shown to be well working as flexible RRAMs [3], but ITO is not suitable for flexible devices. Here, we first report graphene transparent conductive electrode (TCE)-based flexible organic-inorganic perovskite RRAMs. Figure 1(a) shows a typical MAPbI₃ RRAM with graphene TCE on PET. The RRAM shows remarkable bipolar and bistable resistive switching behaviors with an on-off voltage < 1 V. In addition, the RRAM exhibits excellent bending stabilities, maintaining its initial resistive switching behaviors even after 1000 bending cycles at a bending curvature radius of 4 mm, as shown in Figure 1(b). These and other results are discussed based on possible physical mechanisms.

References

- [1] Q. Liu, S. Long, H. Lv, W. Wang, J. Niu, Z. Huo, J. Chen, and M. Liu, ACS Nano, 10 (2010) 6162-6168.
- [2] S. Gao, C. Song, C. Chen, F. Zeng, and F. Pan, J. Phys. Chem. C, 33 (2012) 17955-17959.
- [3] C. Gu and J.-S. Lee, ACS Nano, 10 (2016) 5413-5418.

Figures

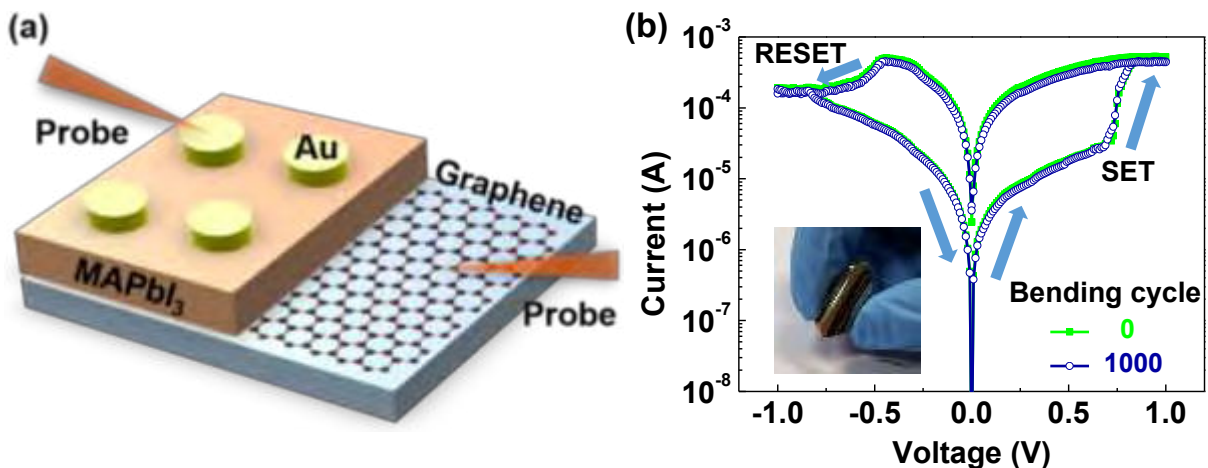


Figure 1: Flexible perovskite RRAM. (a) Schematic diagram of a typical perovskite RRAM with a structure of Au (top electrode)/CH₃NH₃PbI₃ perovskite layer/graphene (bottom electrode)/PET substrate. (b) Resistive switching properties of a typical perovskite RRAM after 1000 bending cycles at bending curvature radius of 4 mm. The inset shows a photograph of a flexible perovskite RRAM.

Kaicheng Jia

Hailin Peng*, Zhongfan Liu*

Peking University & Beijing Graphene Institute, Beijing, China

jiakc-cnc@pku.edu.cn

Copper Containing Carbon Feedstock for Growing High Quality Graphene

Abstract

Chemical vapor deposition (CVD) grown graphene holds great potential in controllable regulation and scalable production, especially for methane gaseous carbon source on Cu substrate. However, it's still unclear about the reaction mechanism of copper and carbon species in the CVD system during high-temperature graphene synthesis. Herein, we choose copper containing carbon feedstock, $\text{Cu}(\text{Ac})_2$, instead of common CH_4 , to change the content of copper in the system and then study the gas-phase reaction kinetics. Meanwhile, additional Cu cluster will catalyze the decomposition of carbon feedstock and graphitization process, giving high-quality graphene film without defects and amorphous carbon by-product. Transmittance is higher than 97.5% at 550 nm and the average sheet resistances are lower than $300 \Omega \text{ sq}^{-1}$, showing improved optical and electrical properties of the graphene grown by $\text{Cu}(\text{Ac})_2$. This work not only opens up new thought for growing high-quality graphene film, but also has reference value and significance for the graphene synthesis mechanism.

References

Li, X; Cai, W.; An, J.; Kim, S.; Nah, J.; Yang, D.; Banerjee, S. K. *Science*, 6 (2011) 1312.

Hao, Y; Bharathi, M. S.; Wang, L; Liu, Y; Chen, H.; Nie, S; Ramanarayan, H. *Science*, 10 (2013) 1243879.

Figures

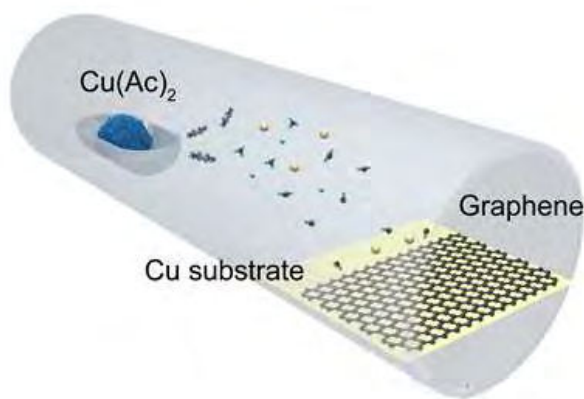


Figure 1: Schematic illustration of the growth of graphene by $\text{Cu}(\text{Ac})_2$

Minwoong Joe¹

Jinhwan Lee¹, and Changgu Lee^{1,2}

¹ School of Mechanical Engineering, Sungkyunkwan University, 2066 Seobu-ro, Jangan-gu, Suwon 440-746, Republic of Korea

² SKKU Advanced Institute of Nanotechnology, Sungkyunkwan University, 2066 Seobu-ro, Jangan-gu, Suwon 440-746, Republic of Korea

mjoe122@gmail.com

Dominant in-plane cleavage direction of CrPS₄ monolayer

In-plane cleavage directions of 2D crystals are displayed and often well-defined in their flakes exfoliated by the widely-used scotch-tape method. Here, we investigate the correlation between dominant in-plane cleavage direction and elastic properties in different directions. CrPS₄ flakes show a preferential in-plane cleavage direction of 67.5°, corresponding to <110> direction. To explain it, we calculated directional dependence of Young's modulus and fracture energy using first-principles density functional theory calculations. We found that fracture energy is directly relevant to the in-plane cleavage direction of CrPS₄. Our study can provide a facile approach to figure out the direction of 2D crystals without complex characterization process, which is valuable for material processing of 2D materials.

References

- [1] Joe, M. et al. A comprehensive study of piezomagnetic response in CrPS₄ monolayer: mechanical, electronic properties and magnetic ordering under strains. *J. Phys. Condens. Matter* 29, (2017) 405801.

Figures

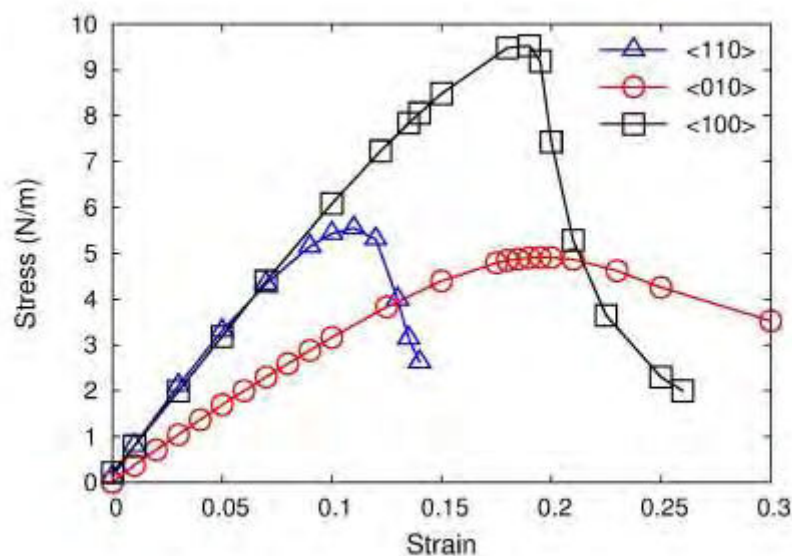


Figure 1: Stress-strain curve of monolayer CrPS₄ under different uniaxial directions.

Gil-Ho Kim

Muhammad Atif Khan and Servin Rathi

School of Electronic and Electrical Engineering and Sungkyunkwan Advanced Institute of Nanotechnology (SAINT), Sungkyunkwan University, Suwon 16419, South Korea

ghkim@skku.edu

Atomically Thin Tunneling Layer for Improved Contact Resistance and Dual Channel Transport in MoS₂/WSe₂ van der Waals Heterostructure

Two-dimensional (2D) material-based heterostructures provide a unique platform where interactions between stacked 2D layers can enhance the electrical and opto-electrical properties as well as give rise to interesting new phenomena. Here, the operation of a van der Waals heterostructure device comprising of vertically stacked bilayer MoS₂ and few layered WSe₂ has been demonstrated in which an atomically thin MoS₂ layer has been employed as a tunneling layer to the underlying WSe₂ layer. In this way, simultaneous contacts to both MoS₂ and WSe₂ 2D layers have been established by forming a direct metal–semiconductor to MoS₂ and a tunneling-based metal–insulator–semiconductor contacts to WSe₂, respectively. The use of MoS₂ as a dielectric tunneling layer results in an improved contact resistance (80 kΩ μm) for WSe₂ contact, which is attributed to reduction in the effective Schottky barrier height and is also confirmed from the temperature-dependent measurement. Furthermore, this unique contact engineering and type-II band alignment between MoS₂ and WSe₂ enables a selective and independent carrier transport across the respective layers. This contact engineered dual channel heterostructure exhibits an excellent gate control and both channel current and carrier types can be modulated by the vertical electric field of the gate electrode, which is also reflected in the on/off ratio of 10⁴ for both electron (MoS₂) and hole (WSe₂) channels.[1] Moreover, the charge transfer at the heterointerface is studied quantitatively from the shift in the threshold voltage of the pristine MoS₂ and the heterostructure device, which agrees with the carrier recombination-induced optical quenching as observed in the Raman spectra of the pristine and heterostructure layers. This observation of dual channel ambipolar transport enabled by the hybrid tunneling contacts and strong interlayer coupling can be utilized for high-performance opto-electrical devices and applications.

References

- [1] Muhammad Atif Khan, Servin Rathi, Changhee Lee, Dongsuk Lim, Yunseob Kim, Sun Jin Yun, Doo-Hyeb Youn, and Gil-Ho Kim, ACS Appl. Mater. Interfaces 10 (2018) 23961–23967

Figures

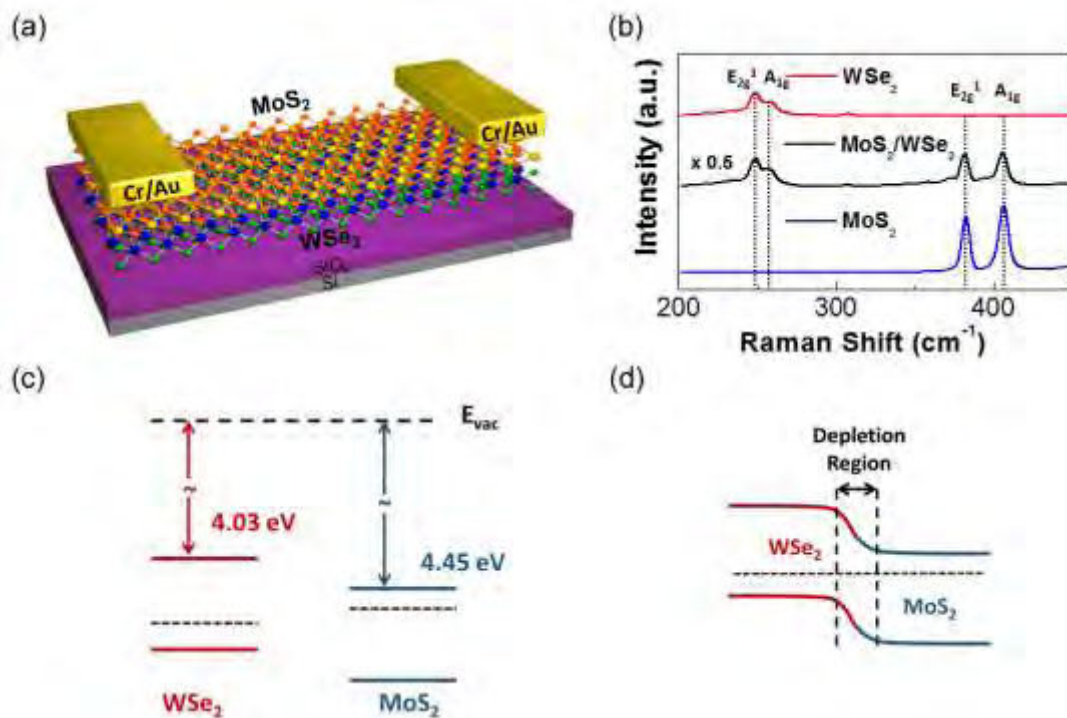


Figure 1: (a). Schematic diagram of dual channel MoS₂-WSe₂ heterostructure FET (b). Raman spectra of MoS₂, WSe₂ and overlapped MoS₂/WSe₂ region (the intensity of overlapped region is reduced by a factor of 0.5) (c) Band diagram showing band structure of pristine MoS₂ and WSe₂ before transfer (d) Band diagram of MoS₂/WSe₂ heterostructure illustrating the formation of depletion region.

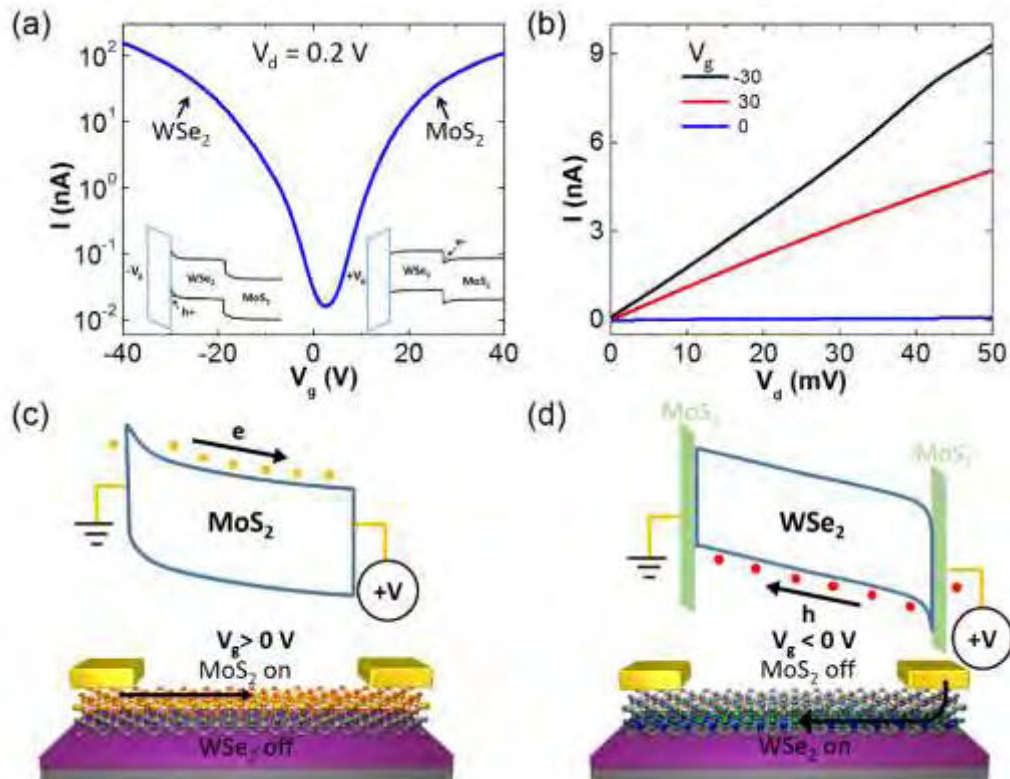


Figure 2: (a). Transfer characteristics curve of dual channel FET at $V_d = 0.2$ V in semi-logarithmic scale (b). Output characteristics curve of dual channel FET at different back gate voltages (c). Schematic band diagram and device schematic illustrating the band structure and current flow for positive V_g (d). Schematic band diagram and device schematic illustrating the band structure and current flow for positive V_g .

Ju Hwan Kim

Dong Hwan Jung, Jong Min Kim, Sung Kim, Suk-Ho Choi

Department of Applied Physics and institute of Natural Sciences, Kyung Hee University, Yongin 17104, Korea

sukho@Khu.ac.kr

Multilayer graphene/conducting polymer/Si nanowires/Si/TiO_x hybrid solar cells

Over the past decade, many researchers have focused on organic materials/Si hybrid solar cells (HSCs) to reduce the production cost of Si-based solar cells [1,2], but several problems such as big reflective index of Si, low aperture ratio of the mesa-type metal transparent conductive electrodes (TCEs), and large recombination loss at Si rear contact should be solved for the practical applications. Especially, poly(3,4-ethylenedioxythiophene): poly(styrenesulfonate) (PEDOT:PSS), a conducting polymer, is not only an antireflective layer for HSCs but also a hole transporting/optical window that serves as a passivation layer [3]. As one approach for further increase of the power conversion efficiency (PCE), it is necessary to find a method of enhancing the light absorption of Si, for example, by lowering the refractive index. Si-based nanostructures such as Si nanowires (NWs) and porous Si are useful for reducing the reflectivity, resulting in higher light absorption than bulk Si [4]. Here, we report a HSC structure of multi-layer graphene (MLG) TCE/PEDOT:PSS/Si NWs/n-Si/TiO_x (back surface passivation layer) to cope with aforementioned problems. Resulting maximum PCE is 12.10 %, much larger than that of the planar-Si-type HSC (10.11 %) as a control sample, mainly due to the lowered reflectance (increased absorption) and recombination loss. As the active area increases from 14 to 50 mm², the PCE decreases by only 2.5 % from 12.10 to 9.60 %, possibly resulting from the area-dependent change in the uniformity of the Si NWs. The PCE shows only a 10% decrease for 30 days under 25 °C temperature and 40% humidity.

References

- [1] J. He, P. Gao, Z. Yang, J. Yu, W. Yu, Y. Zhang, J. Sheng, J. Ye, J. C. Amine, and Y. Cui, *Adv. Mater.* 29 (2017) 1606321.
- [2] R. Liu, J. Wang, T. Sun, M. Wang, C. Wu, H. Zou, T. Song, T. X. Zhang, S.-T. Lee, Z. L. Wang, and B. Sun, *Nano Lett.* 17 (2017) 4240-4247.
- [3] L. He, C. Jiang, H. Wang, D. Lai, and Rusli, *ACS Appl. Mater. Interfaces* 4 (2012) 1704-1708.
- [4] G. Fan, H. Zhu, K. Wang, J. Wei, X. Li, Q. Shu, N. Guo, and D. Wu, *ACS Appl. Mater. Interfaces* 3 (2011) 721-725.

Figures

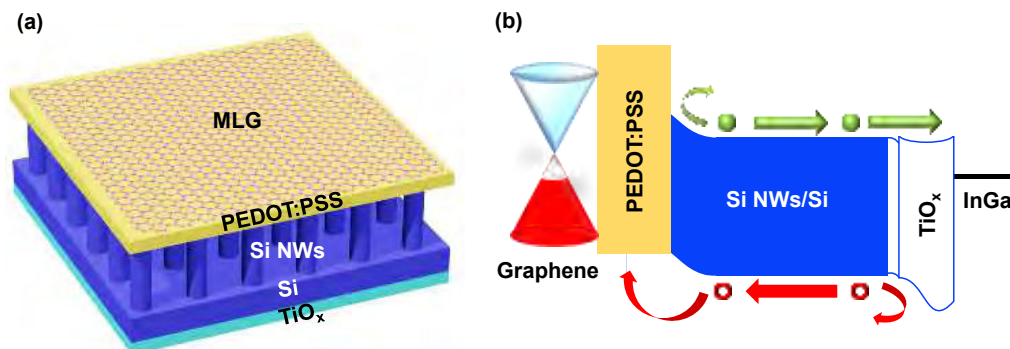


Figure 1: (a) Schematic and (b) energy band diagram of a typical MLG/PEDOT:PSS/Si NWs/n-Si/TiO_x HSC.

Wenjiang Li

Hui Liang¹, Shuang Zhou¹, Rony Snyders^{1,2}, Stephan Werner³, Catharina Haebel³, Peter Guttman³, Wenjiang Li^{1*}, Carla Bittencourt²

¹Key Laboratory of Display Materials & Photoelectric Devices, School of Materials Science and Engineering, Tianjin University of Technology, Tianjin 300384, PR China.

²Chimie des Interactions Plasma Surface, CIRMAP, University of Mons, Mons, Belgium.

³Research group X-ray microscopy, Helmholtz-Zentrum Berlin für Materialien und Energie GmbH, Berlin, Germany.

liwj@tjut.edu.cn

Nanoscale NEXAFS for Probing multi-layer graphene/copper nanowires composite

Fabrication of conductive patterns on flexible substrates is a key step for the engineering of next generation of novel flexible devices. In this context, silver based inks have been the preferred one. ^[1] However, the high cost and electromigration effect in silver limit its applications. An attractive alternative is the use of copper nanoparticles provided that their oxidation can be avoided. ^[2] In this work we report on the synthesis of a graphene /copper nanowires composite based on a scaled up amine-capped and glucose-based reduction method. Graphene oxide and CuCl₂·2H₂O (the precursor), glucose (the reductant), hexadecylamine (HAD) (the capping agent), water (the solvent) were mixed and the final solution was magnetically stirred. The graphene /copper nanowires composite was collected by centrifuging the reaction solution and rinsing with deionized water.

We discuss the potential of graphene as anti-oxidation barrier to avoid an excess of oxidation of the copper nanowires. ^[3] Transmission electron microscopy showed the good dispersion of the metal nanowires on the surface of graphene flakes. X-ray photoelectron spectroscopy was used to evaluate the interaction between the graphene flakes and the copper nanowires. To understand the oxidation and electronic structure of the synthesized copper hybrid, we have recorded linear polarized NEXAFS with the transmission x-ray microscope installed at the new U41-XM beamline of the BESSY II synchrotron, Berlin. ^[4,5] The spectra were normalized using the signal intensity in the proximity of the sample to correct for intensity variations with the photon energy. We observed that the oxidation of the copper nanowires is smaller when graphene is added to the synthesis.

References

- [1] Yang W, Wang C, Journal of Materials Chemistry C, 4 (2016) 7193.
- [2] Kim W J, Lee T J, Han S H, Carbon, 69(2014) 55-65.
- [3] Scardamaglia M, Susi T, Struzzi C, et al., Scientific Reports, 7 (2017) 7960.
- [4] Peter G, Carla B, Beilstein J Nanotechnol, 6 (2015) 595-604.
- [5] Peter G, Stephan W, Stefan R, Catharina H, Gerd S M, Microanal. 24 (2018) 202-203.

Figures

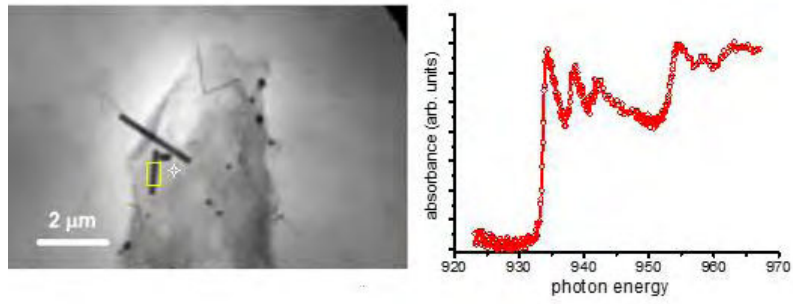


Figure 1: X-ray image at 950 eV photon energy from an image stack recorded on the graphene/copper nanowires composite at the U41 beamline by using the TXM. The NEXAFS-TXM Cu L-edge spectrum was recorded in the area delimited by the rectangle. The spot indicates the point at which the IO was recorded

Integrated paper-based stretchable LIBs

With the development of technologies, the people's comfort level and experience degree of electronics are improving. As one developing direction of electronics is flexible and wearable, it puts forward a new request for energy storage devices.[1] Making energy storage devices flexible and integrating it with flexible electronics can lead a maximally comfort level and experience degree of electronics for people. Currently, the energy storage devices for electronics are lithium ion batteries, as lithium ion batteries owns a series of advantages compared with other energy storage devices. It has a much higher energy density compared with supercapacitors and Na-ion batteries, and it has a much more wonderful cycling stability compared with lithium-sulfur batteries. So the flexible energy storage devices for flexible electronics are mostly based on lithium ion batteries. As traditional lithium ion batteries has no flexible features, lithium ion battery products with excellent flexibility are urgently needed in the market.[2]

In recent years, scientists has achieved much progress in this field. Paper-based, film-like, fiber-like, textile-like and some new structure flexible LIBs have been prepared to achieve excellent stability of LIBs. In these methods, paper-based flexible batteries have advantages like processing easy, low cost and high energy density.[3] For application, the most important flexible form is stretchable. So, based on paper-based flexible LIBs, to realize the stretchability of battery is very important. Kirigami has been confirmed a good method to prepare stretchable LIBs.[4] However, as we known, the inner structure of traditional LIBs may be destroyed when shape change of battery occurs under outside forces.[5] This will cause mismatch of each layer in battery and finally cause deterioration of electrochemical performance and safety problem.[6] The destroy of inner structure of flexible LIBs (especially for kirigami stretchable LIBs) will be more serious as flexible LIBs are working under dynamic environment. So, the stability and safety problem of kirigami stretchable LIBs will be a serious challenge for application. Based on these, we used a simple method to prepare kirigami stretchable LIBs with integrated structure. The alignment quality of each layer is well controlled when stretched and mismatch of the correlated multiple layers when stretched is avoided in this structure.

References

- [1] Zhang, Y.; Zhao, J.; Ren, J.; Weng, W.; Peng, H., *Adv. Mater.*, 28, (2016), 4524-4531.
- [2] Liu, W.; Song, M.; Kong, B.; Cui, Y., *Adv. Mater.*, DOI: 10.1002/adma.201603436.
- [3] Hu, L.; Wu, H.; Mantia, F.; Yang, Y.; Cui, Y., *Acs nano*, 10, (2010), 5843-5848.
- [4] Song, Z.; Wang, X.; Lv, C.; An, Y.; Liang, M.; Ma, T.; He, D.; Zheng, Y.; Huang, S.; Yu, H.; Jiang, H., *Sci. Rep.* | DOI: 10.1038/srep10988.
- [5] Cai, W.; Wang, H.; Maleki, H.; Howard, J.; Curzion, E., *J. Power Sources* 196 (2011) 7779 – 7783
- [6] Zou, B.; Hu, Q.; Qu, D.; Yu, R.; Zhou, Y.; Tang, Z.; Chen, C., *J. Mater. Chem. A*, 2016, 4, 4117 – 4124.

Figures

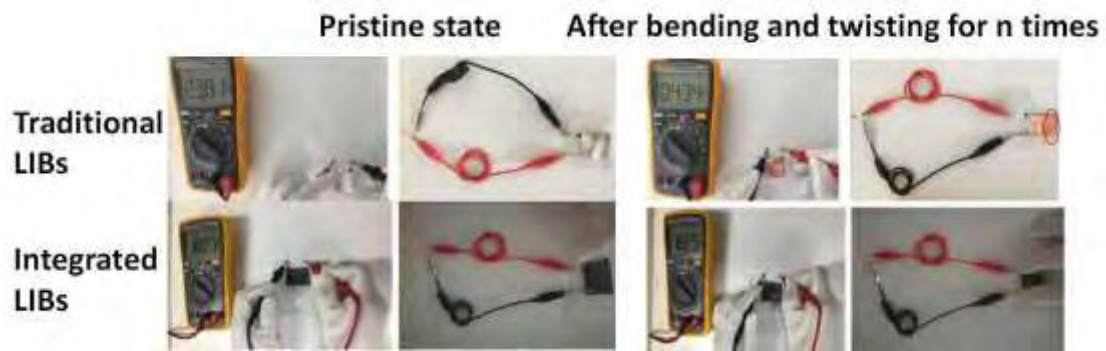


Figure 1: Mismatch of the correlated multiple layers between integrated structure and traditional structure

Oxygen-assisted Growth of Highly Conductive Graphene with Controllable Domain Size on Glass

Abstract

The integration of graphene with glass has broad practical applications, such as smart windows and transparent heating glass, which could benefit people's daily life. Direct growth of graphene over glass is efficient and scalable way to fabricate graphene glass hybrid materials as it avoids the tedious transfer process that involved introduction of defects and contaminations into graphene film. However, the grain boundaries dominant the electrical conductivity of the poly-crystalline graphene films when the grain size is smaller than 800nm. [1] By introducing oxygen into the CVD system, the graphene films directly synthesized on glass with different domain size can be obtained, which performs different electrical properties. In particular, the domain size of graphene can be designed to in the range of 100nm to 800 nm in terms of controlling the amount of oxygen in the gas phase, and the corresponding sheet resistance of the fabricated graphene glass is in the range of 6.1k Ω /sq to 0.9k Ω /sq at the same transmittance of 90%. This method is a simple and effective way to enhance the electrical conductivity of graphene glass, and promote the development of its application in electronic devices.

References

- [1] Ma, T.; Liu, Z. B.; Wen, J. X.; Gao, Y.; Ren, X. B. A.; Chen, H. J.; Jin, C. H.; Ma, X. L.; Xu, N. S.; Cheng, H. M.; Ren, W. C. Nature Communications, (2017) 8, 9.

Figures

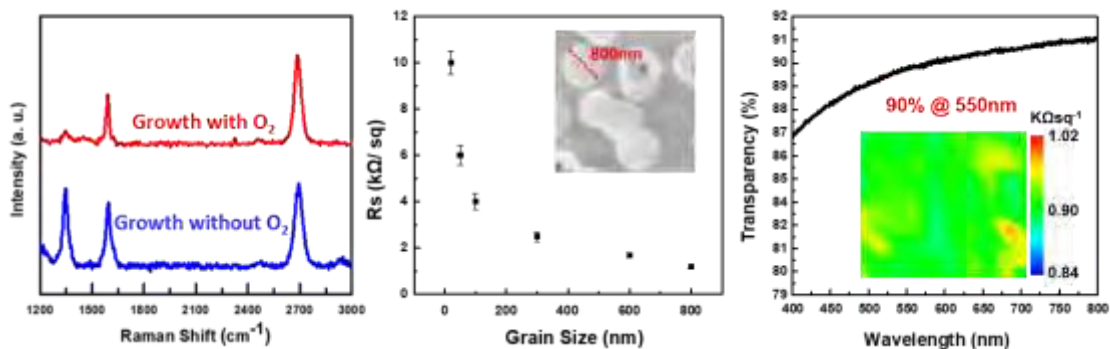


Figure 1: Oxygen-assisted Growth of Graphene with Controllable Domain Size on Glass

Fangming Liu

Zhenhua Yan, Fangyi Cheng* and Jun Chen

Key Laboratory of Advanced Energy Materials Chemistry (Ministry of Education), College of Chemistry, Nankai University, Tianjin 300071, China.

fycheng@nankai.edu.cn

Anions inserted into graphite interlayers enhancing the electrodeposited metal hydroxides for oxygen evolution

Electrochemical deposition is an easy-controlled method to prepare thin films of functional and energy materials. As for energy storage and conversion applications, freestanding films electrodeposited on varied conducting substrates are more competent than their conventional counterparts relied on binder and conducting additives. However, the weak deposit-substrate interaction makes it tough to achieve robust and high-mass deposition especially on flat substrates, which hinders their practical application. Here we report a universal strategy with interface enhancement via insertion and reduction of oxyacid anions to electrosynthesize a variety of metal hydroxides/oxides. Specifically, nitrate ions intercalate into the graphene layers of a graphite substrate driven by electric field, and then are reduced by cathodic current to form hydroxyls, which in-situ precipitate the metal cations from the electrolyte. Thus, the nanocrystalline cerium dioxide and amorphous nickel hydroxide co-electrodeposited on graphite feature a rather tight interface and considerable mass loading after elaborate manipulation. When employed as electrocatalyst for oxygen evolution reaction in alkaline electrolyte, it exhibits a low overpotential of 177 mV@10 mA cm⁻² and sustains long-term durability over 300 h at a large current density of 1000 mA cm⁻², surpassing the state-of-the-art RuO₂ benchmark. The superior electrocatalytic performance of the interface-enhanced self-supporting metal hydroxide/oxide composite indicates promising generalization of this efficient technique to fabricate practical robust and high-activity water splitting electrodes based on low-cost graphite substrates.

References

- [1] Yan, Z.; Sun, H.; Chen, X.; Liu, H.; Zhao, Y.; Li, H.; Xie, W.; Cheng, F.; Chen, J. *Nat. Commun.* 2018, 9, 2373.

Figures

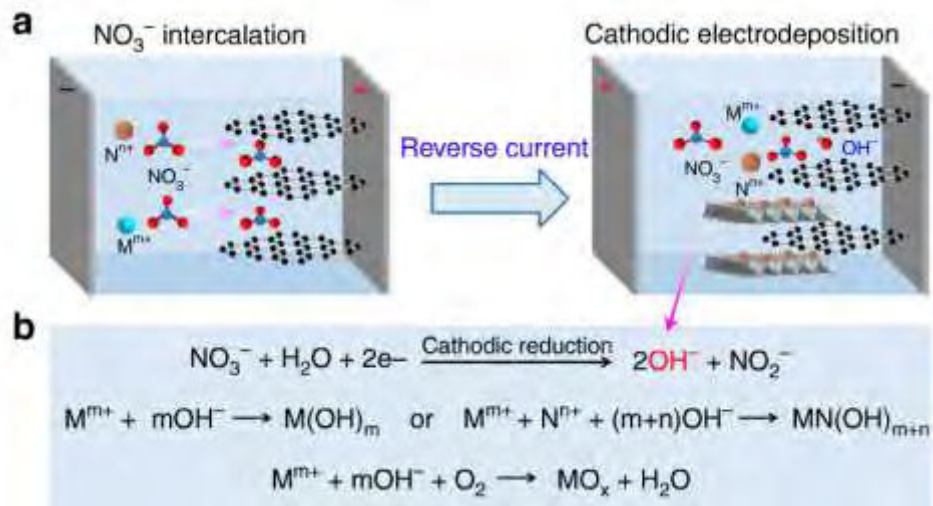


Figure 1: (a) schematic two-step synthesis using graphite substrate and nitrate precursors. (b) the reaction mechanisms of the cathodic electrodeposition of metal hydroxides ($\text{M}(\text{OH})_m$ or $\text{MN}(\text{OH})_{m+n}$), and oxides (MO_x). M^{m+} and N^{n+} are metal cations.

Jiaman Liu

Jiaman Liu, Liwei Yu, Xingke Cai, Zhengyang Cai, Qiangmin Yu, Lei Tang, Azhar Mahmood, Usman Khan, Jingyu Xi, Bilu Liu, and Feiyu Kang
Tsinghua-Berkeley Shenzhen Institute, University Town, Shenzhen, China

liujm15@mails.tsinghua.edu.cn

Synthesis of wafer-scale single-layer h-BN and its use in proton transport membrane

Proton exchange membranes (PEMs), as semi-permeable membranes, are designed to transport protons while impede other species in hydrogen-based technologies such as redox flow battery [1]. Currently, commercialized PEMs like Dupont's Nafion is largely recognized for its excellent proton conductivity, chemical stability and mechanical strength [2]. However, it generally suffers from relatively poor selectivity, leading to ion crossover issue. This can severely deteriorate the overall performance of electrochemical devices. Recent research on proton conductivity and isotope separation through two-dimensional (2D) atomic crystals in several proof-of-concept works show the great potential of these materials, especially graphene and hexagonal boron nitride (h-BN) [3, 4]. Integration of two-dimensional (2D) hexagonal boron nitride (h-BN) onto commercialized proton exchange membranes (PEMs) can maintain proton conductivity while improve ion selectivity simultaneously, a longstanding issue in separation membrane. However, until now, a cost-effective method for centimeter-scale single-layer h-BN thin film fabrication as well as an efficient method for wafer-scale transfer is still lacking. Here, we use a space-confined approach and Nafion-supporting-Functional Layer-assisted (Nafion-sFLa) transfer method to overcome this roadblock, demonstrating the potency of scale-up as PEMs. Around two inch large single-layer h-BN thin film has been synthesized with high uniformity (Raman peak positions at $\sim 1370\text{ cm}^{-1}$) and quality (full width at half maximum of $\sim 16\text{ cm}^{-1}$). With a transfer efficiency as high as 75%, the h-BN functionalized membrane has shown ion selectivity three times higher than that of pristine membrane, reaching more than $30 \times 10^4\text{ S min cm}^{-3}$. In vanadium flow battery (VFB), the resistance to proton transport of the sandwich membrane is not affected by the h-BN but the barrier properties of h-BN inhibit vanadium crossover at low current density ($< 100\text{ mA cm}^{-2}$), resulting in significantly improved coulombic efficiency and energy efficiency, being $\sim 95\%$ and $\sim 92\%$, respectively. Such Nafion/h-BN/SPEEK sandwich structure may be promising for future 2D materials-based membrane in separation technology.

References

- [1] Ding, C.; Zhang, H.; Li, X.; Xing, F., *J Phys Chem Lett*, 4, (2013), 1281-94.
- [2] Mai, Z.; Zhang, H.; Li, X.; Xiao, S.; Zhang, H., *Journal of Power Sources*, 196, (2011), 5737-5741.
- [3] Hu, S.; Lozada-Hidalgo, M.; Wang, F. C.; Mischchenko, A.; Schedin, F.; Nair, R. R.; Hill, E. W.; Boukhvalov, D. W.; Katsnelson, M. I.; Dryfe, R. A.; Grigorieva, I. V.; Wu, H. A.; Geim, A. K., *Nature*, 516, (2014), 227-30.
- [4] Lozada-Hidalgo, M.; Hu, S.; Marshall, O.; Mishchenko, A.; Grigorenko, A. N.; Dryfe, R. A.; Radha, B.; Grigorieva, I. V.; Geim, A. K., *Science*, 351, (2016), 68-70.

Figures

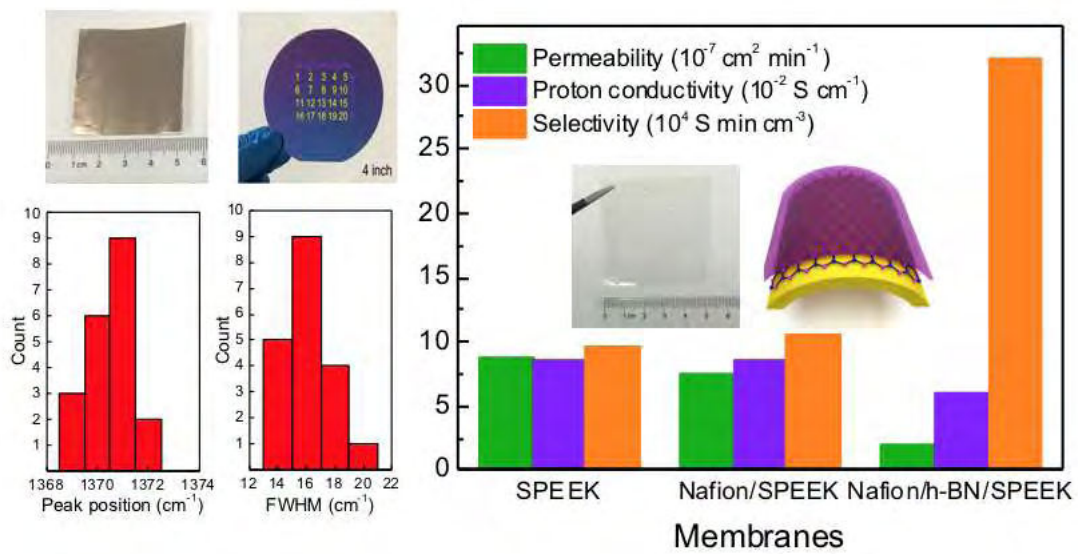


Figure 1: CVD growth of large-area h-BN and its ion transport properties in all vanadium flow battery

Mingqiang Liu

Mingqiang Liu, Yi Hou, Simin Feng, Changjiu Teng, Lei Tang, Jiaman Liu, Jie Ren,

Bilu Liu*

Shenzhen Geim Graphene Center, Tsinghua-Berkeley Shenzhen Institute, Tsinghua University,
518055, Shenzhen, P. R. China

E-mail: bilu.liu@sz.tsinghua.edu.cn

Controlled growth and doping of black phosphorus with tunable properties

Black phosphorus (BP) is a candidate 2D material in optoelectronics owing to its excellent electronic properties and a tunable bandgap in mid-far infrared region. Doping has been a reliable way to tune bandgap and improve the properties of BP. However, a uniform and large amount of doping into BP lattice remains a challenge. Here, a facile approach using CVT reaction furnace under uniform temperature gradient have been applied to synthesize centimeter-sized, high-quality BP crystals. Compared with tradition gradient temperature furnace, much larger crystal yield are obtained (more than 90%) using this new approach. Uniform and controllable doping of various elements are also achieved with the same method. It should be noted that some elements (such as Sb, Bi, Se and Te) that are normally difficult to doped into BP are successfully obtained here and the doping level is the highest reported so far. In addition, to understand the growth mechanism, control experiments have been carried out by tuning various synthesis conditions. Structural and optical characterization show that the synthesized pristine and doped BP crystals exhibit high crystalline quality. Furthermore, our synthetic approach enables uniform doping in the lattice of BP crystals, which is evidenced by the XRD, TEM and Raman spectroscopy. Furthermore, the atomic doping can significantly improve the stability of BP in air, which lays a foundation for the large-scale development of BP in the field of optoelectronic devices. High tunability of bandgap and work function via controlling doping type and concentration provides a large variety of choices in real applications.

References

- [1] Xia, F., Wang, H., Xiao, D., Dubey, M., & Ramasubramaniam, A. *Nature Photonics*, 8, (2014), 899-907.
- [2] Li, L., Yu, Y., Ye, G. J., Ge, Q., Ou, X., & Wu, H., et al. *Nature Nanotechnology*, 9, (2014), 372-7.
- [3] Bilu Liu , Marianne Köpf , Ahmad N. Abbas , Xiaomu Wang , Qiushi Guo, et al. *Advanced Materials*, 27, (2015), 4423-4429.
- [4] Long M, Gao A, Wang P, et al. *Science Advances*, 3, (2017), e1700589.
- [5] Yang B, Wan B, Zhou Q, et al. *Advanced Materials*, 28, (2016), 9408-9415.

Figures

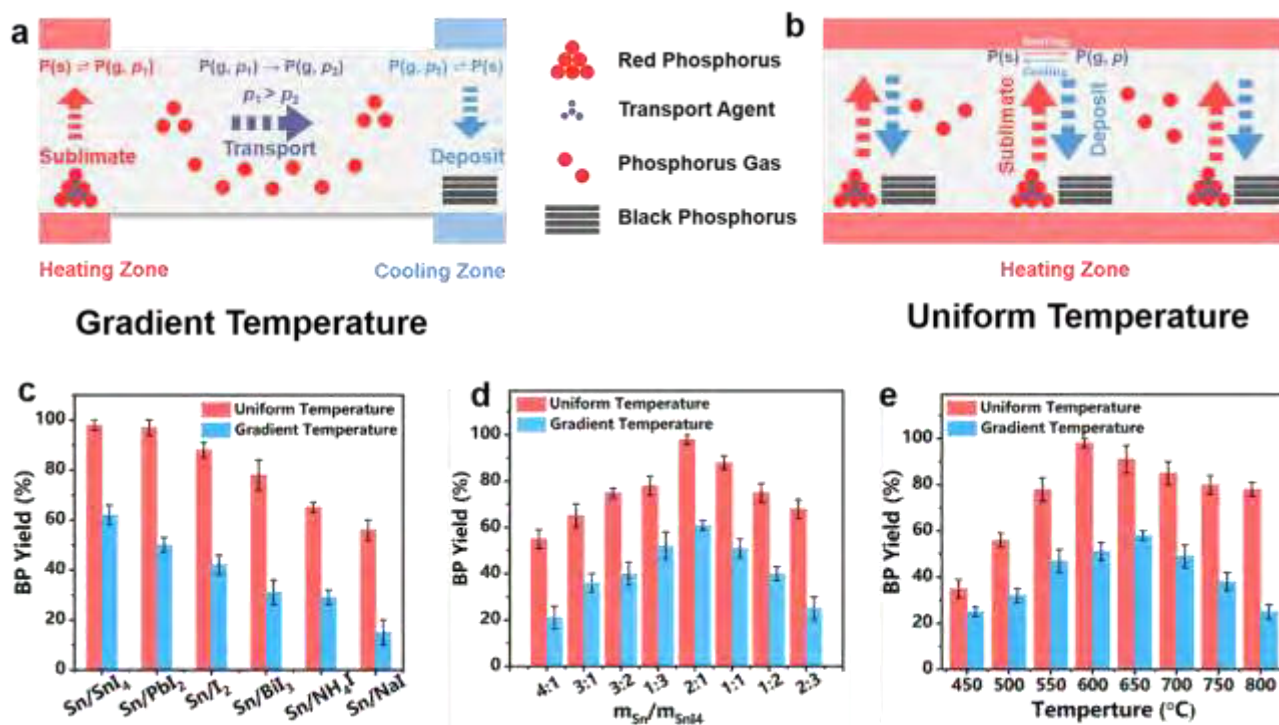


Figure 1. Experimental setup of BP crystal growth with both uniform and gradient temperature furnace and the comparison of BP yield with various growth conditions.

Yang Liu

Yang Liu, Shibin Yin, Pei Kang Shen*

Collaborative Innovation Center of Renewable Energy Materials, Guangxi University, Nanning, China

Contact@liugedayang@foxmail.com

Asymmetric 3d Electronic Structure for Enhanced Oxygen Evolution Catalysis

Abstract

With the deterioration of the environment, human concern with clean energy has increased considerably. Hydrogen is a relatively cleaner energy, and hence has a wide range of applications in various fields. Hydrogen can be obtained through many ways, such as electrolysis of water, photo-catalytic water splitting, etc. The process of water splitting involves the production of hydrogen and oxygen, where the evolution of these gases is interventional.¹ The theoretical voltage of hydrogen and oxygen evolution from water splitting are 0 and 1.23 V, respectively.² The Pt/C and IrO₂ catalysts have been reported as the best hydrogen and oxygen evolution catalysts with overpotentials of 0 and 270 mV, respectively.^{3,4} Obviously, the oxygen evolution reaction (OER) is the biggest obstacle in water splitting. The oxygen evolution reaction (OER) is a four electron transfer process in acid or alkaline medium, where OH⁻ loses electrons to become O₂. Owing to the fact that the transition metals (such as Fe, Co, Ni, etc.) possess unpaired d orbital electrons, they can be used to open the O-H bond. But due to high degree of localization and overspreading of the d orbital, intermediate products (such as O_{ad}, OOH_{ad}) and OH_{ad}, OOH_{ad} could be resulted, which would be difficult to be desorbed and dissociated, respectively. In this work, FeS, Ni₃S₂, Fe₅Ni₄S₈, and N, O, S-doped meshy carbon base were successfully synthesized. The sample containing Fe₅Ni₄S₈ exhibited excellent OER performance. The density functional theory calculations indicate that the partial density of states for 3d electrons (3d-PDOS) of Fe and Ni atoms are changed from monometallic sulfide to bimetallic sulfide at the sulfur vacancy. The asymmetric 3d electronic structure optimizes the 3d-PDOS of Fe and Ni atoms, and leads to an enhanced OER activity. This work provides a new strategy to prepare a low-cost electrocatalyst for oxygen evolution with high-efficiency.

References

- [1] Kanan, M. W.; Nocera, D. G., *Science*, 321 (2008) 1072–1075.
- [2] Zeng, K.; Zhang, D., *Prog. Energy Combust. Sci.*, 36 (2010) 307–326.
- [3] Long, X.; Wang, Z.; Xiao, S.; An, Y.; Yang, S., *Mater. Today*, 19 (2016) 213–226.
- [4] Yu, X.; Zhang, S.; Li, C.; Zhu, C.; Chen, Y.; Gao, P.; Qi, L.; Zhang, X., *Nanoscale*, 8 (2016) 10902–10907.

Acknowledgment

This work was supported by the Guangxi Science and Technology Prject (AA17204083, AB16380030).

Figures

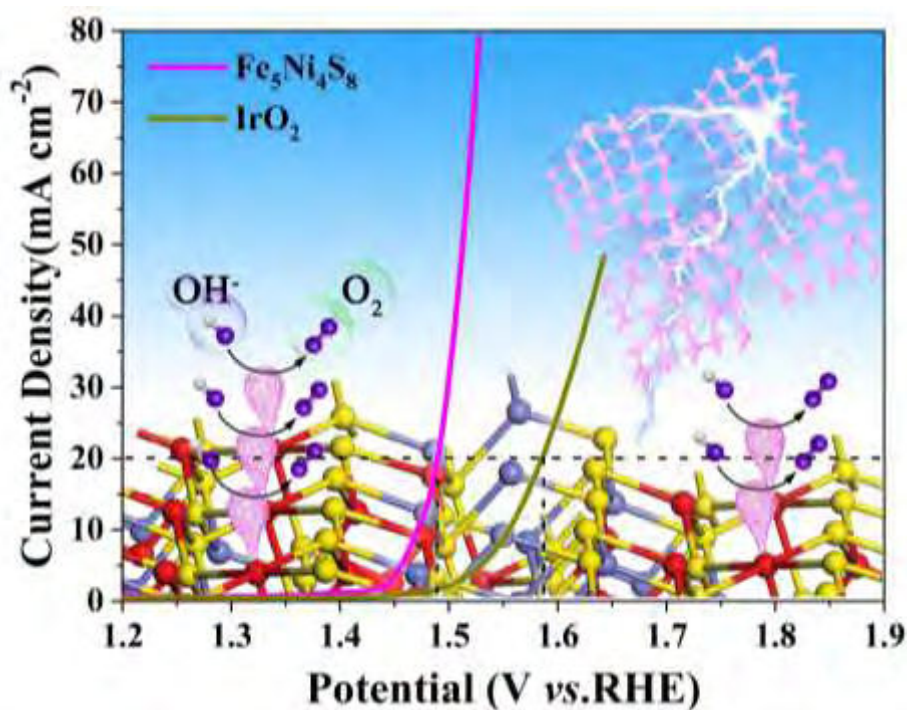


Figure 1: The cover of this paper.

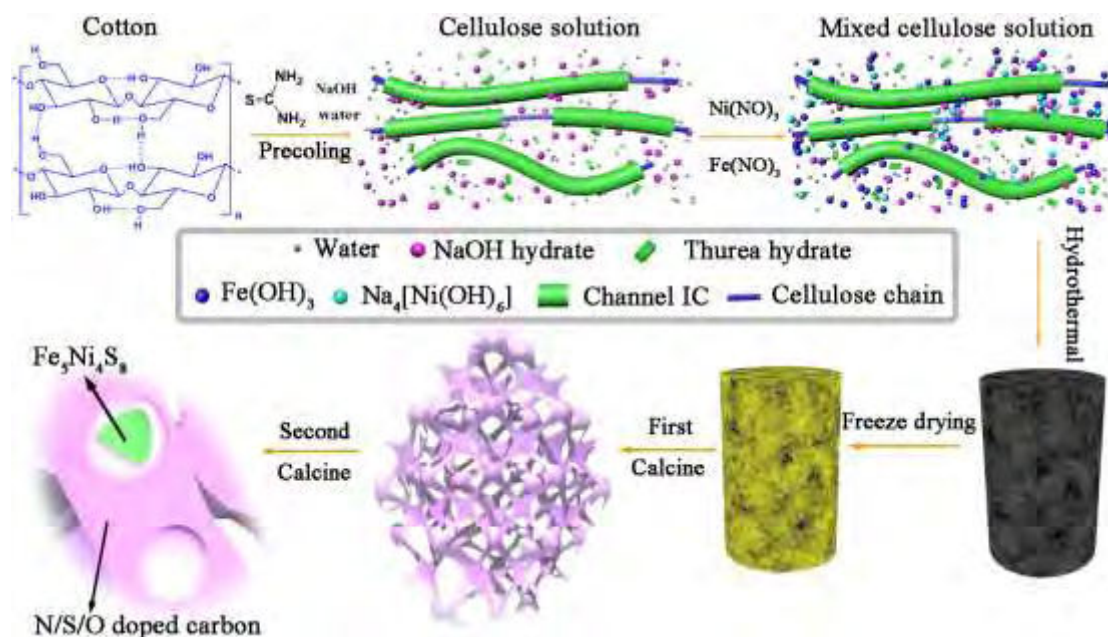


Figure 2. Synthesis procedures for meshy carbon materials loaded by carbon-encapsulated Fe₅Ni₄S₈ nanoparticle.

Tomoaki Oba

Takamasa Kawanago, Shunri Oda

QNERC and Dept. of EE., Tokyo Institute of Technology, 2-12-1-S9-12, Ookayama, Meguro-ku, 152-8550, Tokyo, Japan

oba.t.ae@m.titech.ac.jp

Gated Four-Probe Method for Evaluation of Electrical Characteristics in MoS₂ Field-Effect Transistors

Layered semiconductor of transition metal dichalcogenides (TMDC) has been considerable attention because of their various properties [1]. New classes of semiconductor materials motivate an investigation of carrier mobility and contact resistance in field-effect transistor configuration from the view point of both scientific interests and practical applications. This study describes the gated four-probe method to evaluate the relation between interfacial properties and channel mobility in MoS₂ FETs [2, 3].

Heavily-doped p⁺-type Si wafer was subjected to SPM and 1% HF cleaning. Thermal SiO₂ was grown by dry oxidation at 1000 °C for 5 min. Subsequently, Al₂O₃ was deposited by ALD (TMA, H₂O, 300 °C) on SiO₂. Au (40 nm)/Ti (10 nm) was deposited by thermal evaporation and lift-off for source/drain contact and two potential probes. After removal of back side SiO₂ with BHF, Au (30 nm) / Ti (10 nm) for back gate contact was deposited on the back side of the substrate by thermal evaporation. Next, the substrate was subjected to oxygen plasma to form hydroxyl groups on the surface of Al₂O₃. Then, the substrate was immersed into 2-propanol containing 5 mM n-octadecylphosphonic acid (ODPA) for 4 hours at room temperature [4]. Annealing was conducted at 100 °C in N₂ for 30 min to stabilize ODPA. The gate dielectric consists of hybrid ODPA/Al₂O₃/SiO₂. Mechanically exfoliated MoS₂ were transferred to the substrate with the PDMS elastomer. Finally, devices were annealed in N₂ at 150 °C for 30 min to improve source/drain contact. The fabrication process and device structure are summarized in Fig. 1. Fig.2 shows microscope image of fabricated FET.

The channel mobility were evaluated with four-probe method based on the equations, as shown in Fig. 3. Fig. 4 shows the representative I_d-V_d characteristics of MoS₂ FET with gated four-probe method. The FET operation was observed with this four-probe configuration. Fig. 5 shows the representative I_d-V_g characteristics of MoS₂ FET without SAM. Hysteresis in clockwise direction was observed. On the other hand, formation of SAM can suppress the hysteresis in I_d-V_g characteristics as shown in Fig. 6. The channel potential was estimated during I_d-V_g measurement using internal two probes between source and drain contact. Fig. 7 shows the C-V characteristics of Si MOSCAP for SiO₂ and Al₂O₃/SiO₂ gate dielectric. The physical thickness of SiO₂ was 15.7 nm. The physical thickness of Al₂O₃ corresponds 14 nm when the dielectric constant of Al₂O₃ was assumed to be 8.5. Also, the physical thickness and dielectric constant of ODPA are 2.1 nm and 2.5 [4]. Consequently, the overall capacitance of ODPA/Al₂O₃/SiO₂ is 0.13 μm/cm². Fig. 8 shows V_g dependence of four-probe conductivity (σ). The channel mobility (μ_{4w}) was evaluated from the σ using the equation as shown in Fig. 3. The μ_{4w} with SAM is improved as high as 28 cm²/Vs, while the μ_{4w} without SAM shows 19.7 cm²/Vs. The interfacial properties is responsible for the channel mobility of MoS₂ FET

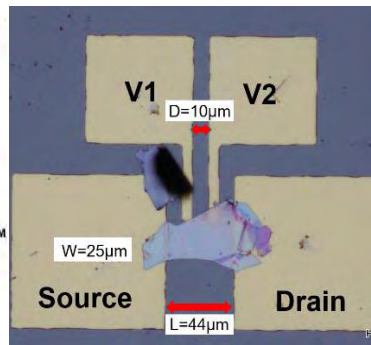
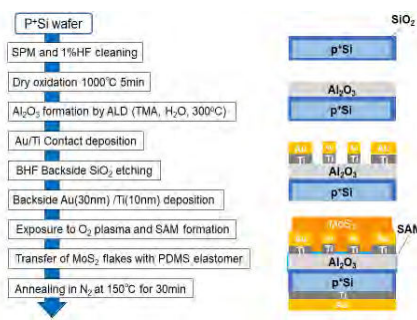
Acknowledgments

The authors would like to thank Prof. Y. Kawano, Prof. K. Kakushima, Prof. H. Wakabayashi, and Prof. K. Tsutsui of Tokyo Institute of Technology for their continuous support in the experiments. This study was supported by JST-CREST (Grant No. JPMJCR16F4), JSPS Grant-in-Aid for Young Scientists (B) (Grant No. 17K14662) and Yazaki Memorial Foundation for Science and Technology.

References

- [1] B.Radisavljevic et al., Nat. Nanotechnol. 6, 147 (2011).
- [2] V. C. Sundar et al., Science, 303, 12, 1644 (2004).
- [3] V. Podzorov et al. Appl. Phys. Lett., 84, 3301 (2004).
- [4] T. Kawanago et al., Appl. Phys. Lett. 108, 041605 (2016).

Figures



Channel Conductivity $\sigma = \frac{I_{SD}}{V_{AW}}$

Intrinsic electron mobility $\mu = \frac{D}{WC_i} \cdot \frac{d\sigma}{dV_G}$

Contact resistance $R_{contact} = \frac{V_{SD}}{I_{SD}} - \frac{L}{D} \cdot \frac{V_{AW}}{I_{SD}}$

D : distance between the voltage probes
 C_i : capacitance of the gate dielectric
 d : derivative operator

Figure 1: Fabrication process and device structure.

Figure 2: Microscope image of fabricated FET.

Figure 3: Equations to evaluate channel mobility & contact resistance with gated four-probe method.

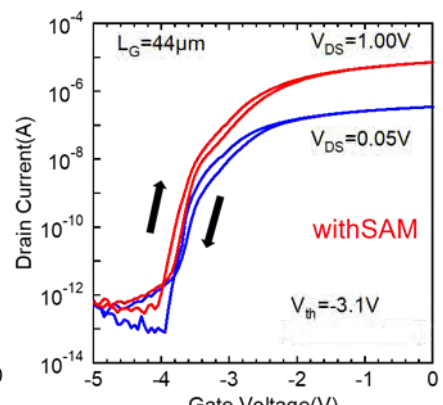
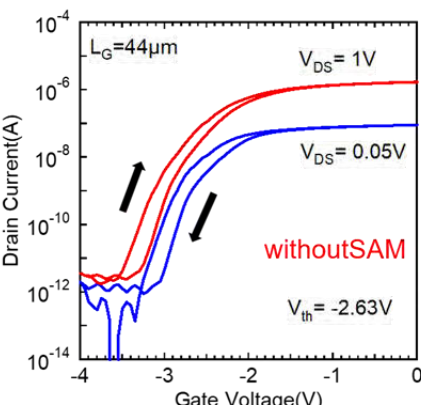
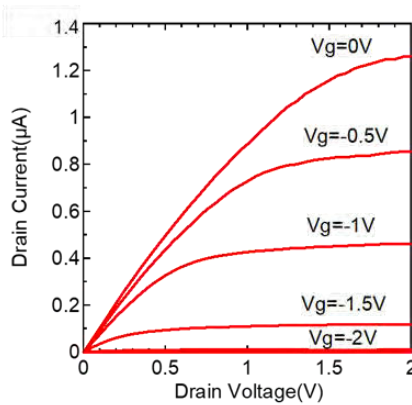


Figure 4: Representative I_d - V_d characteristics of MoS₂ FET with gated four-probe method.

Figure 5: Bidirectional I_d - V_g characteristics of MoS₂ FET without SAM.

Figure 6: Bidirectional I_d - V_g characteristics of MoS₂ FET with SAM.

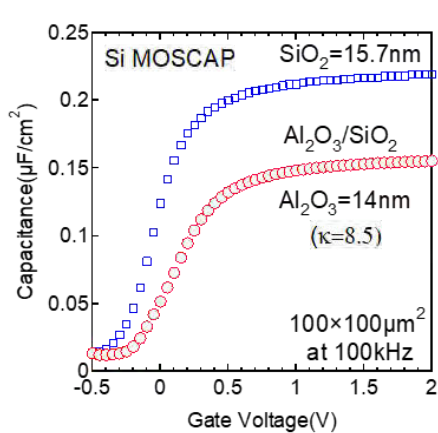


Figure 7: C-V characteristics of Si MOSCAP for SiO₂ and Al₂O₃/SiO₂ gate dielectric.

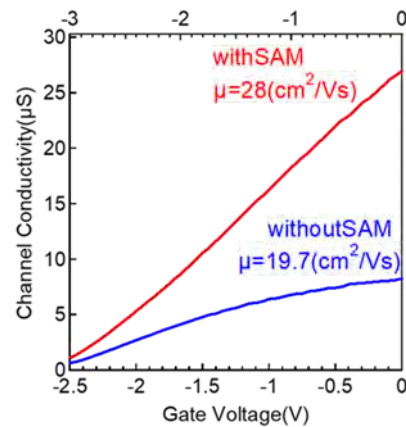


Figure 8: Impact of SAM on channel mobility estimated by four-probe method.

Takuya Okamoto^{1,2}

Yoshikazu Ito³, Naoka Nagamura^{4,5}, Takeshi Fujita⁶, Yukio Kawano^{1,2}

¹ FIRST, Tokyo Institute of Technology, Tokyo, Japan.

² Department of Electrical and Electronic Engineering, Tokyo Institute of Technology, Tokyo, Japan.

³ Institute of Applied Physics, Graduate School of Pure and Applied Science, Tsukuba University, Tsukuba, Ibaraki, Japan

⁴ National Institute for Materials Science (NIMS), Tsukuba, Ibaraki, Japan

⁵ Japan Science and Technology Agency, PRESTO, Kawaguchi, Saitama, Japan

⁶ School of Environment Science & Engineering, Kochi University of Technology, Kochi, Japan

okamoto.t.ap@m.titech.ac.jp

Three-Dimensional Spatial-Topology Effects, Magnetoresistance in Three-Dimensional Porous Graphene

Spatial topology is a critical factor for graphene due to its spatial symmetry arranged in hexagonal lattice. Actually, many studies on spatial-topology modification have been reported, such as 1D or 0D graphene (graphene nanoribbon [1,2] and quantum dot [3], respectively), antidot system [4,5], and strained graphene inducing gauge field [19, 20]. As a new platform, upsizing 2D graphene into 3D architectures is also interesting for exploring new physics. Many theoretical studies on such 3D graphene systems has been reported on viewpoints of 3D-topology effects [6-8]. Particularly topological defects which are geometrically required to form 3D architecture with negative Gaussian curvatures. Since such 3D-topology effects are expected to bring intriguing physics, experimental exploration is strongly demanded.

Recently high-quality 3D graphene which has open porous structure smoothly interconnected graphene network without edge and fringes [9] have been developed with chemical vapor deposition (CVD) method. This 3D porous graphene preserves the properties of Dirac fermion well, allowing us to explore interesting phenomenon only observed in 3D graphene system. Additionally, the 3D-spatial topology such as pore size can be tune by CVD conditions, providing pore size dependence of curvatures and topological defects. It will provide a platform for investigating the topological effect. In this report, we experimentally investigated 3D spatial-topology effects through the electrical transport measurements.

We synthesized open and smoothly inter-connected 3D graphene with different pore size of 100–300 nm and $\sim 1 \mu\text{m}$ (Figs. 1(a,b)). Raman spectra of these samples demonstrated that the 3D graphene is composed by single-layer graphene due to the high 2D/G intensity ratios (Fig. 1(c)). We performed magnetoresistance (MR) measurements at 3.8 K with a standard four probe method in Fig. 2(a). The large pore-sized ($\sim 1 \mu\text{m}$) sample shows a conventional positive MR, whereas the small pore-sized (100–300 nm) sample exhibits negative MR (weak localization). These comparison are a clear indication of the spatial-topology effects on the magnetic-field correction, showing the strong dependence on spatial topology of the pore size.

According to the theoretical report [10], several scattering rates including elastic scattering events can be deduced owing to the nature of quasiparticle chirality in graphene. Figure 2(b) plots the T dependence of the ratio $\tau_i^{-1}/\tau_\phi^{-1}$, where τ_i^{-1} and τ_ϕ^{-1} are the intervalley and dephasing scattering rate, respectively. It is found that intervalley scattering event prevails in the sample with small pores at low temperature, and that inelastic scattering event is dominant regardless of the pore size at high temperature. These results show that the curvature of graphene surface is strongly related with intervalley scattering events.

Through purely geometrical considerations, 3D graphene structures with high curvature require much topological defects according to the Euler's theorem. At topological defects, especially odd-number carbon ring, when the momentum vector k of carriers revolves around the singularity $k = 0$ (Γ point), K point reverses to K' one. It is the main reason of intervalley scattering events. Our findings provide not only deeper understanding of 3D graphene systems but also pave a new way to realize a spatial-topology controllability of valleys.

References

- [1] M. Fujita, et al. Journal of the Physical Society of Japan 65 (1996) 1920.
- [2] X. Li, et al. science 319 (2008) 1229.
- [3] M. Bacon, et al. Particle & Particle Systems Characterization 31 (2014) 415.
- [4] J. Eroms, et al New Journal of Physics 11 (2009) 095021.
- [5] T. G. Pedersen, et al. Physical Review Letters 100 (2008) 136804.
- [6] M. Koshino, et al. Physical Review B 93 (2016) 041412.
- [7] H. Aoki, et al. Physica E 22 (2004) 696.
- [8] M. Fujita, et al. Physical Review B 51 (1995) 13778.
- [9] Y. Ito et, al. Angewandte Chemie International Edition 53 (2014) 4822.
- [10] E. McCann, et al. Physical Review Letters 97 (2006) 146805.

Figures

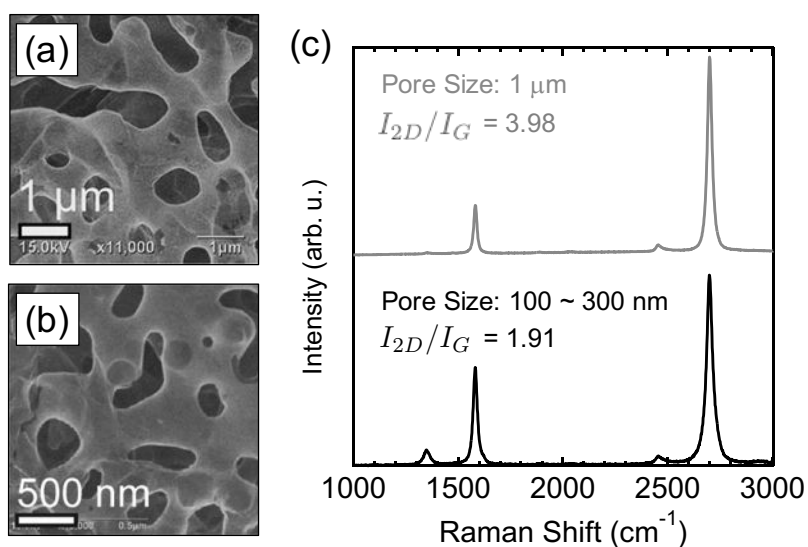


Figure 1: (a,b) Scanning electron microscopy images of the 3D porous graphene with 1 μm (a) and 100-300 nm (b) in a diameter.

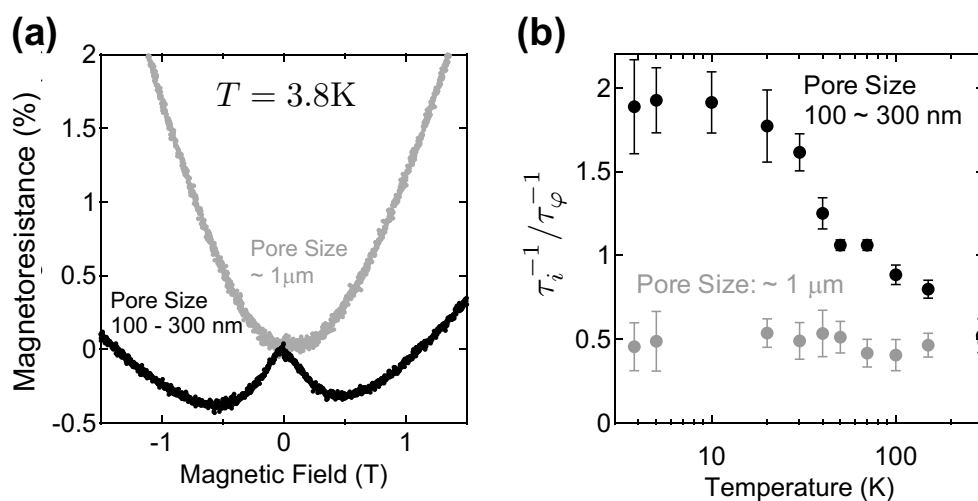


Figure 2: (a) Pore-sized dependence of the normalized magnetoresistance at 3.8 K. (b) Temperature dependence of the ratio $\tau_i^{-1}/\tau_\phi^{-1}$.

Young Hee park

Seunghyun Shin, Jong-Guk Ahn and Hyunseob Lim*

Department of Chemistry, Chonnam National University (CNU), Gwangju, 61186, Republic of Korea

pyh7077@naver.com

Electrochemical Surface Modification of Two-Dimensional Hexagonal Boron Nitride for Generating Midgap Energy States

The surface functionalization has been regarded as one of approaches to modulate the electronic structure of covalent nanomaterials such as carbon nanotube and graphene sheet. Although two dimensional hexagonal boron nitride (h-BN) has the similar chemical structure to that of graphene, the spontaneous chemical reactions for realizing the surface functionalization on h-BN were rarely reported due to its insulating electronic property. In general, single electron transfer (SET) process from nanomaterial to organic molecules is a prerequisite process for radical-based functionalization reactions, but SET from insulating material is restricted because of zero density of states near the Fermi level of insulating material. Herein, we present the new chemical route to facilitate the direct functionalization on insulator, h-BN. Aryl groups were successfully functionalized on the h-BN by the electrochemical reduction reaction of 4-BBDT. The electrochemical process can drive the electron tunneling from working electrode to 4-BBDT through h-BN film (both monolayer and multilayer) by electron tunneling process, and produce the highly reactive diazonium radical on its surface. Then, aryl radicals can be covalently functionalized on h-BN surface. In addition, this rapid reaction process can modulate the electronic structure of h-BN. We believe that our demonstration does not only provide fundamental insights for developing the surface functionalization reaction on 2D materials, but also can advance the applications of h-BN-based optoelectronic devices

References

- [1] Weng, Q.; Wang, X.; Wang, X.; Bando, Y.; Golberg, D. *Chem. Soc. Rev.* 45, (2016), 3989.
- [2] Song, L.; Ci, L.; Lu, H.; Sorokin, P. B.; Jin, C.; Ni, J.; Kvashnin, A. G.; Kvashnin, D. G.; Lou, J.; Yakobson, B. I.; Ajayan, P. M. *Nano Lett.* 10, (2010), 3209.
- [3] Sainsbury, T.; Satti, A.; May, P.; Wang, Z.; McGovern, I.; Gun'ko, Y. K.; Coleman, J. J. *Am. Chem. Soc.* 134, (2012), 18758.

Figures

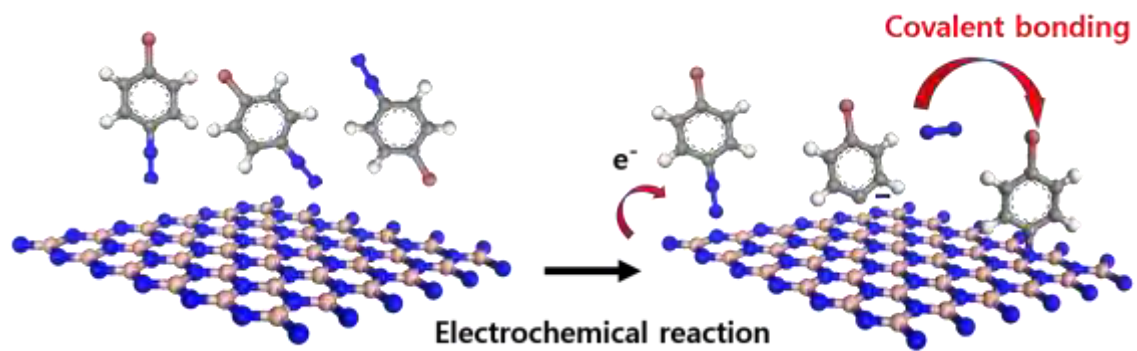


Figure 1: h-BN-4BBDT electrochemical reaction

Two-Dimensional Pseudocapacitive Nanosheets for All-Solid-State Micro-Supercapacitors

Two-dimensional (2D) pseudocapacitive materials, characterized by nanoscale dimension in thickness, infinite length in the plane and reversible redox reactions, are currently regarded as groundbreaking electrode candidates for micro-supercapacitors (MSCs). Here, we synthesized ultrathin MnO_2 nanosheets and mesoporous polypyrrole-based graphene nanosheets uniformly anchored with redox polyoxometalate ($\text{mPPy}@r\text{GO}-\text{POM}$). Further, a novel and universal mask-assisted filtration technology for the simplified fabrication of all-solid-state planar MSCs was developed. Remarkably, the resulting MSCs exhibited outstanding areal capacitance and volumetric capacitance, exceptionally mechanical flexibility, excellent cyclability and impressive serial or parallel integration for modulating the voltage or capacitance.

References

- [1] Qin, J.Q., Wu, Z.-S.*, Zhou, F., Dong, Y.F., Xiao, H., et al. Chinese Chemical Letters, 29 (2018), 582-586.
- [2] Qin, J.Q., Zhou, F., Xiao, H., Ren, R.Y., Wu, Z.-S*. Science China Materials, 61 (2017), 233-242.

Figures

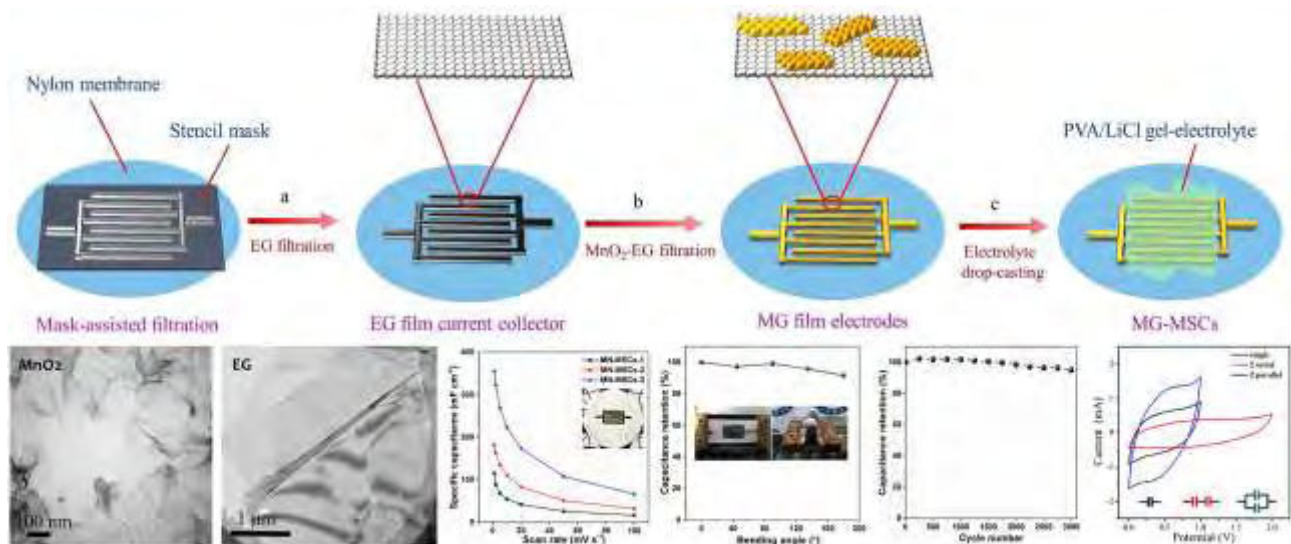


Figure 1: Fabrication schematic, materials characterizations and electrochemical performance of all-solid-state planar MSCs based MnO_2 nanosheets.

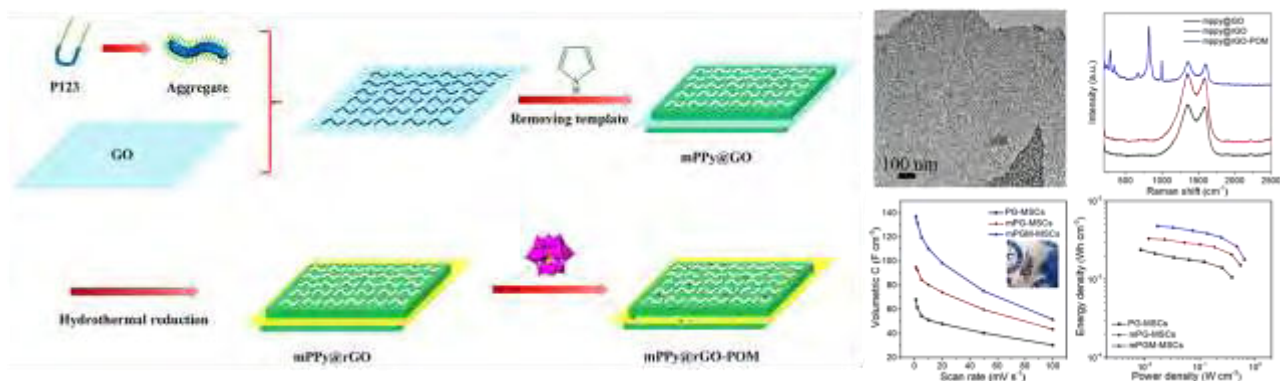


Figure 2: Materials synthesis and characterizations of mesoporous polypyrrole-based graphene nanosheets anchoring redox polyoxometalate for all-solid-state planar MSCs.

A. Sasagawa¹

T. Okamoto¹, Y. Harada², S. Nakano², W. Norimatsu², M. Kusunoki³, and Y. Kawano¹

¹First, Dept of Electrical and Electronic Engineering, Tokyo Institute of Technology, 152-8552, Tokyo, Japan.

²Department of Materials Chemistry, Nagoya University, 464-8603, Nagoya, Japan.

³Institute of Materials and Systems for Sustainability, Nagoya University, 464-8603, Nagoya, Japan.

sasagawa.a.aa@m.titech.ac.jp

Direct observation of Plasmons in Graphene Quantum Dots with Scanning Near-Field Optical Microscopy

Surface Plasmon Polariton (SPP) in two-dimensional graphene has been applied to a wide range of fields such as photo-detectors [1, 2], bio-sensing [3], and optical communications [4]. In recent years, nanostructured graphene such as graphene nanoribbons and graphene quantum dots (GQDs) downsized in dimension attracts much attention as materials with novel SPP characteristics arising from nanostructures. Actually they have been studied by many spectroscopic techniques and these research opens the path for new functionalities [5]. These measurements, however, only show area-averaged optical response and nanoscale measurements have not been made due to diffraction limit. To explore and realize more SPP functionalities, understanding real-space characteristics in detail is indispensable.

To investigate such nanoscale spatial characteristics, a scattering scanning near-field optical microscopy (s-SNOM) provides a strong tool for accessing optical response of nanostructures. Mutual near-field interaction between highly-confined optical fields on an AFM tip and a sample provides high spatial resolution ~ 10 nm beyond the diffraction limit. Through the s-SNOM measurements, many nanoscale investigations have been reported including graphene [6]. In this work, we achieved to directly observe SPP in GQDs by using s-SNOM. Interestingly, the results indicate unique SPP frequency dependence derived from the nanostructure.

We synthesized epitaxial-GQDs with a diameter of ~ 40 nm on SiC substrate by a thermal decomposition method. For optical measurements, we utilized the s-SNOM equipped with a CO₂-gas laser at the wavenumber of 929.02 cm⁻¹. Figure 1 schematically illustrates the experimental setup. Figures 2 (a) and (b) display an AFM phase image and a near-field amplitude image, respectively. We succeeded in directly observing dot-like plasmon luminescence from the GQDs. Additionally, by utilizing monochromatic measurement (CO₂ gas laser) and nanoscale spectroscopy, we observed strong frequency dependence of SPP in GQDs, which is in strong contrast to 2D graphene on SiC.

Our findings indicate the geometric controllability of the SPP characteristics in nanostructured graphene, providing not only a deeper understanding of nanostructured graphene but also a new pathway to realize new functional SPP properties in a wide frequency range from terahertz and infrared regime.

References

- [1] T. Mueller., et al, Nat. Photonics vol.4, 2010, 297-301.
- [2] Y. Liu, et al. Nat. commun vol. 2, 2011, 1-7.
- [3] D. Rodrigo, et al, Science vol. 349, 2015, 165-168.
- [4] A. Pospischil, et al, Nat. Photonics vol. 7, 2013, 892-896.
- [5] V. W. Brar., et al, Nano Letter vol. 13(6), 2013, 2541-2547.
- [6] J. Chen, et al, Nature volume 487, 2012, 77-81.

Figures

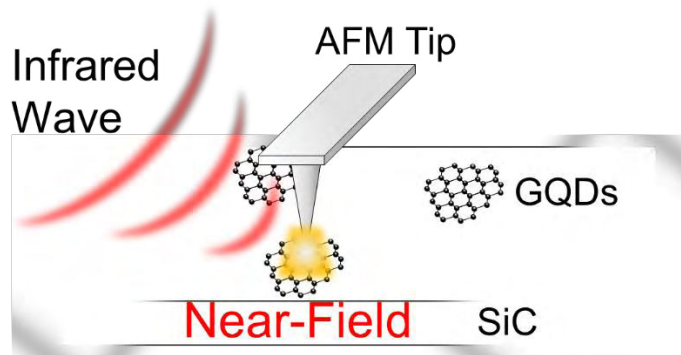


Figure 1: Schematic of the s-SNOM measurement

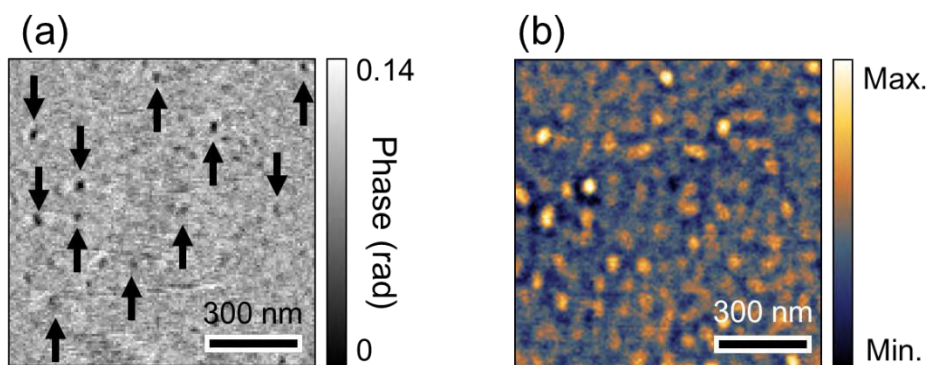


Figure 2: (a) AFM phase image. The black arrows indicate the GQDs with ~40 nm in a diameter. (b) Near-field amplitude image (929.02cm⁻¹) of the GQDs. The dot-like plasmonic luminescence is clearly visible.

Graphene-Armored Aluminum Foil as Current Collectors for High-voltage Lithium-Ion Battery with Enhanced performance

Abstract

Lithium-ion batteries (LIB) have become one of the most promising power sources to meet the ever increasing demand for high-performance electric devices. Recently, the issue of corrosion happened on aluminum (Al) foil began to receive attention. In order to improve the potential of cathode to improve the energy density of LIB, it's crucial to solve the problem of the corrosion of Al foil. Here, we directly grow graphene film on commercial Al foil for current collectors via plasma-enhanced chemical vapor deposition (PECVD) method and take it as electrically conductive coating layers and interfacial barrier layers to enhance the anticorrosion performances of Al foil at high voltage in LIB. It is demonstrated that Al foil armored by such graphene film shows significantly reinforced anodic corrosion resistance and LiNi_{0.5}Mn_{1.5}O₄ cells using graphene-armored Al foil (GAI) as current collectors show enhanced cycling performance compared to the cells with pristine Al foil. Moreover, the rate performance is also improved due to the graphene nanosheet grown by PECVD improving the adhesion between active materials and current collectors. This work not only contributes to the long-term stable operations of LIBs but also provides feasibility for next-generation high-voltage lithium ion batteries.

References

- [1] M. Wang, M. Tang, S. Chen, H. Ci, K. Wang, L. Shi, L. Lin, H. Ren, J. Shan, P. Gao, Z. Liu and H. Peng, *Adv. Mater.*, 2017 1703882.
- [2] T. Ma, G. L. Xu, Y. Li, L. Wang, X. He, J. Zheng, J. Liu, M. H. Engelhard, P. Zapol, L. A. Curtiss, J. Jorne, K. Amine and Z. Chen, *J. Phys. Chem. Lett.*, 8 (2017) 1072.

Figures

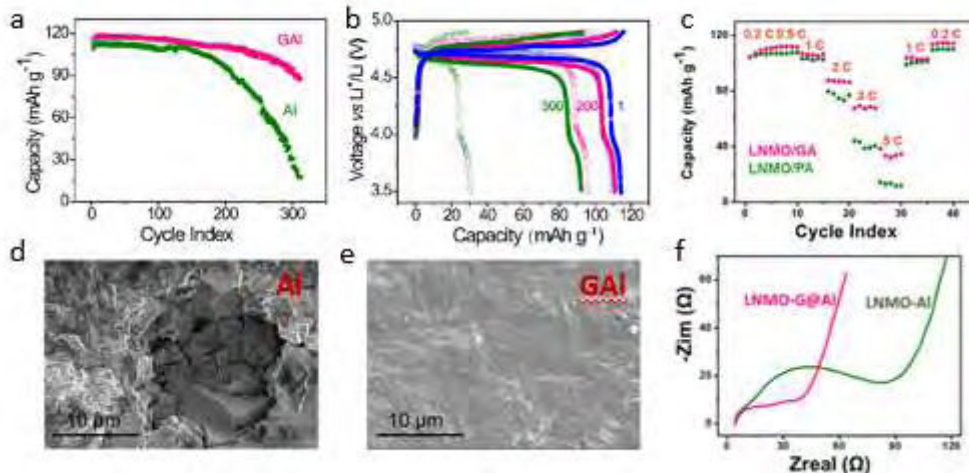


Figure 1: Enhanced anticorrosion performance and electrochemical performance of GAI. (a,b) Long-term cycling performance of LNMO/GAI and LNMO/Al cells; (c) Rate performances of LNMO/GAI and LNMO/Al cells; (d,e) SEM images of pristine Al foil and GAI after cycling; (f) EIS analysis of LNMO/GAI and LNMO/Al cells.

Xiaoyu Shi

Zhong-Shuai Wu and Xinhe Bao

Dalian Institute of Chemical Physics, Chinese Academy of Sciences, 457 Zhongshan Road, Dalian, China.

shixiaoyu@dicp.ac.cn

Graphene based linear tandem micro-supercapacitors

We demonstrate the printable fabrication of new-type planar graphene-based linear tandem micro-supercapacitors (LTMSs) on diverse substrates with symmetric and asymmetric configuration, high-voltage output, tailored capacitance and outstanding flexibility. The resulting graphene-based LTMSs consisting of 10 single device present a high-voltage output of 8 V, the layer by layer graphene/conductive polymer-based LTMSs show enhanced capacitance and the asymmetric LTMSs exhibit higher output voltage and energy density. This work offers numerous opportunities for one-step scalable fabrication of flexible tandem energy storage devices.

References

- [1] X. Shi, Z.-S. Wu, J. Qin, S. Zheng, S. Wang, F. Zhou, C. Sun and X. Bao, *Adv. Mater.* 29 (2017), 1703034.

Figures

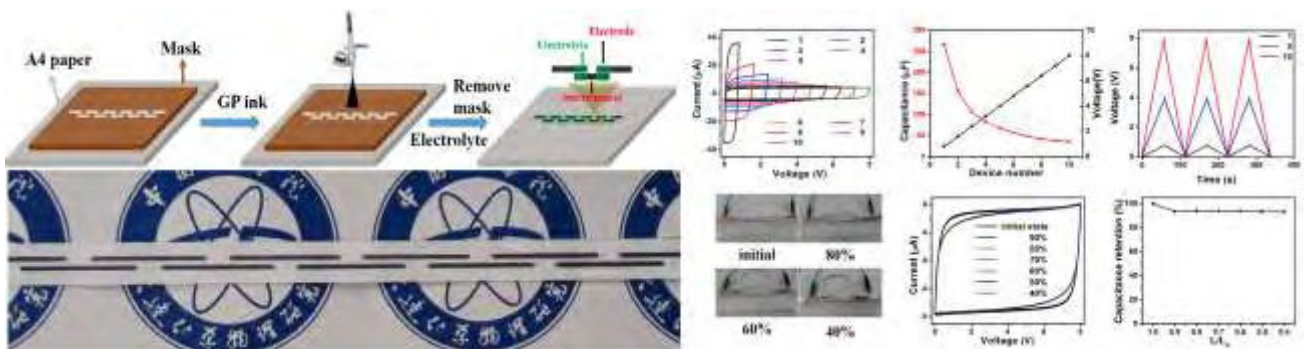


Figure 1: Fabrication schematic and electrochemical performances of graphene based linear tandem micro-supercapacitors consisting of 10 single device.

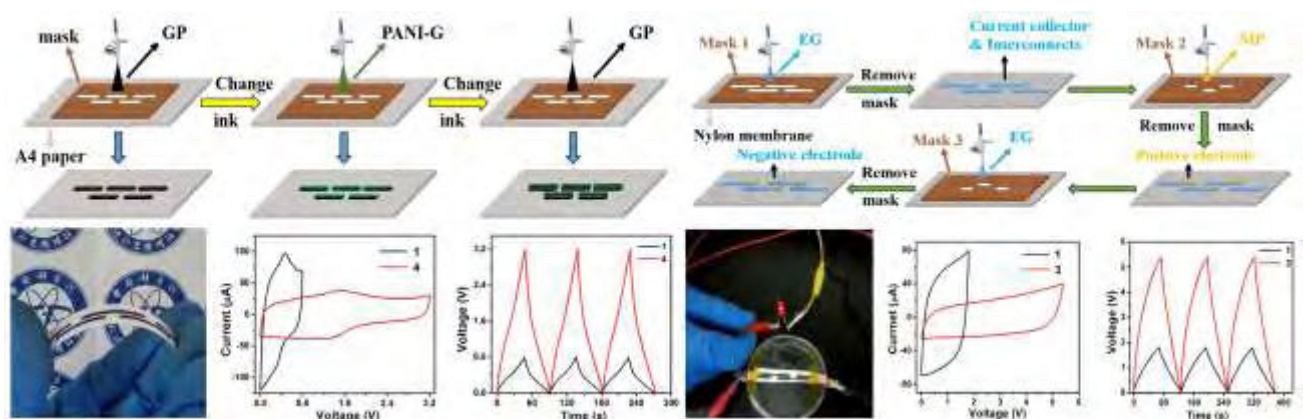


Figure 2: Fabrication schematic and electrochemical performances of high-capacitance and asymmetric graphene based linear tandem micro-supercapacitors.

Seung-Hyun Shin

Dong Hwan Jung, Jong Min Kim, Chan Wook Jang, Sung Kim, Suk-Ho Choi

Department of Applied Physics and Institute of Natural Sciences, Kyung Hee University, Yongin 17104, Korea

sukho@khu.ac.kr

MAPbI₃ Perovskite Solar Cells Employing Flexible n-Type Graphene Transparent Conducting Electrodes

Metal halide-based organic-inorganic hybrid perovskite solar cells (PSCs) have been actively studied in recent years due to the rapid increase in their efficiency [1]. Integrating graphene into PSCs has especially attracted much attention because graphene provides promising flexibilities in device designs due to its excellent structural, electrical, and optical properties [2]. In addition, graphene is very useful as a flexible transparent conductive electrode (TCE) that can replace brittle transparent conductive oxides (TCOs) such as indium tin oxide and F-doped tin oxide [3]. Despite successful application of graphene TCEs for PSCs [4], no use of n-type graphene as a TCE has been reported until now. However, most of the active scaffolds are based on n-type metal-oxide electron transfer layers such as TiO₂, Al₂O₃, and ZnO because they play an important role in achieving high efficiency in PSCs. Therefore, studies on n-type graphene TCEs are very important for PSCs. Here, we fabricate *n-i-p*-type MAPbI₃ PSCs by employing Ag nanowires (Ag NWs)-doped graphene with high transmittance (T) and low sheet resistance (R_s) as an n-type graphene TCE. With increasing the doping concentration (n_A) to 0.3 wt%, the R_s monotonically decreases to ~ 52 Ω/sq whilst the T decreases by about 10%. Due to the n_A-dependent trade-off correlation between the R_s and T, the ratio of DC conductivity/optical conductivity is the highest (~ 62) at n_A = 0.1 wt%, resulting in 15.80 and 13.45% power conversion efficiencies for the PSCs on rigid and flexible substrates, respectively.

References

- [1] Q. Chen, N. De Marco, Y. Yang, T. B. Song, C. C. Chen, H. X. Zhao, Z. R. Hong, H. P. Zhou, and Y. Yang, *Nano Today*, 10 (2015) 355-396.
- [2] H. S. Jung and N. G. Park, *Small*, 11 (2015) 10-25.
- [3] H. Zhou, Q. Chen, G. Li, S. Luo, T. Song, H.-S. Duan, Z. Hong, J. You, Y. Liu, and Y. Yang, *Science*, 345 (2014) 542-546.
- [4] A. Mei, X. Li, L. Liu, Z. Ku, T. Liu, Y. Rong, M. Xu, M. Hu, J. Chen, Y. Yang, M. Grätzel, and H. Han, *Science*, 345 (2014) 295-298.

Figures

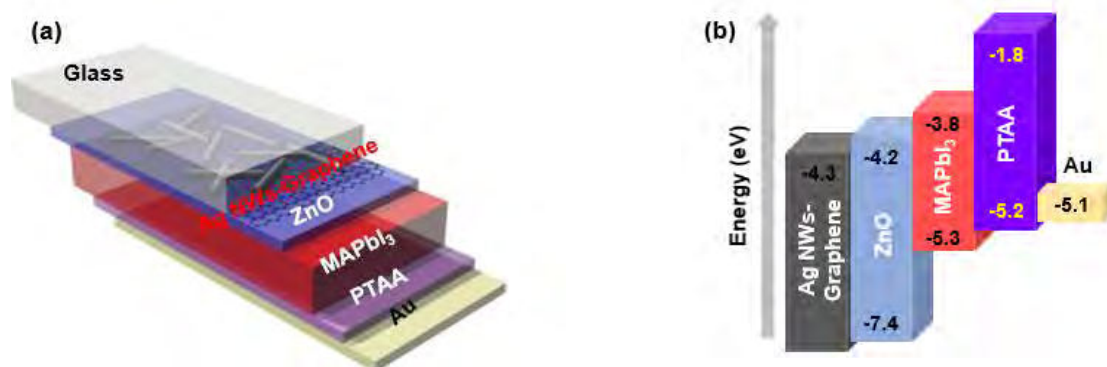


Figure 1: (a) A schematic of a typical TCO-free *n-i-p*-type planar PSC with a structure of glass/Ag NWs-doped graphene/ZnO/MAPbI₃/poly[bis(4-phenyl)(2,4,6-trimethylphenyl)amine] (PTAA)/Au and (b) its band diagram.

Seunghyun Shin, Young Hee Park

Jong-Guk Ahn and Hyunseob Lim

Department of Chemistry, Chonnam National University (CNU), Gwangju, 61186, Republic of Korea

sshssh146@gmail.com

Direct Covalent Functionalization of Single Layer 2H-MoS₂ Electrografting of Diazonium Salt: Influence of S vacancy and S-C bond on Photoluminescence of 2H-MoS₂

Two-dimension materials such as graphene, hexagonal boron nitride (h-BN) and transition metal dichalcogenides (TMD) have lots of advantages for various applications due to their two-dimensional (2D) geometric structure. Among them, 2D-TMD materials, has attracted great attention as an alternative to graphene, since it has semiconducting properties while graphene has metallic properties. Thus, it cannot also be used in electronic applications, but also in optical and optoelectronic applications. Although single layer MoS₂ has a bandgap of ~1.8 eV, the modulation of its bandgap is further required to absorb or emit the wider range of light. Surface modification is one of approaches, but the one-step functionalization on 2H-TMDs has been known to be difficult, while various reactions on 1T- TMDs have been demonstrated. The origin of the limitation is attributed to the difficulty of electron transfer from 2H-TMD to reacting molecules due to its semiconducting property and neutral charge state, which is a prerequisite process for the surface functionalization. Herein, we present the novel approach facilitating the direct surface functionalization of 4-bromobenzene diazonium tetraborate (4BBDT) on 2H-MoS₂, one of TMD materials, by electrochemical process. The successful functionalization was confirmed by Atomic force microscopy, Raman spectroscopy and spatially resolved X-ray photoelectron spectroscopy (XPS) combined with scanning photoelectron microscopy (SPEM). The widened band-gap of modified 2H-MoS₂ was also confirmed by photoluminescence spectroscopy. In addition, the modified optical bandgap was confirmed on the aryl-functionalized MoS₂ sheet by photoluminescence (PL) measurement. The systematic experimental studies combined with theoretical calculation have revealed the influence of S vacancy and S-C bond, created by the electrochemical modification, on the change in PL of the modified MoS₂. We believe that our demonstration does not only provide fundamental insights for developing the surface functionalization reaction on 2D materials, but also can advance the practical applications of TMD-based optoelectric devices.

References

- [1] Chhowalla, M., *et al.*, *Nat. Chem.* **2013**, 5, 263.
- [2] Wang, Q. H., *et al.* *Nat. Nanotechnol.* **2012**, 7, 699.
- [3] Lim, H., *et al.* *Langmuir.* **2010**, 26 (14), 12278-12284.
- [4] Song, I., *et al.* *RSC Adv.* **2015**, 5 (10), 7495-7514.

Figures

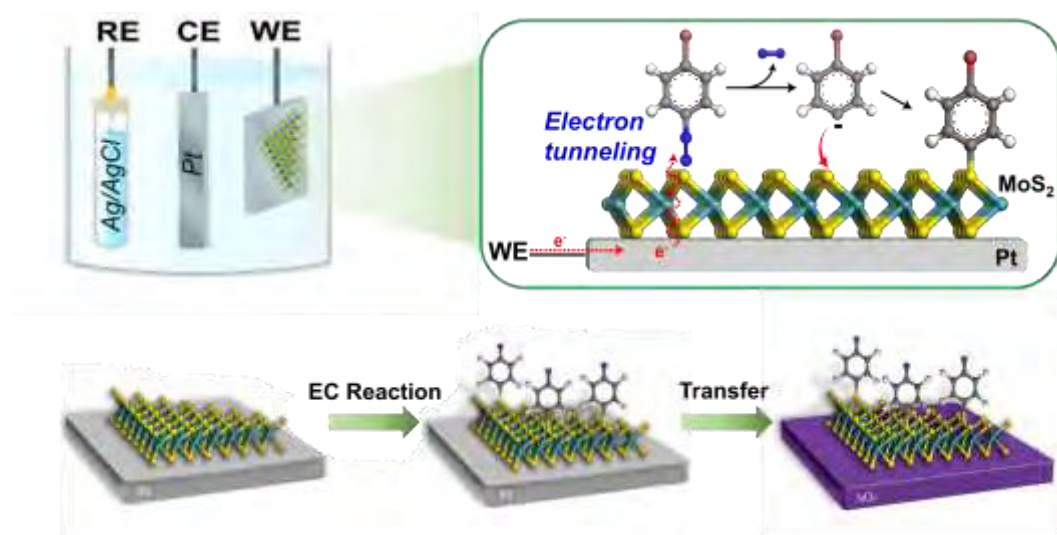


Figure 1: Schematic illustrations showing the experimental set up for electrografting of 4-BBDT on MoS₂/Pt, and the expected reaction

Li Shuan

Wu Yanqing, Li Xingguo, Zheng Jie

College of Chemistry and Molecular Engineering, Peking University, Beijing, China

15652783232@163.com

Annealing temperature effect on microstructure, optical and electrical properties of nanometer GdYO_x high k films

Abstract

In this work, Metal-oxide-semiconductor (MOS) capacitors with sputtering-deposited ternary GdYO_x high k gate dielectric thin films were fabricated by magnetron co-sputtering method on p-type Si substrates. Annealing temperature dependent microstructure, morphology, chemical bonding states, optical and electrical properties of nanometer GdYO_x gate dielectric thin films were systemically investigated by x-ray diffraction, atomic force microscopy, x-ray photoelectron spectroscopy, optical spectroscopy and electrical measurements. Results have shown that the 500°C-annealed GdYO_x composite films as well as those samples annealed at lower temperatures keep amorphous state. With the sample annealed at 600 °C, however, the amorphous phase disappears and the nanometer particles films were formed. The increase in band gap energy has been found with increasing the annealing temperature and maximum band gap is reached to 5.55 eV. Electrical properties of all samples based on Pt/Si/GdYO_x/Pt MOS capacitor have been investigated by means of the high frequency capacitance-voltage (C-V) and the leakage current density-voltage (I-V) characteristics. It shows improved performances at the annealing temperature of 500 °C, such as high dielectric constant (k) of 20.2, lowest current density of $1.44 \times 10^{-2} \text{A/cm}^2$ (at $V_{fb}-1\text{V}$). In addition, the leakage current mechanism for 500 °C-annealed sample has been discussed in detail. 500°C-annealed GdYO_x thin films can be acted as potential high-k gate dielectrics in future CMOS devices.

References

- [1] J. Robertson, R.M. Wallace, *Materials Science & Engineering R-Reports*, 88 (2015) 1-41
- [2] T. Kanashima, R. Yamashiro, M. Zenitaka, K. Yamamoto, *Materials Science in Semiconductor Processing*, 70 (2017) 260-264.
- [3] L. Zhu, G. He, Z.Q. Sun, M. Liu, S.S. Jiang, S. Liang, W.D. Li, *Journal of Sol-Gel Science and Technology*, 83 (2017) 675-682.
- [4] L. Zhu, G. He, W. Li, B. Yang, E. Fortunato, R. Martins, *Nontoxic, Advanced Electronic Materials*, 4 (2018) 1800100.

Figuresa

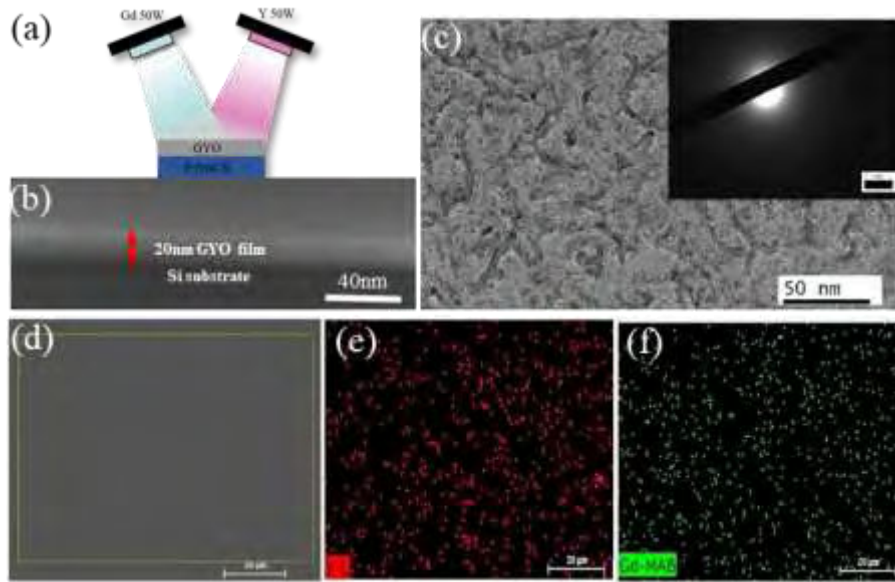


Figure 1:(a) Schematic diagram of $GdYO_x$ film prepared by magnetron sputtering. (b) Cross-sectional SEM image of a $GdYO_x$ film deposited on a silicon substrate. (c) TEM image, (d-f) EDS mapping of original sputtering $GdYO_x$ thin films

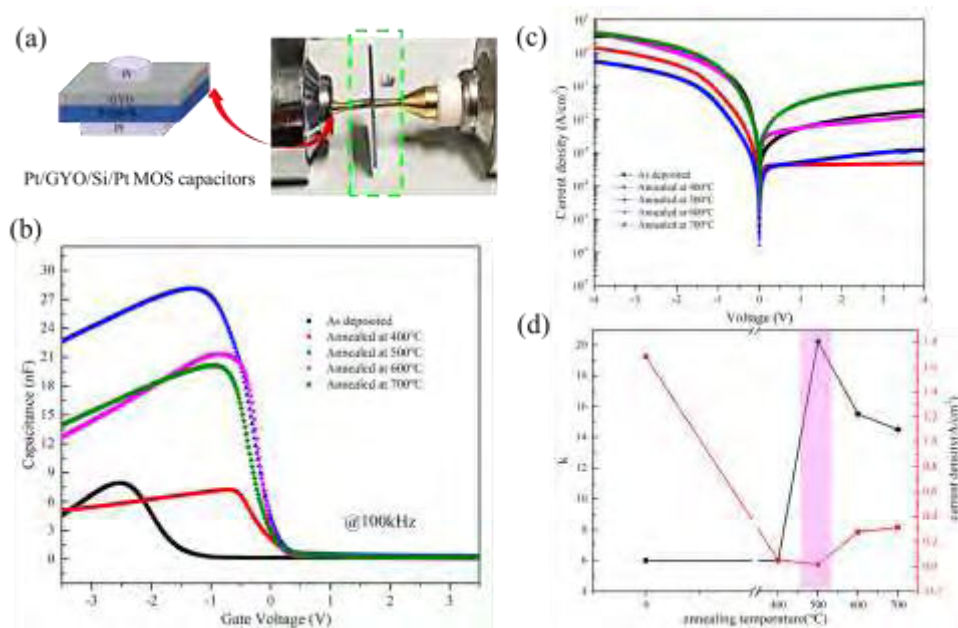


Figure 2: (a) Schematic diagram of Pt/ $GdYO_x$ /p-Si MOS capacitors. (b) C-V characteristics, (c) I-V characteristics and (d) k value and current density of $GdYO_x$ thin films as a function of annealing temperature.

Shubin Su

Haihua Tao, Hao Li, Zhenhua Ni, Dong Qian, Guanghui Yu, Xianfeng Chen

State Key Laboratory of Advanced Optical Communication Systems and Networks, Department of Physics and Astronomy, Shanghai Jiao Tong University, 200240 Shanghai, China.

shubinsu@sjtu.edu.cn

tao.haihua@sjtu.edu.cn

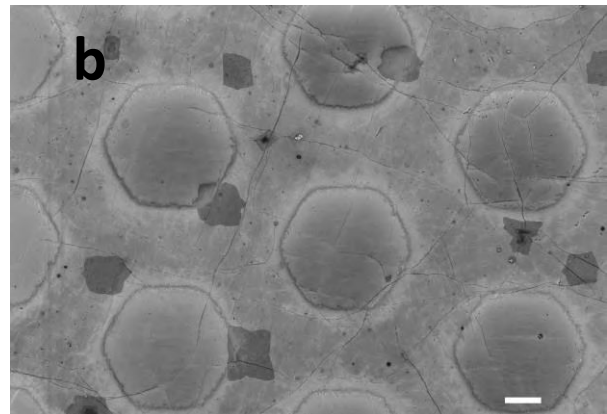
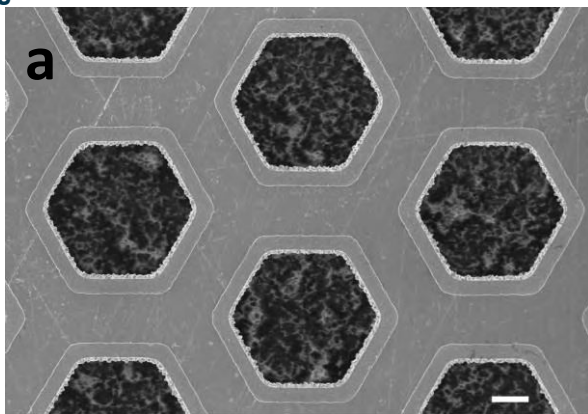
Water-based Graphene Patterning under Ultraviolet Irradiation

Abstract: Magnetic-assisted UV ozonation has been proposed to be an alternative cost-effective method for patterning microscale graphene microstructures, immune to organic contamination and substrate damage [1,2]. However, the low oxidizing intensity and lateral diffusion of the instable intermediate of ozone molecule appear detrimental to the quality of graphene patterning. Herein, we propose to pattern chemical vapor deposition grown graphene film through a stencil mask using a stronger oxidant of paramagnetic OH ($X^2 \Pi$) radicals photodissociated from water (H_2O) molecules under ultraviolet (UV) irradiation [3]. The OH ($X^2 \Pi$) radicals move directionally toward graphene surface in an inhomogeneous vertical magnetic field ($B_z = 0.51 \text{ T}$, $\nabla B_z = 160 \text{ T} \cdot \text{m}^{-1}$), strongly enhancing the oxidation intensity. Another photodissociated product of paramagnetic H (1^2S) radicals together with the stable water molecule explain the improved lateral under-oxidation. The water-based graphene patterning under UV irradiation is applicable to graphene-based electronic and optoelectronic devices.

References

- [1] Y. Wu, H. Tao, S. Su, H. Yue, H. Li, Z. Zhang, Z. Ni and X. Chen. *Sci. Rep.* 7 (2017), 46583–46590.
- [2] H. Yue, H. Tao, Y. Wu, S. Su, H. Li, Z. Ni, X. Chen. *Phys. Chem. Chem. Phys.* 19 (2017), 27353.
- [3] K. H. Welge, and F. Stuhl. *J. Chem. Phys.* 46(1967), 2440.

Figures



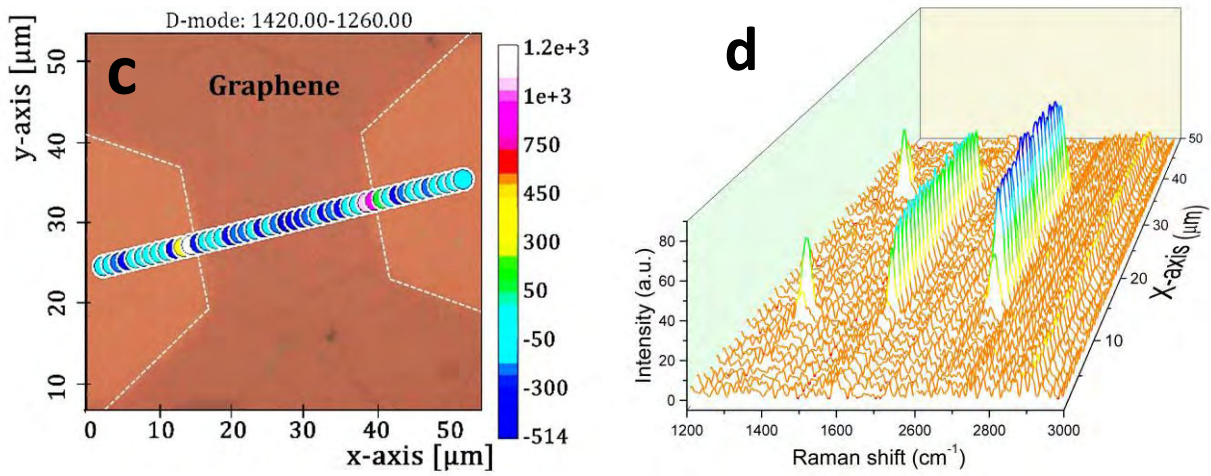


Figure 1: Water-based graphene patterning under UV irradiation through a copper mask. SEM topographical images of (a) the copper mask and (b) the corresponding microstructural graphene pattern; (c) Its optical topographical image with a line representing the defect mode (D band), and (d) the detailed Raman spectrum evolution. Both scale bars are 10 μm.

Chia-Liang Sun^{1,2,*}

Chia-Heng Kuo¹, Cheng-Hsuan Lin¹, Ben-Son Lin¹

¹Department of Chemical and Materials Engineering, Chang Gung University, Taoyuan 33302, Taiwan (ROC)

²Department of Neurosurgery, Linkou Chang Gung Memorial Hospital, Taoyuan 33305 Taiwan (ROC)

sunchialiang@gmail.com

Photoassisted Electrochemical Biosensing Using Graphene Oxide Nanoribbons

We have investigated graphene oxide nanoribbons (GONRs) for a variety of applications since 2011. [1-11] This conference paper presents a photoassisted biosensor based on GONRs. Images and graphitic structures of GONRs were monitored by transmission electron microscopy and Raman spectroscopy, respectively. The C1s spectra and energy bandgaps of GONR were collected by using X-ray photoelectron spectroscopy as well as UV-vis spectroscopy. Finally, the GONRs were adopted to modify the screen print carbon electrodes (SPCE) for the electrochemical detection of uric acid (UA) with the help of AM 1.5 light source in the power density of 100 mW/cm². In cyclic voltammetry analyses, all Faradaic currents for UA oxidation increased more than 20%. In the low concentration region, the photocurrent sensitivity was about 4 times higher than that of dark current. Therefore, the significantly improved UA sensing was demonstrated by photoassisted electrochemical detection by adopting GONRs.

References

- [1] C. L. Sun *et al.* ACS Nano 5 (2011) 7788.
- [2] L. Y. Lin *et al.* J. Mater. Chem. A 1 (2013), 11237.
- [3] Y. J. Lu *et al.* Carbon 74 (2014) 83.
- [4] M. H. Yeh *et al.* J. Phys. Chem. C 118 (2014) 16626.
- [5] C. L. Sun *et al.* Biosens. Bioelectron. 67 (2015) 327.
- [6] X. Lu *et al.* J. Mater. Chem. A 3, (2015) 13371.
- [7] R. Zhang *et al.* Anal. Chem. 87, (2015) 12262.
- [8] Y. W. Lan *et al.* Nano Energy 27, (2016) 114.
- [9] C. H. Su *et al.* ACS Omega 2(8), (2017) 4245.
- [10] T. E. Lin *et al.* Angew. Chem. Int. Ed. 56, (2017) 16498.
- [11] R. Zhang *et al.* Carbon 126, (2018) 328.

Figures

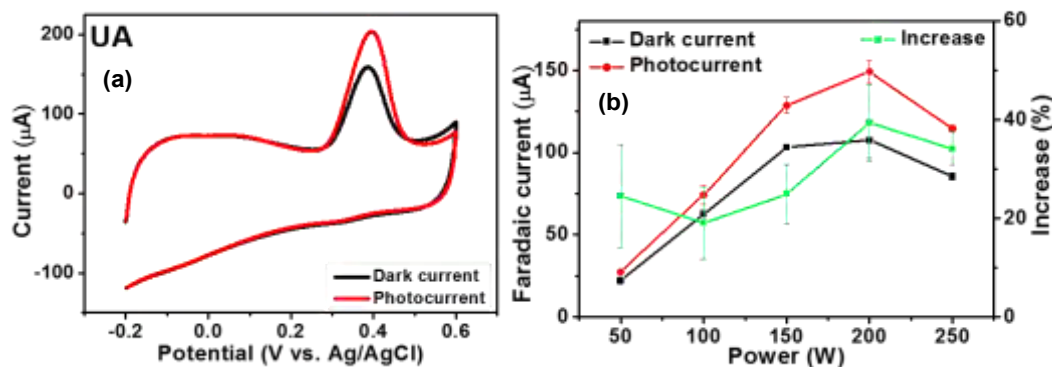


Figure 1: (a) Cyclic voltammograms in the electrolyte containing 0.1 M PBS + 0.3 mM UA using GONR(200 W). (b) Faradaic currents for photoassisted UA oxidation for GONRs unzipped under different microwave powers.

Luzhao Sun

Li Lin, Hailin Peng*, Zhongfan Liu*.

Center for Nanochemistry, Beijing Science and Engineering Center for Nanocarbons, Beijing National Laboratory for Molecular Sciences, College of Chemistry and Molecular Engineering, Peking University, Beijing 100871, P. R. China

Beijing Graphene Institute, Beijing 100094, P. R. China

zfliu@pku.edu.cn, hlpeng@pku.edu.cn

Visualizing the Fast Growth of Large Single-Crystalline Graphene

Chemical vapor deposition (CVD) technique has been demonstrated to be promising in growing large-area and high-quality graphene. However, the CVD-grown graphene is usually polycrystalline, which would degrade the electronic and mechanical properties. Consequently, to decrease the density of grain boundary, large single-crystalline graphene (LSCG) is synthesized via low supply of carbon source, which unfortunately exhibits low growth rate. Thus, fast growth of LSCG is an urging problem to realize the industrial growth of graphene film with high quality, which requires the in-depth understanding of the growth dynamics. Herein, we visualized the entire growth process of LSCG by using carbon isotopic pulse-labelling technique in conjunction with the Raman identification. The investigation of growth dynamics unveils the roles of carbon source in controllable growth of LSCG. By carefully tuning the carbon source supply, centimeter-sized graphene single crystals with high growth rate are realized.

References

Figures

- [1] Sun, L.; Lin, L.; Zhang, J.; Wang, H.; Peng, H.; Liu, Z. *Nano Res.* 10 (2016) 355-363
[2] Lin, L.; Sun, L. Z.; Zhang, J. C.; Sun, J. Y.; Koh, A. L.; Peng, H. L.; Liu, Z. F. *Adv. Mater.* 28 (2016) 4671-4677.

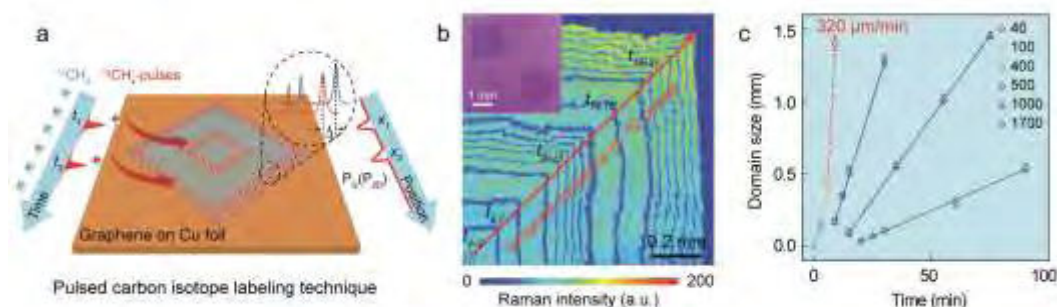


Figure 1: (a) schematic of visualizing fast growth of LSCG. (b) Optical image and Raman intensity maps of isotopic labeled LSCG. (c) Domain size as a function of growth time.

Yan Sun

Yan Sun,^a Wei Li,^a Hui Yang,^b Carla Bittencourt,^c Wenjiang Li,^{a*} Rony Snyders^c

^aKey Laboratory of Display Materials & Photoelectric Devices, School of Materials Science and Engineering, Tianjin University of Technology, Tianjin 300384, PR China.

^bTaizhou Branch of Zhejiang-California International Nan systems Institute, Taizhou, 318000, PR China.

^cChimie des interactions Plasma-surface, University of Mons (Umons), 20 place du parc, 7000 Mons, Belgium.

457479076@qq.com

In-suit Assembled MoS₂/Reduced Graphene Oxide Aerogels as an Efficient Catalyst Application for HER Electro catalysis

Layered transition metal dichalcogenides (TMDs) semiconductor MoS₂ composed of three-atom stacked layers (S-Mo-S) has been recognized as one of the most common candidates of HER electrocatalysts due to their low-cost, naturally abundant and electrocatalytic activities, and somehow can be considered as the pioneer of this class of electrocatalysts [1]. At the same time, it is vital role of carbonaceous nanomaterials that as a catalyst support for the development of any potential HER electrocatalyst, even in the case of noble metal catalysts [2-3]. In this work, the 3D non-noble MoS₂/rGO hybrid aerogels catalysts was successfully synthesized, made up of the 2D layered transition metal dichalcogenides (TMDs) MoS₂ nanoflowers and the 3D carbonaceous nanomaterials rGO aerogels, via a one-pot hydrothermal route. In the hybrid 3D MoS₂/rGO aerogels, rGO aerogels act as catalyst support for MoS₂, while the MoS₂ nanoflowers tight and well-decorated on the rGO nanofilms, which allows the hybrid aerogels with a very large surface area, defective structure, abundance of active sites, and high conductivity. All the above factors make the hybrid aerogels are characterized by excellent optimization in electrocatalytic hydrogen evolution reaction (HER).

References

- [1] Yang S, Feng X, Ivanovici S, Mullen K, *Angewandte Chemie-International Edition*, 49 (2010) 8408-8411.
- [2] Wang H, Robinson J T, Li X, et al., *Journal of the American Chemical Society*, 131 (2009) 9910.
- [3] Zhu C, Liu T, Qian F, et al., *Nano Letters*, 16 (2016) 3448-3456.

Figures

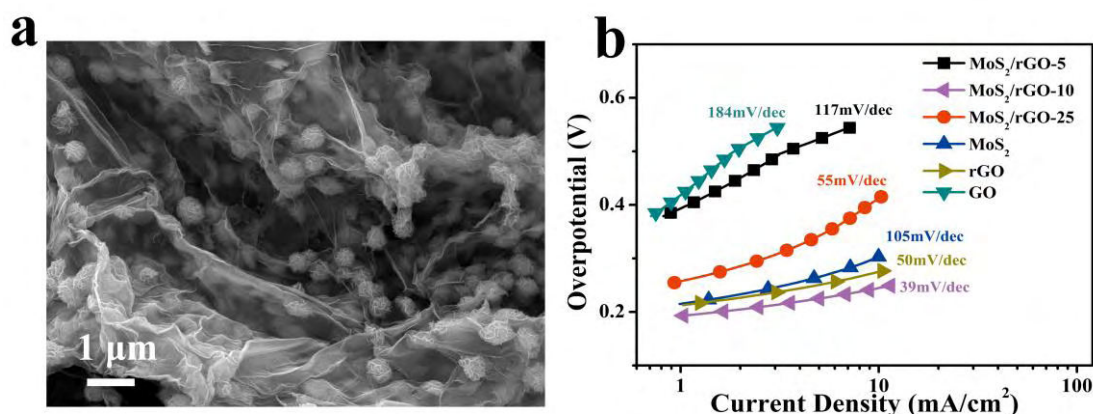


Figure 1: SEM image of MoS₂/rGO-10 sample (a) and the Tafel plots of the MoS₂/rGO with the content of 5 wt%, 10 wt%, 25 wt%, MoS₂, rGO and GO.

Ze Lin Tan

Ken Liu, Zhi Hong Zhu

National University of Defense Technology, No. 109 Deya Road, Kaifu District, Changsha, China

zelin_tan@163.com

Photoluminescence properties of WS₂ under optical irradiation

Two-dimensional transition metal dichalcogenides, like monolayer MoS₂ and WS₂, have been promising materials for on-chip light sources due to its direct-bandgap and convenient transfer characteristics [1]. Though these materials have more efficient optical gain and are easily integrated or transferred on various substrates, their photoluminescence properties can be influenced by ambient environment[2], different from III - V compound semiconductors. We show that the photoluminescence spectra of WS₂ are different on various substrates, and changes under continuous violet laser illumination. Because atmospheric moisture and oxygen adsorbed on WS₂ induce p-doping by chemical reaction [3], the densities of trions and neutral excitons have changed, resulting in the enhancement of photoluminescence intensity. However the monolayer WS₂ will be damaged by long-time laser irradiation. In order to extend the lifetime of WS₂, we coated it with Al₂O₃ to isolate air, and the stability was indeed improved. To design a commercial on-chip light sources, there are further studies required to do on these monolayer materials.

References

- [1] X. Wang, K. Kang, S. Chen, R. Du, E. H. Yang, *2D Mater.* (2017) 4, 025093.
- [2] Y. Yu, Y. Yu, C. Xu, Y. Q. Cai, L. Su, Y. Zhang, Y. W. Zhang, K. Gundogdu, L. Cao, *Adv. Funct. Mater* (2016) 26, 4733.
- [3] N. Peimyoo, W. Yang, J. Shang, X. Shen, Y. Wang, T. Yu, *ACS Nano* (2014) 8, 11320.

Figures

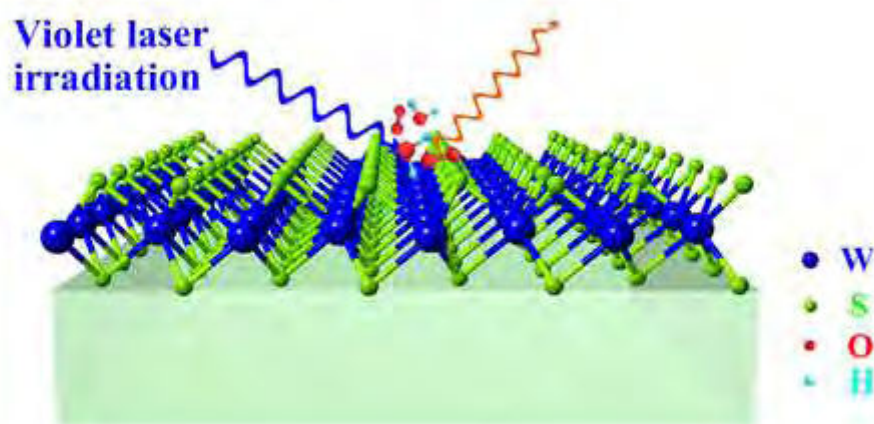


Figure 1: Schematic diagram illustrating light emission from monolayer WS₂ on substrate under violet laser irradiation

Chao Wang^{1,2}

Qiang Fu¹ and Xinhe Bao^{1,3}

¹State Key Laboratory of Catalysis, Dalian Institute of Chemical Physics, Chinese Academy of Sciences, Zhongshan Road 457, Dalian 116023, China

²University of Chinese Academy of Sciences, Beijing 100049, China

³University of Science and Technology of China, Hefei 230026, China

Chao0354@dicp.ac.cn

In-situ investigations of the rechargeable aluminum ion battery by XPS, Raman and optical microscope

Rechargeable aluminum ion battery is one of the most promising energy storage device owing to crustal abundance, high theoretical power density and excellent safety [1]. In 2015, Dai's group developed a novel aluminum ion battery (AIB) consisting graphitic foam cathode, aluminum anode, and AlCl_3 /1-ethyl-3-methylimidazolium chloride (EMIC) ionic liquid (IL) electrolyte exhibited ultrafast rechargeable rate and excellent cycle stability [2]. However, the fundamental science problems of AIB have been rarely studied by researchers. Herein, we built a model battery consisting highly oriented pyrolytic graphite (HOPG) cathode, Al foil anode and AlCl_3 /EMIC IL electrolyte. The same electrochemistry performance as the real ones such that the in-situ studies using Raman, XPS, and optical microscope can be performed with the model battery. By designing the transfer chamber and sample holder, in-situ XPS investigated of the electrochemical intercalation process of chloroaluminate anion-graphite system has been achieved for the first time. Except for XPS Al and Cl signals, we also observed the increase of N1s signal. We believe that there exists the co-intercalation of EMI^+ and AlCl_4^- , which has been further proved by in-situ Raman. By analyzing the binding energy, the electronic structure (work function, charge transfer) change of the graphite cathode has been revealed during the intercalation process. Furthermore, the in-situ observation of the HOPG during charging and discharging process via optical microscope could provide some intuitive information such as the diffusion of ions, color and macrostructure change of HOPG.

References

- [1] Li, Q. & Bjerrum, N. J et al J. Power Sources 110, (2002) 1–10.
- [2] Lin M C, Dai H J et al Nature 520 (2015) 325-328

Figures

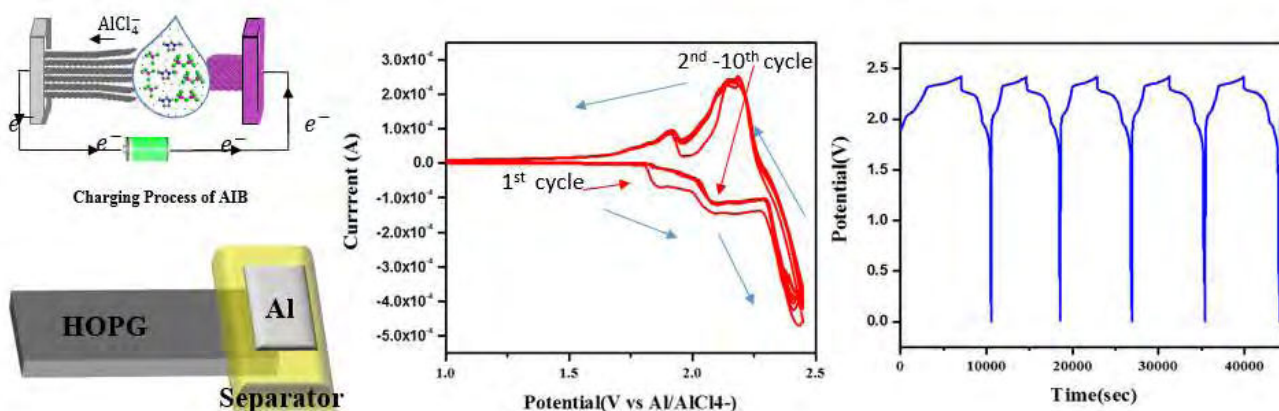


Figure 1: Left: the schematic diagram of the $\text{Al}|\text{EMIC}-\text{AlCl}_3$ (1:1.3 by mole) |HOPG model battery, notice that only one end of HOPG is submerged by electrolyte. Middle and right: CV curve (scan rate is 0.5mV/s) and the voltage profile of first five cycles, which exhibit the same performance with the real ones [2].

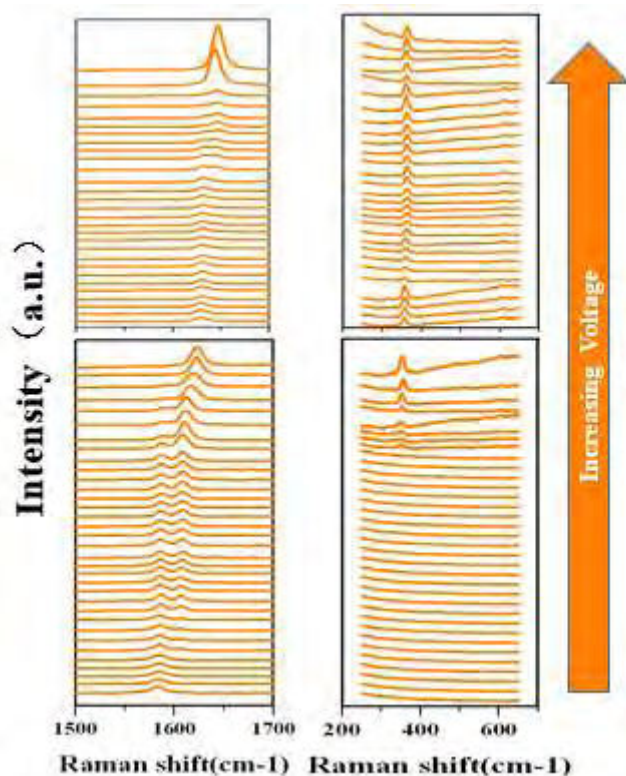


Figure 2: In-situ Raman spectra of the uncovered part of the HOPG electrode during charging process. Except for the typical change of the G band, the AlCl_4^- ($\sim 350\text{cm}^{-1}$) and EMI^+ ($\sim 600\text{cm}^{-1}$) have also been detected.

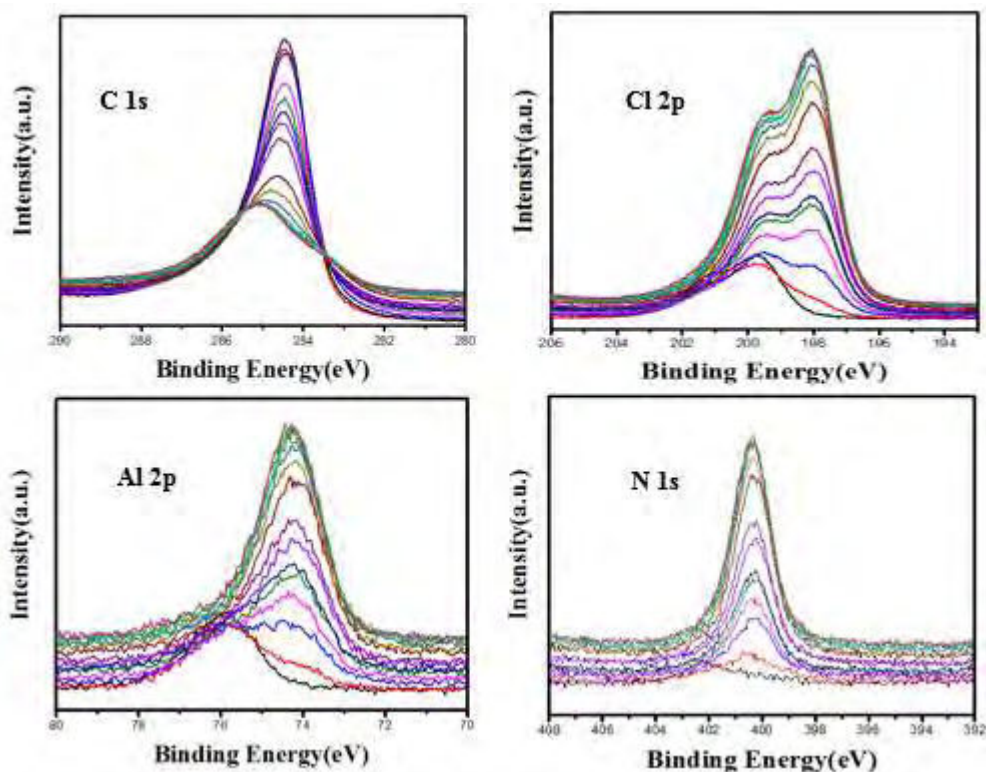


Figure 3: Similarly with the in-situ Raman, in-situ XPS spectra was collected from the uncovered part of HOPG electrode during charging process. As expected, the intensity of Al 2p and Cl 2p would increase because of the intercalation and the C 1s decrease because of the expansion. Furthermore, we also found the increase of N 1s signal. Combined with the Raman spectra, we assumed that there exist the co-intercalation of AlCl_4^- and EMI^+ .

Presenting Author: Sen Wang

Co-Authors: Zhong-Shuai Wu

Dalian Institute of Chemical Physics, CAS., 457 Zhongshan Road, Dalian, China.

Contact@E-mail:senwang@dicp.ac.cn

Scalable Fabrication of Monolithic Micro-Supercapacitors with Tailored Geometries for On-Chip Energy Storage

Abstract

Single-step scalable fabrication of micro-supercapacitors (MSCs) with both high energy and power densities is still challenging. To address this, we demonstrate the scalable fabrication of graphene-based monolithic MSCs with diverse planar geometries and capable of superior integration by photochemical reduction of graphene oxide/TiO₂ nanoparticle hybrid films. The resulting monolithic MSCs can operate well in a hydrophobic electrolyte of ionic liquid (3.0 V) at a high scan rate of 200 V s⁻¹, two orders of magnitude higher than those of conventional supercapacitors. More notably, the MSCs show landmark volumetric power density of 534 W cm⁻³ and energy density of 13.2 mWh cm⁻³, both of which are among the highest values attained for carbon-based MSCs. Therefore, such monolithic MSC devices based on photochemically reduced, compact graphene films possess enormous potential for numerous miniaturized, flexible electronic applications.

References

- [1] S. Wang, Z.S. Wu*, S.H. Zheng, F. Zhou, C.L. Sun, H.M. Cheng, X.H. Bao, ACS Nano, 11, (2017), 4283.
- [2] S. Wang, S.H. Zheng, Z.S. Wu*, C.L. Sun, Sci. Sin. Chim., 46 (2016), 732.
- [3] S.H. Zheng, X.Y. Tang, Z.S. Wu*, Y. Z. Tan, S. Wang, C.L. Sun, H.M. Cheng, X.H. Bao, ACS Nano, 11, (2017), 2171.
- [4] Z. S. Wu*, Y. Z. Tan, S.H. Zheng, S. Wang, K. Parvez, J.Q. Qin, X.Y. Shi, C.L. Sun, X.H. Bao, X.L. Feng*, K. Müllen*, J. Am. Chem. Soc., 139, (2017), 4506.

Figures

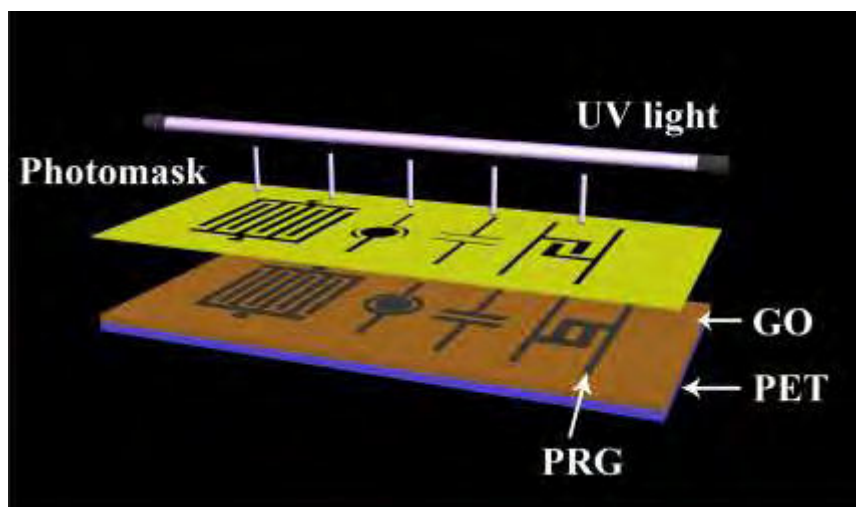


Figure 1: Scheme of fabricating PRG-MSCs with various tailored planar geometries.

Yijing Wang*

Weiqin Li, Yan Zhang, Huinan Guo

Key Laboratory of Advanced Energy Materials Chemistry (Ministry of Education), College of Chemistry, Nankai University, No. 94 Weijin Road, Tianjin, China

E-mail: wangyj@nankai.edu.cn

Rational design of 1D mesoporous MnO@C nanorods as anode material for improved Li-storage properties

As the rapid emerging of portable intelligent products and electromobile, lithium ion batteries (LIBs) have become the leading force of energy storage devices, due to its miniature and portability, high energy density, high working potential (~ 3.7 V) and long life span.^{[1],[2]} As an anode material for commercial LIBs, graphite has not met the demand of energy storage market owing to its low specific capacity ($372.0 \text{ mA h g}^{-1}$) and inferior rate capability.^{[3],[4]} Accordingly, it is of utmost urgency to develop an advanced anode material for LIBs application. Transition metal oxides (TMOs), owing to their high theoretical capacity and abundant resources, have attracted many researchers' attentions. Among them, MnO has been considered as promising anode candidate because of cost-effective, abundant resources and low reduction potential (~ 0.3 V vs. Li⁺/Li).^[5] However, MnO still have not escaped from intrinsic disadvantages, which are low electrical conductivity and large volumetric expansion during the charge-discharge processes. In order to address these challenges, we adopt in situ carbon coating method to synthesize 1D mesoporous MnO@C nanorods via a solvothermal reaction coupled with subsequent thermal treatment. In the preparation process, the homogeneous in situ carbon coating has been realized, and the diameter and pore size of nanorods are well regulated because of the solvent effect. According to different volume ratio of H₂O and isopropanol (IPA) in solvothermal reaction, the resultants are named as MnO@C-1 (the mixture: 40 ml IPA), MnO@C-2 (the mixture: 20 ml IPA and 20 ml H₂O) and MnO@C-3 (the mixture: 40 ml H₂O). As an anode for LIBs, MnO@C-3 displays remarkable excellent rate capability ($1202.6 \text{ mA h g}^{-1}$ at 0.1 A g^{-1} and $1085.7 \text{ mA h g}^{-1}$ at 2.0 A g^{-1} with the capacity retention of 90.3%). This fantastic improvement of electrochemical performances benefits from the synergistic effect of well-designed structure characteristics. Firstly, lots of carbon coating nanoparticles gather into 1D nanorods and form a large conductive network, which can immensely enhance material conductivity. Secondly, mesoporous structure can effectively remit the volume expansion and increase the contact area of electrode/electrolyte, contributing to lithiation and delithiation. These characteristics improve transfer efficiency of ion/electron during the charge-discharge processes, greatly upgrading rate capability.

This work was financially supported by the MOST (2016YFA0202500), NSFC (51471089, 51501072 and 51571124), MOE (IRT13R30), NSFT (17JCYBJC17900), and 111 Project (B12015).

References

- [1] Zheng, M.; Tang, H.; Li, L.; Hu, Q.; Zhang, L.; Xue, H.; Pang, H. *Adv. Sci.*, 3 (2018), 1700592.
- [2] Li, W.; Song, B.; Manthiram, A. *Chem. Soc. Rev.*, 10 (2017), 3006-3059.
- [3] Zhu, S.; Li, J.; Deng, X.; He, C.; Liu, E.; He, F.; Shi, C.; Zhao, N. *Adv. Funct. Mater.*, 9 (2017), 1605017.
- [4] Guo, H.; Chen, C.; Chen, K.; Cai, H.; Chang, X.; Liu, S.; Li, W.; Wang, Y.; Wang, C. *J. Mater. Chem. A*, 42 (2017), 22316-22324.
- [5] Zhang, K.; Han, X.; Hu, Z.; Zhang, X.; Tao, Z.; Chen, J. *Chem. Soc. Rev.*, 3 (2015), 699-728.

Figures

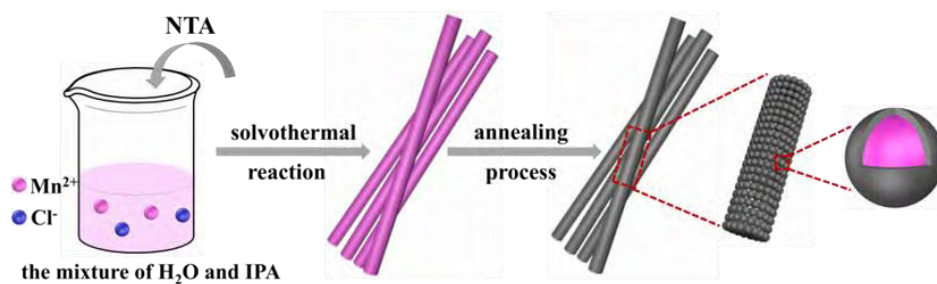


Figure 1: The schematic illustration of preparation process for 1D mesoporous MnO@C nanorods.

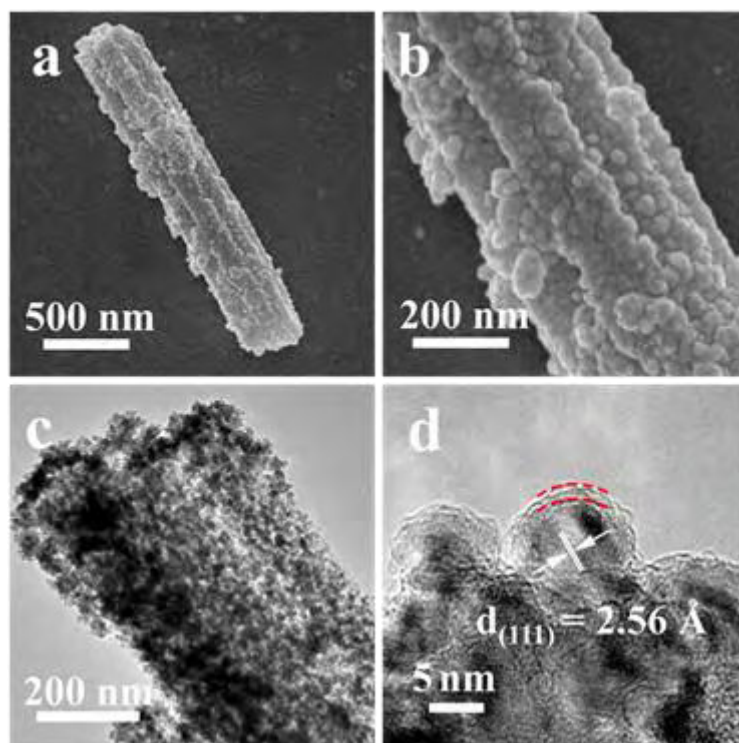


Figure 2: (a-b) SEM images, (c) TEM image and (d) HR-TEM image of MnO@C-3.

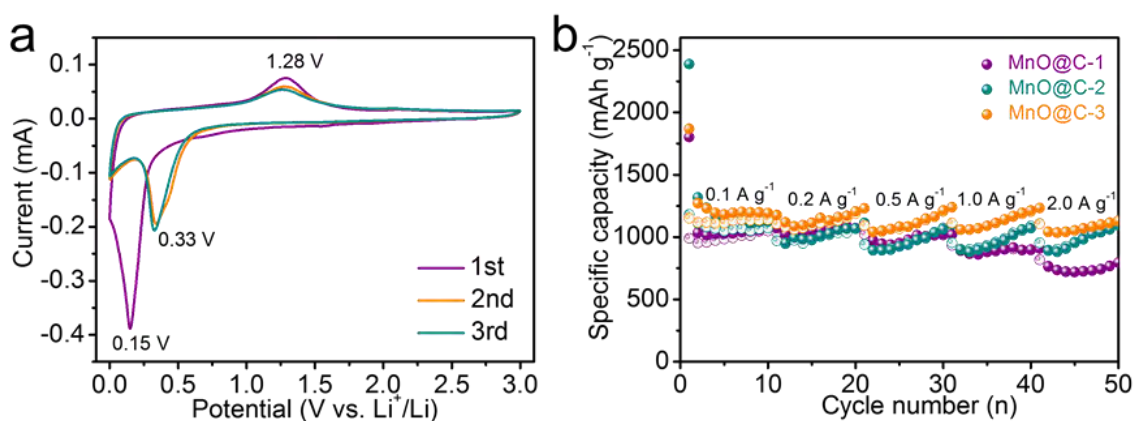


Figure 3: (a) CV curves with the potential of 0-3 V at the scan rate of 0.1 mV s⁻¹ for MnO@C-3. (b) The rate capabilities of MnO@C-1, MnO@C-2 and MnO@C-3.

Jindi Wei

Gengmin Zhang

Key Laboratory for the Physics and Chemistry of Nanodevices and Department of Electronics, Peking University, Beijing, China

weijindi@pku.edu.cn

Fabrication of a graphene edge based field emitter and its electron emission properties

Abstract

Graphene edges based field emitters were designed in this paper, which could be fabricated by using a scalable process. Advantages of the vacuum tube and transistor could be combined. The nanoscale vacuum tubes can provide high frequency/power output while satisfying the metrics of lightness, cost, lifetime, and stability at harsh conditions, and the operation voltage can be decreased comparable to the modern semiconductor devices. TWO pages abstract format: including figures and references.

References

- [1] Han J W, Oh J S, Meyyappan M, Applied Physics Letters, 100 (2012) 1858
- [2] Kumar S, Duesberg G S, Pratap R, et al, Applied Physics Letters, 105 (2014) 927
- [3] Wang H M, Zheng Z, Wang Y Y, et al, Applied Physics Letters, 96 (2010) 666
- [4] Ji X, Wang Q, Zhi T, et al, Acs Applied Material Interfaces, 8 (2016) 3295

Figures

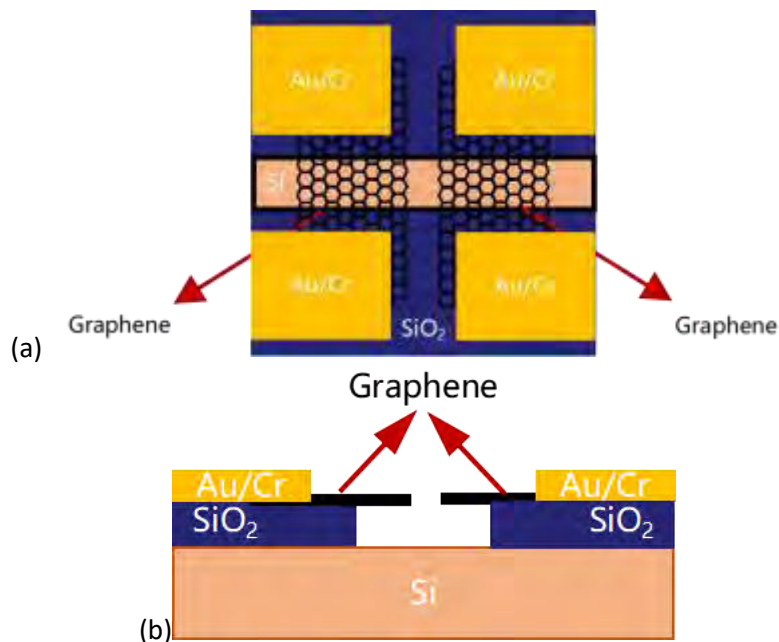


Figure 1: (a)Top and (b) lateral view of the graphene based field emitters

Yongpeng Xia

Li Zhao, Xia Yang, Huanzhi Zhang, Fen Xu, Lixian Sun*

(Guangxi Key Laboratory of Information Materials, School of Material Science and Engineering, Guilin University of Electronic Technology, Guilin, 541004, P. R. China)

sunlx@guet.edu.cn

Significant improved dehydrogenation of LiAlH₄ doped with two-dimensional Ti₃C₂

Lithium alanate (LiAlH₄) has attracted intense interest as one of the most promising candidates for hydrogen storage due to its high hydrogen storage capacity (10.5 wt%) and low cost. However, the drawbacks of its dehydrogenation process are the relatively high temperatures and the slow dehydrogenation kinetics. In this study, a two-dimensional Ti₃C₂ MXene was doped into LiAlH₄ to improve its hydrogen storage properties. The composition evolution and dehydrogenation performance of the as-prepared sample were characterized by means of XRD (X-ray diffraction), FT-IR (Fourier transform infrared spectroscopy) and Sieverts-type pressure-composition-temperature apparatus (PCT) measurements, respectively. LiAlH₄-5 wt% Ti₃C₂ samples start to release hydrogen at 48.8 °C, which is 154.2 °C lower than that of as-received LiAlH₄. Isothermal desorption measurements show that the 5 wt% Ti₃C₂-doped sample releases 5.3 wt% of hydrogen within 15 min at 200 °C.

This work was financially supported by the National Natural Science Foundation of China (Grant No. 51361005, U1501242, 51371060, 51671062, 51102230 and 51462006), the Guangxi Natural Science Foundation (No. 2014GXNSFAA118319, 2014GXNAFDA118005, 2014GXNSFAA118401 and 2013GXNSFBA019244), Guangxi Key Laboratory of Information Materials (161002-Z, 161002-K), Guangxi Scientific Technology Team (2012GXNSFGA06002).

Figures

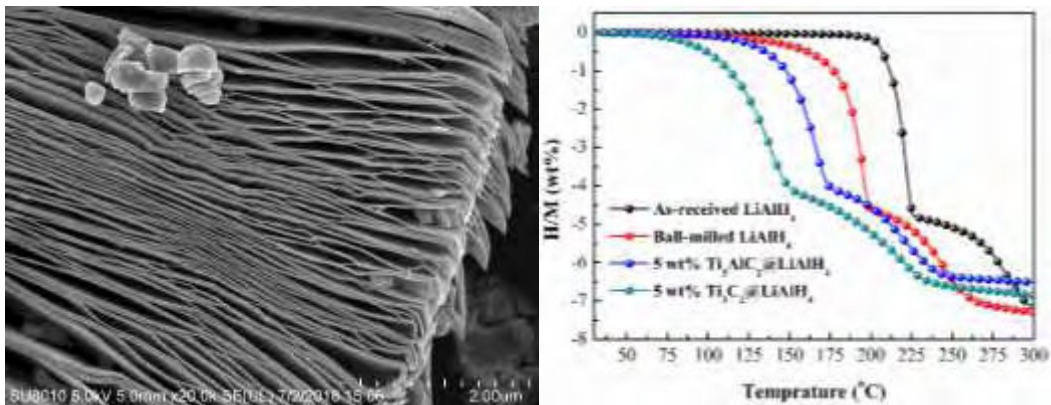


Figure 1: Fig.1 SEM images of Ti₃C₂

Figure 2: Volumetric release curves of the prepared samples.

Fen Xu*

Chaochao Xu, Fen Xu*, Lixian Sun*

(School of Material Science and Engineering, Guilin University of Electronic Technology, Guilin, 541004, P. R. China

xufen@guet.edu.cn

Synthesis of bio-based porous carbon and its application in supercapacitors

Supercapacitors have widespread applications in the field of electrical energy storage devices due to their high power density, fast charge-discharge rate and environmental friendliness¹. Nowadays, porous carbon materials, especially biomass carbons, have been widely used in supercapacitors due to their low cost and sustainability. In this work, we synthesized bio-based porous carbon using cycas leaves as carbon precursor and urea as the nitrogen source; Namely, the dried cycas leaves firstly is burned at 300 °C and then activated by KOH containing urea at 700 °C. Experimental results show that the as-prepared bio-based carbon material displays high specific surface area and suitable pore size for supercapacitor. The supercapacitor performance of as-prepared bio-based carbon material has been investigated in a 2-electrode system (see Fig. 1). As shown in Fig. 1a, the CV curves of as-prepared carbon material show an approximate rectangular shape at all voltage scan rates. Its linear GCD curves at all current densities appear an isosceles triangle (see Fig. 1b). According to literature established equations², their specific capacitances are 260 F/g at 0.5 A/g and 203 F/g at 10 A/g (78% of the capacitance retention), respectively. Meanwhile, its energy density for the supercapacitor is about 9.13 W h/kg at a power density of 125 W/kg. In addition, an energy storage device was fabricated (see Fig.1c). Fig. 1c demonstrates that the simple energy storage device can power for a light-emitting diode (LED).

Acknowledgements

This work was supported by the National Natural Science Foundation of China (U1501242 and 51671062), the Guangxi Collaborative Innovation Centre of Structure and Property for New Energy and Material (2012GXNSFGA06002), Guangxi Science and Technology Project (AD17195073), Guangxi Major Science and Technology Special Project (AA17202030-1) and the Guangxi Key Laboratory of Information Laboratory Foundation (161002-Z, 161002-K and 161003-K).

References

- (1) P. Simon, Y. Gogotsi and B. Dunn, *Science* 343, 2014, 1210–1211.
- (2) Cunjing Wang, Dapeng Wu, Hongju Wang, et al, *Journal of Materials Chemistry A*, 6, 2018, 1244-1254.

Figures

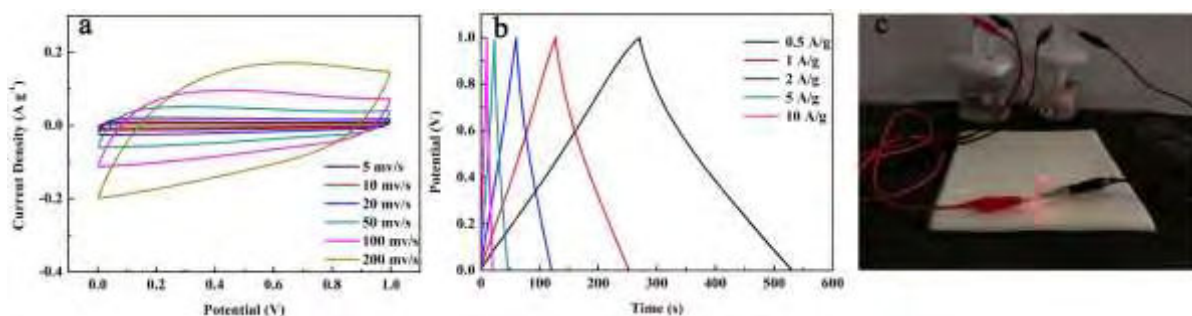


Figure 1: CV curves at various scan rates of 5–200 mV/s; b: GCD curves tested at 0.5 – 10 A/g; c: a energy storage device of supercapacitors made by as-prepared bio-carbon material.

Aikai Yang

Zhiqiang Luo, Qing Zhao, Jun Chen*

Key Laboratory of Advanced Energy Materials Chemistry (MOE), College of Chemistry, Nankai University, Tianjin 300071, China

chenabc@nankai.edu.cn

Organic Molecules Grafted onto Graphene Enable Superior Lithium-Ion Batteries

Abstract

A key challenge faced by organic electrodes is how to promote the redox reactions of functional groups to achieve high-rate capability and long cycling life. One efficient strategy is to stitch organic molecules onto insoluble substrates and inhibit the dissolution. Graphene is a promising alternative with high electronic conductivity, two-dimensional pores and intrinsically insoluble features, which favors promoting the diffusion of ions and conduction of electrons and suppressing the dissolution of organic active materials into aprotic electrolytes. Here we report that the combination of poly(imide-benzoquinone) (PIBN) and tetralithium salts of 2,5-dihydroxyterephthalic acid ($\text{Li}_4\text{C}_8\text{H}_2\text{O}_6$) with the graphene substrate exhibits high electrochemical performance in lithium ion batteries for organic electrodes based on the in-situ synthesis and recrystallization method. This enables large reversible specific capacities of 271 (0.1 C) and 193 (10 C) mA h g^{-1} and retention of 86% after 300 cycles for PIBN-graphene (PIBN-G) composite as well as over 1000 cycles at 10 C and high capacities of 191 and 121 mA h g^{-1} after 100 and 500 cycles for the $\text{Li}_4\text{C}_8\text{H}_2\text{O}_6$ -graphene ($\text{Li}_4\text{C}_8\text{H}_2\text{O}_6$ -G) composite. Our results indicate a useful strategy for obtaining high-performance organic batteries and a practical way of application of graphene.

References

- [1] Z. Luo, L. Liu, J. Ning, K. Lei, Y. Lu, F. Li, J. Chen, *Angew. Chem. Int. Ed.*, 57(2018) 9443-9446
- [2] Q. Zhao, J. Wang, C. Chen, T. Ma, J. Chen, *Nano Res.*, 10(2017) 4245-4255

Figures

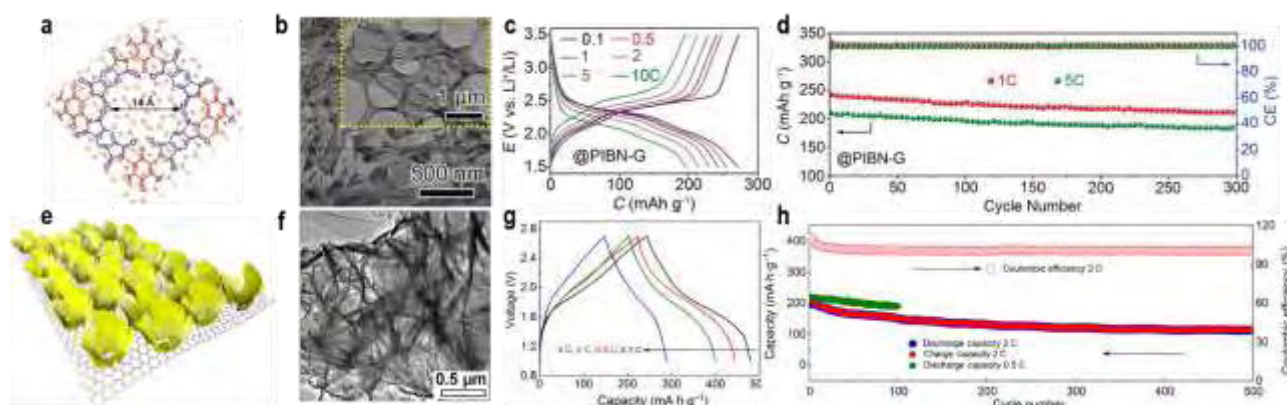


Figure 1: a. Schematic of PIBN-G composite. b. SEM image with an inset of TEM image of PIBN-G. c and d. Discharge/charge profiles and cycle stability of PIBN-G. e. Schematic of $\text{Li}_4\text{C}_8\text{H}_2\text{O}_6$ -G composite. f. TEM image of $\text{Li}_4\text{C}_8\text{H}_2\text{O}_6$ -G composite. g and h. Discharge/charge profiles and cycle stability of all-organic symmetrical cells with the $\text{Li}_4\text{C}_8\text{H}_2\text{O}_6$ -G composite as both the anode and the cathode.

Yusi Yang

Xia Wang, Shun-Chang Liu, Zongbao Li, Zhaoyang Sun, Chunguang Hu, Ding-Jiang Xue,* Gengmin Zhang* and Jin-Song Hu*

Key Laboratory for the Physics and Chemistry of Nanodevices and Department of Electronics, Peking University, Beijing, China

yangys1995@pku.edu.cn

Weak Interlayer Interaction in Anisotropic GeSe₂

As an emerging anisotropic material with wide band gap, GeSe₂ is regarded as a promising candidate for polarization-dependent devices, such as polarization-sensitive photodetectors and optical waveplates. Except for in-plane anisotropies, another unique property, weak interlayer coupling, is firstly discovered in this work. Here, electronic structures of GeSe₂ are investigated and a minor change is found from monolayer to bulk. Cleavage energy, interlayer binding energy and interlayer differential charge density are also calculated, demonstrating that GeSe₂ processes much weaker interlayer coupling when compared with BP, a typical represent of anisotropic materials. Experimental studies including Raman spectra of different thickness and temperature-dependent Raman spectroscopy further confirm weakly coupled layers in GeSe₂. Our results introduce GeSe₂ as a complement to anisotropic two-dimensional material family with weak interlayer interaction.

References

- [1] S. Tongay, H. Sahin, C. Ko, A. Luce, W. Fan, K. Liu, J. Zhou, Y.-S. Huang, C.-H. Ho, J. Yan, D. F. Ogletree, S. Aloni, J. Ji, S. Li, J. Li, F. M. Peeters, J. Wu, *Nature Communications* 5(2014), 3252.
- [2] Y. Jing, Y. Ma, Y. Li, T. Heine, *Nano Lett.* 17(2017), 1833-1838.
- [3] Y. Zhao, J. Qiao, P. Yu, Z. Hu, Z. Lin, S. P. Lau, Z. Liu, W. Ji, Y. Chai, *Adv. Mater.* 28(2016), 2399-2407.

Figures

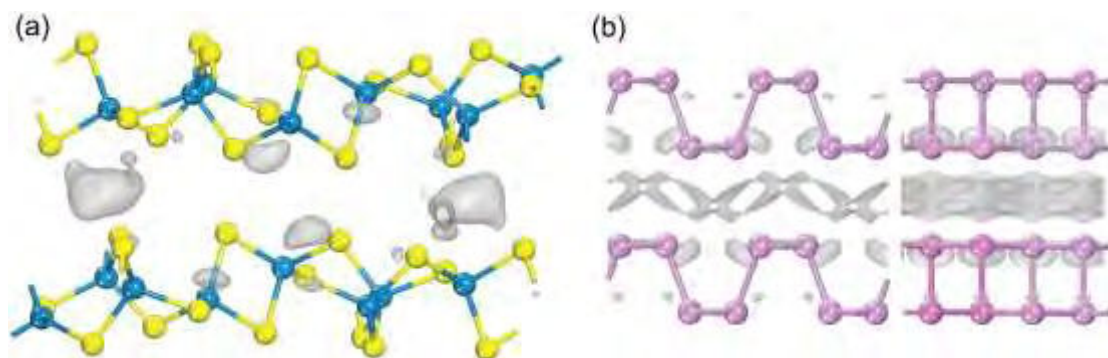


Figure 1: Interlayer differential charge density of (a) GeSe₂ and (b) BP, respectively.

Minjie Yao

Xinyu Wang, Zhiqiang Niu*, Jun Chen

Key Laboratory of Advanced Energy Materials Chemistry (MOE), College of Chemistry, Nankai University, Tianjin 300071, China

zqniu@nankai.edu.cn

Large-Area Reduced Graphene Oxide Composite Films for Flexible Asymmetric Sandwich and Microsized Supercapacitors

Abstract

Asymmetric supercapacitors have attracted tremendous attention in energy storage devices due to their enhanced energy density. The development of asymmetric supercapacitor matching with diverse and flexible electronic devices depends mainly on the preparation of flexible components and the design of various configurations. Graphene and its derivatives are typical 2D materials and can serve as the building blocks to construct freestanding macroscopic graphene with porous structures, high electrical conductivity and excellent mechanical flexibility. Herein, a spontaneously reducing/assembling strategy in alkaline condition is developed to fabricate large-area reduced graphene oxide (RGO) and RGO-metal oxide/hydroxide composite films or microsized structures. The obtained pure RGO and RGO/Mn₃O₄ composite films possessing porous structure and superior mechanical property can directly serve as the electrodes of flexible asymmetric sandwich supercapacitors. Furthermore, the interdigital RGO and RGO/Mn₃O₄ patterns are also assembled via a selectively reducing/assembling process to achieve the asymmetric microsized supercapacitors. These asymmetric supercapacitors with different configurations exhibit excellent electrochemical performance and flexibility. Such reducing and assembling strategy provides a route to achieve large-area RGO-based films and microsized structures for the applications in the various fields such as energy storage and photocatalysis.

References

- [1] X. Wang, Niu Z.*, et al. Adv. Funct. Mater. 2018,28,1707247

Figures

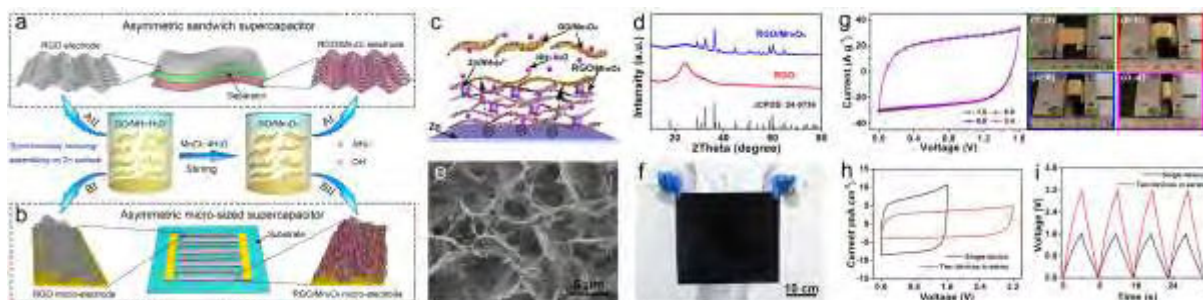


Figure 1: Schematic illustrating the synchronously reducing/assembling strategy in an alkaline solution to prepare the RGO and RGO/Mn₃O₄ electrodes of a) asymmetric sandwich and b) microsized supercapacitors. c) Schematic mechanism of synchronously reducing and assembling RGO/Mn₃O₄ composite film in NH₃·H₂O solution on Zn surface. d) XRD patterns of RGO and RGO/Mn₃O₄ films. e) SEM image of RGO/Mn₃O₄ composite film. f) Optical image of a RGO/Mn₃O₄ composite film (≈1200 cm⁻²). g) CV curves under different values of L/L_0 , inset optical images: L_0 is the initial length of substrates, and L is the distance between two ends of films in different bending states. h) CV curves of two asymmetric microsized supercapacitors in series and a single device, scan rate: 10 V s⁻¹. i) GCD curves of the two asymmetric microsized supercapacitors in series and a single device, current density: 0.4 mA cm⁻².

Shilu Yin

Lixian Sun, Fen Xu, Yongpeng Xia, Feifei Wang, Jinyang Hu, Jinghua Li

Guilin University of Electronic Technology, 1 Jinji Road, Guilin, China

shiluy@foxmail.com

Synthesis and electrochemical properties of phosphorus doped GO/porous carbon

Supercapacitor is a kind of green device between traditional capacitor and battery, because of its high power density, light weight, multiple charge and discharge, long cycle life as well as maintenance-free, and become a new type of energy storage device^[1]. As an useful, efficient, environmental friendly energy storage device, It has broad prospects. Graphene has excellent optical, mechanical and electrical properties. Graphene oxide has attracted much attention because of its lamellar structure and high conductivity. In recent years, many researchers have used GO to make electrode materials for supercapacitors. Porous carbon as one of promising materials is widely used in supercapacitors. And adding GO in carbon materials can effectively improve the conductivity of carbon materials. However, pure carbon material due to its surface hydrophobicity, large internal resistance, its development has been severely constrained^[2]. The introduction of phosphorus elements, can effectively enhance the performance of porous carbon^[3]. Therefore, phosphorus doped GO/porous carbon materials in recent years has been a wide range of attention and research.

In this study, As the precursor, phosphorus doped GO/sodium alginate composite by sol-gel method. At the same time, sodium alginate and GO as carbon source, sodium hypophosphite as phosphorus source while Iron nitrate as catalyst and porogenic agent. The precursor was freeze-dried for 48 hours and activated by KOH. Finally, the mixture was carbonized to 700 degrees in N₂ atmosphere to obtain phosphorus doped GO/porous carbon. The results showed that the mass ratio of sodium alginate to sodium hypophosphite was 1:1, the porous carbon material possesses the best electrochemical performance with a high specific capacitance of about 348 F g⁻¹ at a current density of 0.5 A g⁻¹. Moreover, its cyclic voltammetry curve shows a good rectangular shape. From the SEM, It was obviously find that the GO lamellar structure interspersed and constructed three-dimensional porous carbon materials. As a result, the composite porous carbon materials demonstrate an effective improvement of the performance for the electric double layer capacitor and great potential in supercapacitors.

References

- [1]. Q Long ,W Chen ,H Xu ,X Xiong ,Y Jiang etc. *Energy & Environmental Science* , 2013,6 (8) :2497-2504
- [2]. X Yan ,Y Liu ,X Fan ,X Jia ,Y Yu etc, *Journal of PowerSources* , 2014 , 248 (248) :745-751
- [3]. J Chen ,H Wei ,H Chen ,W Yao , H Lin etc, *Electrochimica Acta* , 2018 , 271

Figures

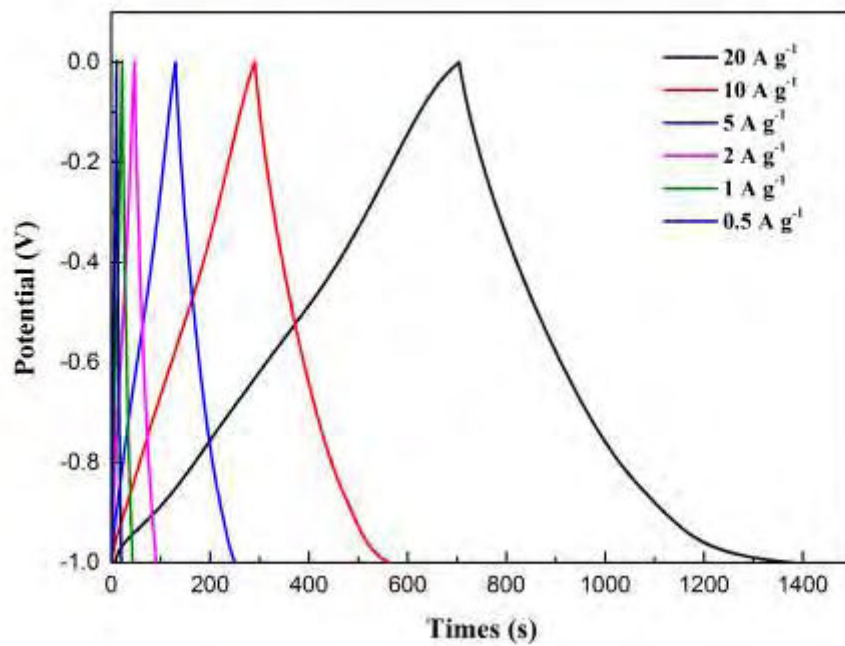


Figure 1. the charge discharge curves of 0.40-GO/SA at current density from $0.5 A g^{-1}$ to $20A g^{-1}$

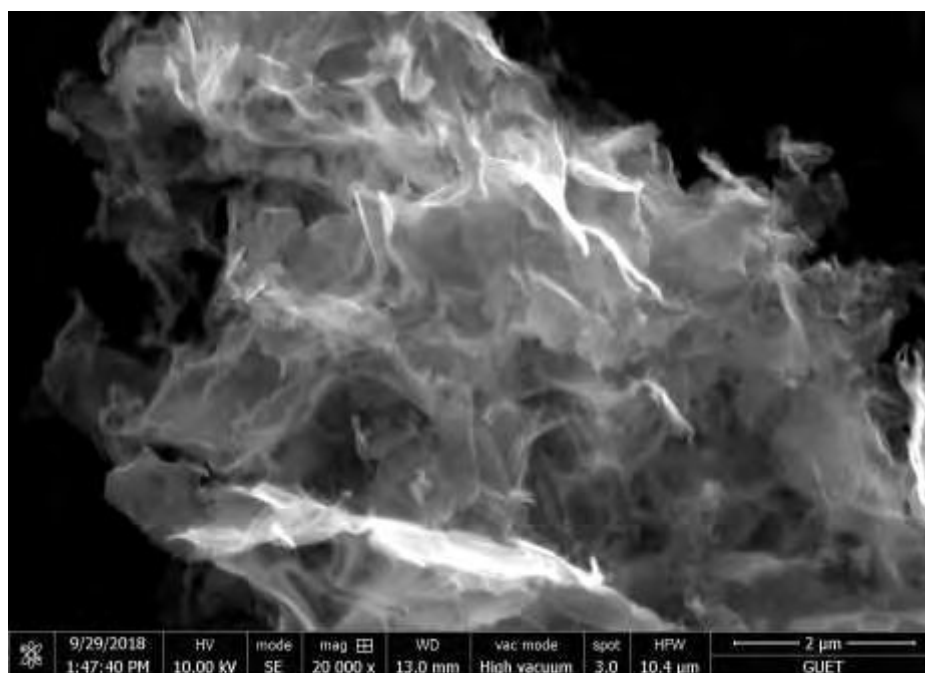


Figure2. SEM of 0.40-GO/SA at 20K magnification

Zhengxuan Yin

Chenchen Wang, Kaixiang Lei, Fujun Li

Key Laboratory of Advanced Energy Materials Chemistry (Ministry of Education), College of Chemistry, Nankai University, Tianjin 300071, PR China

fujunli@nankai.edu.cn

High Na/K-storage performance of bismuth enabled by ether-based electrolytes

Abstract

Sodium and potassium-ion batteries have attracted extensive attention due to the abundance and low cost of sodium and potassium resource. However, large size of Na⁺/K⁺ and formation of dendrite make it hard to find appropriate anode materials. Alloying anodes provide high capacity and modest voltage but suffer from large volume change and pulverization. Here, we reported bulk bismuth with excellent Na/K-storage performance enabled by ether-based electrolytes. During cycling, the electrode undergoes reversible phase reactions of Bi ↔ NaBi ↔ Na₃Bi and KBi₂ ↔ K₃Bi₂ ↔ K₃Bi, respectively. In ether-based electrolytes, a stable solid electrolyte interface is formed and the morphology of the electrode also gradually develops into a porous network, realizing fast kinetics and tolerance of its volume change. Both stable solid electrolyte interface and porous morphology contribute to the good performance in sodium-ion battery and potassium-ion battery. This interplay between electrolyte and electrode to boost Na/K-storage performance will pave a new way in energy storage.

References

- [1] Kaixiang Lei, Chenchen Wang, Luojia Liu, Yuwen Luo, Chaonan Mu, Fujun Li, and Jun Chen *Angew .Chem.* 2018, 57,4687–469
- [2] Chenchen Wang, Liubin Wang, Fujun Li, Fangyi Cheng, and Jun Chen *Adv. Mater.* 2017, 29, 1702212

Huanzhi Zhang

Yongpeng Xia, Rong ji, Chaowei Huang, Fen xu, Lixian Sun*

Guilin University of Electronic Technology, No.1 Jinji Road, Guilin, China

zhanghuanzhi@guet.edu.cn; sunlx@guet.edu.cn

Graphene-enhanced Composite Phase Change Materials for Thermal Energy Storage

Abstract

Graphene is quite famous for its high specific surface area ($\geq 2600 \text{ m}^2 \text{ g}^{-1}$) and superior thermal conductivity of $5000 \text{ W}/(\text{m} \cdot \text{K})$ [1]. Thus, graphene has been used widely as a filler to fabricate highly thermal conductive composites. [2] In addition, graphene is light in weight and meanwhile possesses inherent good flexibility, high tensile modulus or Young's modulus (1100 GPa) and the ultimate strength (116 GPa) [3]. Consequently, graphene was considered as an ideal material to improve thermal conductivity and comprehensive performances of composite phase change materials (PCMs) in our present studies. Firstly, three-dimensional graphene (3D-GA) was creatively synthesized through hydrothermal methods using graphene oxide (GO) as a precursor and ethylenediamine (EDA) as a moderate reducing agent. And *n*-octadecane (OD)/3D-GA composite PCMs were successfully prepared by solution impregnation and vacuum impregnation methods. Structural characterization and morphology of the composite PCMs confirm that there was no strong chemical interaction between OD and 3D-GA, and OD was successfully filled into the porous structure of 3D-GA by physical interaction (observed from Figure 1(a)). Furthermore, the composites have a much better phase change property, and the melting enthalpy and crystallization enthalpy can reach 195.70 J g^{-1} and 196.67 J g^{-1} , respectively. Moreover, the composite PCM has excellent thermal cycling stability and the phase change enthalpy almost has no obvious change after 60 times of DSC thermal cycling (observed from Figure 1(b)). The thermal conductivity of the composite PCMs can be enhanced to $1.636 \text{ W m}^{-1} \text{ K}^{-1}$ indicating a connected thermal conductive network between OD and 3D-GA. Secondly, we used PEG as PCMs, 4,4'-diphenylmethane diisocyanate (MDI) as the cross-linking agent, and GO was selected as a supporting skeleton to design a novel polymer based solid-solid composite PCMs. Results reveal that GO nano-sheets induced a regular lamellar structure and an interconnected thermal conductive network for the composite PCMs, and PEG was homogeneously intercalated into the GO nano-sheets (observed from Figure 2). This molecular structure supplies the SSPCMs with excellent phase change behavior, good thermal cycling stability and high thermal conductivity. As a result, the SSPCMs display a fast thermal-response rate and outstanding thermal regulating performance, which can maintain their temperature in the range of $50 \text{ }^\circ\text{C} \sim 57 \text{ }^\circ\text{C}$ for about 410 s.

References

- [1] O. C. Compton, S. B. T. Nguyen, Graphene Oxide, Highly Reduced Graphene Oxide, and Graphene: Versatile Building Blocks for Carbon-Based Materials, *Small* 6 (2010) 711-723
- [2] S. Park, S. He, J. Wang, A. Stein, C. W. Macosko, Graphene-polyethylene nanocomposites: Effect of graphene functionalization, *Polymer* 104 (2016) 1-9.

Figures

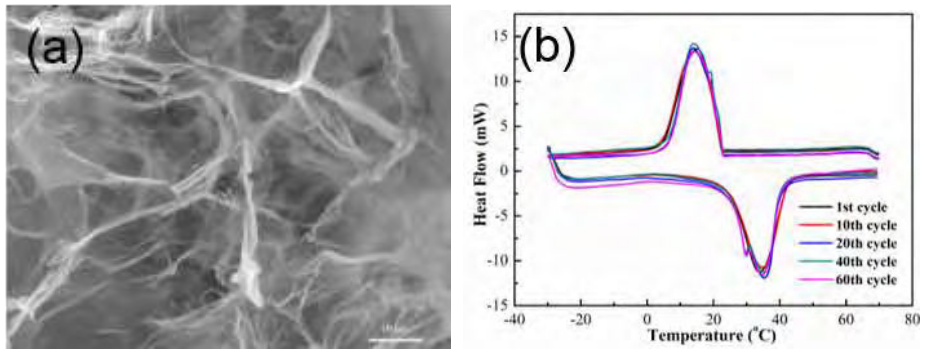


Figure 1: SEM images and thermal -regulating properties of OD/3D-GA composite PCMs

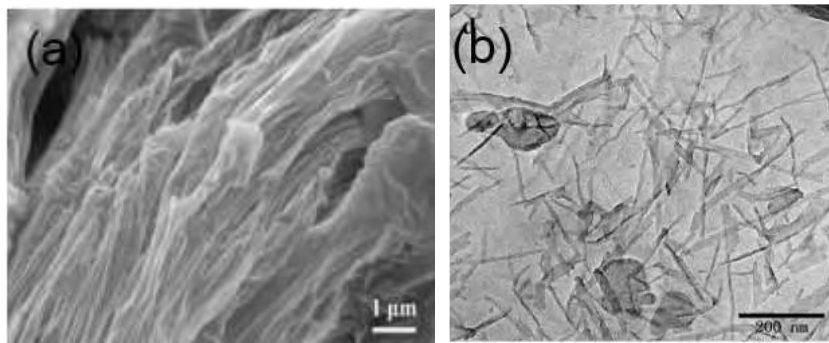


Figure 2: SEM images (a) and TEM images (b) of solid-solid composite PCMs

Super-clean graphene film: synthesis, transfer and applications

Abstract

The atomically thin two-dimensional nature of suspended graphene membranes holds promising in numerous technological applications. In particular, the outstanding transparency to electron beam endows graphene membranes great potential as a candidate for specimen support of transmission electron microscopy (TEM). However, major hurdles remain to be addressed to acquire an ultraclean, high-intactness, and defect-free suspended graphene membrane. Here, we have achieved a polymer-free clean transfer of sub-centimeter-sized graphene single crystals onto TEM grids to fabricate large-area and high-quality suspended graphene membranes. Through the control of interfacial force during the transfer, the intactness of large-area graphene membranes can be as high as 95%, prominently larger than reported values in previous works. Graphene liquid cells are readily prepared by π - π stacking two clean single-crystal graphene TEM grids, in which atomic-scale resolution imaging and temporal evolution of colloid Au nanoparticles were recorded. This facile and scalable production of clean and high-quality suspended graphene membrane is promising towards their wide applications for electron and optical microscopy.

References

- [1] Hao, Y.; Bharathi, M. S.; Wang, L.; Liu, Y.; Chen, H.; Nie, S. *Science* 342, 720 (2013).
- [2] Lin, Y. C.; Lu, C. C.; Yeh, C. H.; Jin, C. *Nano Lett.* 12, 414 (2012).

Figures

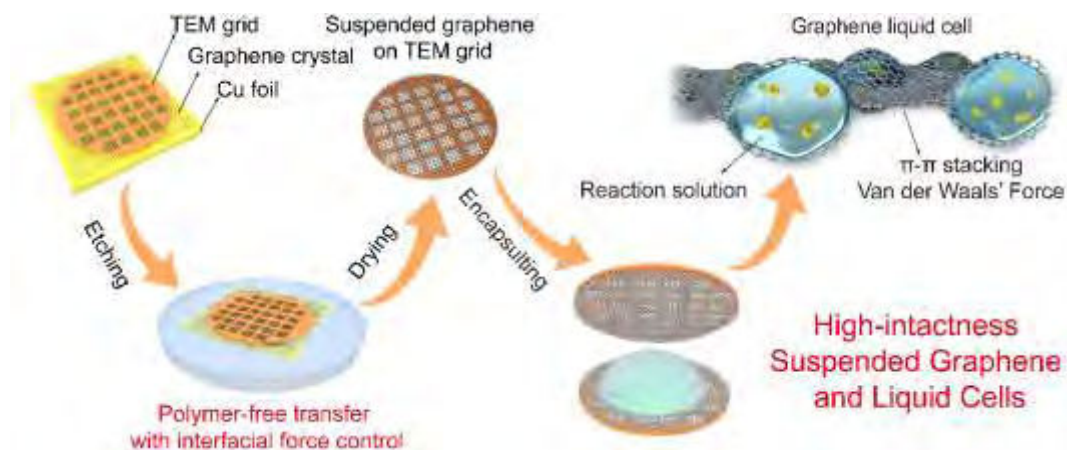


Figure 1: Schematic illustration of the procedures from clean transfer of graphene single crystals to fabrication of graphene liquid cells

Two-dimension Sulfide Anodes for Sodium-ion Batteries

Two-dimension (2D) materials, such as molybdenum disulfide (MoS_2), iron disulfide (FeS_2), have received widely interest in electrode materials for rechargeable batteries owing to their 2D structure, low cost, natural abundance and high theoretical capacity. Here, we report the application of MoS_2 [1], FeS_2 [2] as the anodes of sodium-ion batteries. Based on the selected compatible ether-based electrolyte and the tuned cut-off voltage, both of two sulfides show an intercalation mechanism rather than a conversion reaction, refraining from the huge volume change caused by phase conversion. MoS_2 nanoflower with expanded interlayer shows high discharge capacities of 350 mAh g^{-1} at 0.05 A g^{-1} , and 195 mAh g^{-1} at 10 A g^{-1} . FeS_2 microsphere exhibits high-rate capability (170 mAh g^{-1} at 20 A g^{-1}) and long-term cycling ($\sim 90\%$ capacity retention for 20000 cycles). The superior electrochemical performance of the two sulfides demonstrates the feasibility for their practical application.

References

- [1] Z. Hu, L. Wang, K. Zhang, J. Wang, F. Cheng, Z. Tao, J. Chen, *Angew. Chem. Int. Ed.*, 53(2014), 12794–12798.
- [2] Z. Hu, Z. Zhu, F. Cheng, K. Zhang, J. Wang, C. Chen, J. Chen, *Energy Environ. Sci.*, 8(2015), 1309–1316.
- [3] Y. Lu, N. Zhang, S. Jiang, Y. Zhang, M. Zhou, Z. Tao, L. A. Archer, J. Chen, *Nano Lett.*, 17(2017), 3668–3674.

Figures

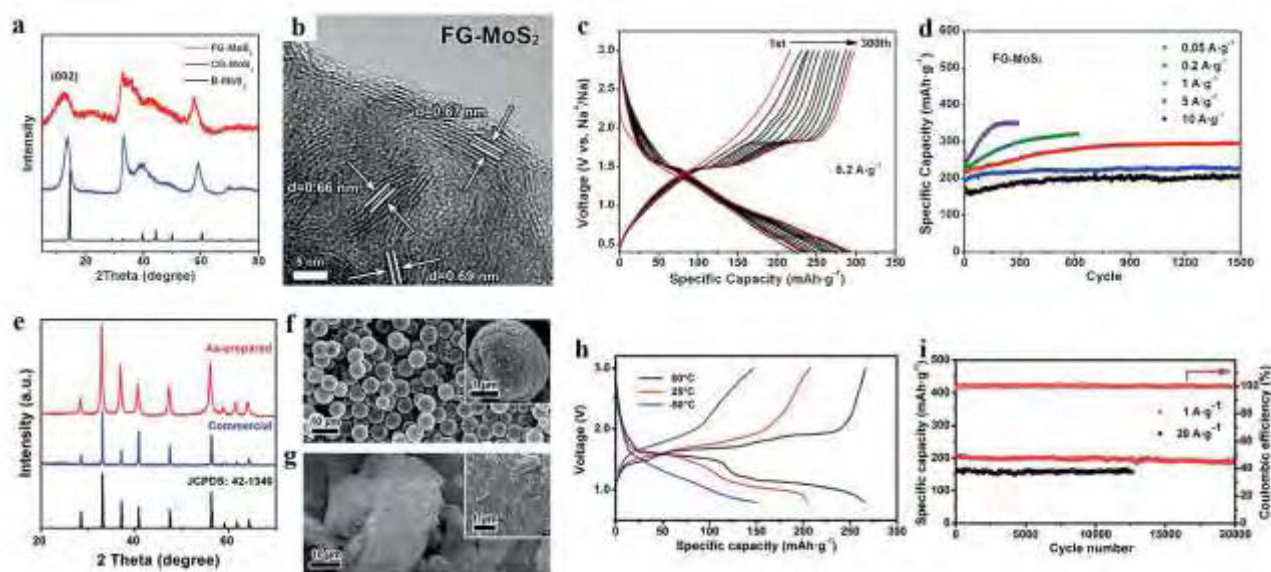


Figure 1: (a) XRD patterns of the MoS_2 samples and (b) HRTEM images of FG- MoS_2 . (c) The charge-discharge curves from 1st to 300th cycle and (d) the cyclic properties at different rates of FG- MoS_2 . (e) XRD patterns and (f,g) SEM images of FeS_2 microspheres and commercial FeS_2 . (h) Charge-discharge profiles at 1 A g^{-1} at different temperatures. (i) Cycling performance of FeS_2 microspheres.

Shuqing Zhang

Xiaolong Zou, Huiming Cheng

Tsinghua-Berkeley Shenzhen Institute, Nanshan I Park, Shenzhen, China

zhangshuqing@sz.tsinghua.edu.cn

High temperature half-metallicity in 2D CoGa_2X_4 ($\text{X}=\text{S}, \text{Se}, \text{Te}$)

The recent discovery of intrinsic ferromagnetic CrI_3 and $\text{Gr}_2\text{Ge}_2\text{Te}_6$ within 70 K creates huge potential for spintronic applications of 2D van der Waals crystals.^[1, 2] However, large spin polarization, high phase transition temperature and controllable spin direction are crucial requirements for the spintronic applications of atomically thin magnets. Here, we discover a class of CoGa_2X_4 ($\text{X}=\text{S}, \text{Se}$ or Te) monolayer with triangular lattice exhibiting intrinsic half-metallic ferromagnetism. They have large spin gaps in the semiconducting channel, ranging from 2.7 eV for CoGa_2S_4 to 1.7 eV for CoGa_2Te_4 , which makes them stable against the spin flip under weak external disturbances. The magnetocrystalline anisotropy (MAE) calculation with spin-orbital coupling SOC indicates CoGa_2X_4 possesses easy plane magnetization, which is expected to have a Berezinskii–Kosterlitz–Thouless transition by classical XY model. The critical temperatures are 886 K, 752 K, and 719 K for CoGa_2S_4 , CoGa_2Se_4 and CoGa_2Te_4 , respectively. The MAE of CoGa_2X_4 are 47 μeV for $\text{X}=\text{S}$, 84 μeV for $\text{X}=\text{Se}$ and 622 μeV for $\text{X}=\text{Te}$. The in-plane magnetic moments change to out-of-plane direction if the lattice constants increase from 3.623 Å to 3.75 Å (increase 3.5%), which can be realized through substrate mismatch or other bilayer strain methods. The proposed half-metallic CoGa_2X_4 system belongs to the big family of layered AB_2X_4 compounds, which is a significant part of layer-type phases. The stable and steerable magnetization with 100% spin-polarization ratio of CoGa_2X_4 would broaden the available design space for spintronics, and connect the magnetic with electronic properties together in 2D materials.

References

- [1] Huang, B.; Clark, G.; Navarro-Moratalla, E.; Klein, D. R.; Cheng, R.; Seyler, K. L.; Zhong, D.; Schmidgall, E.; McGuire, M. A.; Cobden, D. H.; Yao, W.; Xiao, D.; Jarillo-Herrero, P.; Xu, X.; *Nature* 546 (2017), 270-273.
- [2] Gong, C.; Li, L.; Li, Z.; Ji, H.; Stern, A.; Xia, Y.; Cao, T.; Bao, W.; Wang, C.; Wang, Y.; Qiu, Z. Q.; Cava, R. J.; Louie, S. G.; Xia, J.; Zhang, X., *Nature* 546 (2017), 265-269.

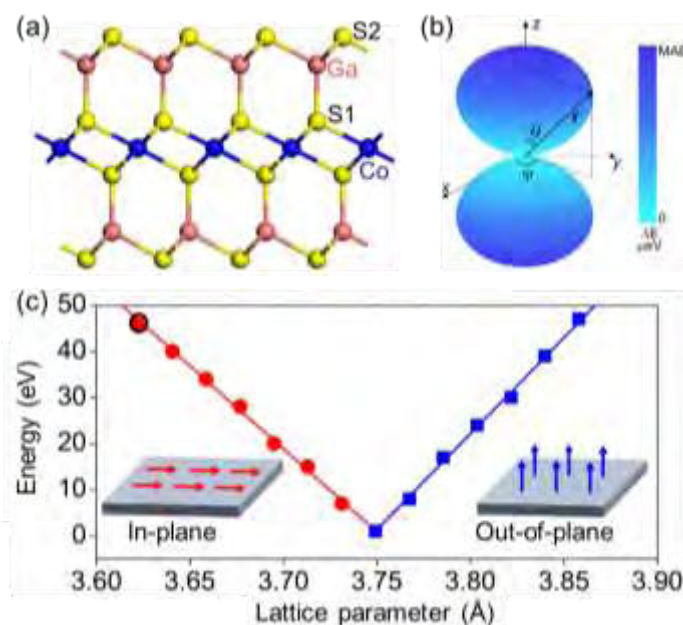


Figure 1: (a) Side view of CoGa_2X_4 structure; (b) Schematic map of MAE for CoGa_2X_4 monolayer. (c) With the increase of lattice parameters, the in-plane magnetic moments vary to out-of-plane direction.

Shuang Zhou

Shuang Zhou¹, Carla Bittencourt², Stephan Werner³, Catharina Haebel³, Peter Guttman³, Wenjiang Li^{1*}, Rony Snyders^{1,2}

¹Key Laboratory of Display Materials & Photoelectric Devices, School of Materials Science and Engineering, Tianjin University of Technology, Tianjin 300384, PR China.

²Chimie des Interactions Plasma Surface, CIRMAP, University of Mons, Mons, Belgium.

³Research group X-ray microscopy, Helmholtz-Zentrum Berlin für Materialien und Energie GmbH, Berlin, Germany.

1467693061@qq.com

Reduced graphene oxide/carbon hybrid aerogels from cellulose and graphene oxide for oil/water separation

Recently, reduced graphene oxide/carbon hybrid (RGO/CH) aerogels with outstanding physicochemical properties have exhibited potential application in widespread fields, and therefore attracted extensive attention. RGO/CH aerogels are synthesized by pyrolysis of graphene oxide /cellulose aerogels that are prepared by dissolving of cellulose in N-methylmorpholine-N-oxide (NMMO) monohydrate solvent, a nontoxic and environmentally friendly solvent, followed by gelation, regeneration and freeze drying. The prepared RGO/CH aerogel possesses a low apparent density in the range of 0.073-0.156 g cm⁻³, and presents highly hydrophobic and oleophobic properties with a high water contact angle up to 112° (Figure 1a). The porous 3D network structure of RGO/CH aerogels makes it to be an excellent candidate as absorber for oil/water separation (Figure 1b). Moreover, the absorbed oil could be removed by burning, and the oil sorption was still as high as 90% of the original sorption capacity after 5 cycles.

References

- [1] Li C, Wu Z Y, Liang H W, et al., *Small*, 13(2017)
- [2] Meng Y, Young T M, Liu P, et al., *Cellulose*, 22(2015) 435-447.
- [3] Yin T, Zhang X, Liu X, et al., *Rsc Advances*, 6(2016) 98563-98570.
- [4] Zu G, Shen J, Zou L, et al., *Carbon*, 99 (2016) 203-211.

Figures

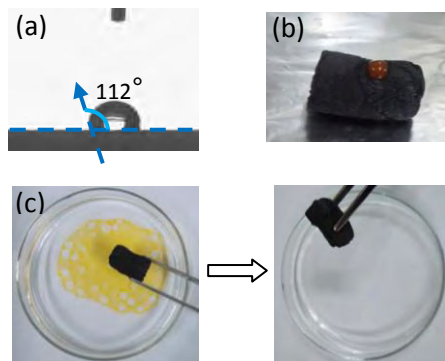


Figure 1: (a) The water contact angle of RGO/CH aerogels (b) Water stained with Sudan I was dropped on the surface of RGO/CH aerogel (c) Removal of corn oil from the water surface using RGO/CH aerogels

Yongjin Zou

Cuili Xiang, Fen Xu, Lixian Sun*

Material Science and Engineering, Guilin University of Electronic Technology, 1# Jinji Road, Guilin, 541004
Chinazouy@guet.edu.cn

Functionalized porous carbon for high performance supercapacitors

Porous carbon-based nanomaterials such as graphene, carbon nanotubes, carbon nanosheets and carbon nanosphere are still the first choices for fabricating the electrodes of supercapacitor because of their excellent stability, good conductivity, and large surface area [1]. However, the capacitance of carbon-based materials is intrinsically low, which limit their wide application. Doping carbonaceous materials with a conducting polymer or transition metal compounds to generate pseudocapacitance is effective way to improve their electrochemical performance [2-4]. In this study, porous carbon was functionalized with transition metal oxides, conducting polymer and heteroatom for the purpose of supercapacitive enhancement. The electrochemical performance of the supercapacitor was studied in detail.

References

- [1] Y. Zou, Q. Wang, C. Xiang, Z. She, et al., *Electrochim. Acta*, 2016,188, 126-134.
- [2] C. Xiang, Q. Wang, Y. Zou, et al. *J. Mater. Chem. A*, 2017,5, 9907-9916.
- [3] Y. Zou, C. Cai, C. Xiang, et al. *Electrochim.a Acta*, 2018,261,537-547.
- [4] C. Cai, Y. Zou, C. Xiang, et al., *Appl. Surface Sci.*, 2018, 440, 47-54.



GRAFOID

A Complete Solutions Graphene Company

GRAFOID: POSITIONED FOR COMMERCIALIZATION

Grafoid is a world-leading graphene research and application development company moving towards the commercialization of mass produced, next generation products in partnership with leading global corporations and institutions.

Grafoid has achieved:

- An Expanding Global Presence
- A World Class R&D Facility
- A Critical Energy Materials Business Platform
- A Multi-country Application Development Partnership
- Security of Supply of Source Graphite

Grafoid's business innovation and management vision, our science, in-house engineering, quality control and investments in next generation materials and products leave us well positioned to commercialize our inventions in the global marketplace

www.GRAFOID.com